

精工锻造的钉砧使钳口压力增强且一致  
三点控制系统确保缝钉排列整齐，成型良好  
独有金色钉仓，提供1.8mm 成钉高度

60  
Echelon

45  
Echelon

腔镜直线型切割吻合器和钉仓 (商品名: ECHELON 60)  
注册证号: 国食药监械(进)字2011第3220273号  
腔镜直线型切割吻合器和钉仓 (商品名: ECHELON 45)  
注册证号: 国食药监械(进)字2009第3651686号  
广告批准文号:

强生(上海)医疗器材有限公司  
地址: 上海市徐汇区虹桥路355号城开国际大厦4楼  
邮编: 200030  
电话: 021-22058888  
传真: 021-22058868  
网址: www.jmc.com.cn  
生产企业地址: Ethicon Endo-Surgery, LLC

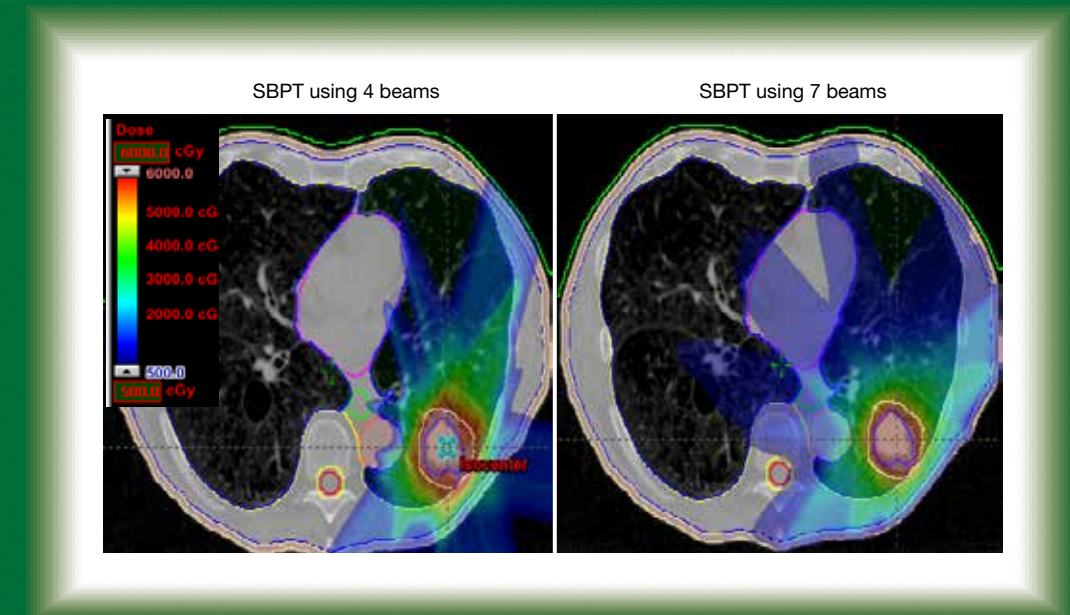


# JOURNAL of THORACIC DISEASE



www.jthoracdis.com

**FOCUSED ISSUE:** Hypo- and hyper-fractionated radiotherapy in NSCLC using cutting-edge technologies  
**Guest Editors:** Joe Y. Chang, Dirk De Ruyscher



Published by Pioneer Bioscience Publishing Company

Indexed in PubMed, SCI

## Now Indexed in PubMed

### Aims and Scope

The *Journal of Thoracic Disease* (JTD, J Thorac Dis, pISSN: 2072-1439; eISSN: 2077-6624) was founded in Dec 2009, indexed in Pubmed/Pubmed Central in Dec 2011, and Science Citation Index (SCI) on Feb 4, 2013. It is published quarterly (Dec 2009- Dec 2011), bimonthly (Jan 2012- Dec 2013), and monthly (Jan 2014-), and openly distributed worldwide. JTD publishes manuscripts that describe new findings in the field to provide current, practical information on the diagnosis and treatment of conditions related to thoracic disease (lung disease, cardiac disease, breast disease and esophagus disease). Original articles are considered most important and will be processed for rapid review by the members of Editorial Board. Clinical trial notes, Cancer genetics reports, Epidemiology notes and Technical notes are also published. Case reports implying new findings that have significant clinical impact are carefully processed for possible publication. Review articles are published in principle at the Editor's request. There is no fee involved throughout the publication process. The acceptance of the article is based on the merit of quality of the manuscripts. All the submission and reviewing are conducted electronically so that rapid review is assured.

### The Official Publication of:

- ❖ Guangzhou Institute of Respiratory Disease (GIRD)
- ❖ China State Key Laboratory of Respiratory Disease
- ❖ First Affiliated Hospital of Guangzhou Medical University
- ❖ Society for Thoracic Disease (STD)

### Endorsed by:

- ❖ International COPD Coalition (ICC)

### Editorial Correspondence

Daoyuan Wang, MD

Managing Editor

Pioneer Bioscience Publishing Company

Address: 9A Gold Shine Tower, 346-348 Queen's Road Central, Sheung Wan, Hong Kong. Tel: +852 3488 1279; Fax: +852 3488 1279.

Email: [jtd@thepbpc.org](mailto:jtd@thepbpc.org)  
[www.jthoracdis.com](http://www.jthoracdis.com)

### Note to NIH Grantees

Pursuant to NIH mandate, Pioneer Bioscience Publishing Company will post the accepted version of contributions authored by NIH grant-holders to PubMed Central upon acceptance. This accepted version will be made publicly available 2 months after publication. For further information, see [www.thepbpc.org](http://www.thepbpc.org)

### Conflict of Interest Policy for Editors

The full policy and the Editors' disclosure statements are available online at: [www.jthoracdis.com](http://www.jthoracdis.com)

### Disclaimer

The Publisher and Editors cannot be held responsible for errors or any consequences arising from the use of information contained in this journal; the views and opinions expressed do not necessarily reflect those of the Publisher and Editors, neither does the publication of advertisements constitute any endorsement by the Publisher and Editors of the products advertised.

### Cover image:

Comparison of stereotactic body proton therapy (SBPT) and stereotactic body radiation therapy (SBRT) plans for early-stage lung cancer. (See P349 in this issue).

For submission instructions, subscription and all other information visit [www.jthoracdis.com](http://www.jthoracdis.com)

© 2014 Pioneer Bioscience Publishing Company

**Editor-in-Chief**

Nanshan Zhong, MD

*Academician, Chinese Academy of Engineering. Guangzhou Institute of Respiratory Disease, Guangzhou, China***Executive Editor-in-Chief**

Jianxing He, MD, FACS

*The First Affiliated Hospital of Guangzhou Medical University, Guangzhou, China***Executive Editor-in-Chief (Cardiovascular Surgery)**

Tristan D. Yan, BSc, MBBS, MS, MD, PhD

*Department of Cardiothoracic Surgery, Royal Prince Alfred Hospital, University of Sydney, Sydney, Australia; The Collaborative Research (CORE) Group, Sydney, Australia***Deputy Editors-in-Chief**Jin-Shing Chen, MD, PhD  
*Taipei, Taiwan*Rongchang Chen, MD, PhD  
*Guangzhou, China*

Yi-Jen Chen, MD, PhD

*Duarte, USA*Kwun Fong, MBBS (Lon), FRACP, PhD  
*Brisbane, Australia*Lawrence Grouse, MD, PhD  
*Gig Harbor, USA*

Shahzad G. Raja, MBBS, MRCSEd, FRCSEd (C-Th)

*London, United Kingdom*Gaetano Rocco, MD, FRCS (Ed), FETCS, FCCP  
*Naples, Italy***Editorial Co-Directors & Executive Editors**

Guangqiao Zeng, MD

*Guangzhou, China*

Daoyuan Wang, MD

*Guangzhou, China***Statistical Editors**

Jiqian Fang, PhD

*Guangzhou, China*

Baoliang Zhong, MD, PhD

*Hong Kong, China***Associate Editors**

Hatem A Azim Jr, MD

*Brussels, Belgium*

Kazuaki Takabe, MD, PhD, FACS

*Richmond, United States*

Gary Y. Yang, MD

*Loma Linda, United States*

Paul Zarogoulidis, MD, PhD

*Thessaloniki, Greece*

Junya Zhu, MS, MA

*Boston, United States***Section Editor (Systematic Review and Meta-analysis)**

Zhi-De Hu, M.M Jinan, China

Wan-Jie Gu, MSc *Guangzhou, China*Zhi-Rui Zhou, MD *Changchun, China***Section Editor (Cancer Registry, Prevention and Control)**

Wanqing Chen, MD

*Beijing, China***Editorial Board**

James S Allan, MD

Rahul J Anand, MD

Emilio Bajetta, MD, SC

Peter J Barnes, DM, DSc, FRCP,

FCCP, FMedSci, FRS

J. Patrick Barron, MD

Bruno R. Bastos, MD

Luca Bertolaccini, MD, PhD

Peter Calverley, MD

Weiguo Cao, MD

Mario Cazzola, MD

Joe Y Chang, MD, PhD

Wanqing Chen, MD

Yi-han Chen, MD, PhD

Leo L Cheng, PhD

Xiangyang Chu, MD

Kian Fan Chung, MD, DSc, FRCP

Henri G. Colt, MD, FCCP

Thomas A. D'Amico, MD

Giovanni Dapri, MD, FACS,

FASMSB

Keertan Dheda, MBBCh,

FCP(SA), FCCP, PhD(Lond),

FRCP(Lond)

Peter V. Dicpinigaitis, MD

Leonardo M. Fabbri

Yoshinosuke Fukuchi, MD, PhD

Diego Gonzalez-Rivas, MD,

FECTS

Cesare Gridelli, MD

Tomas Gudbjartsson, MD, PhD

Don Hayes, Jr, MD, MS, Med

Andrea Imperatori, MD

Mary Sau Man Ip, MBBS(HK),

MD(HK), FRCP (London,

Edinburgh, Glasgow), FHKCP,

FHKAM, FAPSR, FCCP

Ki-Suck Jung, MD, PhD

Alexander Sasha Krupnick, MD

Hyun Koo Kim, MD, PhD

Anand Kumar, MD

Aseem Kumar, PhD

Y. C. Gary Lee, MBChB, PhD,

FCCP, FRCP, FRACP

Mario Leoncini, MD

Jian Li, MD

Tianhong Li, MD, PhD

Wenhua Liang, MD

Yang Ling, MD

Deruo Liu, MD

Lunxu Liu, MD

Hui-Wen Lo, PhD

Kevin W. Lobbell, MD

Jiade J. Lu, MD, MBA

Giovanni Mariscalco, MD, PhD

Doug McEvoy, MBBC, FRACP

Mark J. McKeage, MD

Walter McNicholas, MD, FRCPI,

FRCPC, FCCP

Michael T. Milano, MD, PhD

John D. Mitchell, MD

Alyn H Morice MD

Akio Niimi, MD, PhD

Antonio Passaro, MD

Georgios Plataniotis, MD, PhD

David Price, M.B B.Chir, MA,

DRCOG, FRCGP

Gui-bin Qiao, MD, PhD

Klaus F Rabe, MD, PhD

Dominik Rüttinger, MD, PhD,

FACS

Sundeep Salvi, MD, DNB, PhD,

FCCP

Martin Schweiger, MD

Suresh Senan, MD

Charles B. Simone, II, MD

Yong Song, MD, PhD

Ross Soo, MD

Joerg S. Steier, MD (D), PhD (UK)

Robert Sturm, MSc, PhD

Lijie Tan, MD, Vice Chief

Kosmas Tsakiridis, MD, PhD

Kenneth WT Tsang, MD, FRCP

Mark I. van Berge Henegouwen,

MD, PhD

Ko Pen Wang, MD, FCCP

Qun Wang, MD

Yi-Xiang Wang, MD

Zheng Wang, MD

Zhimin Wang, PhD

Bryan A Whitson, MD, PhD

Yunlong Xia, MD, PhD

Jin Xu, MS

Ping Yang, MD, PhD

Stephen C. Yang, MD

Kazuhiro Yasufuku, MD, PhD

Anthony P.C. Yim, BM

BCh(Oxon), DM(Oxon),

FRCS(Eng)

Xiuyi Zhi, MD

Caicun Zhou, MD, PhD

Qinghua Zhou, MD

Zhi-hua Zhu, MD, PhD

**Journal Club Director**

Bing Gu, MD

**Editorial Assistants**Maria Karina, MD, PhD,  
FRCP

Parag Prakash Shah, PhD

**Managing Editor**

Katherine L. Ji

**Senior Editors**Grace S. Li (Corresponding  
Editor)

Eunice X. Xu

Elva S. Zheng

Nancy Q. Zhong

**Science Editors**

Melanie C. He

Tina C. Pei

Molly J. Wang

Rui Wang

**Executive Copyeditor**

Benti L. Peng

**Executive Typesetting Editor**

Jian Li

**Production Editor**

Emily M. Shi

# Table of Contents

## Preface

- 285 **Individualized hypo/hyperfractionated radiotherapy for non-small cell lung cancer**  
*Joe Y. Chang, Dirk De Ruyscher*

## Review Article

- 287 **Exploiting sensitization windows of opportunity in hyper and hypo-fractionated radiation therapy**  
*Anish Prasanna, Mansoor M. Ahmed, Mohammed Mobiuddin, C. Norman Coleman*
- 303 **Improving radiotherapy planning, delivery accuracy, and normal tissue sparing using cutting edge technologies**  
*Carri K. Glide-Hurst, Indrin J. Chetty*
- 319 **Imaging techniques for tumour delineation and heterogeneity quantification of lung cancer: overview of current possibilities**  
*Wouter van Elmpt, Catharina M.L. Zegers, Marco Das, Dirk De Ruyscher*
- 328 **Hyperfractionated and accelerated radiotherapy in non-small cell lung cancer**  
*Kate Haslett, Christoph Pöttgen, Martin Stuschke, Corinne Faivre-Finn*
- 336 **Radiation dose effect in locally advanced non-small cell lung cancer**  
*Feng-Ming (Spring) Kong, Jing Zhao, Jingbo Wang, Corrine Faivre-Finn*
- 348 **Accelerated dose escalation with proton beam therapy for non-small cell lung cancer**  
*Daniel R. Gomez, Joe Y. Chang*
- 356 **Combining targeted agents and hypo- and hyper-fractionated radiotherapy in NSCLC**  
*Fiona McDonald, Sanjay Papat*

## Original Article

- 369 **Local control rates with five-fraction stereotactic body radiotherapy for oligometastatic cancer to the lung**  
*Deepinder Singh, Yuhchayou Chen, Mary Z. Hare, Kenneth Y. Usuki, Hong Zhang, Thomas Lundquist, Neil Joyce, Michael C. Scbell, Michael T. Milano*

## Review Article

- 375 **New techniques for assessing response after hypofractionated radiotherapy for lung cancer**  
*Sarah A. Mattonen, Kitty Huang, Aaron D. Ward, Suresh Senan, David A. Palma*
- 387 **Molecular markers to predict clinical outcome and radiation induced toxicity in lung cancer**  
*Joshua D. Palmer, Nicholas G. Zaorsky, Matthew Witek, Bo Lu*

## Between You and Me

- E37 **Stories of *Special K* patients**  
*Peng Wu*

# PREFACE

---

## Individualized hypo/hyperfractionated radiotherapy for non-small cell lung cancer

Radical radiotherapy has a crucial role in the management of non-small cell lung cancer (NSCLC). Stereotactic ablative radiotherapy [SABR, also known as stereotactic body radiotherapy (SBRT)], which involves the administration of biologically effective doses (BEDs) in excess of 100 Gy in a few large radiation doses in a short overall treatment time, for stage I NSCLC has produced local control rates in excess of 90% and survival comparable to that after lobectomy. Indeed, SABR has become standard treatment for medically inoperable stage I NSCLC. For locally advanced inoperable NSCLC, the standard treatment in the United States and Europe is concurrent chemoradiotherapy, with the radiation delivered in 2-Gy fractions. However, the optimal radiation dose and fractionation remain controversial. Retrospective and phase II clinical studies have shown that radiation doses with higher BEDs are associated with improved local control and potentially with better survival. Unfortunately, a recent phase III randomized study [Radiation Therapy Oncology Group (RTOG) 0617] indicated that a high radiation dose (74 Gy, BED 88.8 Gy) given with concurrent carboplatin-paclitaxel chemotherapy was associated with poorer local control and survival than the conventional 60-Gy dose (BED 72 Gy) in that study. Underreported severe toxicity of high radiation doses, especially given concurrently with carboplatin-paclitaxel chemotherapy, could be the main reason for the poor survival, as well as the prolonged treatment time (37 fractions) and the lack of adequate image-guided radiotherapy and quality assurance in this study could explain the poor local control. On the other side, the nearly 29 months of overall survival in the 60 Gy arm is the best ever achieved in a multi-centre phase III trial and should be regarded as a benchmark result.

Advances in radiotherapy technologies allow the radiation dose to be precisely focused to the target while minimizing the inadvertent dose to nearby organs at risk, which may translate into improved local control and reduced toxicity. Thus, although 60 Gy with concurrent chemotherapy remains the “standard of care” for inoperable stage III NSCLC at this time, issues of dose escalation and acceleration should continue to be explored as new techniques and technologies emerge. In addition, not all cases of NSCLC will need radiation dose escalation. Moreover, some patients may not be able to tolerate dose escalation or acceleration. Individualized radiotherapy dose escalation, acceleration, or both that is based on the biological and physical features of tumors and normal tissues should be considered in future studies.

Altered radiotherapy fractionation schedules including hyperfractionated or hypofractionated accelerated radiotherapy regimens have been used for NSCLC in Europe and have shown promising clinical outcomes. In addition to potential reductions in cost (from shortening the treatment period), altered fractionation and image-guided hyper/hypofractionated radiotherapy can be used to safely increase the BED and thereby potentially improve local control and survival for selected patients. However, the greater risk of late toxic effects when higher BEDs are delivered to critical structures remains a concern. Also unknown is how these regimens are best combined with chemotherapy or molecular targeted therapy.

In this special issue of the *Journal of Thoracic Disease*, experts from around the world discuss the potential role of, and associated challenges with, the use of hyper/hypofractionated accelerated radiotherapy for the treatment of lung cancer. This special issue addresses the unique biological, physical, and clinical aspects of altered radiotherapy fractionation regimens for early-stage disease, locally advanced disease, and metastatic NSCLC. The biological rationale underlying the use of altered fractionation and molecular marker-based personalized targeted therapy is discussed as well. Cutting-edge technologies to improve local control while reducing normal-tissue toxicity through the use of 4D CT-based motion management and radiotherapy planning, and image-guided radiotherapy delivery with intensity-modulated radiotherapy, stereotactic ablative radiotherapy, and proton therapy are presented. The novel concept of using radical radiotherapy as a component of systemic treatment, particularly for tumors that are resistant to chemotherapy or targeted therapies, and the potential of synergizing immunotherapy and radiotherapy are also explored.

The challenges of financial constraints and upcoming “bundled” reimbursements for oncologic care, both in the United States, Europe and elsewhere, underscore the urgency of the need to evaluate, verify, and consider adopting these strategies for treating some patients with lung cancer, if hyper/hypofractionated radiotherapy can be shown to improve or at least maintain the efficacy of conventional radiotherapy while minimizing toxic effects to normal tissues.

**Joe Y. Chang<sup>1</sup>, MD, PhD****Dirk De Ruyscher<sup>2</sup>, MD**

<sup>1</sup>Professor, Clinical Section Chief of Thoracic Radiation Oncology; Director of Stereotactic Ablative Radiotherapy Program, Department of Radiation Oncology, The University of Texas MD Anderson Cancer Center, Houston, TX 77030, USA;

<sup>2</sup>Professor, Radiation Oncologist, Department of Radiation Oncology, University Hospitals Leuven/KU Leuven, Belgium  
(Email: [jychang@mdanderson.org](mailto:jychang@mdanderson.org); [dirk.deruyscher@uzleuven.be](mailto:dirk.deruyscher@uzleuven.be).)

doi: 10.3978/j.issn.2072-1439.2013.12.47

Disclosure: The authors declare no conflict of interest.



**Cite this article as:** Chang JY, De Ruyscher D. Individualized hypo/hyperfractionated radiotherapy for non-small cell lung cancer. *J Thorac Dis* 2014;6(4):285-286. doi: 10.3978/j.issn.2072-1439.2013.12.47

## Exploiting sensitization windows of opportunity in hyper and hypofractionated radiation therapy

Anish Prasanna<sup>1</sup>, Mansoor M. Ahmed<sup>1</sup>, Mohammed Mohiuddin<sup>2</sup>, C. Norman Coleman<sup>1</sup>

<sup>1</sup>Radiation Research Program, Division of Cancer Treatment and Diagnosis, National Cancer Institute, National Institutes of Health, Rockville, MD, USA; <sup>2</sup>Oncology Centre, King Faisal Specialist Hospital and Research Centre, Riyadh, Kingdom of Saudi Arabia

### ABSTRACT

In contrast to the conventional radiotherapy/chemoradiotherapy paradigms used in the treatment of majority of cancer types, this review will describe two areas of radiobiology, hyperfractionated and hypofractionated radiation therapy, for cancer treatment focusing on application of novel concepts underlying these treatment modalities. The initial part of the review discusses the phenomenon of hyper-radiation sensitivity (HRS) at lower doses (0.1 to 0.6 Gy), describing the underlying mechanisms and how this could enhance the effects of chemotherapy, particularly, in hyperfractionated settings. The second part examines the radiobiological/physiological mechanisms underlying the effects of high-dose hypofractionated radiation therapy that can be exploited for tumor cure. These include abscopal/bystander effects, activation of immune system, endothelial cell death and effect of hypoxia with re-oxygenation. These biological properties along with targeted dose delivery and distribution to reduce normal tissue toxicity may make high-dose hypofractionation more effective than conventional radiation therapy for treatment of advanced cancers. The novel radiation physics based methods that take into consideration the tumor volume to be irradiated and normal tissue avoidance/tolerance can further improve treatment outcome and post-treatment quality of life. In conclusion, there is enough evidence to further explore novel avenues to exploit biological mechanisms from hyper-fractionation by enhancing the efficacy of chemotherapy and hypo-fractionated radiation therapy that could enhance tumor control and use imaging and technological advances to reduce toxicity.

### KEYWORDS

Low Doses Fractionated Radiation Therapy (LDFRT); hyper-radiation sensitivity (HRS); induced radiation resistance (IRR); hyperfractionation; chemopotential; stereotactic body radiation therapy (SBRT); stereotactic ablative radiosurgery (SARS); stereotactic ablative radiotherapy (SABR); stereotactic radiosurgery (SRS); spatially fractionated GRID radiotherapy (SFGRT); lattice

*J Thorac Dis 2014;6(4):287-302. doi: 10.3978/j.issn.2072-1439.2014.01.14*

### Introduction

Approximately 60% of patients with solid tumors are treated with radiation therapy, which highlights its importance in cancer

treatment. For 15% of patients radiation therapy is the only form of treatment and the remaining 45% are treated with radiation combined with chemotherapy. The latter includes breast, lung, prostate, head & neck, bladder, gynecological, pancreas, colorectal and anal cancers and brain tumors (1). The efficacy of radiation therapy, whether treated alone or in combination, can be further improved by adopting recent technological advances and biological approaches. These advances in technology include improved dose distribution with intensity modulated and image guided radiotherapy (IMRT and IGRT), dose escalation (higher dose) and dose intensification (higher and more focused dose). Biological approaches include (I) adopting time-honored, "classical" concepts such as DNA damage repair, tumor cell repopulation and cell cycle distribution; (II) exploiting tumor microenvironmental changes such as hypoxia, reoxygenation,

Correspondence to: Mansoor M. Ahmed, PhD. Radiotherapy Development Branch (RDB), Radiation Research Program (RRP), Division of Cancer Treatment and Diagnosis (DCTD), National Cancer Institute/National Institutes of Health, 9609 Medical Center Drive, Rm. 3W224, Rockville, MD 20850-7440, USA. Email: ahmedmm@mail.nih.gov.

Submitted Dec 04, 2013. Accepted for publication Jan 12, 2014.  
Available at [www.jthoracdis.com](http://www.jthoracdis.com)

ISSN: 2072-1439

© Pioneer Bioscience Publishing Company. All rights reserved.

vasculature, etc.; (III) use of different types of particles (e.g., protons and carbon ions), which may have a high-linear energy transfer for improved radiobiological effectiveness; (IV) use of altered dose and schedule such as hyper- and hypo-fractionation; and (V) use of radiation protectors and sensitizers including concurrent chemotherapy. In this paper, we define standard fractionation as conventional 1.8 to 2.2 Gy (one fraction per day, five days a week continuing for 3-7 weeks), hyperfractionation as 0.5 to 2.2 (two fractions per day, 2-5 days a week, for 2-4 weeks), and hypofractionation as doses of 3-20 Gy (one fraction a day given for 1-3 days for doses 8-20 Gy).

As with cancer treatment in general, progress in radiation therapy has been steady with much more organ preservation (e.g., head & neck cancer, anal and rectal cancer, esophageal cancer) because of (I) patient selection based on improved clinical parameters, mostly of tumor stage but some with biomarkers such as proliferation and metabolism (e.g., PET scanning); (II) modified surgical/radio-surgical approaches; and (III) use of chemo/hormonal therapy based on pathological and molecular subtype (e.g., breast cancer). Progress is likely to accelerate with the incorporation of emerging new knowledge in cancer biology including tumor classification by molecular characterization and precision medicine, i.e., providing right treatment to right patient. Key to progress relies on well done randomized clinical trials that need to be based on improved preclinical models and careful post-trial analysis because well-conceived hypotheses may not be confirmed for a variety of reasons (2).

It is always wise to exploit what can be exploited based on careful clinical observation—some of which may have been hypothesis driven but much of it may be hypothesis generating based on thorough observations and innovative analyses. Examples from clinical treatments based on so-called “classical” radiation biology includes modifying radiation dose and treatment volume based on the shape of the survival curve (alpha and beta components of the linear-quadratic curve) but it would be preferable to understand the benefits of a particular dose size at the molecular, cellular, and tissue levels. Understanding what happens in various tumor types and relevant normal tissues at the clinically relevant dose fractions of 2 Gy is important, as there are extensive historical clinical-outcome data over many decades. This may help identify targets such as radiation-induced pro-survival factors that can confer induced radiation resistance (IRR). Were those the situation, one could use a particular radiation dose window (below threshold IRR dose) and schedule it in such a way that it does not activate pro-survival events. Resistance to treatment could relate more to factors within the heterogeneous tumor microenvironment niche or to other factors that might benefit from the use of chemotherapy

as part of the regimen. The first part of the review will focus on low-dose hyperfractionation (below IRR dose or HRS-inducing dose) and chemopotiation providing evidence both at pre-clinical and clinical level. In the second part, we provide data that support the contention that high-dose radiation has the potency to induce a robust bystander effect, as well as abscopal (distant) effects (3). Since high-dose hypofractionation regimens are now commonly adopted in the clinic (such as stereotactic radiation surgery), is there a defined dose/fractionation window to exploit certain potential sensitization avenues initiated by abscopal factors that can be potentially combined with agents (including immune modulating agents) or subsequent radiotherapy?

### Low-dose hyperfractionation and chemopotiation

In the past 100 years, the biological effects of various size doses of low-LET radiation have been examined in the clinic as well as by *in vitro* clonogenic assay since first reported by Puck and Marcus in 1955. Radiation hormesis or an effect of radiation at very low doses which can stimulate the repair mechanisms on the cellular level and thereby potentially protect cells from future exposure, are known to be induced at 0.1 to 0.2 Gy (100 to 200 mGy) (4). There is controversy as to what is the lowest radiation dose that can produce radiation-inducible cancer however, at doses above 0.10 Gy there is a risk of radiation-induced carcinogenesis, which increases with dose (5). Generally, at doses above 1 Gy growth arrest occurs and cell killing predominates above 2 Gy. A daily dose size in the range of 2-3 Gy and multiple dose schedules had been empirically selected over the years based on both normal tissue sparing from fractionation and evidence of clinical efficacy. However, as the biological effects of dose have been examined, novel regimens are being explored.

### *Low dose hyper-radiosensitivity (HRS) and induced radiation resistance (IRR)*

Although, there is an understanding of the mechanism of cell death by radiation at conventional doses (1.5-2.2 Gy per fraction), the mechanism of radiation effects at lower doses (<1 Gy) is still emerging (6). The initial slope of the radiation cell-survival curve (doses of 0.1-1 Gy) was presumed to be ineffective for human tumor therapy, however, with dynamic microscopic imaging to study the effects of low dose radiation on individual cells within a larger cell population, it was demonstrated that X-rays are effective at cell killing at very low doses, around 0.1 Gy, then become less effective as the dose increased with

**Table 1.** Potential underlying mechanisms in HRS and IRR doses and in chemopotiation settings.

| Treatments              | Mechanisms  |   |
|-------------------------|---|---|
|                         | Normal cells                                      | Tumor cells   |
| HRS LDFRT (<0.6 Gy)     | ATM activation and DNA repair programs initiated. | Bax upregulation with bcl-2 down regulation; pro-apoptotic proteins upregulated   |
| IRR dose (>1 Gy)        | ATM activation and DNA repair programs initiated. | ATM activation, pro-survival transcription factors (NFκB and NF-Y) upregulated, MDR-1 upregulated   |
| LDFRT + chemotherapy    | No data   | Bax upregulation with bcl-2 down regulation, cytochrome C release; several pro-apoptotic proteins are upregulated<br>XIAP was downregulated, but upregulated in LDFRT-resistant cells |
| IRR dose + chemotherapy | No data   | Bcl-2 and MDR1 protein increased; increase in NFκB and NF-Y activity<br>XIAP is significantly upregulated   |

IRR, induced radiation resistance; HRS, hyper-radiation sensitivity; LDFRT, Low Doses Fractionated Radiation Therapy.

minimal effectiveness at about 0.6 Gy, and then becoming more effective again as the dose increased to 1.5 Gy and above. This phenomenon is referred to as hyper radiation sensitivity (HRS) (6,7). At doses <1 Gy, many cell lines show low dose HRS (8-10). Interestingly, the HRS is most pronounced in radio-resistant cells, defined in this case as those with mutant p53 expression (11,12). Enns *et al.* (13) examining the response of human A549 lung carcinoma, T98G glioma, and MCF7 breast carcinoma cell lines to gamma radiation in the dose range 0 to 2 Gy, showed marked HRS at doses below 0.5 Gy. It was further determined that low dose hypersensitivity is possibly related to p53-dependent apoptosis, as treatment of cells with Pifithrin, an inhibitor of p53 function, completely ablated HRS. Thus, the role of p53 function in HRS is still unclear and requires further investigation using p53 knockout cell lines and validation in GEMMs.

HRS is evident in murine models (14), but it appears to be an underexplored phenomenon in humans. Since development of resistance is a major cause of treatment failure, circumventing resistance by exploiting HRS would greatly benefit in the treatment of many cancer types. Further, as seen *in vitro* HRS does not involve activation of pro-survival pathways [found at higher doses (15)] (16), providing a mechanism to explain the efficacy of radiation at these low doses. However, as Short and Joiner have pointed out, in order to benefit from low dose-per-fraction radiation in the clinical setting, therapy needs to be extended over 7-12 weeks for sufficient total dose to be delivered. During this prolonged period of treatment, tumor proliferation can occur, which would abate the gain due to enhanced cell killing at HRS radiation doses (17). Prolonged treatment in clinic, lasting 7-12 weeks, will result in several logistic issues as well as increasing cost. Hence, it is logical to combine a radiation

dose that results in HRS with chemotherapy to potentiate the effects of chemotherapy and also shorten the treatment time.

In summary, there is a functional evidence for the existence of HRS *in vitro* and its exploitation in the clinic can be challenging. One possibility is to benefit in the clinic from HRS is by using Low Doses Fractionated Radiation Therapy (LDFRT) as a potentiator of systemic chemotherapy that would not trigger the activation of pro-survival pathways in the tumors. Here below, we describe the preclinical evidence to this end.

#### ***HRS-inducing LDFRT as a potentiator of chemotherapy: preclinical evidence***

Extensive data are available on the HRS/IRR phenomenon observed in more than 40 tumor cell lines in response to single low dose radiation (18,19). HRS occurs after fractionated low doses in *in vitro* (18,19). Pretreatment with paclitaxel followed by multi-fractionated low dose radiation (0.5- or 1-Gy fractions for a total dose of 2 Gy) significantly enhanced the radiosensitizing effect in both HCT-116 and HT-29 cells when compared to single fraction 2 Gy dose (12). LDFRT was found to potentiate the effects of taxanes in head and neck cancer cell lines *in vitro* (15,20) as well as cisplatin in lung cancer cells *in vitro* (21).

The molecular mechanisms underlying the process of chemopotiation by LDFRT are shown in Table 1. In brief, there is involvement of NFκB, NF-Y, bcl-2, XIAP and MDR1 in IRR and at the same time p53, bax, and pro-apoptotic effectors such as cytochrome C seems to be involved (Figure 1). Further, in a recent meeting presentation, HDAC inhibitor SAHA (Vorinostat) was combined with LDFRT in GBM cells lines D54 and U118. Findings of this study demonstrated that LDFRT potentiated the effect of Vorinostat in p53 dependent manner

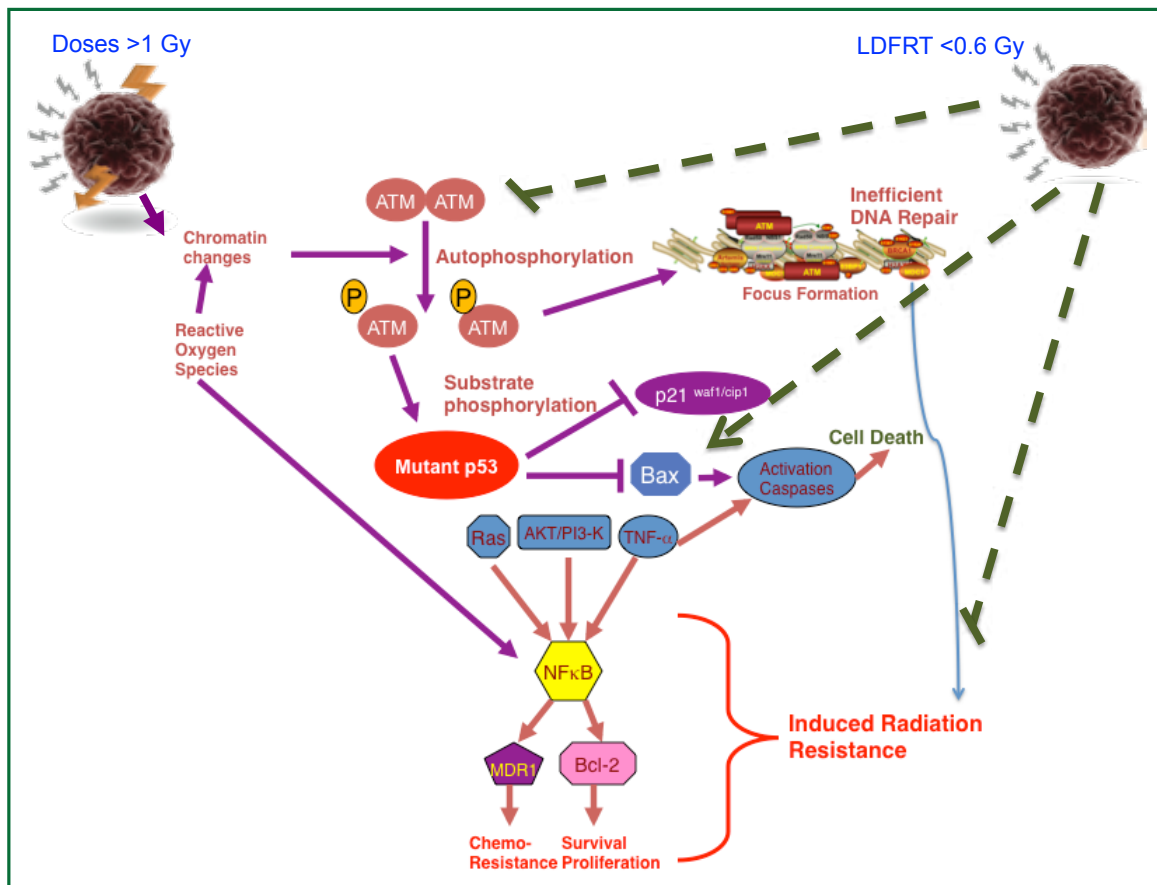


**Figure 1.** Reported molecular events in IRR and LDFRT. IRR is achieved similarly as DNA damage repair programs such as by activation of ATM, inefficient DNA repair, increase in NFκB, Bcl-2 and MDR1 (purple arrows); along with minimal extrinsic apoptotic induction via TNFα (orange arrows). In LDFRT settings in tumor cells (not in normal cells), ATM kinase is not activated and hence no DNA-repair, lack of increase in NFκB activity as well as in Bcl-2 and MDR1 proteins (green dashed lines). LDFRT activates directly bax to induce an intrinsic apoptotic killing (green dashed lines).

with the requirement of PTEN (22). It is important to note that at doses of approximately 0.5 Gy, ATM autophosphorylation occurs in normal cells such as skin fibroblast (23) and peripheral blood lymphocytes (24) resulting in activation of DNA repair programs, but in cancer cells the dose to activate ATM pathways is  $>1$  Gy (25). Thus, it appears that HRS is due to a lack of activation of ATM autophosphorylation pro-survival pathways (Figure 1) (modification of apoptosis, NFκB). Thus, these mechanistic data from cell culture studies indicate that chemopotentialization by LDFRT is primarily due to cell killing, thus leading to further studies *in vivo*.

HRS inducing doses in fractionation setting were tested alone or with combination of chemotherapy in several mouse models and the results have not always been reflective of data obtained using cell cultures. For example one study, compared the effect of low dose ultra-fractionation schedule (0.4 Gy/fraction—126

fractions in six weeks; an approach to exploit the HRS) with the conventional fractionation schedule (1.68 Gy/fraction, 30 fractions in six weeks) of a total dose of 50.4 Gy for inhibiting A7 tumor growth in nude mice (26). Although, ultrafractionation resulted in a significant decrease in tumor growth delay, it also showed a significant increase of the top-up TCD<sub>50</sub> dose (the dose needed to cure 50% of animals) compared with conventional fractionation dose, but failed to prove the existence of HRS in *in vivo* (26). Thus, despite a pronounced HRS phenomenon observed *in vitro*, ultrafractionation appeared to be significantly less effective than conventional fractionation in the above nude mice xenograft model. The results from this study simply indicate that extrapolation of such data on single dose exposure or a few fractionated doses in *in vivo* is not always predictive of *in vitro* data and does not exclude the potential clinical value (27).

Low dose fractionation allows the delivery of a higher total radiation dose to the tumor for a better result as indicated in the studies below. In a mouse glioma tumor xenograft model, repeated irradiation with low dose (0.8 Gy 3 times/day  $\times$  4 days/wk  $\times$  2 wks, total dose of 19.2 Gy) was markedly more effective compared to a conventional fractionated dose schedule (2 Gy/day  $\times$  4 days/wk  $\times$  2 wks; total dose of 16 Gy) in inhibiting tumor growth (28). Similarly, Spring *et al.* (29) showed that LDFRT (0.5 Gy 2 times/day  $\times$  2 days/wk  $\times$  6 wks; total dose of 12 Gy) significantly prolonged tumor re-growth delay compared to a conventional fractionation dose schedule (2 Gy one fraction/day  $\times$  1 wk  $\times$  6 wks) in a SCCHN xenograft mouse model (29).

Recently, Tyagi *et al.* demonstrated the capability to deliver ten 0.2 Gy pulses in 8 mins [referred to as Pulsed Low-Dose Radiation (PLRT)] (30). This approach of dose-escalated PLRT was compared with standard radiation therapy (Std-RT), where 2 Gy fractions were delivered continuously in a single fraction in eight minutes, in an intracranial U87MG GBM nude mice tumor model (31). Both PLRT and Std-RT groups received treatments for 5 days/wk. One cohort of mice was treated with 20 Gy Std-RT or 20 Gy PLRT; a second cohort was treated with 30 Gy. Results showed that the mean survival was significantly better with 34.2 days for 30 Gy PLRT compared to 29 days with Std-RT, although there was no tumor cure in either of the groups.

Even though these results imply a minimally a better outcome when radiation is used alone as LDFRT in preclinical models, because of the existence of HRS at lower radiation doses as described above, there exists potential to benefit from the effects of chemotherapy when LDFRT is used in conjunction with chemotherapy. However, demonstration of efficacy of combination of chemotherapy with LDFRT in animal model(s) optimizing dose, time, and sequence is a critical prerequisite for a successful clinical translation.

Below we discuss three such studies in which combination of LDFRT or PLRT with chemotherapy has been used that substantiate potential opportunities for enhancing chemotherapy effects for better treatment outcome. (I) Complete tumor cure was demonstrated in the studies by Spring *et al.* (29), that evaluated the efficacy of LDFRT in potentiating tumoricidal properties of taxotere in SCCHN tumor xenograft animal model. Tumor regression was significant in all LDFRT groups. Mechanistic studies involving molecular analyses of resected tumor specimens showed an increase in Bax levels with an increase in cytochrome c release suggesting an apoptotic mode of cell death in LDFRT chemopotentialization of taxotere effects rather than clonogenic inhibition, albeit G2M cell cycle arrest by taxotere also appears to be an important sequencing

component of chemopotentialization. (II) PLRT in combination with Temozolamide (TMZ) was more effective in reducing tumor volume and normal tissue damage and improving survival compared to standard fractionation RT with TMZ in an orthotopic GBM xenograft murine model (32). Increased and differential vascularization and significantly fewer degenerating neurons were seen in normal brain after PLRT with TMZ compared to standard RT with TMZ. (III) Similarly, in an on-going study in a mouse ovarian cancer model, combination of LDFRT with paclitaxel showed significantly improved survival over paclitaxel alone or LDFRT alone. A similar trend was noted when cisplatin was combined with LDFRT in the treatment of ovarian cancer (33) as well as when TMZ was used with LDFRT in the treatment of GBM in mouse models (unpublished observations).

The above preclinical *in vivo* studies assessing the benefit of combining LDFRT or PLRT with chemotherapy demonstrating improved efficacy and survival as well as reducing normal tissue toxicity together with supporting mechanistic evidences provided adequate rationale for conducting safety and efficacy trials in the clinic as these studies might unlock novel treatment avenues for radio-resistant and/or aggressive tumors with poor clinical outcome (e.g., GBM and ovarian cancers). LDFRT can be exploited to potentiate the effect of chemotherapy for achieving maximum tumor cell killing with significantly reduced toxicity and a favorable clinical translation of the HRS phenomenon observed at low radiation doses to help overcome IRR at radiation doses above 0.6 Gy seen in standard fractionated chemo-radiotherapy regimen. In summary, there is strong pre-clinical evidence and mechanistic reasoning for using HRS low-doses of radiation to potentiate the effects of chemotherapy particularly in hyperfractionated settings.

#### ***HRS-inducing LDFRT as a potentiator of chemotherapy: clinical evidence***

Several clinical trials have been conducted to assess the benefit of combining LDFRT with standard chemotherapeutic agents for improved outcome (Table 2). Arnold *et al.* (34) studied LDFRT as a chemopotentializer of paclitaxel and carboplatin in 40 patients with locally advanced SCCHN. LDFRT was given in two doses of 0.80 Gy (based on the average dose that yielded maximal HRS in four SCCHN cell lines each on days 1 and 2, administered 4-6 hours apart, and the sequence was repeated on days 22 and 23. Definitive RT began three weeks after the last dose of chemotherapy and LDFRT. The combinations of LDFRT, carboplatin and paclitaxel were extremely well-tolerated, with toxicity comparable to that of carboplatin and paclitaxel

**Table 2.** Reported clinical trials combining LDFRT with chemotherapy in solid tumors.

| Clinical trial parameters | Induction regimen  |   | Phase I  |  |  |   | Phase II  |
|---------------------------|--|---|--|--|--|---|---|
|                           | Locally advanced SCCHN   | Recurrent ovarian fallopian tube/peritoneal cancers   | Locally advanced pancreatic or small bowel adenocarcinoma  | Stage III/IV endometrial carcinoma   | Recurrent/progressive GBM  | Stage IIA/B-III A breast cancer   | Recurrent NSCLC   |
| Design                    | Paclitaxel (225 mg/m <sup>2</sup> ), carboplatin (area under the curve of 6), and four 80-cGy fractions of radiotherapy (two each on days 1 and 2). This sequence was repeated on days 22 and 23 | One of three dose levels of docetaxel (20, 25, or 30 mg/m <sup>2</sup> ) weekly with concurrent LDFRT given as 60 cGy bid 2 days weekly for 6 weeks | Gemcitabine 1,250 mg/m <sup>2</sup> at 10 mg/m <sup>2</sup> /min on days 1 and 8 of a 3-week cycle. LDFRT at two dose levels: 60 cGy per fraction and 70 cGy per fraction on days 1, 2, 8, and 9 for 4 weeks | Six weekly cycles of FD-CDDP (40 mg/m <sup>2</sup> , maximum 70 mg IV) + LDFRT at 0.5 Gy/tx (total 3 Gy) and 0.75 Gy/tx (total 4.5 Gy) | LDFRT 0.3 Gy twice daily with cisplatin and fotemustine if progressing on temozolomide, or 0.4 Gy twice daily with temozolomide if recurrent | LDFRT 0.4 Gy/ per fraction, 2 fractions per day, for 2 days, every 21 days for 6-8 cycles) with non-pegylated liposomal doxorubicin and docetaxel | Pemetrexed (500 mg/m <sup>2</sup> IV) and concurrent LDFRT (40 cGy bid on days 1 and 2) was repeated fourfold every 21 days |
| Duration                  | 5 years  | 2 years   | 37 months  | 27 months  | 20 months  |   | 2 years   |
| Recruitment               | 40   | 13  | 10   | 12   | 26   | 10  | 19  |
| References                | Arnold et al. (34); Gleason Jr et al. (35)   | Kunos et al. (36)   | Regine et al. (37)   | Wrenn et al. (38)  | Balducci et al. (39)   | Nardone et al. (40)   | Mantini et al. (41)   |

LDFRT, Low Doses Fractionated Radiation Therapy.

alone in a similar patient cohort.

Recently, the Arnold group reported 5-year results of the above prospective Phase II SCCHN trial (35). After a median follow-up of 83 months, LRC was 80% and distant control was 77%. Out of 39 evaluable patients, 5-year OS, diseases specific survival (DSS), and PFS were 62%, 66%, and 58%, respectively. These data strongly indicate a favorable outcome compared to historical controls and excellent compliance with definitive therapy.

In the above trial, the status of p16 was evaluated, which is a validated marker for HPV status and an important predictor of response to various treatment modalities for SCCHN (42). Immunohistochemistry analysis of available 42 pre-treatment specimens showed 15 HPV positive (ten were oropharynx sub group) and 27 (seven were oropharynx subgroup) were negative. Of 15 patients with p16 positive tumors CR, PR, SD and SD were 5 (33.3%), 8 (53.3%) 1 (6.7%), and 1 (6.7%) respectively,

compared to 2 (7.4%), 18 (66.7%), 6 (22.2%) and no PD among 27 patients with p16 negative tumors ( $P=0.0616$ ), respectively. Similar results were also found in HPV positive oropharynx sub-group. Two-year OS was 93.3% for p16 positive patients compared to 73.08% in p16 negative patients ( $P=0.0252$ ); two-year PFS was 80% (p16 + ve) and 69.23% (p16 - ve). In oropharyngeal subgroup, the 2-year OS was 100% (p16 + ve) and 42.86% (p16 - ve) tumors respectively ( $P=0.001$ ). These results stress the point that p16 status can be an important predictor of response to LDFRT mediated chemopotential induction treatment similar to that seen in standard of care, in head and neck cancer treatment an observation recently described (43,44).

Based on the pre-clinical data (33), the Gynecology Oncology Group (GOG) conducted a feasibility study (36), of whole abdomen LDFRT for patients with recurrent epithelial ovarian fallopian tube, or peritoneal cancers along with weekly

**Table 3.** Open clinical trials combining LDFRT with chemotherapy in solid tumors.

| Clinical trial parameters     |   | Phase II                       |   |
|-------------------------------|---|--------------------------------|---|
| Site                          | Recurrent Anaplastic Astrocytoma and Glioblastoma Multiforme  | Recurrent and Inoperable SCCHN | Recurrent Unresectable Locally Advanced SCCHN   |
| Design                        | Temozolomide (150 to 200 mg per square meter for 5 days during each 28-day cycle). LDFRT 0.5 Gy of radiation therapy twice daily with the first six 28-day cycles of temozolomide | No description available       | Erbitux 400 mg/m <sup>2</sup> as a loading dose one week prior to radiation and taxotere, and then at 250 mg/m <sup>2</sup> given weekly on Mondays. Taxotere 20 mg/m <sup>2</sup> IV once a week on Mondays on weeks 2 to 7. LDFRT 0.5 Gy per fraction BID at least 6 hours apart on Tuesday and Wednesday of weeks 2 to 7 for a total dose of 12 Gy |
| Duration                      | 1 year  | Not available                  | 3.5 years   |
| Recruitment                   | 49  | 38                             | 35  |
| ClinicalTrials.gov identifier | NCT01466686   | NCT01820312                    | NCT01794845   |

LDFRT, Low Doses Fractionated Radiation Therapy.

treatment of docetaxel 25 mg/m<sup>2</sup>. LDFRT was delivered in 60 cGy fractions, twice daily for two days, with a minimum of 4 hr inter-fraction interval, starting on day 1 of each chemotherapy cycle. Three out of four patients completed therapy and none of the toxicities were dose limiting. Another phase I study (38), delivering once a week for six consecutive weeks of morning cisplatin followed 6-8 hours later by afternoon low dose-whole abdomen radiation therapy (LD-WART), enrolled 12 patients with optimally debulked Stage III/IV endometrial cancer. The results suggested feasibility of using LD-WART as a novel chemopotentiator to cisplatin in combination therapy as an adjuvant regimen (38). This trial showed no dose-limiting toxicities with follow-up that ranged from 4-36 months (median: 14 months). These data as well as the data from the GOG trial does indicate that 0.60 Gy/fraction was well tolerated.

Regine *et al.* (37) studied upper abdominal LDFRT given as a chemopotentiator for gemcitabine in patients with locally advanced pancreatic or small bowel adenocarcinoma. Gemcitabine was given at 1,250 mg/m<sup>2</sup> at 10 mg/m<sup>2</sup>/min on days 1 and 8 of a 3-week cycle. Low-dose fractionated radiotherapy was tested at two dose levels: 0.6 Gy and 0.7 Gy/fraction. Radiotherapy was given b.i.d. on days 1, 2, 8, and 9. Two of the four patients at dose level 0.7 Gy/fraction experienced dose-limiting toxicity, therefore 0.6 Gy/fraction was deemed the MTD.

Balducci *et al.* (39) reported a study of LDFRT and chemotherapy for recurrent or progressive GBM in 17 patients who had previously received radiotherapy and recurred: they received total LDFRT dose of 7.2 Gy in 0.3 Gy fractions with concomitant chemotherapy (TMZ and Fotemustine). LDFRT

regimen was well tolerated. In reality, a robust randomized clinical is warranted to establish as a new treatment modality for GBM patients with poor prognosis.

In recurrent NSCLC, Mantini *et al.* (41) found that LDFRT was safe when added to 500 mg/m<sup>2</sup> Pemetrexed as a 10-minute intravenous infusion on day 1 of a 21-day cycle, concurrent with LDFRT on days 1 and 2 at 0.4 Gy twice daily with each fraction given 5-6 hrs apart, and the median total dose was 6.40 Gy. LDFRT was also tested in combination with liposomal doxorubicin and docetaxel in stage IIA/B-IIIA breast cancer that led to higher histological response rates compared to the sequential application of the same two drugs (40).

There are three more clinical trials ongoing (<http://www.clinicaltrials.gov>), which are summarized in Table 3. Unfortunately, as with the trials discussed above, none of them is randomized for evaluating the efficacy of LDFRT using robust end-points such as survival or quality of life.

### Summary of hyperfractionation

- Over the years clear evidence has emerged from the cell culture studies on the existence of HRS and IRR phenomena that have provided adequate mechanistic rationale for using radiation dose in the HRS range to potentiate the effects of chemotherapy.
- Preclinical *in vivo* animal studies using mouse xenograft tumor models, as discussed above, assessing the benefit of combining LDFRT or PLRT with chemotherapy demonstrate improved efficacy and survival as well as a

reduction in normal tissue toxicity and have helped optimize dose, time, and sequence schedule in experimental setting and lead to clinical trials.

- Several Phase I/II clinical trials conducted in different cancer organ sites, such as SCCHN, GBM, ovarian, pancreatic, breast and lung cancers, are in process for an optimized LDFRT dose and schedule in order to potentiate the effects of chemotherapeutic drugs such as cisplatin, taxanes, TMZ, and also demonstrated improved efficacy.
- More randomized clinical trials are warranted to study the role of LDFRT as an adjuvant for chemotherapy in definite settings rather than induction regimen.

In conclusion, LDFRT has some very intriguing preclinical data, however, despite the fact that about ten clinical trials have been or are being performed, at present, it can be concluded that this technique appears to be relatively safe. Based on the reported as well as on-going clinical trials, it still remains unclear whether the patients can be benefited from the addition of LDFRT to chemotherapy and hence better designed prospective trials (randomized against chemotherapy-only controls, and with more robust endpoints such as survival and quality of life) must be conducted to ascertain the value of LDFRT in the management of solid tumors.

### Hypofractionation: novel windows of opportunity

To take advantage of the technological ability to deliver precision radiation therapy and to utilize the biological effects of a large dose per fraction as well as the smaller dose per fraction just described, hypofractionated radiation therapy can provide a different pathway of biological effects either used alone or combined with chemoradiotherapy. A potential advantage of hypofractionated radiation therapy, which makes it an attractive approach for the management of advanced cancers, is the reduction in treatment time and cost and reduced burden of frequent and numerous radiotherapy sessions.

Hypofractionated radiation therapy can be approached in two different ways: (I) is to consider  $\alpha/\beta$  ratio and Biologically Effective Dose (BED), where the “classical” concepts of repair, re-assortment, re-oxygenation and re-population (4-Rs) are applicable. This is a categorical approach for hypofractionated radiotherapy that uses 3 to 6 Gy dose fractions; (II) Hypofractionation schedule that uses above 8 Gy doses/fraction in radiotherapy, in which the biological changes different than the “classical” 4-Rs are felt to be applicable, generally known as high-dose hypofractionation radiation therapy (HDHRT). This section of the review will focus HDHRT with more detailed understanding of new radiobiology.

There are data to suggest that the use of HDHRT radiation

is effective as an alternative means of dose escalation with conventional fractionation treatment schedule. The results with HDHRT in the early-stage lung cancer population have thus far been very encouraging with local control rates up to 90% (45,46), being superior to the control rates obtained with conventionally fractionated radiation. Biologically, new mechanistic insights suggest that HDHRT may cause four unique effects that can be further exploited for sensitization. HDHRT can (I) cause non-targeted pharmacodynamics effects (such as intra-tumoral bystander as well as abscopal effects) mediated by TNF- $\alpha$ , TRAIL, PAR-4 and ceramide (47-49); (II) robustly induce tumor endothelial death at doses above 8-11 Gy (50); (III) increase host immune recognition of radiation-induced enhanced antigen presentation, such that a single fraction may incite an immune response that enhances the effects of radiation (51); and (IV) result in a better response of that tumors that are heterogeneous with different cell populations, whose clonal radiosensitivity considerably differ (52).

The interaction between HDHRT and hypoxia needs to more fully understood. The effects would depend in part on the initial hypoxic fraction, the dose size used and fractionation, as reoxygenation could occur. Brown *et al.* (53), Song *et al.* (54), suggest the need for drugs to treat the hypoxic fraction whereas Meyer *et al.* (55) suggest that reoxygenation and the selection of a dose at the “hypoxia transition zone” could overcome hypoxia. With other potential mechanism of action of HDHRT, as noted above, studies that determine changes in hypoxia including imaging and biomarkers of hypoxia, as well as studies to modify hypoxia and or use cytotoxic agents would be needed to dissect out the complexity of the effect of hypoxia. Another interesting consideration could be the use of conventional radiation therapy following single high dose or high dose in combination with chemotherapeutic drugs to improve the response of tumors to treatment. There are strong biological data to suggest that a large induction dose of radiation preceding conventional fractionated radiation therapy results in significantly greater tumor regression (56,57). However, high doses of radiation prescribed uniformly to large tumor volumes are generally associated with significant side effects and potentially serious late toxicity, which can take many years to be manifest. At this point in time, there is limited use of high-dose-per-fraction radiation to smaller targets, as in the case of SABR for T1-2N0 lung cancer. In patients with stage III lung cancer, high-dose-per-fraction radiation to the entire target volume is precluded due to normal tissue tolerance. Therefore, future approaches could combine the capability of new imaging and treatment technology for target selection, including novel approaches described next, including HDHRT and its biological properties.

### **Technical aspects of hypofractionated radiation therapy**

The challenges of hypofractionated radiotherapy for better treatment outcome primarily include development of optimal radiation dose delivery techniques. We provide a very brief account of technical development of SRS, SBRT and 3D lattice radiotherapy (LRT), with the understanding that high-dose rate brachytherapy with radionuclides or miniature X-ray source can also be an effective way of delivering highly localized radiation.

Traditionally SRS refers to single fraction stereotactic delivery of an intended ablative dose (58). The first full-scale successful radiosurgery system, Leksell Gamma Knife, was developed in the late 1960s. Since then its successful clinical utilization has established the foundations for intracranial radiosurgery and radiosurgery, in general. Following its success, a number of LINAC-based systems were developed since 1980s (59) and protons beams are also being used (60).

The concept of intracranial radiosurgery was first applied to other body sites in the early 1990s using modified conventional LINACs. The introduction of dedicated radiosurgery systems has widened the application, most noticeably from the early 2000s and clinical efficacy has been well demonstrated (61). In current terminology, SBRT refers to stereotactic body radiation treatments delivered in more than one fraction. While the term SBRT has been widely adopted, it is noteworthy that the difference between radiotherapy and radiosurgery is in the fractional-dose size that ostensibly leads to their differences in therapeutic effects—as a result of different radiobiological effects. The term stereotactic only indicates the method of target localization.

The goal of SABR is to administer a markedly higher dose to the treatment target volume without damaging the surrounding normal tissue thereby achieving enhanced local control and less normal tissue toxicity compared to conventional radiotherapy. The unique physical characteristics of traditional SRS are: high precision (sub-millimeter), highly-focused dose distribution (about a 10% dose fall-off per millimeter outside the treatment margin) and high dose (10 Gy and higher) (58).

In traditional SRS or SBRT, the coverage of prescribed dose to the treatment target volume is to be maximized. In contrast, the spatially fractionated high dose radiation therapy delivered in forms of spatially fractionated GRID radiotherapy (SFGRT) technique covers only partial tumor volume with the prescribed dose (48,49,62).

In the last decade, improvements in GRID design, ability to deliver higher tumor dose by improved target penetration along with reduced normal tissue damage as well as superior dosimetry have resulted in dramatic improvements in clinical responses

(62-67). Unnecessary high dose exposure of the surrounding normal tissue can be significantly reduced by reconfiguring the GRID treatment into a 3D GRID dose in form of LATTICE. We now define 3D GRID as LATTICE which is a new approach to spatially fractionated radiation that takes advantage of modern-era technology of SABR systems in a safer and efficient way (68). The difference in the dose delivery is shown at the URL (<http://assets.cureus.com/uploads/figure/file/538/13fig1.png>) published by Wu *et al.* (68). Using this technique, high doses of radiation are concentrated at vertices within the tumor volume, with drastically lower dose between vertices (peak-to-valley effect) and leaving anything outside of tumor volume minimally exposed. Because more pronounced radiation dose peaks and valleys are generated using LATTICE technique compared to 2D-GRID, it may be more radio-biologically effective, with lower radiation dose to adjacent normal tissues resulting in a reduction in normal tissue toxicity.

### **Hypofractionation and normal tissue toxicity**

The  $\alpha/\beta$  ratios derived from linear quadratic model of the radiation survival curve describes the effectiveness of the dose and is used to model cell survival at different conventional doses used in radiation therapy (69). A similar approach has also been adapted to model cell survival with the large doses for hypofractionation studies (70,71). However, this approach may overestimate tumor control. Because of the improvements in radiotherapy planning and delivery, targeting accuracy of radiation to the tumor is also improved with a reduction in surrounding normal tissue damage. It is feasible to use higher doses of radiation per fraction without inducing significant acute and late radiation induced toxicity with SABR. However, concerns still remain on the late toxicity with high dose hypofractionation and it must be emphasized that these may take many years or a decade or more to be seen. An intriguing concept for both technological limitations and capabilities and also for biological advantages is to consider irradiating only limited portions of the tumor and still achieve similar or better outcomes with SABR as discussed next.

When large doses of radiation are delivered to only a fraction of the target volume, scaling back on the irradiated tumor volume invariably results in a reduction of dose to the adjacent normal tissues. Such scaling back of target treatment volume may not compromise the benefits of high dose per fraction for better control because underlying radiobiological mechanisms of damage by large dose per fractions remain the same. SFGRT (2D-Grid) and now LATTICE (3D-Grid), results in a better dose distribution in tumor spatially rather than temporally,

which results in significantly improved sparing of normal tissue achieving a better tumor control.

Next we discuss the role of three underlying radiobiological mechanisms of bystander/abscopal effects, activation of immune system, and damage to endothelial cells, that might contributing to a better tumor control with SFGRT and LATTICE in salvage settings, however, needs randomized trials for definitive treatment practices.

### **High dose radiation-induces factors leading to bystander/abscopal effects**

Brooks *et al.* reported the first observation of radiation-induced non-targeted effects in a hamster model (72). Although evidences for these effects have accumulated over time, the exact mechanisms by which they cause tumor regression distant to site of irradiation remains somewhat speculative. A few major mechanistic categories have been proposed to account for abscopal effects based on studies involving different malignancies: immune system, cytokines and pseudo-abscopal effect (73).

Cell-cell communication appears to play an important role in mediating the bystander effect, and there may also be contributions from the transfers of soluble mediators generated in irradiated medium. It is most likely that multiple mechanisms are involved in bystander effects. The presence of gap junctions is not essential. Transfer of radiation-conditioned medium (RCM) from confluent cell culture is more effective, a phenomenon that is termed as “indirect radiation effects” (74-77). Irradiated cells may release clastogenic factors into serum that will induce chromosomal damage when transferred to cultured cells from unirradiated donors (78-80). In a study in rats, for example, clastogenic activity persisted in circulating plasma of irradiated animals for the 10-week duration of the study, and was not abrogated by diluting with non-irradiated serum. Serum irradiated *in vitro* was not clastogenic suggesting that these factors were released from the irradiated cells (81).

Although evidence for the presence of these factors has been accumulating over past decades, their exact nature as well as the mechanisms by which they cause the distant bystander effects (more of an abscopal effect) has proven elusive. One such mechanism might be through radiation-induced early genes and induction of cytokines. Indeed, TNF- $\alpha$  and TRAIL are directly involved in apoptosis and are induced by ionizing radiation (82-86). There is a demonstrated correlation of therapeutic efficacy following SFGRT with TNF- $\alpha$  induction in the serum obtained from these patients as well as ceramide production (48,49).

For SFGRT, the “bystander effect” is within the GRID irradiated tumor volume that falls directly under shielded regions (low-dose regions) of the GRID. Bystander factors, such as

TNF- $\alpha$  shown by Sathishkumar *et al.* (49) and Shareef *et al.* (47); TRAIL shown by Shareef *et al.* (47) and ceramide shown by Sathishkumar *et al.* (48) are induced in cells that are under the open field of the high-dose GRID areas and are hypothesized to be responsible for initiating the cell death cascade both in the epithelial and endothelial compartments of the tumor micro-environment. Recent reports have demonstrated the presence of radiation-induced signal transduction leading to significant DNA damage and cellular stress (87,88). In addition to the bystander effect within the GRID-irradiated tumor, Peters *et al.* (3) reported that there is robust “abscopal effect” in distant tumors or metastatic lesions that are not irradiated or treated and has been reported clinically with the use of large doses (89).

In this respect, recently using SFGRT we found both bystander and abscopal effects in mice bearing A549 lung adenocarcinoma xenograft contra-lateral tumors (90). Maximal abscopal effect was observed in unirradiated right tumor when mice was exposed to 15 Gy SFGRT followed by 5 fractions of 2 Gy to the left tumor suggesting that the abscopal effect can be amplified by sequential combination of SFGRT with conventional fractionation. More recently, using LATTICE therapy we obtained similar results in mice bearing syngenic Lewis Lung Carcinoma (LLC) contra-lateral tumors (91). These findings strongly suggest that SFGRT is more potent in eliciting evident abscopal effect in the un-irradiated tumor than conventional dosimetric approaches.

### **High dose radiation activates immune system**

There are quite a few reports that support the important role of immune factors in mediating the abscopal effects (92,93). In contrast to the generally believed notion that radiation therapy is immunosuppressive, recent reports indicate ablative high dose radiation therapy could activate immune system and reduce the primary tumor burden as well as distant metastasis (51,94). These effects were mediated by radiation therapy induced disruption of physical and immunologic barriers, stimulation of danger signaling pathways, increase in dendritic cells cross-presentation of tumor antigen, and possibly reversal of T-cell unresponsiveness in tumor-bearing hosts, leading to a rejection of local and distant tumors (51). Subsequently these authors demonstrated that IFN- $\alpha/\beta$  produced by tumor-infiltrating myeloid cells in an autocrine fashion is required to endow tumor-infiltrating dendritic cells with T-cell cross-priming capacity following local RT; however, T cells do not need to bear the type I IFN receptor to mediate tumor rejection (94). Together, these results score the importance of cytotoxic T-cell mediated antitumor immunity that mediates tumor regression. Our unpublished results show that RCM obtained from lymphoblasts

is able to induce killing of lung cancer (A549) cells, suggesting that the immune factors in addition to cytokines and ceramide pathway may be involved. However, in our contra-lateral tumor xenograft athymic nude mice, we observed significant bystander and abscopal effects indicating that not only the T-cell mediated immune factors but also humoral immunity may play an important role in the radiation-induced abscopal effects. These observations suggest potential therapeutic role for immune factors.

Lee *et al.* (51) reported that reduction of tumor burden after ablative radiation depends largely on T-cell responses as it dramatically increases T-cell priming in draining lymphoid tissues, leading to reduction/eradication of the primary tumor or distant metastasis in a CD8(+) T cell-dependent fashion. Interestingly, this study observed that ablative radiation-initiated immune responses and tumor reduction are abrogated by conventional fractionated RT or adjuvant chemotherapy (if given after a week of single ablative dose) but greatly amplified by local immunotherapy. However, in SFGRT settings we observed significant enhanced response when the high dose radiation was followed by fractionated 2 Gy fractions (given after 24 hrs), implying that spatial fractionation of radiation delivery might activate immune factors that can synergize with the conventional fractionated radiation. These results strongly argue for more detailed investigations to elucidate the role of immune factors in radiation therapy.

#### **High dose radiation induces damage to endothelium**

Engagement of the vascular component in tumor response to radiation therapy has been a topic of interest in recent literature. However, in addition to release of cytokines, impaired blood vessel formation and induction of endothelial cell death in tumors not exposed to radiation have been demonstrated to play a role in abscopal effect (95). Endothelial cells generate 20-fold more of a unique form of acid sphingomyelinase (ASMase), termed Secretory ASMase, than any other cell type in the body. Secretory ASMase activation is required for ionizing radiation to kill endothelium (96), as endothelium in lung, gut, and brain are totally resistant to radiation-induced apoptotic death in the absence of ASMase. Garcia-Barros *et al.* (50) have postulated that high dose radiation-induced damage (15 Gy) to the endothelial cells could convert Potentially Lethal Damage (PLD) in tumor cells and cancer stem cells to lethal damage resulting in tumor cell death. Animal studies have shown that radiation at doses higher than 10 Gy induces endothelial apoptosis by activation of acid sphingomyelinase (ASMase) and ceramide generation (50,96-99); these effects that are not observed with conventional radiation doses. Findings

by Garcia-Barros *et al.* (50) suggest that high-dose radiation-induced tumor regression can be entirely dependent on tumor endothelium apoptosis since these effects were abolished in ASMase knockout animals implanted with functional ASMase MCA/129 fibrosarcomas and B16F1 melanomas and restored upon bone marrow transplantation of ASMase functional stem cells. Further, elevated sphingomyelinase activity and ceramide concentration in the serum of patients undergoing high dose spatially fractionated radiation treatment were observed (48). Our unpublished findings in A549 xenografts showed increased elevation of ceramide in the serum of nude mice treated with SFGRT (90).

Although direct killing effect of tumor cells with SFGRT occurs, it cannot completely account for tumor regression observed after treatment. Recently, we demonstrated that treatment of 11 patients with various types of cancer with 15 Gy SFGRT therapy followed by multiple consecutive doses of 2 Gy each led to an increase in the activity of ASMase in serum and a corresponding elevation in the concentration of LDL-enriched ceramide. These changes correlated with the clinical outcome of the treatment, as they were found only in the 76% of patients with CR or PR and not in non-responders (48). It is evident that there is a biologic/therapeutic consequence of this response, whereby high single dose radiotherapy requires ceramide-driven endothelial apoptosis for tumor cure (50,100). This observation has broad implications for cancer treatment and is a subject of active debate in the field, as it is generally believed that radiation therapy works by partly targeting tumor stem cells and it is unclear which components of tumor microenvironment play important role in radiation cure.

There exists data on ceramide production, its relation to endothelial apoptosis and induction of abscopal regression of distant tumor with radiation exposure, however, there is little or any information available on the impact of negative regulators of ceramide pathway in radioresistance/radiosensitivity, their association with release of cytokines, and finally any possible cross-talks during cellular events associated with abscopal phenomena.

#### **Hypofractionation and hypoxia**

Tumor hypoxia has been observed in many human cancers and has been a major impediment for the success of radiotherapy. Generally, the phenomenon of re-oxygenation of hypoxic cells between several fractions of conventionally fractionated radiation therapy is considered to increase the sensitivity of the cells that were previously hypoxic. With the encouraging results using SABR or other hypofractionation strategies, this

is a point of considerable debate whether the issue of hypoxia under such therapy settings. Taking into account several factors such as the potential over-estimation of cell killing and tumor control by the linear quadratic model at large doses, high dose hypofractionation has actually resulted in greater than expected tumor control. It is possible that single dose hypofractionation induced specific mechanisms abate hypoxia, or that the extreme ablative doses currently used in many SABR protocols are already high enough to overcome hypoxic radioresistance or both. The latter hypothesis implies that concurrent strategies (such as hypoxic cytotoxin) targeted directly at hypoxic cells might improve the therapeutic ratio of SABR and allow clinicians to treat with a larger fraction in the patient population.

Fractional doses in hypofractionation schemes vary significantly in clinical practice, from 3 Gy/fraction to 20 Gy/fraction. There are a number of processes that will be effected by dose size and fractionation that could be exploited, including changes in the “4-R’s” (repair, repopulation, redistribution and reoxygenation), consequence of endothelial damage (which could worsen hypoxia) or tumor shrinkage (which could lessen hypoxia) and impact of the high dose on factors secreted by the tumor.

An example of the latter comes from our unpublished results (101). In two lung cancer cell lines, we observed that conditioned media collected from 10 Gy-irradiated hypoxic A549 cells (H-RCM) showed highly reduced cell proliferation effect on normoxic A549 cells when compared to media collected from irradiated normoxic A549 cells (N-RCM). Interestingly, with H-RCM obtained from 10 Gy irradiated hypoxic H-460 cells showed a significantly decreased cell proliferation in H460 cells but such reduced cell proliferation was absent with H-RCM obtained from 2 Gy irradiated hypoxic H-460 cells (101). This suggests that oxygen may potentially negate bystander effect. Nonetheless more data are needed, including modeling that would help define the potential complexities, for example, one recently published that aims to account for intercellular signaling (102).

How to best take advantage of the high dose effect but also not damage normal tissue remains to be established. This could include partial treatment of the tumor to high dose using a variety of technique such as the high-dose LATTICE approach. That might have positive effects on damaging the endothelial compartment and/or immune activation. Another important aspect that is not discussed in detail could be differential effect of hypofractionation on cancer stem cells.

### *Summary of new biology of hypofractionation*

- Hypofractionated radiotherapy (>12 Gy) is an attractive

approach in the management of cancer although long-term toxicity in patients with curative tumors remains to be evaluated as series mature.

- Success of hypofractionated radiotherapy is dependent on its ability to deliver a markedly higher dose to the target volume without damage to surrounding normal tissue. Over the last decade, technological improvement in terms of dose delivery and intra-tumoral spatial distribution of dose seems to have been achieved, with long-term data needed to see if the spatial distribution of dose can reduce normal tissue injury and maintain or even improve tumor control.
- The underlying radiobiological mechanisms for improved outcome obtained by high dose hypofractionated radiation therapy could be multifactorial, which include differential endothelial and cancer stem cell killing, overcoming hypoxic radioresistance, activation of complex immunological pathways, and bystander/abscopal tumoricidal effects, resulting in improved treatment outcome (Figure 2).
- There appears to be opportunities to achieve better response of tumors to high dose fractionated radiotherapy by the use of chemotherapeutic drugs or hypoxic cell radiosensitizers.
- While speculative, the use of spatial fractionation in the form of 2D SFGRT and 3D LATTICE in combination with conventional fractionated radiation therapy or chemotherapeutic drugs or hypoxic cytotoxins might be able to counteract the effects of hypoxia with simultaneous normal tissue sparing. In conclusion, ablative hypofractionation schemes are effective in certain solid tumors that may take advantage of new aspects of radiation biology by involving certain components of tumor microenvironment such as effects on vasculature as well as immunologic modulation. SFGRT provided some mechanistic insights pre-clinically as well as from patients (who received SFGRT as salvage therapy), however, to bring SFGRT in the mainstream needs more well designed trials. Lattice (3D-Grid) has some promise in the main realm of definitive treatment, however, this approach warrants robust randomized trials. Overall, it is the ablative dose (delivery approaches may differ with or without homogenous dose distribution) that needs further exploration based on clinical observation of its efficacy and preclinical studies.

### **Overall conclusions**

While hyper- and hypo-fractionation are presented as distinctly

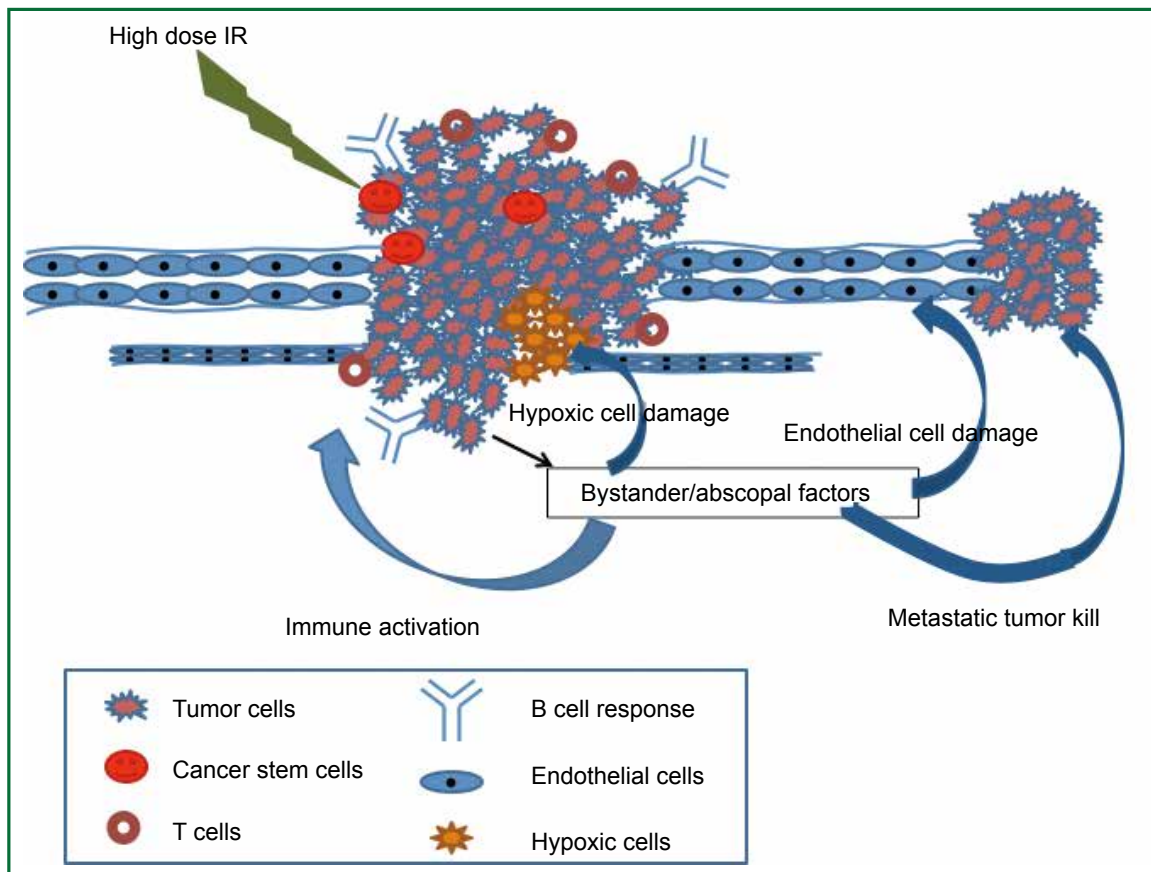


**Figure 2.** Impact of high-dose ablative RT on tumor micro-environment components. High-dose ablative RT given in lattice (2 vertices) to the tumor induces bystander/abscopal factors, endothelial cell death coupled with immune activation. The underlying radiobiological mechanisms for improved outcome obtained by high dose hypofractionated radiation therapy could be multifactorial. The differential effects on tumor endothelium and cancer stem cells could be responsible for this enhanced response. Further, complex immunological pathways could be linked to high dose radiation-induced mechanisms. All of these pathways could be affected by the bystander/abscopal factors released from the tumor following spatially fractionated radiation therapy. An animation of these events can be found at URL: <http://youtu.be/KvQ8z91J6A8>.

different, a key point to emphasize is that radiation fraction size and schedule have properties that can be exploited using radiation alone and in combination with immunotherapy, molecular target treatment and cytotoxic chemotherapy. Improvements in imaging and technology of treatment delivery can allow improvement in anatomical targeting and also in treating based on the physiological and biological processes as they present and evolve. New techniques such as LATTICE may be able to take advantage of heterogeneous dose delivery.

While there is a good deal of new and exciting data there is much research to do and, of course, the ultimate proof will be from well-designed clinical trials. Radiation therapy and radiation biology are far from static and with the ability for precision targeting and dose delivery, radiation “as a drug” can have a major impact in multi-modality cancer treatment.

## Acknowledgements

Authors acknowledge Dr. Bhadrasain Vikram for critical reading and suggestions.

*Disclosure:* The authors declare no conflict of interest.

## References

1. Delaney G, Jacob S, Featherstone C, et al. The role of radiotherapy in cancer treatment: estimating optimal utilization from a review of evidence-based clinical guidelines. *Cancer* 2005;104:1129-37.
2. Liu FF; workshop participants, Okunieff P, Bernhard EJ, et al. Lessons learned from radiation oncology clinical trials. *Clin Cancer Res* 2013;19:6089-100.
3. Peters ME, Shareef MM, Gupta S, et al. Potential Utilization of Bystander/

- Abscopal-Mediated Signal Transduction Events in the Treatment of Solid Tumors. *Current Signal Transduction Therapy* 2007;2:129-43.
4. Feinendegen LE. Evidence for beneficial low level radiation effects and radiation hormesis. *Br J Radiol* 2005;78:3-7.
  5. Brenner DJ, Doll R, Goodhead DT, et al. Cancer risks attributable to low doses of ionizing radiation: assessing what we really know. *Proc Natl Acad Sci U S A* 2003;100:13761-6.
  6. Joiner MC. Induced radioresistance: an overview and historical perspective. *Int J Radiat Biol* 1994;65:79-84.
  7. Lambin P, Marples B, Fertl B, et al. Hypersensitivity of a human tumour cell line to very low radiation doses. *Int J Radiat Biol* 1993;63:639-50.
  8. Wouters BG, Skarsgard LD. The response of a human tumor cell line to low radiation doses: evidence of enhanced sensitivity. *Radiat Res* 1994;138:S76-80.
  9. Marples B, Wouters BG, Collis SJ, et al. Low-dose hyper-radiosensitivity: a consequence of ineffective cell cycle arrest of radiation-damaged G2-phase cells. *Radiat Res* 2004;161:247-55.
  10. Marples B, Wouters BG, Joiner MC. An association between the radiation-induced arrest of G2-phase cells and low-dose hyper-radiosensitivity: a plausible underlying mechanism? *Radiat Res* 2003;160:38-45.
  11. Short S, Mayes C, Woodcock M, et al. Low dose hypersensitivity in the T98G human glioblastoma cell line. *Int J Radiat Biol* 1999;75:847-55.
  12. Chendil D, Oakes R, Alcock RA, et al. Low dose fractionated radiation enhances the radiosensitization effect of paclitaxel in colorectal tumor cells with mutant p53. *Cancer* 2000;89:1893-900.
  13. Enns L, Bogen KT, Wizniak J, et al. Low-dose radiation hypersensitivity is associated with p53-dependent apoptosis. *Mol Cancer Res* 2004 Oct;2:557-66.
  14. Joiner MC, Johns H. Renal damage in the mouse: the response to very small doses per fraction. *Radiat Res* 1988;114:385-98.
  15. Dey S, Spring PM, Arnold S, et al. Low-dose fractionated radiation potentiates the effects of Paclitaxel in wild-type and mutant p53 head and neck tumor cell lines. *Clin Cancer Res* 2003;9:1557-65.
  16. Short SC, Mitchell SA, Boulton P, et al. The response of human glioma cell lines to low-dose radiation exposure. *Int J Radiat Biol* 1999;75:1341-8.
  17. Skov KA. Radioresponsiveness at low doses: hyper-radiosensitivity and increased radioresistance in mammalian cells. *Mutat Res* 1999;430:241-53.
  18. Joiner MC, Marples B, Lambin P, et al. Low-dose hypersensitivity: current status and possible mechanisms. *Int J Radiat Oncol Biol Phys* 2001;49:379-89.
  19. Short SC, Kelly J, Mayes CR, et al. Low-dose hypersensitivity after fractionated low-dose irradiation in vitro. *Int J Radiat Biol* 2001;77:655-64.
  20. Shareef MM, Brown B, Shajahan S, et al. Lack of P-glycoprotein expression by low-dose fractionated radiation results from loss of nuclear factor-kappaB and NF-Y activation in oral carcinoma cells. *Mol Cancer Res* 2008;6:89-98.
  21. Gupta S, Koru-Sengul T, Arnold SM, et al. Low-dose fractionated radiation potentiates the effects of cisplatin independent of the hyper-radiation sensitivity in human lung cancer cells. *Mol Cancer Ther* 2011;10:292-302.
  22. Carrier F, Diss E, Nalobothula N, et al. The Histone Deacetylase Inhibitor Vorinostat Induces Hyper-radiosensitivity (HRS) In P53 Wild Type Glioblastoma Cells. In *The 53rd Annual Meeting of American Society for Radiation Oncology*. 2011. Miami Beach, FL: ASTRO.
  23. Bakkenist CJ, Kastan MB. DNA damage activates ATM through intermolecular autophosphorylation and dimer dissociation. *Nature* 2003;421:499-506.
  24. Suzuki K, Kodama S, Watanabe M. Low-dose radiation effects and intracellular signaling pathways. *Yakugaku Zasshi* 2006;126:859-67.
  25. Tichý A, Zászkodová D, Rezacová M, et al. Gamma-radiation-induced ATM-dependent signalling in human T-lymphocyte leukemic cells, MOLT-4. *Acta Biochim Pol* 2007;54:281-7.
  26. Krause M, Hessel F, Wohlfarth J, et al. Ultrafractionation in A7 human malignant glioma in nude mice. *Int J Radiat Biol* 2003;79:377-83.
  27. Krause M, Joiner M, Baumann M. Ultrafractionation in human malignant glioma xenografts. *Int J Cancer* 2003;107:333; author reply 334.
  28. Beauchesne PD, Bertrand S, Branche R, et al. Human malignant glioma cell lines are sensitive to low radiation doses. *Int J Cancer* 2003;105:33-40.
  29. Spring PM, Arnold SM, Shajahan S, et al. Low dose fractionated radiation potentiates the effects of taxotere in nude mice xenografts of squamous cell carcinoma of head and neck. *Cell Cycle* 2004;3:479-85.
  30. Tyagi N, Yang K, Sandhu R, et al. External beam pulsed low dose radiotherapy using volumetric modulated arc therapy: planning and delivery. *Med Phys* 2013;40:011704.
  31. Dilworth JT, Krueger SA, Dabjan M, et al. Pulsed low-dose irradiation of orthotopic glioblastoma multiforme (GBM) in a pre-clinical model: effects on vascularization and tumor control. *Radiother Oncol* 2013;108:149-54.
  32. Lee DY, Chunta JL, Park SS, et al. Pulsed versus conventional radiation therapy in combination with temozolomide in a murine orthotopic model of glioblastoma multiforme. *Int J Radiat Oncol Biol Phys* 2013;86:978-85.
  33. Modesitt SC, Gupta S, Brandon J, et al. Low dose fractionated radiation as a chemopotentiator for in vitro and in vivo ovarian cancer models. *Proc Amer Assoc Cancer Res* 2005;46:abstr 4748.
  34. Arnold SM, Regine WF, Ahmed MM, et al. Low-dose fractionated radiation as a chemopotentiator of neoadjuvant paclitaxel and carboplatin for locally advanced squamous cell carcinoma of the head and neck: results of a new treatment paradigm. *Int J Radiat Oncol Biol Phys* 2004;58:1411-7.
  35. Gleason JF Jr, Kudrimoti M, Van Meter EM, et al. Low-dose fractionated radiation with induction chemotherapy for locally advanced head and neck cancer: 5 year results of a prospective phase II trial. *Int J Radiat Oncol Biol Phys* 2013;2:35-42.
  36. Kunos CA, Sill MW, Buekers TE, et al. Low-dose abdominal radiation as a docetaxel chemosensitizer for recurrent epithelial ovarian cancer: a phase I study of the Gynecologic Oncology Group. *Gynecol Oncol* 2011;120:224-8.
  37. Regine WF, Hanna N, Garofalo MC, et al. Low-dose radiotherapy as a chemopotentiator of gemcitabine in tumors of the pancreas or small bowel: a phase I study exploring a new treatment paradigm. *Int J Radiat Oncol Biol Phys* 2007;68:172-7.
  38. Wrenn DC, Saigal K, Lucci JA 3rd, et al. A Phase I Study using low-dose fractionated whole abdominal radiotherapy as a chemopotentiator to

- full-dose cisplatin for optimally debulked stage III/IV carcinoma of the endometrium. *Gynecol Oncol* 2011;122:59-62.
39. Balducci M, Chiesa S, Diletto B, et al. Low-dose fractionated radiotherapy and concomitant chemotherapy in glioblastoma multiforme with poor prognosis: a feasibility study. *Neuro Oncol* 2012;14:79-86.
40. Nardone L, Valentini V, Marino L, et al. A feasibility study of neo-adjuvant low-dose fractionated radiotherapy with two different concurrent anthracycline-docetaxel schedules in stage IIA/B-IIIa breast cancer. *Tumori* 2012;98:79-85.
41. Mantini G, Valentini V, Meduri B, et al. Low-dose radiotherapy as a chemopotentiator of a chemotherapy regimen with pemetrexed for recurrent non-small-cell lung cancer: a prospective phase II study. *Radiother Oncol* 2012;105:161-6.
42. Silver NL, Arnold S, Gleason JF, et al. p16 status predicts response to low dose fractionated radiation as a chemopotentiator of neoadjuvant chemotherapy for locally advanced squamous cell carcinoma of the head and neck. In 8th International Conference on Head and Neck Cancer. 2012. Toronto, Ontario, Canada: American Head & Neck Society.
43. Ang KK, Sturgis EM. Human papillomavirus as a marker of the natural history and response to therapy of head and neck squamous cell carcinoma. *Semin Radiat Oncol* 2012;22:128-42.
44. Snow AN, Laudadio J. Human papillomavirus detection in head and neck squamous cell carcinomas. *Adv Anat Pathol* 2010;17:394-403.
45. Baumann P, Nyman J, Hoyer M, et al. Outcome in a prospective phase II trial of medically inoperable stage I non-small-cell lung cancer patients treated with stereotactic body radiotherapy. *J Clin Oncol* 2009;27:3290-6.
46. Fakiris AJ, McGarry RC, Yiannoutsos CT, et al. Stereotactic body radiation therapy for early-stage non-small-cell lung carcinoma: four-year results of a prospective phase II study. *Int J Radiat Oncol Biol Phys* 2009;75:677-82.
47. Shareef MM, Cui N, Burikhanov R, et al. Role of tumor necrosis factor- $\alpha$  and TRAIL in high-dose radiation-induced bystander signaling in lung adenocarcinoma. *Cancer Res* 2007;67:11811-20.
48. Sathishkumar S, Boyanovsky B, Karakashian AA, et al. Elevated sphingomyelinase activity and ceramide concentration in serum of patients undergoing high dose spatially fractionated radiation treatment: implications for endothelial apoptosis. *Cancer Biol Ther* 2005;4:979-86.
49. Sathishkumar S, Dey S, Meigooni AS, et al. The impact of TNF- $\alpha$  induction on therapeutic efficacy following high dose spatially fractionated (GRID) radiation. *Technol Cancer Res Treat* 2002;1:141-7.
50. Garcia-Barros M, Paris F, Cordon-Cardo C, et al. Tumor response to radiotherapy regulated by endothelial cell apoptosis. *Science* 2003;300:1155-9.
51. Lee Y, Auh SL, Wang Y, et al. Therapeutic effects of ablative radiation on local tumor require CD8<sup>+</sup> T cells: changing strategies for cancer treatment. *Blood* 2009;114:589-95.
52. Bao S, Wu Q, McLendon RE, et al. Glioma stem cells promote radioresistance by preferential activation of the DNA damage response. *Nature* 2006;444:756-60.
53. Brown JM, Diehn M, Loo BW Jr. Stereotactic ablative radiotherapy should be combined with a hypoxic cell radiosensitizer. *Int J Radiat Oncol Biol Phys* 2010;78:323-7.
54. Song CW, Levitt SH, Park H. Response to "tereotactic ablative radiotherapy in the framework of classical radiobiology: response to Drs. Brown, Diehn, and Loo." (*Int J Radiat Oncol Biol Phys* 2011;79:1599-1600) and "influence of tumor hypoxia on stereotactic ablative radiotherapy (SABR): response to Drs. Mayer and Timmerman." *Int J Radiation Oncol Biol Phys* 2011;78:1600). *Int J Radiat Oncol Biol Phys* 2011;81:1193; author reply 1193-4.
55. Meyer J, Timmerman R. Stereotactic ablative radiotherapy in the framework of classical radiobiology: response to Drs. Brown, Diehn, and Loo. *Int J Radiat Oncol Biol Phys* 2011;79:1599-600; author reply 1600.
56. Schenken LL, Poulakos L, Hagemann RF. Responses of an experimental solid tumour to irradiation: A comparison of modes of fractionation. *Br J Cancer* 1975;31:228-36.
57. Sakamoto K, Sakka M. The effect of bleomycin and its combined effect with radiation on murine squamous carcinoma treated in vivo. *Br J Cancer* 1974;30:463-8.
58. Phillips MH, Stelzer KJ, Griffin TW, et al. Stereotactic radiosurgery: a review and comparison of methods. *J Clin Oncol* 1994;12:1085-99.
59. Thariat J, Hannoun-Levi JM, Sun Myint A, et al. Past, present, and future of radiotherapy for the benefit of patients. *Nat Rev Clin Oncol* 2013;10:52-60.
60. Levin WP, Kooy H, Loeffler JS, et al. Proton beam therapy. *Br J Cancer* 2005;93:849-54.
61. Kavanagh BD, Timmerman RD. Stereotactic radiosurgery and stereotactic body radiation therapy: an overview of technical considerations and clinical applications. *Hematol Oncol Clin North Am* 2006;20:87-95.
62. Mohiuddin M, Fujita M, Regine WF, et al. High-dose spatially-fractionated radiation (GRID): a new paradigm in the management of advanced cancers. *Int J Radiat Oncol Biol Phys* 1999;45:721-7.
63. Meigooni AS, Parker SA, Zheng J, et al. Dosimetric characteristics with spatial fractionation using electron grid therapy. *Med Dosim* 2002;27:37-42.
64. Reiff JE, Huq MS, Mohiuddin M, et al. Dosimetric properties of megavoltage grid therapy. *Int J Radiat Oncol Biol Phys* 1995;33:937-42.
65. Mohiuddin M, Curtis DL, Grizos WT, et al. Palliative treatment of advanced cancer using multiple nonconfluent pencil beam radiation. A pilot study. *Cancer* 1990;66:114-8.
66. Huhn JL, Regine WF, Valentino JP, et al. Spatially fractionated GRID radiation treatment of advanced neck disease associated with head and neck cancer. *Technol Cancer Res Treat* 2006;5:607-12.
67. Neuner G, Mohiuddin MM, Vander Walde N, et al. High-dose spatially fractionated GRID radiation therapy (SFGRT): a comparison of treatment outcomes with Cerrobend vs. MLC SFGRT. *Int J Radiat Oncol Biol Phys* 2012;82:1642-9.
68. Wu X, Ahmed MM, Wright J, et al. On Modern Technical Approaches of Three-Dimensional High-Dose Lattice Radiotherapy (LRT). *Cureus* 2010. doi: 10.7759/cureus.9.
69. Williams MV, Denekamp J, Fowler JF. A review of alpha/beta ratios for experimental tumors: implications for clinical studies of altered fractionation. *Int J Radiat Oncol Biol Phys* 1985;11:87-96.

70. Joiner MC. A simple alpha/beta-independent method to derive fully isoeffective schedules following changes in dose per fraction. *Int J Radiat Oncol Biol Phys* 2004;58:871-5.
71. Hoban PW, Jones LC, Clark BG. Modeling late effects in hypofractionated stereotactic radiotherapy. *Int J Radiat Oncol Biol Phys* 1999;43:199-210.
72. Brooks AL, Benjamin SA, McClellan RO. Toxicity of 90Sr-90Y in Chinese hamsters. *Radiat Res* 1974;57:471-81.
73. Kaminski JM, Shinohara E, Summers JB, et al. The controversial abscopal effect. *Cancer Treat Rev* 2005;31:159-72.
74. Lyng FM, Seymour CB, Mothersill C. Early events in the apoptotic cascade initiated in cells treated with medium from the progeny of irradiated cells. *Radiat Prot Dosimetry* 2002;99:169-72.
75. Lyng FM, Seymour CB, Mothersill C. Initiation of apoptosis in cells exposed to medium from the progeny of irradiated cells: a possible mechanism for bystander-induced genomic instability? *Radiat Res* 2002;157:365-70.
76. Hall EJ. The bystander effect. *Health Phys* 2003;85:31-5.
77. Hall EJ, Hei TK. Genomic instability and bystander effects induced by high-LET radiation. *Oncogene* 2003;22:7034-42.
78. Goh K, Sumner H. Breaks in normal human chromosomes: are they induced by a transferable substance in the plasma of persons exposed to total-body irradiation? *Radiat Res* 1968;35:171-81.
79. Hollowell JG Jr, Littlefield LG. Chromosome damage induced by plasma of x-rayed patients: an indirect effect of x-ray. *Proc Soc Exp Biol Med* 1968;129:240-4.
80. Sharpe HB, Scott D, Dolphin GW. Chromosome aberrations induced in human lymphocytes by x-irradiation in vitro: the effect of culture techniques and blood donors on aberration yield. *Mutat Res* 1969;7:453-61.
81. Faguet GB, Reichard SM, Welter DA. Radiation-induced clastogenic plasma factors. *Cancer Genet Cytogenet* 1984;12:73-83.
82. Ahmed MM, Sells SF, Venkatasubbarao K, et al. Ionizing radiation-inducible apoptosis in the absence of p53 linked to transcription factor EGR-1. *J Biol Chem* 1997;272:33056-61.
83. Hallahan DE, Spriggs DR, Beckett MA, et al. Increased tumor necrosis factor alpha mRNA after cellular exposure to ionizing radiation. *Proc Natl Acad Sci U S A* 1989;86:10104-7.
84. Hallahan DE, Haimovitz-Friedman A, Kufe DW, et al. The role of cytokines in radiation oncology. *Important Adv Oncol* 1993:71-80.
85. Hallahan DE, Virudachalam S, Sherman ML, et al. Tumor necrosis factor gene expression is mediated by protein kinase C following activation by ionizing radiation. *Cancer Res* 1991;51:4565-9.
86. Unnithan J, Macklis RM. TRAIL induction by radiation in lymphoma patients. *Cancer Invest* 2004;22:522-5.
87. Asur R, Butterworth KT, Penagaricano JA, et al. High dose bystander effects in spatially fractionated radiation therapy. *Cancer Lett* 2013. [Epub ahead of print].
88. Asur RS, Sharma S, Chang CW, et al. Spatially fractionated radiation induces cytotoxicity and changes in gene expression in bystander and radiation adjacent murine carcinoma cells. *Radiat Res* 2012;177:751-65.
89. Konoeda K. Therapeutic efficacy of pre-operative radiotherapy on breast carcinoma: in special reference to its abscopal effect on metastatic lymph-nodes. *Nihon Gan Chiryo Gakkai Shi* 1990;25:1204-14.
90. Gupta S, Zagurovskaya M, Wu X, et al. Spatially Fractionated Grid High-dose radiation-induced tumor regression in A549 lung adenocarcinoma xenografts: cytokines and ceramide regulators balance in abscopal phenomena. *Sylvester Comprehensive Cancer Center*, 2014:20.
91. Kanagavelu S, Gupta S, Wu X, et al. In vitro and in vivo effects of lattice radiation therapy on local and distant lung cancer. *Sylvester Comprehensive Cancer Center*, 2014:19.
92. Dewan MZ, Galloway AE, Kawashima N, et al. Fractionated but not single-dose radiotherapy induces an immune-mediated abscopal effect when combined with anti-CTLA-4 antibody. *Clin Cancer Res* 2009;15:5379-88.
93. Ilnytsky Y, Koturbash I, Kovalchuk O. Radiation-induced bystander effects in vivo are epigenetically regulated in a tissue-specific manner. *Environ Mol Mutagen* 2009;50:105-13.
94. Burnette BC, Liang H, Lee Y, et al. The efficacy of radiotherapy relies upon induction of type I interferon-dependent innate and adaptive immunity. *Cancer Res* 2011;71:2488-96.
95. Camphausen K, Moses MA, Ménard C, et al. Radiation abscopal antitumor effect is mediated through p53. *Cancer Res* 2003;63:1990-3.
96. Santana P, Peña LA, Haimovitz-Friedman A, et al. Acid sphingomyelinase-deficient human lymphoblasts and mice are defective in radiation-induced apoptosis. *Cell* 1996;86:189-99.
97. Lin X, Fuks Z, Kolesnick R. Ceramide mediates radiation-induced death of endothelium. *Crit Care Med* 2000;28:N87-93.
98. Haimovitz-Friedman A, Balaban N, McLoughlin M, et al. Protein kinase C mediates basic fibroblast growth factor protection of endothelial cells against radiation-induced apoptosis. *Cancer Res* 1994;54:2591-7.
99. Haimovitz-Friedman A, Kan CC, Ehleiter D, et al. Ionizing radiation acts on cellular membranes to generate ceramide and initiate apoptosis. *J Exp Med* 1994;180:525-35.
100. Truman JP, García-Barros M, Kaag M, et al. Endothelial membrane remodeling is obligate for anti-angiogenic radiosensitization during tumor radiosurgery. *PLoS One* 2010;5:e12310.
101. Gupta S, Tubin S, Ahmed MM. Radiation-induced bystander effects in normoxic and hypoxic conditions in human lung cancer cells. In 14th International Congress of Radiation Research, Warsaw, Poland, 2011:71.
102. McMahon SJ, McGarry CK, Butterworth KT, et al. Implications of intercellular signaling for radiation therapy: a theoretical dose-planning study. *Int J Radiat Oncol Biol Phys* 2013;87:1148-54.



**Cite this article as:** Prasanna A, Ahmed MM, Mohiuddin M, Coleman CN. Exploiting sensitization windows of opportunity in hyper and hypo-fractionated radiation therapy. *J Thorac Dis* 2014;6(4):287-302. doi: 10.3978/j.issn.2072-1439.2014.01.14

## Improving radiotherapy planning, delivery accuracy, and normal tissue sparing using cutting edge technologies

Carri K. Glide-Hurst, Indrin J. Chetty

Henry Ford Health Systems, Detroit, MI, USA

### ABSTRACT

In the United States, more than half of all new invasive cancers diagnosed are non-small cell lung cancer, with a significant number of these cases presenting at locally advanced stages, resulting in about one-third of all cancer deaths. While the advent of stereotactic ablative radiation therapy (SABR, also known as stereotactic body radiotherapy, or SBRT) for early-staged patients has improved local tumor control to >90%, survival results for locally advanced stage lung cancer remain grim. Significant challenges exist in lung cancer radiation therapy including tumor motion, accurate dose calculation in low density media, limiting dose to nearby organs at risk, and changing anatomy over the treatment course. However, many recent technological advancements have been introduced that can meet these challenges, including four-dimensional computed tomography (4DCT) and volumetric cone-beam computed tomography (CBCT) to enable more accurate target definition and precise tumor localization during radiation, respectively. In addition, advances in dose calculation algorithms have allowed for more accurate dosimetry in heterogeneous media, and intensity modulated and arc delivery techniques can help spare organs at risk. New delivery approaches, such as tumor tracking and gating, offer additional potential for further reducing target margins. Image-guided adaptive radiation therapy (IGART) introduces the potential for individualized plan adaptation based on imaging feedback, including bulky residual disease, tumor progression, and physiological changes that occur during the treatment course. This review provides an overview of the current state of the art technology for lung cancer volume definition, treatment planning, localization, and treatment plan adaptation.

### KEYWORDS

Lung cancer; motion management; dose calculation; treatment planning

*J Thorac Dis 2014;6(4):303-318. doi: 10.3978/j.issn.2072-1439.2013.11.10*

### Introduction

In the United States, lung cancer constitutes 56% of all new invasive cancers diagnosed, accounting for ~30% of deaths resulting from all cancers (1). Non-small cell lung cancers (NSCLC) account for 80-85% of all lung cancers (2), with locally advanced, stage III disease representing about 40% of the total cases. The prognosis of these patients, even with aggressive chemoradiation techniques, is quite poor, with 5-year overall survival rates of only 10-15% (3). Given the recent seminal finding

that low-dose computed tomography (CT) for lung cancer screening reduces lung cancer mortality ~20% when compared to radiography (4), with widespread acceptance, it may be postulated that lung cancers will be found more frequently, and at earlier stages. For early-stage, medically inoperable NSCLC, stereotactic ablative radiation therapy (SABR, also known as stereotactic body radiotherapy, SBRT) has shown remarkable promise, yielding ~90% local tumor control and, in one study, ~55% overall survival at a time point of three years (5).

Recent retrospective research has shown a dose-effect correlation for lung tumors (6-8), however safe radiation dose escalation is complicated by the close proximity of critical organs, and is further complicated by respiration-induced tumor displacement. However, interim analysis of Radiation Therapy Oncology Group (RTOG) 0617, comparing high dose (74 Gy) versus standard dose (60 Gy) radiation therapy (RT) with and without Cetuximab for Stage III NSCLC patients (9), revealed that the high dose arm did not improve overall survival, with no

Correspondence to: Indrin J. Chetty, Henry Ford Health Systems, Detroit, MI, USA.  
Email: [ichetty1@hfhs.org](mailto:ichetty1@hfhs.org).

Submitted Sep 12, 2013. Accepted for publication Nov 07, 2013.  
Available at [www.jthoracdis.com](http://www.jthoracdis.com)

ISSN: 2072-1439

© Pioneer Bioscience Publishing Company. All rights reserved.

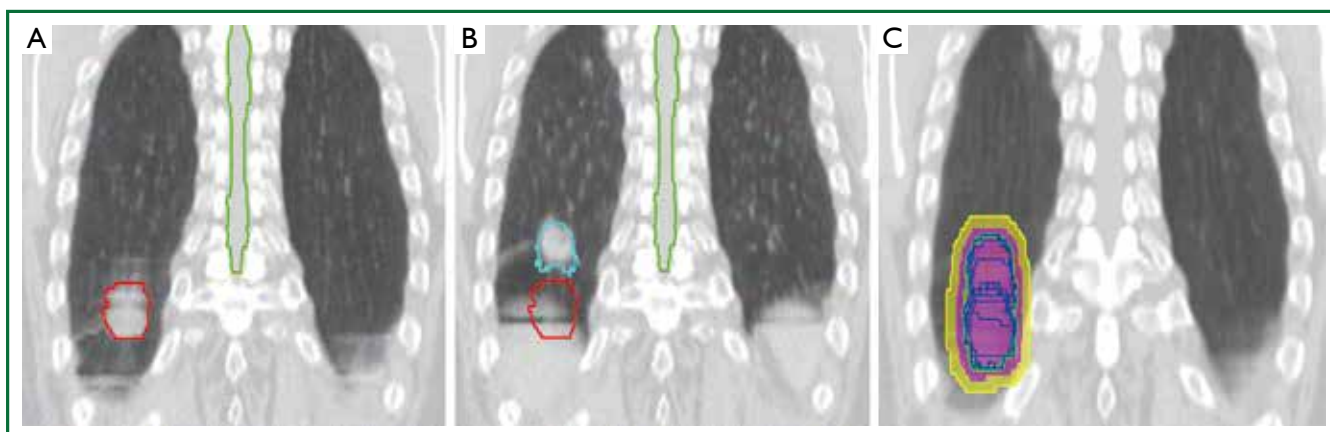


**Figure 1.** 4DCT images of an early-stage lung cancer patient at end-inhalation (A); end exhalation (B); and contours from all 10 phases of the 4DCT combined (C). Abbreviation: 4DCT, four-dimensional computed tomography.

significant differences in toxicity between treatment arms (10). While mature results are still lacking, the results of this clinical trial prompted a considerable amount of uncertainty in the Radiation Oncology community (11). It has been suggested that requiring the use of technical advances such as image-guided radiation therapy (IGRT), patient-specific dose levels based on nearby organs at risk (i.e., healthy lung tissue and heart), and motion management may be advantageous in future trials (11,12). Motion management is currently recommended on a patient-specific basis for tumor excursions greater than 5 mm in any direction (13). To further facilitate dose escalation and increase local control, considerable effort has been made to characterize patient-specific tumor motion using the tumor (14-16), the organ in which it is embedded (17), implanted fiducial markers (18,19), or another part of the anatomy presumed to be related to tumor motion (i.e., diaphragm or abdomen surface) (20-22).

Advances in imaging, including four-dimensional computed tomography (4DCT) and volumetric cone-beam computed tomography (CBCT) have enabled more accurate target definition and precise tumor localization for both advanced stage lung cancer treatment and SBRT to further support dose escalation efforts while sparing nearby organs at risk. In addition, advances in dose calculation algorithms have allowed for more accurate dosimetry in heterogeneous media, thereby providing a clearer picture of dose distributions. Finally, new delivery approaches, such as tumor tracking or gating, offer additional mechanisms to reduce target margins. This work will provide an overview of the current state of the art for lung cancer volume definition, treatment planning, localization, and treatment plan adaptation.

### Internal target volume (ITV)

In 1999, ICRU Report 62 introduced the concept of the “internal margin”, which is meant to incorporate uncertainties arising from physiological variations, such as respiratory motion (23). When the internal margin is combined with the clinical target volume, or CTV, the ITV is formed, which represents the “envelope” encompassing tumor movement determined during the simulation 4D-CT acquisition. The internal margin is expanded to form the planning target volume (PTV), which accounts for geometric variation in the CTV due to day-to-day (interfraction) uncertainties in the patient setup. A margin (planning risk volume, PRV) should also be added to an organ-at-risk to account for interfraction variation in the OAR position (23). Margins for the PTV must be designed with an understanding of the random and systematic errors associated with patient setup (24). For locally advanced stage NSCLC, typical margins for the PTV are on the order of 5-10 mm if an ITV is used for motion compensation and daily IGRT is often employed during treatment. In the absence of motion compensation or IGRT, margins should be much larger (10-20 mm) to minimize the chance of missing the target as a result of motion.

The American Association of Physicists in Medicine (AAPM) Task Group Report No. 76 (13) recommends a variety of approaches to account for respiratory motion. One such example is respiratory-correlated or 4DCT (14,25-27), where organ and tumor motion are both inherently provided during different phases of the respiratory cycle, often sampling data over 10-20 breathing cycles. Figure 1A and 1B illustrate the end-inhale and end-exhale phases of respiratory motion, respectively,

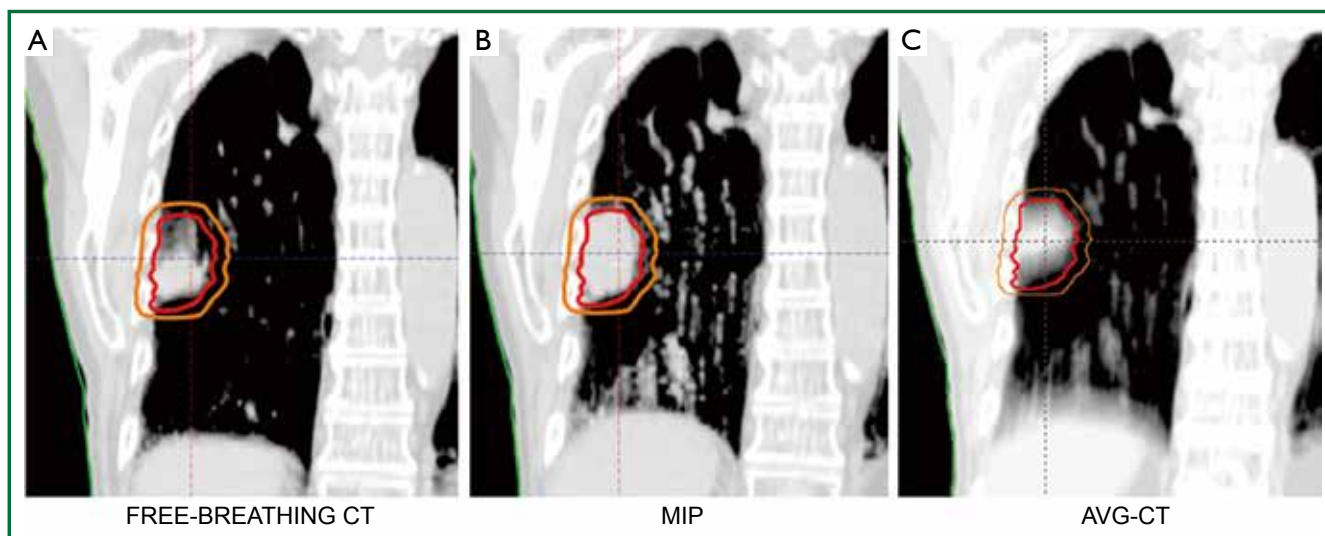


**Figure 2.** (A) Positional differences between the tumor position on the free-breathing CT; (B) maximum intensity projection (MIP); and (C) AVG-CT, indicating that the FBCT was acquired at an extreme phase of the breathing cycle. Contours show the ITV and PTV. Abbreviations: AVG-CT, average computed tomography; ITV, internal target volume; PTV, planning target volume.

for a highly mobile lung tumor. Tumors can be delineated on all 4DCT phases, and a union can be derived to generate the ITV as shown in Figure 1C. By contrast, conventional free-breathing CTs (FBCTs) are acquired at arbitrary states of the breathing cycle, during which tumors, nearby critical structures, and corresponding tissue densities are not static, as shown in Figure 2. Furthermore, due to the fast acquisition time of FBCT, it is possible to acquire imaging data at an extreme phase of the breathing cycle (i.e., end-inhale or end-exhale). Typically, conventional CT-simulator software employs retrospective temporal (i.e., phase-based) 4DCT sorting into 2-10 different phases, although artifact reduction has been realized through the use of amplitude-based 4DCT binning, particularly for irregular breathing patterns (28). Ten-phase 4DCTs often contain >1,000 CT slices, and may result in reconstruction and sorting artifacts introduced by varied respiratory patterns during a single 4DCT acquisition. This is of particular consequence in lung cancer radiotherapy due to patients presenting with compromised pulmonary function. 4DCT artifacts can lead to discrepancies in target and critical structure delineation, as well as impact the accuracy of dose calculation.

Furthermore, the vast amount of data generated via 4DCT may substantially increase the time needed for image review and target/critical structure delineation. Therefore, a problem arises in how to fully exploit 4DCT data for treatment planning with an emphasis on clinical efficiency without compromising accuracy. To reduce the workload of contouring multiple

target volumes in 4DCT, post-processing can be conducted to generate derivative datasets such as the average CT (AVG-CT) and maximum intensity projection (MIP). The AVG-CT data set provides a 3DCT scan with voxels equal to the arithmetic mean of the 4DCT, while the MIP image corresponds to the greatest voxel intensity values throughout the 4DCT. Another commonly used dataset is the mid-ventilation CT scan, corresponding to the specific 4DCT phase with the tumor center of mass closely representing the time-averaged position over the respiratory cycle (29). To further address large 4DCT datasets, several groups have worked toward developing automated contour delineation (30,31), deformable image registration (DIR) techniques (32-34), treatment planning on fewer breathing phases (35), the mid-ventilation phase (29,36), or AVG-CT over the entire breathing cycle (37,38). If 4DCT is not available, end-inspiration and end-exhalation images can be acquired to assess tumor excursion, or the tumor can be observed under fluoroscopy, such as with a conventional simulator.

### Dose calculation

Dose calculation accuracy is of paramount importance in the clinical treatment process. The AAPM Report No. 85 (39) on Tissue Inhomogeneity Corrections for Megavoltage (MV) Beams notes that a 5% change in dose may result in a 10% to 20% change in tumor control probability (TCP) at 50%, and 20% to 30% impact on normal tissue complication probabilities

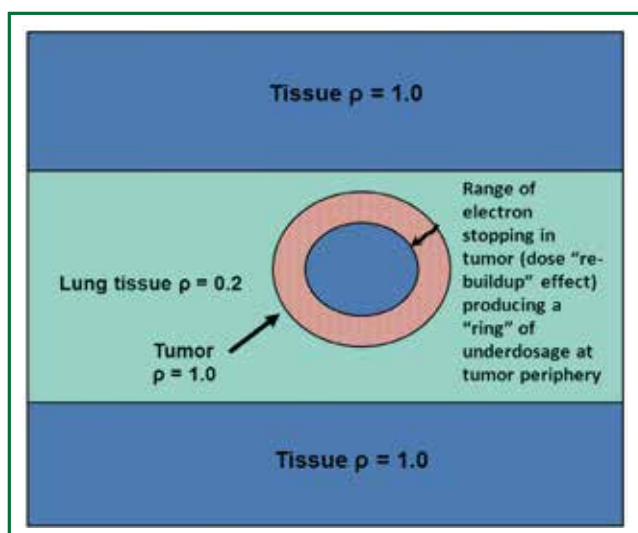


**Figure 3.** Geometry of an “island-like” lung tumor where electrons scatter laterally into lower density lung tissue, carrying dose away from the tumor. Electrons “stopping” within the tumor deposit dose over a finite range, resulting in an underdosage at the periphery of the tumor. Dose algorithms incorporating 3D scatter corrections, including the effects of electron scattering, must be used to properly characterize dose deposition within the tumor and surrounding healthy lung tissue. Abbreviation: 3D, three-dimensional.

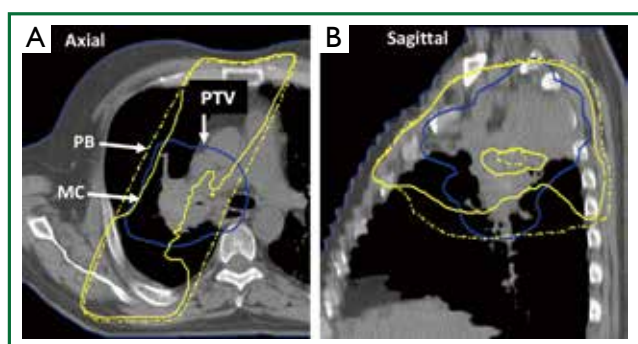


**Figure 4.** Comparison of 100 % isodose line in a treatment plan for a patient with locally advanced stage non-small cell lung cancer, shown in the axial (A) and sagittal (B) views. Dose calculations performed using a pencil-beam-type algorithm (dashed line) and the Monte Carlo (MC) method (solid line). Significant underdosage of the PTV (solid line) is noted with the MC algorithm using UMPlan (University of Michigan) treatment planning system.

(NTCP). The report further cites two examples where a 7% difference in dose delivered to different groups of patients was discovered by a radiation oncologist through clinical observations (39).

### Dosimetric considerations

The presence of low-density lung tissue surrounding thoracic tumors complicates radiation dose computation in lung cancer treatment planning. Conditions of loss of charged-particle equilibrium (CPE) are produced when the field size is reduced such that the lateral ranges of the secondary electrons become comparable to (or greater than) the field size; such conditions occur for larger field sizes in lung than in water-equivalent tissues due to the increased electron range in lung. Under such circumstances, the dose to the target is determined primarily by secondary electron interactions and dose deposition. Because conventional dose algorithms do not explicitly account for transport of secondary electrons, they can be severely limited in accuracy under non-equilibrium conditions. In low density, lung-equivalent tissues, the reduction of dose due to electron scattering in the lung and the “re-buildup” of dose in the tumor at the lung-tumor interface, as electrons begin to stop in the tumor over a finite range, can produce significant underdosage at the tumor periphery (Figure 3). The reduction of dose at the tumor periphery is also exacerbated at higher beam energies, due to the increased electron range. Based on these dosimetric considerations, the RTOG No. 0236 (40) excluded the use of radiation field sizes less than 3.5 cm and restricted the use of beam energies above 10 MV. The article by Reynaert *et al.* (41) and the AAPM Task Group No. 105 (42) provide examples of numerous studies reported on the inaccuracies associated with conventional algorithms for dose calculations in the lung. For lung cancer treatment planning, and especially when dealing with smaller tumors with field sizes  $<5 \times 5 \text{ cm}^2$ , algorithms including three-dimensional (3D) scatter integration such as convolution/superposition, or the Monte Carlo (MC) method are necessary—the latter accounts explicitly for electron transport (43,44).

The AAPM TG Report No. 101 (43) and other articles (45) recommend that pencil-beam algorithms not be utilized for SBRT-based lung dose calculations. The report also states that for the most complex situations, involving small, peripheral lung tumors, surrounded entirely by lung (“island-like” lesions), the MC method is ideal (43). Figure 4 provides a comparison of the 100% isodose line in a treatment plan for a patient with locally advanced stage NSCLC. Dose calculations were performed using a pencil-beam-type algorithm (dashed line) and the MC method (solid line). Whereas the pencil-beam-based calculation shows good dose coverage of the PTV, significant underdosage is noted with the MC algorithm. This example illustrates that PB-based algorithms are relatively insensitive to the presence of low-density lung tissue and do not account for electron scattering within the surrounding lung tissues. Consequently dose to the

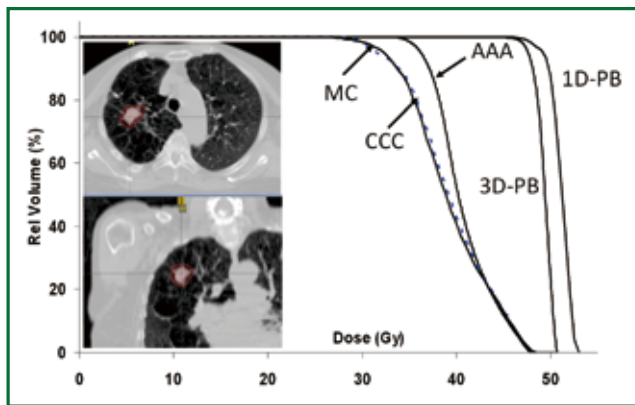


**Figure 5.** Dose volume histograms (DVHs) for the planning target volume (PTV) for a peripherally located lung tumor with PTV dimensions of ~4.5 cm planned with 6 MV photons. Algorithms include pencil beam-type (1D-PB and 3D-PB), convolution/superposition type (AAA and CCC) and Monte Carlo (MC). All calculations were done using treatment planning systems at the Henry Ford Hospital. Figure adapted from reference 46.

tumor is overestimated using PB algorithms, and the “actual” dose delivered, as properly predicted with the MC method, is much lower.

Figure 5 shows dose volume histograms (DVHs) for the PTV for a peripherally located lung tumor with PTV dimensions of ~4.5 cm planned with six MV photons. The prescription dose was 48 Gy (delivered in four 12 Gy fractions) to the 95% line. The initial 3D conformal (3D-CRT) treatment plan was computed with the 1-D PB algorithm. When re-computed with the convolution/superposition and MC-type algorithms, the “actual” dose to the PTV was much lower than that predicted with the PB algorithm. Both the MC and CCC algorithms show underdosage of the minimum PTV dose of 75% relative to PB (27 vs. 48 Gy). Differences in the minimum PTV dose of 25% were noted between MC or CCC and the AAA algorithm; the former which were lower. The substantial differences observed between pencil beam and convolution/superposition or MC-based algorithms for this particular case can be attributed to several factors, including “island-like” geometry (where the tumor is surrounded entirely by lung), relatively small tumor size, and beam arrangements/trajectories. Such conditions amplify the effects of electron scattering and the importance of electron transport; differences are therefore not unexpected.

Table 1 provides the results of a retrospective dose calculation study consisting of 135 patients with early stage NSCLC treated with SBRT (46). As in the example provided in Figure 5, doses were planned initially using a 1D-PB algorithm to a total dose of 48 Gy (in 12 Gy fractions); treatment plans were recomputed

using convolution/superposition type and MC-based algorithms. A recently available algorithm, AcurosXB, uses a discrete-ordinates approach to solve the radiation transport equation. It is similar to the MC method but is deterministic in nature. Results in Table 1 show that the convolution/superposition, MC and discrete ordinates algorithms predict differences of ~-10% and ~-20% in the PTV mean and dose to 95% of the volume (D95) values relative to the 1D-PB algorithm. 1D and 3D PB algorithms are generally within 5% agreement. Differences in mean lung dose (MLD) are not significant, in part because the MLD values are low (~3 Gy). These results confirm that pencil-beam type algorithms should be avoided for thoracic cancer treatment planning, particularly for SBRT.

### *Treatment planning considerations*

Beam arrangements for treatment planning of lung cancers can range from simple two-field, parallel opposed fields (e.g., anterior-posterior, opposed, AP/PA) for late stage NSCLC to complex multiple gantry angle, intensity modulated beams for local or locally advanced disease. Beams are shaped with a multileaf collimator (MLC) which enables conformation of radiation to the target. Treatment plans should be designed to minimize dose to surrounding normal organs and thereby limit the risk of treatment toxicity, implying sharp gradients in the dose fall-off outside the target (43). AP/PA fields may be considered with more extensive, centrally located disease to help reduce dose to the unaffected lung volume. The goal in such cases is to produce a homogeneous dose distribution across the treated volume to encompass the extent of the disease. However, AP/PA beams can only be used for cumulative PTV doses in the range of 45-50 Gy (in 1.8-2 Gy per fraction) due to spinal cord tolerance. “Off-cord” fields are required beyond 45-50 Gy. When treating large volumes of lung, it is especially important to design treatment plans that adhere to normal lung tolerance doses. Dose indices, such as V20, V5 and MLD must be closely observed to avoid radiation pneumonitis and other catastrophic consequences (47,48). For treatment planning of local or locally advanced NSCLC, more conformal dose distributions employing multiple beam angles are warranted. Treatment plans can be developed using 3D-CRT or intensity modulated radiation therapy (IMRT) techniques and must include beams from multiple gantry angles (five or more beams), particularly in the context of SBRT (43), to limit normal tissue sequelae, such as skin erythema, which has been observed clinically.

For IMRT-based planning, one must bear in mind the interplay effect, which describes the interplay between a given MLC position and instance of radiation delivery with the

**Table 1.** Absolute dose values (in Gy) of the PTV mean (Dmean), D95, and MLD early stage NSCLC treatment plans treated with SBRT.

| Algorithm | Dmean (Gy) |           | D95 (Gy) |           | MLD (Gy) |          |
|-----------|------------|-----------|----------|-----------|----------|----------|
|           | Avg.       | Range     | Avg.     | Range     | Avg.     | Range    |
| EPL-1D    | 49.2       | 46.8-53.6 | 48.0     | 38.5-51.8 | 3.0      | 0.6-10.3 |
| EPL-3D    | 47.9       | 44.3-53.4 | 45.9     | 38.7-51.4 | 3.0      | 0.4-10.6 |
| AAA       | 44.7       | 37.9-52.5 | 40.8     | 31.5-48.7 | 2.8      | 0.5-9.7  |
| CCC       | 45.1       | 37.4-52.8 | 40.9     | 30.0-48.6 | 2.9      | 0.5-10.1 |
| AcurosXB  | 44.3       | 34.2-52.1 | 39.8     | 29.8-47.6 | 3.0      | 0.5-10.4 |
| MC        | 45.0       | 36.2-52.4 | 40.9     | 30.5-49.0 | 2.9      | 0.5-10.6 |

Abbreviations: PTV, planning target volume; D95, dose corresponding to 95% of the volume; MLD, mean lung dose. Both average dose and the range are presented for the EPL-1D (pencil beam 1D), EPL-3D (pencil beam 3D), AAA (convolution/superposition type), CCC (convolution/superposition type), AcurosXB (discrete ordinates-type), and Monte Carlo (MC) algorithms. The dose prescription was 48 Gy (in 12 Gy per fraction) to the 95% line, computed initially using the 1D-PB algorithm. The same monitor units and plan parameters as in the 1D-PB plan were used for computation with all other algorithms. All calculations were done using treatment planning systems at the Henry Ford Hospital, adapted from Reference (46).

position of the tumor in the respiratory-induced motion cycle at the same instance (49). For conventional 3D treatment, small dose gradients can be expected and moving anatomy within the treatment field will blur the dose distribution, effectively increasing the beam penumbra (13). Conversely, for IMRT, this effect is more marked due to the interplay between the MLC leaf motions and the target motion perpendicular to the treatment beam. To account for this, the dose deposited for each respiratory phase can be computed by the subset of MLC sequences delivered to that specific phase, rather than by the entire MLC sequence delivered in aggregate. The interplay effect has been evaluated for intra-fraction cumulative dose and while the interplay effect was significant for individual phases, it “washed out” in dose accumulation over ten phases. The interplay effect caused less than 1% discrepancy in the PTV and ITV minimum doses using an energy mapping algorithm (50). Similarly, the interplay effect averages out over 30 or more treatment fractions (49,51). However, in the SBRT setting, where 3-5 dose fractions are delivered, it is not clear how the interplay will impact dose distributions.

Treatment planning for SBRT must be done with an understanding of the dose gradients so as to develop dose distributions with sharp gradients. This is typically achieved using multiple non-overlapping, and non-coplanar beams as necessary, and a MLC with 5 mm or smaller leaf width (43). The dose prescription line can be low (e.g., 80%) with much smaller margins for beam penumbra (“block edge”) than conventional radiotherapy; the motivation is to produce a faster dose falloff and thereby improve sparing of surrounding healthy tissues (43). AAPM Task Group No. 101 discourages the use of calculation grid sizes greater than 3 mm for SBRT planning (43).

Recently, volumetric modulated arc therapies (VMAT) have become available for SBRT-based treatments. The delivery

of radiation in significantly less time with VMAT is likely to substantially mitigate patient movement on the treatment table as a result of discomfort during a long treatment procedure, and thereby improve delivery quality (52). Another advantage of VMAT is the ability to deliver multiple beams in different directions and preferentially spare neighboring critical structures. However, one must be cognizant of “low-dose” spread with VMAT, which may be higher than IMRT due to the rotational delivery. As such, parameters such as V5 to the healthy lung tissue must be carefully assessed when using VMAT. Nevertheless, comparisons of VMAT and 3DCRT have revealed no early clinical or radiographic changes in the lung post-treatment (53). Also, as with conventional IMRT, VMAT-based plans are subject to the interplay effect, which must be considered depending on the mobility of the tumor and the degree of modulation of the MLC fields.

#### 4D dose accumulation

With widespread 4DCT implementation, a natural progression has been made to estimating the delivered dose during respiration through the use of 4D treatment planning and dose accumulation (32,54,55). Because the tumor and nearby organs at risk change in density and shape during the different phases of respiration, it is advantageous to calculate dose on each, or a subset, of breathing phases, and accumulate the dose to a reference phase. To accomplish this, DIR is necessary to generate the displacement vector field (DVF) between the source and reference images. DVFs describe the voxel-by-voxel correlation across multiple CT sets, and can be used to map the doses deposited during other phases back to the reference phase. The most straightforward, although not efficient, implementation of 4D dose accumulation is to perform a full 4D dose calculation

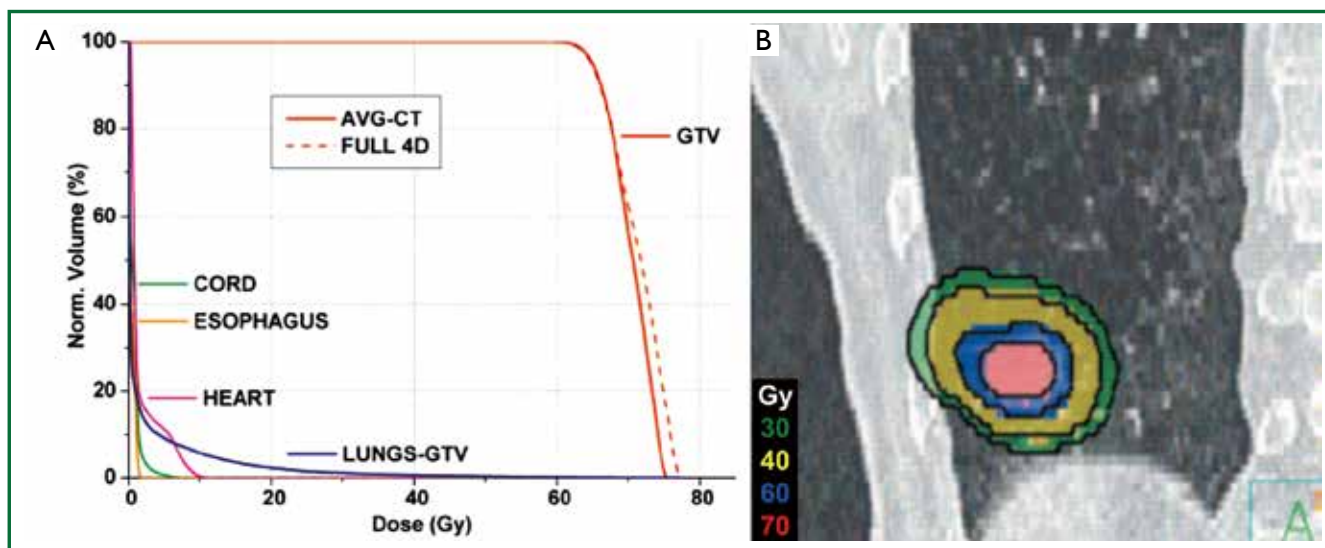


**Figure 6.** Dose volume histogram (A) and coronal 4DCT data set (B) demonstrating the close association between deformable image registration coupled with full 4D dose summation or using the AVG-CT as an approximation for a patient with 2 cm superior-inferior tumor excursion. Isodose washes represent the AVG-CT approximation while the black isodose lines represent the corresponding full 4D dose summation. Figure adapted from Ref (56). Abbreviations: 4DCT, four-dimensional computed tomography; AVG-CT, average computed tomography; 4D, four-dimensional.

and calculate the weighted average over the breathing course (35). In an effort to simplify 4D dose calculation and computational expense, reduction in datasets have been proposed such as coupling the DVFs with the AVG-CT to estimate cumulative dose (56), using fewer breathing phases (35), or using the midventilation phase (54,57). All of these approaches have revealed close approximations to a full 4D dose accumulation, thereby supporting integration of cumulative dose into clinical treatment planning. For example, in a patient case that was considered to be the worst-case scenario (tumor abutted the diaphragm with ~2 cm of superior-inferior motion), the largest deviation observed between DIR coupled with full 4D dose accumulation or the AVG-CT was 2% for the maximum dose and dose to 1% of the gross target volume (56) as shown in Figure 6.

Another method that has been proposed is to determine the actual energy and mass transferred to that voxel, and then divide the energy by mass to get the dose (termed energy/mass transfer mapping) (58-61). A comparison of direct dose mapping and energy/mass transfer mapping in ten patients with demonstrable tumor excursion revealed similar cumulative doses to the ITV and PTV, although minimum dose differences of up to 11% in the PTV and 4% in the ITV minimum doses were observed between the two dose mapping algorithms with treatment plans computed with AAA (62).

While DIR facilitates cumulative dose estimation, propagated DIR errors will lead to irregularities in automatic contouring, dose warping, and overall dose accumulation. However,

verification of DIR is challenging due to the absence of “ground truth”. Commonly, visual assessment of the DIR results is conducted, sometimes evaluating propagated contours or the deformed image set (63,64). Others have evaluated DIR performance against physician delineations or noted landmarks (65,66). However, large registration errors are often observed in regions of uniform intensity, and errors estimated by feature-guided evaluation methods may not represent voxel registration accuracy away from those landmarks. Approaches such as evaluating the curl vector (67) or warping images with known DVFs and evaluate the recovered deformations have been implemented (64). Stanley *et al.* benchmarked and evaluated DIR algorithms using patient-specific finite element models (FEM) and a physical deformable phantom (68). Figure 7A shows a programmable deformable phantom that contains a heterogeneous sponge with average density equivalent to lung (Figure 7B) that can be deformed. The modular phantom can be disassembled to insert film or thermoluminescent dosimeters for 4D dose verification.

### On-line IGRT

On-line IGRT verifies the target volume and organ at risk locations before daily treatment (inter-fraction) and can also be used to monitor the target during treatment (intra-fraction). Daily IGRT-based setup has been shown to significantly reduce residual errors, and consequently planning margins (69,70). For

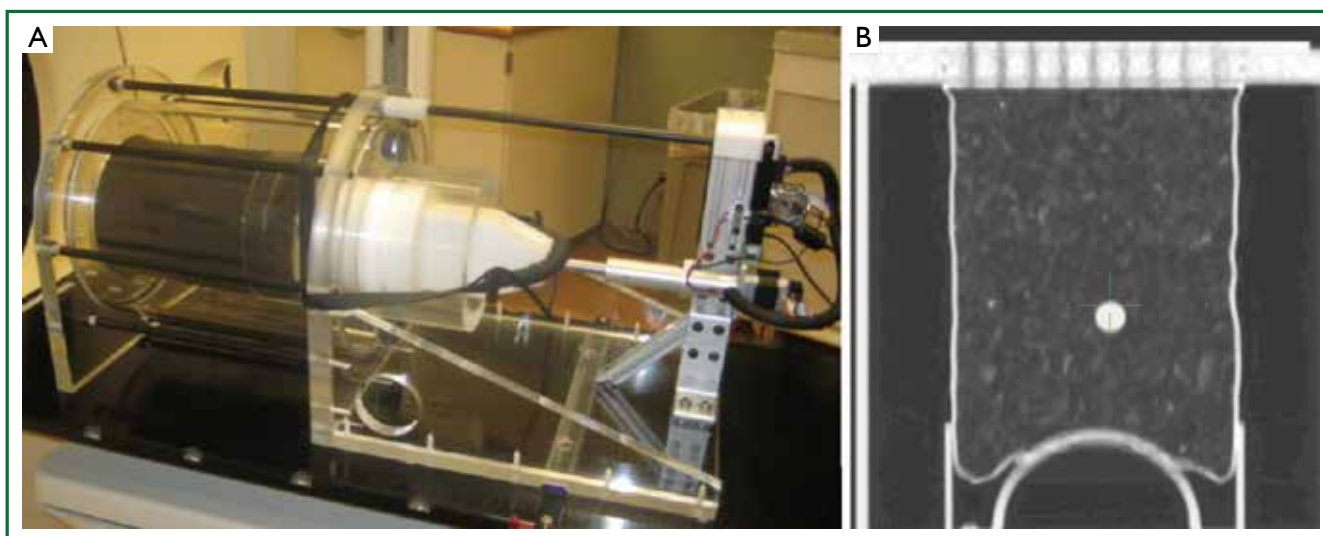


**Figure 7.** In-house developed deformable lung phantom (A) and coronal cross section (B) showing implanted tumor embedded in the lung material (Courtesy of Hualiang Zhong, Henry Ford Health System).

SBRT-based treatments, where motion management and IGRT are the recommended standard-of-care (43), PTV margins can range from 3-6 mm (69,71-73). On-board imaging can include a kilovoltage (kV) source and flat-panel detector mounted orthogonal to the MV therapy beam axis on the linear accelerator gantry. Image acquisition includes planar radiographic (i.e., kV images), fluoroscopic (cine loops of triggered planar kV images), and volumetric (series of angular projection images reconstructed to generate CBCT datasets (74-78)). A chief advantage of kV imaging, particularly CBCT, is the soft tissue visibility, which has been a key component of implementing lung SBRT (70,79,80). Furthermore, because CBCTs are acquired over ~1 minute, the 3D volume represents a time-averaged scan, often indicating the average position of the tumor. Most linear accelerators are also equipped with MV electronic portal imaging devices (EPIDs) mounted at the exit of the treatment beam, which can be used to verify bony landmarks. MV CBCT is also available using an EPID mounted on the treatment beam axis, allowing for volumetric MV imaging.

At Henry Ford Hospital, volumetric CBCT-based imaging is employed to visualize the tumor with respect to organs at risk, for lung SBRT cases. The localization procedure includes setting the patient to tattoos, acquiring a CBCT image, and using automatic image registration tools to align the CBCT to the reference CT. Bony alignment is first verified by the physicist, and manually adjusted if deemed necessary. The physician and physicist then review the registration using soft-tissue window/level and verify that the ITV contour encompasses the lesion. If the lesion falls outside the ITV contour, the physician will manually adjust the

registration until the targets are aligned. The image registration is then approved by the physician, and resulting couch corrections are applied. Verification imaging is performed via an orthogonal pair of MV/kV images that are automatically registered to the digitally reconstructed radiograph (DRR). MV/kV matching ensures the proper couch shift has been applied and the patient has not moved between the original CBCT acquisition and treatment. If the registration result is <2 mm/1 degree (not including shifts made for soft tissue matching in the previous step), treatment commences at the CBCT position. Otherwise, another CBCT is performed and the process is repeated.

Ideally, respiratory-correlated CBCT (or 4D-CBCT) would be implemented to mitigate breathing artifacts while providing the tumor mean position, trajectory, and shape over respiration (81). While the feasibility of 4D-CBCT has been demonstrated on different linear accelerators (82,83), scan times can be on the order of four minutes, yielding ~700 projections of data for sorting, and delivering 2-4 cGy/scan depending on area of interest evaluated (81). Another solution that has been integrated into some clinical workflows include a multiple breath-hold CBCT, often called the “stop and go” CBCT (84,85). Here, CBCT acquisition is paused over multiple breath-holds and the resulting datasets are combined into one final reconstruction.

## Tracking

### Tumor tracking

Lung tumor motion can be measured and monitored using

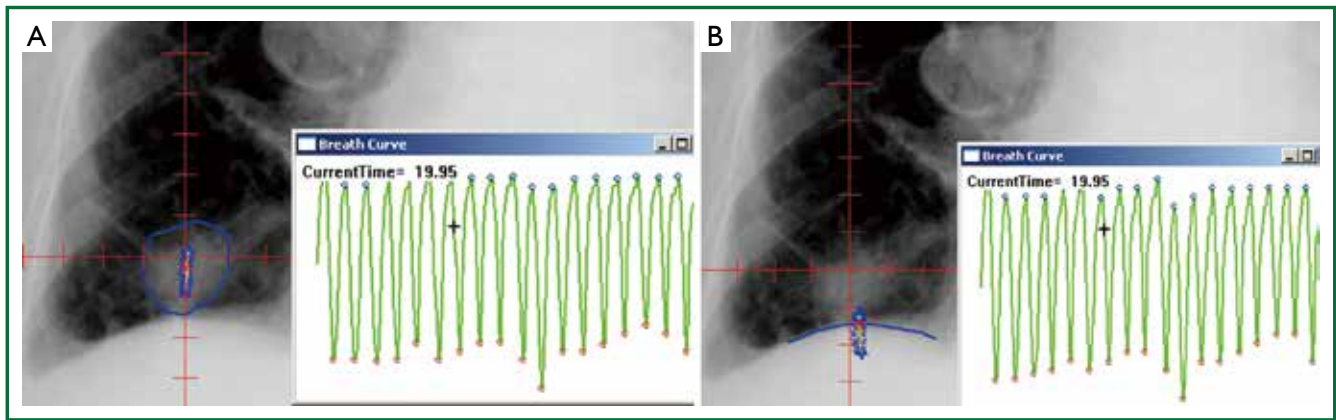


**Figure 8.** AP fluoroscopy images of an advanced stage lung cancer patient with the tumor (A) and diaphragm (B) tracked using automated in-house software [Courtesy of Jian Liang, William Beaumont Hospital, adapted from Reference (86)].

techniques such as fluoroscopy (15,86), real-time tumor tracking radiotherapy (RT-RT) (18,19), or using implanted fiducials. An example of an in-house analysis program designed to track the tumor and diaphragm in fluoroscopy frames is shown in Figure 8A and B, respectively. Details and validation can be found elsewhere (20,36), but briefly, a region of interest (ROI) is contoured on a single frame, and a template-matching technique using rigid-body registration and nearest-neighbor interpolation propagated the ROI to all other frames. For patients, ROIs can include the tumor or nearby ROI, apex of the diaphragm, or any other anatomy of interest. Centroids of the propagated contours can then be exported to generate the tumor or surrogate trajectories over fluoroscopic frames.

The fluoroscopic real-time tumor-tracking system (RTRT system) (Mitsubishi Electronics Co. Ltd., Tokyo, Japan) uses four sets of diagnostic X-ray systems oriented with the central axis at isocenter to track gold markers implanted at or near moving tumors (15,87-90). 3D marker positioning is determined via a template-matching algorithm applied to the digital images, and if the measured and expected marker positions do not match inside pre-determined tolerances, a machine interlock is asserted. Clinical outcome data suggests similar local control and overall survival rates for RTRT as compared to SBRT without gating (91). One caveat is that significant skin surface doses (29-1,182 mGy/h) have been reported (92).

Another external-internal tumor tracking modality is the Synchrony™ Respiratory Tracking System (Accuray, Inc., Sunnyvale, CA, USA) integrated with the CyberKnife robotic linear accelerator. Briefly, the Synchrony camera array tracks three external LED markers affixed to the patient's chest while orthogonal stereoscopic X-ray images are obtained to localize

two to four fiducial markers implanted at or near the tumor (93). Real-time feedback from patient monitoring is used to develop a correspondence model, inferring internal tumor positioning from the external surrogates. The correspondence model predicts tumor position, sends feedback to the robotic linear accelerator, and the robot realigns the beam with the tumor. A soft-tissue tracking algorithm has also been reported that can be used for peripheral tumors (diameter >15 mm) in the lung (94). A few disadvantages include the use of ionizing radiation and the additional margin required to account for deformation (94).

The implantation of electromagnetic transponders [e.g., Calypso wireless transponders (Beacons™) currently part of Varian Medical Systems, Palo Alto, CA] at or near the tumor has been widely implemented in prostate cancer RT (95). Briefly, the system uses an array of AC magnetic coils to generate a resonant response in implanted transponders (8 mm length, 2 mm diameter) subsequently detected using a separate array of receiver coils. Beacons' coordinates are identified on a treatment planning CT, and the offset between the beacons' centroid and intended isocenter is reported. During treatment, the Calypso system continuously monitors and reports the 3D offset between the actual and desired isocenter locations at a frequency of 10 Hz. Transponders have been implanted into canine lungs, although migration and transponder expulsion were challenges for the original beacon design (96,97). As a result, a new anchored beacon was devised under an Investigational Device Exemption (IDE) granted by the FDA, and clinical trials are currently underway (98). While tracking implanted markers within the tumor is optimal, the invasiveness of implantation, increased risk of pneumothorax (99), and potential "dropping" or migration of markers from the implantation location (87) can also be deterrents.

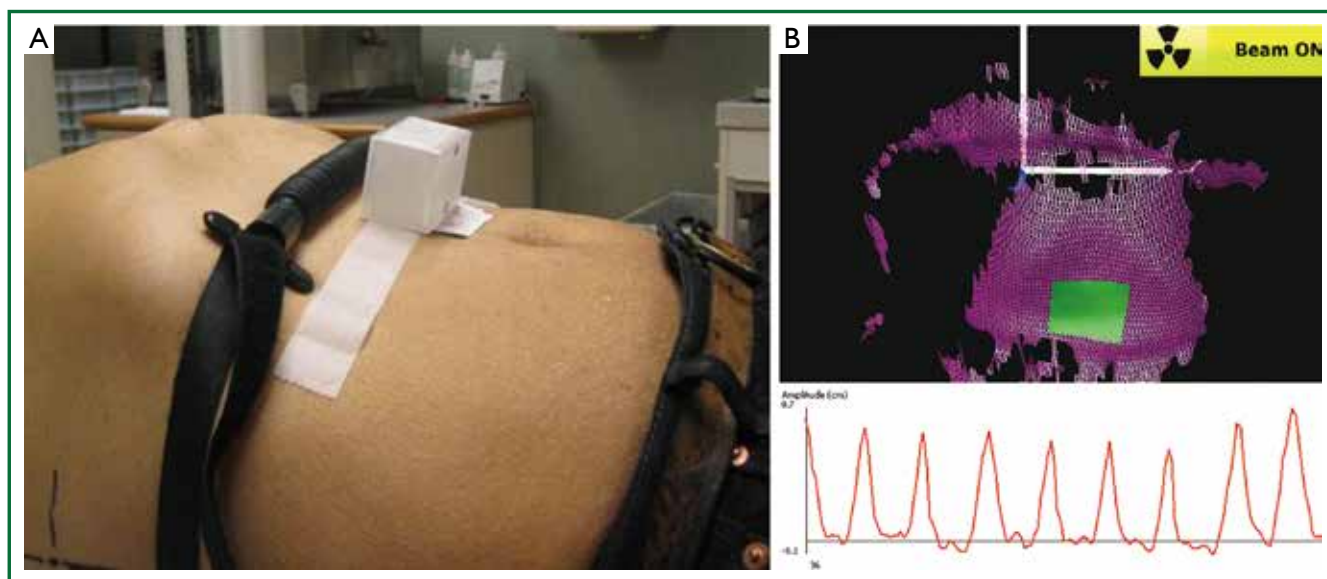


**Figure 9.** Examples of external surrogates used for patient monitoring. (A) Pneumatic belt placed superiorly of the RPM block; (B) surface images obtained from AlignRT [adapted from Reference (86)]. Abbreviation: RPM, Respiratory Gating System.

### External surrogate tracking

External surrogates can infer tumor motion, although they can be limited by the need to verify the relationship with the tumor motion, the potential for external marker placement to affect this correlation (100), and time-dependent characteristics (101). External surrogates of the abdomen can be derived from pressure-sensitive belts, infrared blocks, or surface images. One such example is the Real-Time Position Management Respiratory Gating System (RPM) (Varian Medical Systems, Palo Alto, CA, USA). Briefly, the RPM system uses a plastic block containing two to six markers that reflect infrared light (Figure 9A). These markers are subsequently tracked with an infrared-sensitive charge-coupled device camera, and this video signal is transferred back to the RPM computer. RPM can be used for 4DCT sorting, or coupled with respiratory gating with linear accelerators. Another device that derives an external surrogate includes a pneumatic belt (bellows) (Philips Medical Systems, Cleveland, OH, USA) consisting of a rubber belt that expands and contracts as patients' breathing volumes change (Figure 9A). Changes in the pressure are converted via a transducer to a voltage signal that is then digitized and sent to the CT scanner system for 4DCT sorting. In a simultaneous comparison of bellows and RPM, slight differences in waveform and latency analyses were observed, particularly for low amplitude motions. However, these did not adversely impact image quality or delineations (102). Another example of a pressure sensor is Anzai Medical's small

pneumatic sensor.

Video camera-based, 3D imaging systems are available that are used to derive 3D surface images during RT, for example AlignRT (VisionRT Ltd., London, UK) and C-Rad Sentinel™ (C-RAD AB, Uppsala, Sweden). AlignRT uses two or three cameras combined with a projected speckled-light pattern to derive 3D surface images (shown in Figure 9B), whereas C-Rad uses a line scanning mode with a single camera and laser system. Reference datasets can be derived from RT structure sets (i.e., a CT external structure) or from a previously acquired 3D surface acquisition. Rigid body transformations are used by the systems to perform a least square fit to minimize the difference between the planned 3D model of the patient relative to isocenter and the observed surface model of the patient (103). In a study of simultaneous surface imaging and kV fluoroscopy acquisition of three lung cancer patients in the treatment position, most patient fractions studied showed associations between the abdomen and tumor were equivalent or better than those observed between the diaphragm and tumor. Improved internal-to-external associations have been observed when multiple markers or deformed surface images were used as external surrogates (104-106), although these approaches can be computationally expensive and are not currently incorporated into standard clinical practice. One study explored implementing multiple internal surrogates, such as the air content, lung area, lung density, and body area for 4D CT sorting, and found strong agreement with external surrogates recorded by RPM (107).

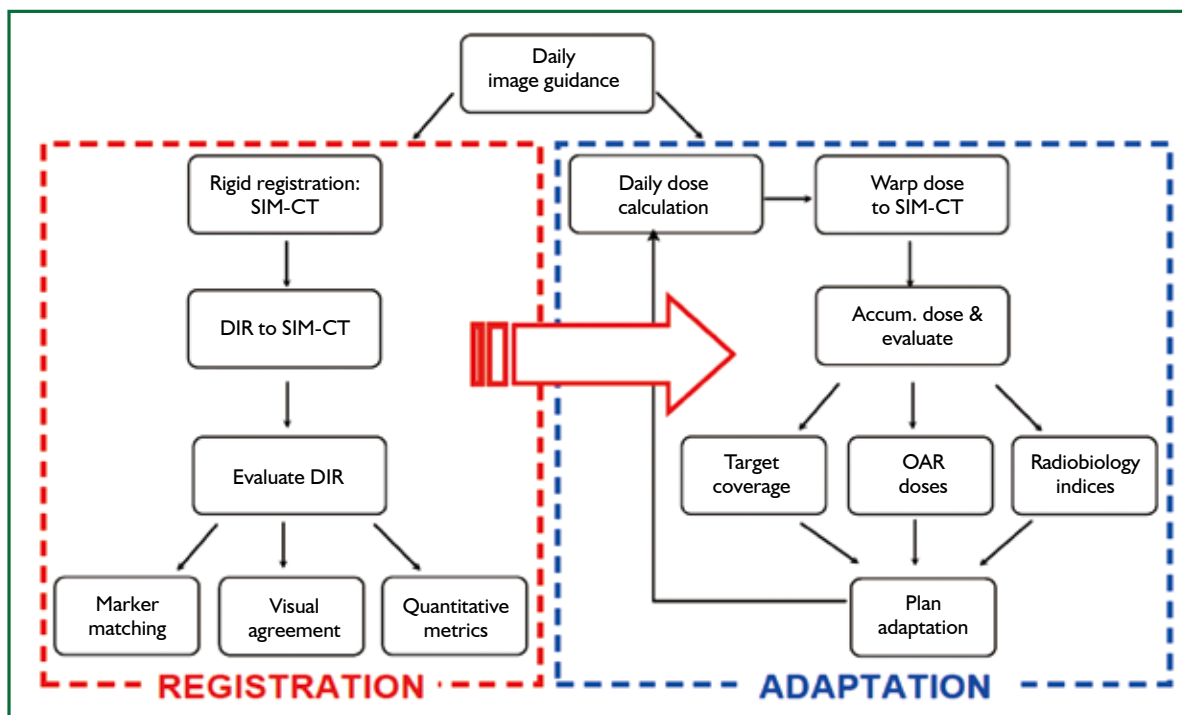


**Figure 10.** Image-guided adaptive radiation therapy framework developed at Henry Ford Health System. Figure adapted from Ref (120).

### Image-guided adaptive radiation therapy (IGART)

While IGRT, such as CBCT, has improved target localization accuracy by providing daily positional information used for online repositioning, daily target and critical structure deformation cannot be fully accounted for using IGRT alone. To combat this, IGART can be implemented. IGART uses patient-specific dynamic/temporal information for potential treatment plan modification during the treatment course (108-110). IGART can address tumor volume and positional changes, as well as other pathologic changes and deformations occurring during the RT treatment course. For lung cancer, inter-fraction baseline variability in lung tumor position, its respiratory trajectory, and normal structures relative to the bony anatomy have been observed (20,36,111-115). Without adjustment, marginal misses can occur. Two cases in point are where a bronchial obstruction is relieved and collapsed lung is re-expanded, resulting in possible tumor shift (116) or in a patient with fluid accumulation in the lungs over the treatment course due to pneumonia (115). Significant reduction in tumor size, particularly for large tumors, has been observed throughout treatment for conventional fractionated radiotherapy of NSCLC (117,118), suggesting that this lung cancer population may benefit most from ART techniques.

Conversely, for SBRT, ART has been shown to offer limited value due to the small amount of target volume changes over the shortened time course (119).

To accomplish IGART, a workflow is needed that includes high-quality, temporal volumetric information that is used as a feedback loop in the DIR, dose reconstruction, dose accumulation, and plan adaptation processes (120) as shown in Figure 10. An offline IGART framework has been implemented consisting of a closed-loop system incorporating feedback from updated patient geometry (i.e., CBCTs) and anatomical information to recompute dose and determine the actual dose delivered to the target and surrounding healthy tissues (120). Similar concepts have been proposed previously (108,121), although a unique feature of the presented framework is that it includes a systematic validation of the DIR algorithm and dose accumulation techniques.

On-line plan re-optimization using an “anatomy of the day” approach has also been implemented. Li *et al.* have developed new IMRT plans using daily IGRT images using a two-step process: segment aperture morphing (SAM), to correct for target deformation/translation using the MLC, and segment weight optimization (SWO), to determine the optimal MU for each segment (122). Full plan re-optimization can be accomplished in ~10 minutes. While this would be challenging to implement

in the clinic, on-line IGART is becoming more realistic due to recent advances in computing such as implementing the graphics processing unit (GPU) (123-125), which has reduced online optimization time from minutes down to seconds.

A prospective, randomized, multi-institutional clinical trial is currently underway to incorporate a during-RT PET/CT-adapted boost for patients with large lung tumors that may potentially benefit from dose escalation (12). In this manner, individualized ART will be performed for patients with inoperable or unresectable stage III NSCLC, a population in which overall prognosis currently remains quite poor despite advances in RT techniques including IMRT and IGRT. Controlled clinical trials such as this will help streamline IGART approaches into clinical practice.

### Conclusions and future directions

Lung cancer RT is complicated by tumor motion, challenges of accurate dose calculation in low density media, and changing anatomy over the treatment course, in addition to radiobiologic and individual patient-response-specific issues. As tumor localization improves, whether via high quality daily IGRT images or tumor tracking, margin reduction and further dose escalation is possible. Furthermore, dose calculation accuracy has substantially improved in recent years, including the ability to incorporate 3D scatter and implement MC for modeling electron transport, and these algorithms are now available in the clinic. 4DCT and DIR have made dose accumulation and IGART possible, and advances in computational speed will continue to make on-line IGART more clinically plausible over the treatment course.

Some promising new techniques currently being evaluated include incorporating biological feedback into treatment planning, such as dynamic contrast-enhanced MRI (DCE-MRI) as an early indicator of treatment response and perfusion changes (126,127), exploring the role of nanoparticles in lung cancer (128), and exploiting radiosensitizers during RT (129). Finding new ways to assess dose response, normal tissue sparing, and identify opportunities for dose escalation, particularly for advanced stage lung cancer patients, is advantageous.

### Acknowledgements

*Disclosure:* HFHS, Department of Radiation Oncology receives grant funding from the NIH/NCI and industrial partners, Varian Medical Systems and Philips Health Care.

### References

- Jemal A, Siegel R, Ward E, et al. Cancer statistics, 2008. *CA Cancer J Clin* 2008;58:71-96.
- Kong FM, Chetty IJ. Advancements in radiation therapy for medically inoperable early stage non-small cell lung cancer: leading article. *Current Medical Literature, Respiratory Medicine* 2006;20:57-65.
- Hayman JA, Martel MK, Ten Haken RK, et al. Dose escalation in non-small-cell lung cancer using three-dimensional conformal radiation therapy: update of a phase I trial. *J Clin Oncol* 2001;19:127-36.
- National Lung Screening Trial Research Team, Aberle DR, Adams AM, et al. Reduced lung-cancer mortality with low-dose computed tomographic screening. *N Engl J Med* 2011;365:395-409.
- Timmerman R, Paulus R, Galvin J, et al. Stereotactic body radiation therapy for inoperable early stage lung cancer. *JAMA* 2010;303:1070-6.
- Kong FM, Ten Haken RK, Schipper MJ, et al. High-dose radiation improved local tumor control and overall survival in patients with inoperable/unresectable non-small-cell lung cancer: long-term results of a radiation dose escalation study. *Int J Radiat Oncol Biol Phys* 2005;63:324-33.
- Movsas B, Moughan J, Swann S, et al. Back to B.E.D. predictors of outcome in RTOG non-operative non-small cell lung cancer (NSCLC) trials. *Int J Radiat Oncol Biol Phys* 2005;63:S230-231.
- Wang L, Correa CR, Zhao L, et al. The effect of radiation dose and chemotherapy on overall survival in 237 patients with Stage III non-small-cell lung cancer. *Int J Radiat Oncol Biol Phys* 2009;73:1383-90.
- Bradley J. Radiation Therapy Oncology Group (RTOG 0617): A randomized phase III comparison of standard dose (60Gy) versus high-dose (74Gy) conformal radiotherapy with concurrent and consolidation carboplatin/ paclitaxel in patients with stage IIIA/IIIB non-small cell lung cancer. Available online: <http://www.rtog.org/ClinicalTrials/ProtocolTable/StudyDetails.aspx?study=0617>
- Bradley J, Paulus R, Komaki R, et al. A randomized phase III comparison of standard-dose (60 Gy) versus high-dose (74 Gy) conformal chemoradiotherapy +/- cetuximab for stage IIIA/IIIB non-small cell lung cancer: preliminary findings on radiation dose in RTOG 0617. 53rd Annual Meeting of the American Society of Radiation Oncology 2011:2-6.
- Cox JD. Are the results of RTOG 0617 mysterious? *Int J Radiat Oncol Biol Phys* 2012;82:1042-4. Available online: <http://dx.doi.org/10.1016/j.ijrobp.2011.12.032>
- RTOG 1106/ACRIN 6697, randomized phase II trial of individualized adaptive radiotherapy using during-treatment FDG-PET/CT and modern technology in locally advanced non-small cell lung cancer (NSCLC). Available online: <http://www.rtog.org/ClinicalTrials/>, (2012).
- Keall PJ, Mageras GS, Balter JM, et al. The management of respiratory motion in radiation oncology report of AAPM Task Group 76. *Med Phys* 2006;33:3874-900.
- Mageras GS, Pevsner A, Yorke ED, et al. Measurement of lung tumor motion using respiration-correlated CT. *Int J Radiat Oncol Biol Phys* 2004;60:933-41.
- Seppenwoolde Y, Shirato H, Kitamura K, et al. Precise and real-time measurement of 3D tumor motion in lung due to breathing and heartbeat,

- measured during radiotherapy. *Int J Radiat Oncol Biol Phys* 2002;53:822-34.
16. Liu HH, Balter P, Tutt T, et al. Assessing respiration-induced tumor motion and internal target volume using four-dimensional computed tomography for radiotherapy of lung cancer. *Int J Radiat Oncol Biol Phys* 2007;68:531-40.
  17. Davies SC, Hill AL, Holmes RB, et al. Ultrasound quantitation of respiratory organ motion in the upper abdomen. *Br J Radiol* 1994;67:1096-102.
  18. Shimizu S, Shirato H, Ogura S, et al. Detection of lung tumor movement in real-time tumor-tracking radiotherapy. *Int J Radiat Oncol Biol Phys* 2001;51:304-10.
  19. Shirato H, Shimizu S, Kunieda T, et al. Physical aspects of a real-time tumor-tracking system for gated radiotherapy. *Int J Radiat Oncol Biol Phys* 2000;48:1187-95.
  20. Hugo G, Vargas C, Liang J, et al. Changes in the respiratory pattern during radiotherapy for cancer in the lung. *Radiother Oncol* 2006;78:326-31.
  21. Mageras GS, Yorke E, Rosenzweig K, et al. Fluoroscopic evaluation of diaphragmatic motion reduction with a respiratory gated radiotherapy system. *J Appl Clin Med Phys* 2001;2:191-200.
  22. Juhler Nøttrup T, Korreman SS, Pedersen AN, et al. Intra- and interfraction breathing variations during curative radiotherapy for lung cancer. *Radiother Oncol* 2007;84:40-8.
  23. ICRU report 62. Prescribing, recording, and reporting photon beam therapy (Supplement to ICRU report 50), (International Commission on Radiation Units and Measurements, Bethesda, MD, 1999).
  24. van Herk M, Remeijer P, Rasch C, et al. The probability of correct target dosage: dose-population histograms for deriving treatment margins in radiotherapy. *Int J Radiat Oncol Biol Phys* 2000;47:1121-35.
  25. Keall PJ, Starkschall G, Shukla H, et al. Acquiring 4D thoracic CT scans using a multislice helical method. *Phys Med Biol* 2004;49:2053-67.
  26. Vedam SS, Keall PJ, Kini VR, et al. Acquiring a four-dimensional computed tomography dataset using an external respiratory signal. *Phys Med Biol* 2003;48:45-62.
  27. Ford EC, Mageras GS, Yorke E, et al. Respiration-correlated spiral CT: a method of measuring respiratory-induced anatomic motion for radiation treatment planning. *Med Phys* 2003;30:88-97.
  28. Wink N, Panknin C, Solberg TD. Phase versus amplitude sorting of 4D-CT data. *J Appl Clin Med Phys* 2006;7:77-85.
  29. Wolthaus JW, Schneider C, Sonke JJ, et al. Mid-ventilation CT scan construction from four-dimensional respiration-correlated CT scans for radiotherapy planning of lung cancer patients. *Int J Radiat Oncol Biol Phys* 2006;65:1560-71.
  30. Zhang T, Chi Y, Meldolesi E, et al. Automatic delineation of on-line head-and-neck computed tomography images: toward on-line adaptive radiotherapy. *Int J Radiat Oncol Biol Phys* 2007;68:522-30.
  31. Rietzel E, Chen GT, Choi NC, et al. Four-dimensional image-based treatment planning: Target volume segmentation and dose calculation in the presence of respiratory motion. *Int J Radiat Oncol Biol Phys* 2005;61:1535-50.
  32. Flampouri S, Jiang SB, Sharp GC, et al. Estimation of the delivered patient dose in lung IMRT treatment based on deformable registration of 4D-CT data and Monte Carlo simulations. *Phys Med Biol* 2006;51:2763-79.
  33. Keall PJ, Siebers JV, Joshi S, et al. Monte Carlo as a four-dimensional radiotherapy treatment-planning tool to account for respiratory motion. *Phys Med Biol* 2004;49:3639-48.
  34. Orban de Xivry J, Janssens G, Bosmans G, et al. Tumour delineation and cumulative dose computation in radiotherapy based on deformable registration of respiratory correlated CT images of lung cancer patients. *Radiother Oncol* 2007;85:232-8.
  35. Rosu M, Balter JM, Chetty IJ, et al. How extensive of a 4D dataset is needed to estimate cumulative dose distribution plan evaluation metrics in conformal lung therapy? *Med Phys* 2007;34:233-45.
  36. Hugo GD, Yan D, Liang J. Population and patient-specific target margins for 4D adaptive radiotherapy to account for intra- and inter-fraction variation in lung tumour position. *Phys Med Biol* 2007;52:257-74.
  37. Admiraal MA, Schuring D, Hurkmans CW. Dose calculations accounting for breathing motion in stereotactic lung radiotherapy based on 4D-CT and the internal target volume. *Radiother Oncol* 2008;86:55-60.
  38. Soofi W, Starkschall G, Britton K, et al. Determination of an optimal organ set to implement deformations to support four-dimensional dose calculations in radiation therapy planning. *J Appl Clin Med Phys* 2008;9:2794.
  39. Papanikolaou N, Battista J, Boyer A, et al. AAPM Report No. 85: Tissue inhomogeneity corrections for megavoltage photon beams. AAPM Report No. 85. Medical Physics Publishing, Madison, WI, 2004:1-135.
  40. Radiation Therapy Oncology Group. RTOG 0236: a phase II trial of stereotactic body radiation therapy (SBRT) in the treatment of patients with medically inoperable stage i/ii non-small cell lung cancer. 2005. Available online: <http://www.rtog.org/ClinicalTrials/>
  41. Reynaert N, van der Marck SC, Schaart DR, et al. Monte Carlo treatment planning for photon and electron beams. *Rad Phys Chem* 2007;76:643-86.
  42. Chetty IJ, Curran B, Cygler JE, et al. Report of the AAPM Task Group No. 105: Issues associated with clinical implementation of Monte Carlo-based photon and electron external beam treatment planning. *Med Phys* 2007;34:4818-53.
  43. Benedict SH, Yenice KM, Followill D, et al. Stereotactic body radiation therapy: the report of AAPM Task Group 101. *Med Phys* 2010;37:4078-101.
  44. Das IJ, Ding GX, Ahnesjö A. Small fields: nonequilibrium radiation dosimetry. *Med Phys* 2008;35:206-15.
  45. Frago M, Wen N, Kumar S, et al. Dosimetric verification and clinical evaluation of a new commercially available Monte Carlo-based dose algorithm for application in stereotactic body radiation therapy (SBRT) treatment planning. *Phys Med Biol* 2010;55:4445-64.
  46. Chetty IJ, Devpura S, Liu D, et al. Correlation of dose computed using different algorithms with local control following stereotactic ablative radiotherapy (SABR)-based treatment of non-small-cell lung cancer. *Radiotherapy and Oncology* 2013;109:498-504.
  47. Allen AM, Czermanska M, Janne PA, et al. Fatal pneumonitis associated

- with intensity-modulated radiation therapy for mesothelioma. *Int J Radiat Oncol Biol Phys* 2006;65:640-5.
48. Marks LB, Bentzen SM, Deasy JO, et al. Radiation dose-volume effects in the lung. *Int J Radiat Oncol Biol Phys* 2010;76:S70-6.
  49. Bortfeld T, Jokivarsi K, Goitein M, et al. Effects of intra-fraction motion on IMRT dose delivery: statistical analysis and simulation. *Phys Med Biol* 2002;47:2203-20.
  50. Li H, Zhong H, Kim J, et al. Investigation of the interplay effect between MLC and lung tumor motions using 4DCT and RPM profile data. *Med Phys* 2011;38:3692.
  51. Yu CX, Jaffray DA, Wong JW. The effects of intra-fraction organ motion on the delivery of dynamic intensity modulation. *Phys Med Biol* 1998;43:91-104.
  52. Matuszak MM, Yan D, Grills I, et al. Clinical applications of volumetric modulated arc therapy. *Int J Radiat Oncol Biol Phys* 2010;77:608-16.
  53. Palma DA, Senan S, Haasbeek CJ, et al. Radiological and clinical pneumonitis after stereotactic lung radiotherapy: a matched analysis of three-dimensional conformal and volumetric-modulated arc therapy techniques. *Int J Radiat Oncol Biol Phys* 2011;80:506-13.
  54. Guckenberger M, Wilbert J, Krieger T, et al. Four-dimensional treatment planning for stereotactic body radiotherapy. *Int J Radiat Oncol Biol Phys* 2007;69:276-85.
  55. Hugo GD, Campbell J, Zhang T, et al. Cumulative lung dose for several motion management strategies as a function of pretreatment patient parameters. *Int J Radiat Oncol Biol Phys* 2009;74:593-601.
  56. Glide-Hurst CK, Hugo GD, Liang J, et al. A simplified method of four-dimensional dose accumulation using the mean patient density representation. *Med Phys* 2008;35:5269-77.
  57. Wolthaus JWH, Schneider C, Sonke JJ, et al. Mid-ventilation CT scan construction from four-dimensional respiration-correlated CT scans for radiotherapy planning of lung cancer patients. *Int J Radiat Oncol Biol Phys* 2006;65:1560-71. Available online: <http://dx.doi.org/10.1016/j.ijrobp.2006.04.031>
  58. Zhong H, Siebers JV. Monte Carlo dose mapping on deforming anatomy. *Phys Med Biol* 2009;54:5815-30.
  59. Zhong H, Weiss E, Siebers JV. Assessment of dose reconstruction errors in image-guided radiation therapy. *Phys Med Biol* 2008;53:719-36.
  60. Heath E, Seuntjens J. A direct voxel tracking method for four-dimensional Monte Carlo dose calculations in deforming anatomy. *Med Phys* 2006;33:434-45.
  61. Heath E, Tessier F, Kawrakow I. Investigation of voxel warping and energy mapping approaches for fast 4D Monte Carlo dose calculations in deformed geometries using VMC++. *Phys Med Biol* 2011;56:S187-202.
  62. Li HS, Zhong H, Kim J, et al. Direct dose mapping versus energy/mass transfer mapping for 4D dose accumulation: fundamental differences and dosimetric consequences. *Phys Med Biol* 2014;59:173-88.
  63. Rueckert D, Sonoda LI, Hayes C, et al. Nonrigid registration using free-form deformations: application to breast MR images. *IEEE Trans Med Imaging* 1999;18:712-21.
  64. Lu W, Chen ML, Olivera GH, et al. Fast free-form deformable registration via calculus of variations. *Phys Med Biol* 2004;49:3067-87.
  65. Brock KK. Results of a multi-institution deformable registration accuracy study (MIDRAS). *Int J Radiat Oncol Biol Phys* 2010;76:583-96.
  66. Hardcastle N, Tomé WA, Cannon DM, et al. A multi-institution evaluation of deformable image registration algorithms for automatic organ delineation in adaptive head and neck radiotherapy. *Radiat Oncol* 2012;7:90.
  67. Schreiber E, Pantalone P, Waller A, et al. A measure to evaluate deformable registration fields in clinical settings. *J Appl Clin Med Phys* 2012;13:3829.
  68. Stanley N, Glide-Hurst C, Kim J, et al. Using patient-specific phantoms to evaluate deformable image registration algorithms for adaptive radiation therapy. *J Appl Clin Med Phys* 2013;14:4363.
  69. Bissonnette JP, Purdie T, Sharpe M, et al. Image-guided stereotactic lung radiation therapy. *Radiat Oncol* 2005;76:S15-S16.
  70. Grills IS, Hugo G, Kestin LL, et al. Image-guided radiotherapy via daily online cone-beam CT substantially reduces margin requirements for stereotactic lung radiotherapy. *Int J Radiat Oncol Biol Phys* 2008;70:1045-56.
  71. Shah C, Grills IS, Kestin LL, et al. Intrafraction Variation of Mean Tumor Position During Image-guided Hypofractionated Stereotactic Body Radiotherapy for Lung Cancer. *Int J Radiat Oncol Biol Phys* 2012;82:1636-41.
  72. Slotman BJ, Lagerwaard FJ, Senan S. 4D imaging for target definition in stereotactic radiotherapy for lung cancer. *Acta Oncol* 2006;45:966-72.
  73. Timmerman R, Abdulrahman R, Kavanagh BD, et al. Lung cancer: a model for implementing stereotactic body radiation therapy into practice. *Front Radiat Ther Oncol* 2007;40:368-85.
  74. Jin JY, Ren L, Liu Q, et al. Combining scatter reduction and correction to improve image quality in cone-beam computed tomography (CBCT). *Med Phys* 2010;37:5634-44.
  75. Wang J, Li T, Xing L. Iterative image reconstruction for CBCT using edge-preserving prior. *Med Phys* 2009;36:252-60.
  76. Feldkamp LA, Davis LC, Kress JW. Practical cone-beam algorithm. *J Opt Soc Am A* 1984;1:612-9.
  77. Wang G, Zhao S, Heuscher D. A knowledge-based cone-beam x-ray CT algorithm for dynamic volumetric cardiac imaging. *Med Phys* 2002;29:1807-22.
  78. Jaffray DA, Siewerdsen JH, Wong JW, et al. Flat-panel cone-beam computed tomography for image-guided radiation therapy. *Int J Radiat Oncol Biol Phys* 2002;53:1337-49.
  79. Purdie TG, Bissonnette JP, Franks K, et al. Cone-beam computed tomography for on-line image guidance of lung stereotactic radiotherapy: localization, verification, and intrafraction tumor position. *Int J Radiat Oncol Biol Phys* 2007;68:243-52.
  80. Guckenberger M, Meyer J, Wilbert J, et al. Cone-beam CT based image-guidance for extracranial stereotactic radiotherapy of intrapulmonary tumors. *Acta Oncol* 2006;45:897-906.
  81. Sonke JJ, Zijp L, Remeijer P, et al. Respiratory correlated cone beam CT.

- Med Phys 2005;32:1176-86.
82. Li T, Xing L, Munro P, et al. Four-dimensional cone-beam computed tomography using an on-board imager. *Med Phys* 2006;33:3825-33.
83. Dietrich L, Jetter S, Tücking T, et al. Linac-integrated 4D cone beam CT: first experimental results. *Phys Med Biol* 2006;51:2939-52.
84. Thompson BP, Hugo GD. Quality and accuracy of cone beam computed tomography gated by active breathing control. *Med Phys* 2008;35:5595-608.
85. Boda-Heggemann J, Fleckenstein J, Lohr F, et al. Multiple breath-hold CBCT for online image guided radiotherapy of lung tumors: simulation with a dynamic phantom and first patient data. *Radiother Oncol* 2011;98:309-16.
86. Glide-Hurst CK, Ionascu D, Berbeco R, et al. Coupling surface cameras with on-board fluoroscopy: a feasibility study. *Med Phys* 2011;38:2937-47.
87. Harada T, Shirato H, Ogura S, et al. Real-time tumor-tracking radiation therapy for lung carcinoma by the aid of insertion of a gold marker using bronchofiberscopy. *Cancer* 2002;95:1720-7.
88. Shimizu S, Shirato H, Ogura S, et al. Detection of lung tumor movement in real-time tumor-tracking radiotherapy. *Int J Radiat Oncol Biol Phys* 2001;51:304-10.
89. Shirato H, Shimizu S, Kitamura K, et al. Four-dimensional treatment planning and fluoroscopic real-time tumor tracking radiotherapy for moving tumor. *Int J Radiat Oncol Biol Phys* 2000;48:435-42.
90. Shirato H, Shimizu S, Kunieda T, et al. Physical aspects of a real-time tumor-tracking system for gated radiotherapy. *Int J Radiat Oncol Biol Phys* 2000;48:1187-95.
91. Onimaru R, Fujino M, Yamazaki K, et al. Steep dose-response relationship for stage I non-small-cell lung cancer using hypofractionated high-dose irradiation by real-time tumor-tracking radiotherapy. *Int J Radiat Oncol Biol Phys* 2008;70:374-81.
92. Shirato H, Oita M, Fujita K, et al. Feasibility of synchronization of real-time tumor-tracking radiotherapy and intensity-modulated radiotherapy from viewpoint of excessive dose from fluoroscopy. *Int J Radiat Oncol Biol Phys* 2004;60:335-41.
93. Seppenwoolde Y, Berbeco RI, Nishioka S, et al. Accuracy of tumor motion compensation algorithm from a robotic respiratory tracking system: a simulation study. *Med Phys* 2007;34:2774-84.
94. Lu XQ, Shanmugham LN, Mahadevan A, et al. Organ deformation and dose coverage in robotic respiratory-tracking radiotherapy. *Int J Radiat Oncol Biol Phys* 2008;71:281-9.
95. Kupelian P, Willoughby T, Mahadevan A, et al. Multi-institutional clinical experience with the Calypso System in localization and continuous, real-time monitoring of the prostate gland during external radiotherapy. *Int J Radiat Oncol Biol Phys* 2007;67:1088-98.
96. Mayse ML, Parikh PJ, Lechleiter KM, et al. Bronchoscopic implantation of a novel wireless electromagnetic transponder in the canine lung: a feasibility study. *Int J Radiat Oncol Biol Phys* 2008;72:93-8.
97. Lechleiter K, Chaudhari A, Malinowski K, et al. SU-FF-J-75: the effect of time on inter-transponder distance implanted in lung: an initial study in a canine mode. *Med Phys* 2007;34:2385.
98. Cook A. FDA grants calypso medical IDE approval for pivotal lung cancer study. 2011.
99. Kupelian PA, Forbes A, Willoughby TR, et al. Implantation and stability of metallic fiducials within pulmonary lesions. *Int J Radiat Oncol Biol Phys* 2007;69:777-85.
100. Gierga DP, Brewer J, Sharp GC, et al. The correlation between internal and external markers for abdominal tumors: implications for respiratory gating. *Int J Radiat Oncol Biol Phys* 2005;61:1551-8.
101. Ionascu D, Jiang SB, Nishioka S, et al. Internal-external correlation investigations of respiratory induced motion of lung tumors. *Med Phys* 2007;34:3893-903.
102. Glide-Hurst CK, Schwenker Smith M, Ajlouni M, et al. Evaluation of two synchronized external surrogates for 4D CT sorting. *J Appl Clin Med Phys* 2013;14:4301.
103. Willoughby T, Lehmann J, Bencomo JA, et al. Quality assurance for nonradiographic radiotherapy localization and positioning systems: report of Task Group 147. *Med Phys* 2012;39:1728-47.
104. Yan H, Zhu G, Yang J, et al. The investigation on the location effect of external markers in respiratory-gated radiotherapy. *J Appl Clin Med Phys* 2008;9:2758.
105. Gianoli C, Riboldi M, Spadea MF, et al. A multiple points method for 4D CT image sorting. *Med Phys* 2011;38:656-67.
106. Schaerer J, Fassi A, Riboldi M, et al. Multi-dimensional respiratory motion tracking from markerless optical surface imaging based on deformable mesh registration. *Phys Med Biol* 2012;57:357-73.
107. Li R, Lewis JH, Cerviño LI, et al. 4D CT sorting based on patient internal anatomy. *Phys Med Biol* 2009;54:4821-33.
108. Yan D, Vicini F, Wong J, et al. Adaptive radiation therapy. *Phys Med Biol* 1997;42:123-32.
109. Yan D, Wong J, Vicini F, et al. Adaptive modification of treatment planning to minimize the deleterious effects of treatment setup errors. *Int J Radiat Oncol Biol Phys* 1997;38:197-206.
110. Yan D, Ziaja E, Jaffray D, et al. The use of adaptive radiation therapy to reduce setup error: a prospective clinical study. *Int J Radiat Oncol Biol Phys* 1998;41:715-20.
111. Sonke JJ, Belderbos J. Adaptive radiotherapy for lung cancer. *Semin Radiat Oncol* 2010;20:94-106.
112. Wulf J, Hädinger U, Oppitz U, et al. Stereotactic radiotherapy of extracranial targets: CT-simulation and accuracy of treatment in the stereotactic body frame. *Radiother Oncol* 2000;57:225-36.
113. Chang J, Mageras GS, Yorke E, et al. Observation of interfractional variations in lung tumor position using respiratory gated and ungated megavoltage cone-beam computed tomography. *Int J Radiat Oncol Biol Phys* 2007;67:1548-58.
114. Sonke JJ, Lebesque J, van Herk M. Variability of four-dimensional computed tomography patient models. *Int J Radiat Oncol Biol Phys* 2008;70:590-8.

115. Glide-Hurst CK, Gopan E, Hugo GD. Anatomic and pathologic variability during radiotherapy for a hybrid active breath-hold gating technique. *Int J Radiat Oncol Biol Phys* 2010;77:910-7.
116. Cohade C, Wahl RL. Applications of positron emission tomography/computed tomography image fusion in clinical positron emission tomography-clinical use, interpretation methods, diagnostic improvements. *Semin Nucl Med* 2003;33:228-37.
117. Woodford C, Yartsev S, Dar AR, et al. Adaptive radiotherapy planning on decreasing gross tumor volumes as seen on megavoltage computed tomography images. *Int J Radiat Oncol Biol Phys* 2007;69:1316-22.
118. Kupelian PA, Ramsey C, Meeks SL, et al. Serial megavoltage CT imaging during external beam radiotherapy for non-small-cell lung cancer: observations on tumor regression during treatment. *Int J Radiat Oncol Biol Phys* 2005;63:1024-8.
119. Haasbeek CJ, Lagerwaard FJ, Cuijpers JP, et al. Is adaptive treatment planning required for stereotactic radiotherapy of stage I non-small-cell lung cancer? *Int J Radiat Oncol Biol Phys* 2007;67:1370-4.
120. Wen N, Glide-Hurst C, Nurushev T, et al. Evaluation of the deformation and corresponding dosimetric implications in prostate cancer treatment. *Phys Med Biol* 2012;57:S361-79.
121. de la Zerda A, Armbruster B, Xing L. Formulating adaptive radiation therapy (ART) treatment planning into a closed-loop control framework. *Phys Med Biol* 2007;52:4137-53.
122. Li XA, Liu F, Tai A, et al. Development of an online adaptive solution to account for inter- and intra-fractional variations. *Radiother Oncol* 2011;100:370-4.
123. Men C, Jia X, Jiang SB. GPU-based ultra-fast direct aperture optimization for online adaptive radiation therapy. *Phys Med Biol* 2010;55:4309-19.
124. Men C, Gu X, Choi D, et al. GPU-based ultrafast IMRT plan optimization. *Phys Med Biol* 2009;54:6565-73.
125. Prax G, Xing L. GPU computing in medical physics: a review. *Med Phys* 2011;38:2685-97.
126. Hugo G, Olsen K, Ford J, et al. WE-C-WAB-03: Correspondence Between FDG-PET and Diffusion-Weighted MRI After Deformable Registration in Locally-Advanced Non-Small Cell Lung Cancer. *Med Phys* 2013;40:477.
127. Ohno Y, Koyama H, Yoshikawa T, et al. Diffusion-weighted MRI versus 18F-FDG PET/CT: performance as predictors of tumor treatment response and patient survival in patients with non-small cell lung cancer receiving chemoradiotherapy. *AJR Am J Roentgenol* 2012;198:75-82.
128. Sukumar UK, Bhushan B, Dubey P, et al. Emerging applications of nanoparticles for lung cancer diagnosis and therapy. *Int Nano Lett* 2013;3:45.
129. Holgersson G, Bergström S, Ekman S, et al. Radiosensitizing biological modifiers enhancing efficacy in non-small-cell lung cancer treated with radiotherapy. *Lung Cancer Management* 2013;2:251-5.



**Cite this article as:** Glide-Hurst CK, Chetty IJ. Improving radiotherapy planning, delivery accuracy, and normal tissue sparing using cutting edge technologies. *J Thorac Dis* 2014;6(4):303-318. doi: 10.3978/j.issn.2072-1439.2013.11.10

## Imaging techniques for tumour delineation and heterogeneity quantification of lung cancer: overview of current possibilities

Wouter van Elmpt<sup>1</sup>, Catharina M.L. Zegers<sup>1</sup>, Marco Das<sup>2</sup>, Dirk De Ruyscher<sup>3</sup>

<sup>1</sup>Department of Radiation Oncology (MAASTRO), <sup>2</sup>Department of Radiology, GROW, School for Oncology and Developmental Biology, Maastricht University Medical Centre, Maastricht, The Netherlands; <sup>3</sup>Radiation Oncology, University Hospitals Leuven/KU Leuven, Leuven, Belgium

### ABSTRACT

Imaging techniques for the characterization and delineation of primary lung tumours and lymph nodes are a prerequisite for adequate radiotherapy. Numerous imaging modalities have been proposed for this purpose, but only computed tomography (CT) and FDG-PET have been implemented in clinical routine. Hypoxia PET, dynamic contrast-enhanced CT (DCE-CT), dual energy CT (DECT) and (functional) magnetic resonance imaging (MRI) hold promise for the future. Besides information on the primary tumour, these techniques can be used for quantification of tissue heterogeneity and response. In the future, treatment strategies may be designed which are based on imaging techniques to optimize individual treatment.

### KEY WORDS

Lung cancer; imaging; tumour delineation; heterogeneity

*J Thorac Dis 2014;6(4):319-327. doi: 10.3978/j.issn.2072-1439.2013.08.62*

### Introduction

Lung cancer is the single most important cause of cancer deaths in all developed countries (1). In the upcoming countries such as China, it is expected that lung cancer will have epidemic proportions within a few decades (2). Radiotherapy plays an increasing role in all stages of lung cancer: stage I non-small cell lung cancer (NSCLC) is treated with stereotactic body radiotherapy (SBRT) (3), also called stereotactic ablative radiotherapy or SABR with results that equal those of surgery. Stage III NSCLC and small cell lung cancer (SCLC) is most often treated with combined chemotherapy and radiotherapy and patients with oligometastases may experience long-term disease-free survival with treatment that includes radiotherapy (4,5).

However, a thorough definition of the tumour to be irradiated is a prerequisite for successful radiotherapy. Visualisation of the

tumour boundaries using morphological imaging techniques such as computed tomography (CT) or magnetic resonance imaging (MRI) are of importance, but also the biological characteristics of the cancer and of the organs at risk (OAR) can nowadays be visualized using molecular imaging e.g., positron emission tomography (PET) techniques. Assessment of this biological heterogeneity of tumours using imaging may lead to more individualized therapy. Using the knowledge of characteristics of the tumour and of the OARs should enable an optimised therapeutic ratio. Although seemingly obvious, reality shows that achieving this goal has been proven to be difficult. Definition of the tumour boundaries with high accuracy and low inter- and intra-observed variability is hampered by the lack of validated automated systems that work well for complicated volumes that are surrounded by OARs with similar densities. Biological characteristics can be imaged, but their implementation in standard practice requires prospective clinical studies showing improved outcomes.

The present manuscript will focus on the delineation and characterization of primary tumour and lymph node involvement in lung cancer patients using the latest available imaging techniques. Some of these techniques are already applied in clinical practice and some of them are still on a research level. Furthermore, an outlook is given how to use these methods in the future to individualize lung cancer treatment and to optimize the balance between local tumour control and organ toxicity.

Correspondence to: Wouter van Elmpt, Ph.D. Department of Radiation Oncology (MAASTRO), GROW, School for Oncology and Developmental Biology, Maastricht University Medical Centre, Dr. Tanslaan 12, NL-6229 ET Maastricht, The Netherlands. Email: wouter.vanelmpt@maastro.nl.

Submitted Aug 05, 2013. Accepted for publication Aug 21, 2013.  
Available at [www.jthoracdis.com](http://www.jthoracdis.com)

ISSN: 2072-1439

© Pioneer Bioscience Publishing Company. All rights reserved.

## Imaging modalities for target volume delineation and quantification

### FDG-PET/CT

The accuracy of FDG-PET is higher than CT for the staging of mediastinal lymph nodes in advanced stage lung cancer. Hence, the incorporation of PET in the treatment planning process of radiotherapy is logical. In many planning studies in NSCLC, the use of FDG-PET has resulted in a decrease of the irradiated volumes of the OARs, which may lead to less side effects or to the possibility of radiation dose-escalation with the aim to improve local tumour control (6,7). Prospective studies both in NSCLC and in SCLC indeed showed that selective mediastinal node irradiation based on FDG-PET scans did not lead to higher isolated nodal recurrences (8-10).

The use of FDG-PET in radiotherapy planning was shown to reduce variability of tumour delineation amongst radiation oncologists and allows automatic tumour delineation that can be followed with manual editing if required (11-13). To use PET/CT equipment directly for radiotherapy treatment planning purposes, some additional criteria have to be considered. A detailed overview on the basic technical aspects and recommendations for radiotherapy treatment planning is described in Thorwarth *et al.* (14). On a standard 3D PET/CT acquisition, small lesions might be difficult to detect due to the intrinsic blurring of breathing motion and might also lead to inaccurate quantification of the standardized uptake value (SUV) compared to respiratory correlated 4D acquisitions (15). PET/CT scanners have options for acquiring the images in a respiration correlated (4D) mode to compensate for breathing motion in thorax. Furthermore, several publications have shown that 4D PET indeed improves lesion detectability (16,17). The 4D scan is usually reconstructed as a set of 5, 8 or 10 3D PET/CT scans representing the different phases of the respiratory cycle (18). Acquiring such a 4D PET scan together with a 4D CT scan is however not yet widely implemented in practice. A drawback of the 4D image acquisition is the somewhat prolonged acquisition times that might limit throughput on the PET/CT scanners and not all software systems are able to visualize this large amount of imaging data. However by using more advanced reconstruction algorithms that use only the part of the acquisition without breathing motion (e.g., the exhale phase) (19,20) or (non-rigidly) register the various breathing phases of the PET image to a single image (21) the workflow might be improved.

Tumour delineation for radiotherapy treatment planning purposes is a time-consuming manual procedure that is associated with a lot of intra- and inter-observer variability (22).

Although the use of strict delineation protocols decrease variability (23), the time investment for delineation still remains and is limiting for adaptation protocols as well. As in radiotherapy the CT scan is used as the primary dataset because of the accurate quantification of (electron) density necessary for the dose calculation of the radiotherapy treatment plan, automatic segmentation based on CT scans are logical. Moreover, 4D-CT scans have been implemented in routine practice and this movement information can readily be accounted for in automatic delineation protocols. On the other hand, FDG-PET scans do correlate better with anatomical boundaries than CT if the tumour is surrounded by lung (24). Combining CT and FDG-PET is therefore logical and automatic segmentation methods could reduce delineation time. However, only few studies have validated their automated segmentation method with pathology (22,25-28) and there is a lack of technical validation and accuracy as well (29,30). Fully automated tumour segmentation has therefore not been implemented in routine clinical practice.

### Hypoxia PET

Tumour cell hypoxia is a known characteristic of solid tumour lesions, which negatively influences treatment efficacy (31). Accurate identification of tumour hypoxia is of importance to select patients which will benefit from specific anti-hypoxic treatments. The use of the Eppendorf electrode is the gold standard to assess tumour hypoxia, however this method has the disadvantage to be invasive, limiting its use to well accessible superficial tumours (32). Hypoxia PET imaging allows a non-invasive detection and quantification of tumour hypoxia and it provides the opportunity to display the spatial distribution of hypoxia, which is essential for its integration in radiation dose distribution. The most common mechanism to detect tumour hypoxia is the use of 2-nitroimidazoles PET tracers which show a selective binding and retention in the hypoxic tumour cells.

Several 2-nitroimidazoles, labelled with fluor-18 [<sup>18</sup>F], have already been applied in patients to identify hypoxia. The first and most familiar hypoxia PET tracer is [<sup>18</sup>F]MISO, however, a slow accumulation in the hypoxic lesions and limited normal tissue clearance limits its clinical use (33). Therefore, alternative tracers are developed to improve the pharmacokinetic properties of the hypoxia tracer by enhancing the hydrophilicity and clearance of the tracer, examples are [<sup>18</sup>F]AZA, [<sup>18</sup>F]ETNIM, [<sup>18</sup>F]EF3, [<sup>18</sup>F]HX4 and the nucleoside conjugate Cu-ATSM.

Quantification of tumour hypoxia based on PET imaging can be performed on static images, acquired at a certain time-point post-injection, or based on dynamic acquisitions, which takes also perfusion of the lesion into account (34). Figure 1 shows an

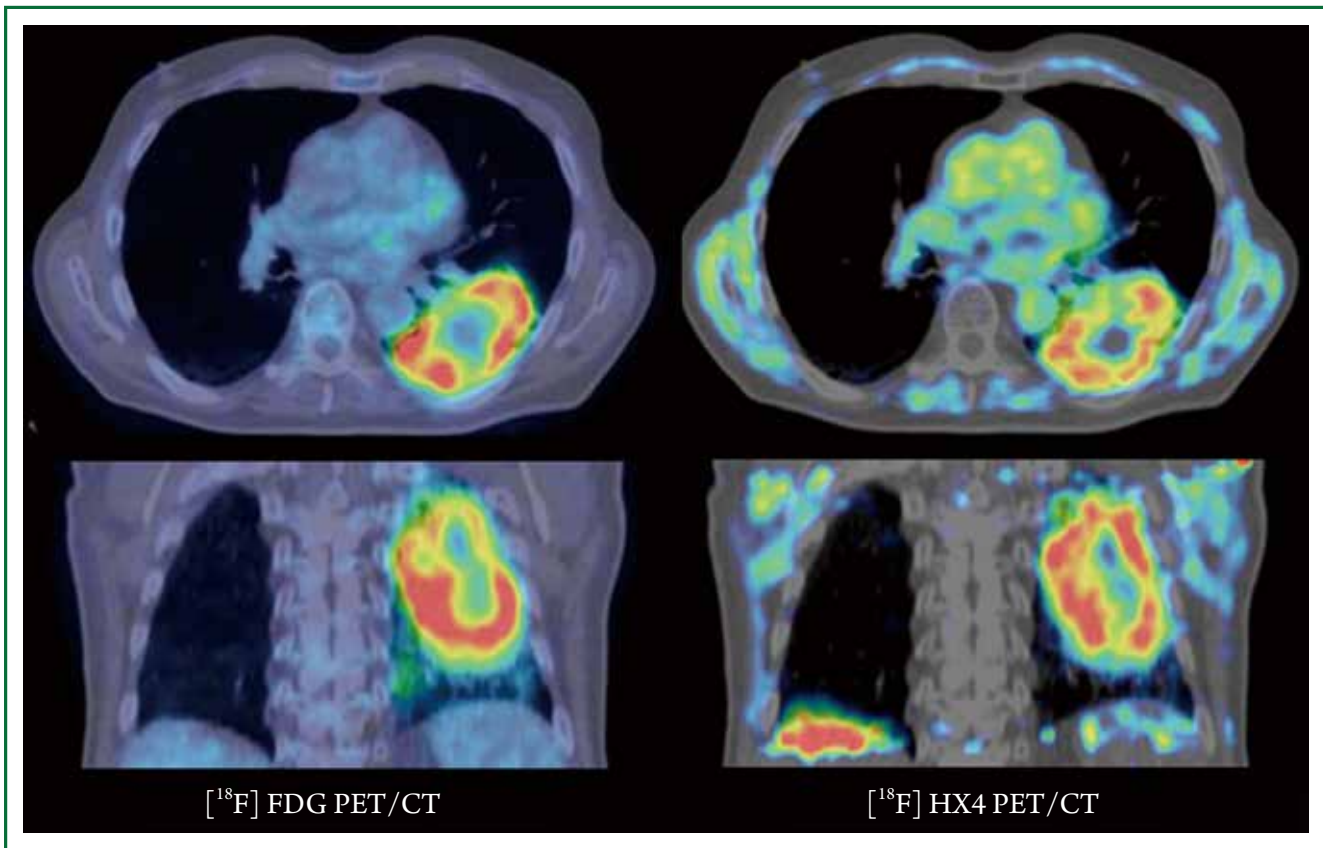


**Figure 1.** Example of a NSCLC patient having both an FDG-PET/CT scan (left) and a hypoxia HX4-PET/CT scan. Clearly visible is the tumour heterogeneity both on the metabolic (FDG) and hypoxic (HX4) PET image.

example of a lung cancer patient having both an FDG-PET/CT scan and an hypoxia [ $^{18}\text{F}$ ]HX4-PET/CT scan. In NSCLC patients, hypoxia PET has shown to be correlated with prognosis and to give different information than FDG uptake (35,36). Studies with hypoxia PET imaging show the presence of tumour cell hypoxia in the majority of NSCLC lesions (37-40). The extent of tumour hypoxia correlates with tumour response and risk of relapse after radiotherapy (41,42). Recent theoretical studies show that boosting or dose painting by numbers based on hypoxia imaging is feasible and that an increased radiation dose to the radio-resistant/hypoxic areas may result in an increased local control (43-45).

### **MRI**

MRI provides high-resolution anatomical information with excellent soft-tissue contrast. Its use for delineation of the tumour and lymph nodes has been investigated. A major issue is obviously the movement of tumours that may cause significant artefacts. To deal with motion, two particular acquisition

sequences have been useful: fast low-angle shot (FLASH) and true fast imaging with steady-state precession (TrueFISP) (46,47). Both techniques showed regular and synchronous diaphragm and chest-wall motion of diagnostic quality. Dynamic MRI can be used to define an Internal Target Volume (ITV) as it allows imaging of the entire lung volume over the breathing cycle. However, dynamic MRI scans of the lung are still prone to artefacts, which affect registration accuracy.

To the best of our knowledge, there have been no contouring studies comparing MRI to CT or FDG-PET-CT in lung cancer, neither have there been validation studies with pathology. Nevertheless, to differentiate benign from malignant nodules, Diffusion Weighted MRI (DW-MRI) may have similar accuracy as FDG-PET scans (48).

### **Dynamic contrast-enhanced CT (DCE-CT)**

DCE-CT (or perfusion CT) imaging is a relatively new method for tumour characterization. It offers a fast way to assess functional parameters in lung cancer patients. To date DCE-CT is still a

research tool, but initial results are showing promising results for the future. DCE-CT scans give information on the blood flow (BF), blood volume (BV) and permeability of the vessels (49-52). Whereas in the literature some DCE-CT studies were hampered by the limited field-of-view (e.g., 3-5 cm) of the scanner in the cranial-caudal direction, the technical infrastructure nowadays has the ability to capture DCE-CT scans of large volumes up to 12 cm. The reproducibility of the extracted parameters of the DCE-CT scan is also within an acceptable range (49,50,53) and allows larger patient studies to look at prognostic factors for treatment outcome. These parameters are related to accessibility for chemotherapy or anti-angiogenesis drugs (54) and shown to be different between treatment responders and non-responders (53). In some series, DCE-CT extracted values correlated with prognosis and with the histological subtype of NSCLC (55). DCE-CT values give other information than FDG uptake and therefore may be complementary to characterise tumours. The clinical and prognostic implications are not yet fully understood and the number of patients who have been studied with DCE-CT is still low. Thus further clinical studies are needed to assess the value of DCE-CT for the future individualized treatment and prognosis. In a recent study by Mandeville *et al.* DCE-CT parameters were evaluated in relation to markers of hypoxia (56). It was shown that BV and BF was inversely correlated to immuno-histochemical markers for hypoxia. Recently it has been shown by Lee *et al.* that reproducibility is high in DCE-CT (57). If DCE-CT is used to measure enhancement curves over time Hwang *et al.* could show that enhancement patterns correspond to tumor staging (58). Interestingly, looking into other body regions DCE-CT parameters might be able to predict survival, as, e.g., was shown by Koh *et al.* in patients with colorectal cancer (59). Spira *et al.* evaluated DCE-CT parameters in correlated these to histopathological findings, showing good correlation especially for microvascular density (MVD) (60). Fraioli *et al.* could demonstrate the correlation between altered perfusion parameters after treatment—indicating treatment response (61).

### **Dual energy CT (DECT)**

Newest CT scanner technology is capable of applying two different kV setting simultaneously or rapidly after each other. The two different resulting scans can be used for tissue characterization and iodine mapping. Some studies tried to use iodine mapping for lung tumour characterization, showing initially promising results (62-64). Initial differentiation between benign and malignant pulmonary nodules seems possible, but

the number of studied patients is still too low and the real clinical problem of small pulmonary nodules <8 mm currently cannot be solved sufficiently (65-67).

### **Imaging modalities for normal tissue characterization**

Radiotherapy is always pushing the optimization of maximum tumour control with an accepted (low) level of side-effects. Radiation induced lung toxicity (RILT) is one of the major dose limiting factor in escalating the dose to lung tumours; Therefore assessment of the lung function could potentially play an important role in the design of the treatment plan. Various imaging techniques can be utilized to quantify the lung function also on a local scale, besides the general pulmonary lung function tests that only give a global assessment of the lung function.

#### **SPECT/CT**

The use of SPECT/CT for quantification of perfusion and ventilation defects in the lung is a frequently used modality for assessing lung function using imaging although the spatial resolution of the SPECT scan is limited. Radiotherapy has been shown to cause lung perfusion alterations in NSCLC patients with perfusion (68-70). Knowledge about the regional sensitivity and functioning of the lung may also guide the treatment plan design to avoid highly functioning regions inside the lung (71-74). However the hypothesis of reduced lung toxicity still has to be validated in clinical trials.

#### **CT**

CT density changes have been described after radiotherapy and show remarkable variability between patients (75,76). In depth analysis of CT characteristics of the lungs may lead to the definition of risk groups for radiation-induced lung damage.

#### **PET/CT**

The uptake of FDG in the lungs probably reflects the inflammatory status. It was found that a high FDG uptake in the lungs before radiotherapy is an independent risk factor to develop subsequent radiation pneumonitis (77). FDG-avid areas in the lungs were at the highest susceptibility for pneumonitis. Further studies are needed to elaborate on these findings before this can be used to change radiation dose distributions in the

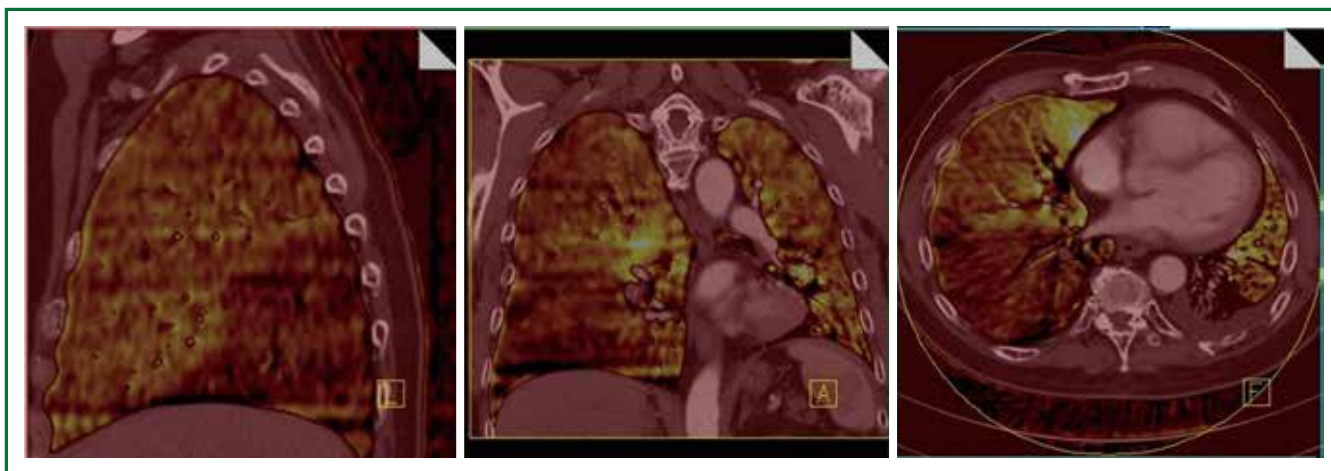


**Figure 2.** An example of a patient with emboli in the segmental arteries causing a large perfusion defect of the right lower lobe.

lungs on the basis of FDG uptake patterns.

### **MRI**

MRI scans using inert hyperpolarised helium-3 gas that is inhaled by the patient show ventilated areas in the lungs (78). Non-ventilated regions do not show an MRI signal. In theoretical studies, the incorporation of this information decreased the V20 of the lungs significantly (78). However, this strategy was never investigated in prospective trials and thus remains investigational.

### **DECT**

DECT for visualizing lung perfusion is often used in the context of the detection of pulmonary embolism (PE) (79-83). An iodine contrast material (CM) is administered and using 2 energy settings of the CT scanner (usually 80/140 kV) it is possible to visualize the distribution of iodine in the lungs. CT is the method of choice to rule out acute PE, nicely showing the emboli up to the sub-segmental level. With the use of DECT it has become possible not only to show the embolus, but also to show corresponding perfusion defects. This is of clinical importance, as was shown in earlier studies—single sub-segmental emboli (not causing significant perfusion defects) can be left untreated (84). Based on the assumption that radiation therapy of the lung may also alter CM perfusion in the lung, this technique offers potential for further assessment of patients treated for lung cancer with radiotherapy. Figure 2 shows an example of a PE in the right lower lobe causing a large perfusion defect.

While DECT is primarily used for iodine perfusion maps of the lung, Xenon ventilation consequently adds the missing

part of ventilation maps for the patients. In the last years some study groups could show that the use of Xenon ventilation is feasible and safe and could also show that ventilation maps may add additional value in different pathologies such as asthma, in intensive care patients or even in children (85-93).

### **Treatment individualization using imaging**

The next major step forward that is currently tested in clinical trials is the dose-painting hypothesis (94,95). The rationale for this is the heterogeneous nature of tumours. Differences in biological characteristics throughout tumours make them respond non-uniformly to treatment (96). Hence treatment resistant parts of the tumours are with the current homogeneous irradiation treatment techniques not optimally treated. Individualizing the treatment by using imaging information to guide or define the actual dose-response relationship is the next phase of treatment individualization (97). A currently on-going multi-centric trial in advanced NSCLC is testing the hypothesis whether a uniform dose or a boost dose to the high metabolic active volumes gives rise to better local control rates (98).

Another way of using imaging information to individualize treatment is in the context of response assessment. Using repeated imaging during treatment may provide predictive information to treatment success. Hypoxic (e.g., HX4, FAZA, FMISO), metabolic (e.g., FDG) or proliferation [e.g., FLT, (99)] PET tracers allow early in the course of treatment already an assessment of treatment (100). MRI scans can be used to evaluate changes in tumours during radiotherapy as well (101). DW-MRI derived ADC (apparent diffusion coefficient) values changes correlate well with survival. However, ADC and FDG

changes also correlate significantly. It remains unclear what the clinical value is of these predictive parameters.

With the current fractionated radiotherapy schedules in lung cancer of 4-6 weeks, there is still room for adaptation of the treatment. As previously stated, these adaptations of the treatment plan can be based either on reducing side-effects or increasing the chance of local tumour control.

## Conclusions

Imaging is an integral part of target volume delineation used in current clinical practice. Tumour characterization is the next step that needs to be exploited. To fully optimize the therapeutic ratio also normal tissue toxicity is of importance. Assessment of imaging features to characterize tissue functioning should be explored as well in the context of individualized treatment optimization.

## Acknowledgements

One of the authors (W.v.E.) would like to acknowledge funding (KWF MAC 2011-4970) from the Dutch Cancer Society.

*Disclosure:* The authors declare no conflict of interest.

## References

1. Simard EP, Ward EM, Siegel R, et al. Cancers with increasing incidence trends in the United States: 1999 through 2008. *CA Cancer J Clin* 2012. [Epub ahead of print].
2. She J, Yang P, Hong Q, et al. Lung cancer in China: challenges and interventions. *Chest* 2013;143:1117-26.
3. Lagerwaard FJ, Haasbeek CJ, Smit EF, et al. Outcomes of risk-adapted fractionated stereotactic radiotherapy for stage I non-small-cell lung cancer. *Int J Radiat Oncol Biol Phys* 2008;70:685-92.
4. De Ruyscher D, Belderbos J, Reymen B, et al. State of the art radiation therapy for lung cancer 2012: a glimpse of the future. *Clin Lung Cancer* 2013;14:89-95.
5. De Ruyscher D, Wanders R, van Baardwijk A, et al. Radical treatment of non-small-cell lung cancer patients with synchronous oligometastases: long-term results of a prospective phase II trial (Nct01282450). *J Thorac Oncol* 2012;7:1547-55.
6. Nestle U, Kremp S, Grosu AL. Practical integration of [18F]-FDG-PET and PET-CT in the planning of radiotherapy for non-small cell lung cancer (NSCLC): the technical basis, ICRU-target volumes, problems, perspectives. *Radiother Oncol* 2006;81:209-25.
7. van Der Wel A, Nijsten S, Hochstenbag M, et al. Increased therapeutic ratio by 18FDG-PET CT planning in patients with clinical CT stage N2-N3M0 non-small-cell lung cancer: a modeling study. *Int J Radiat Oncol Biol Phys* 2005;61:649-55.
8. De Ruyscher D, Wanders S, van Haren E, et al. Selective mediastinal node irradiation based on FDG-PET scan data in patients with non-small-cell lung cancer: a prospective clinical study. *Int J Radiat Oncol Biol Phys* 2005;62:988-94.
9. Belderbos JS, Heemsbergen WD, De Jaeger K, et al. Final results of a Phase I/II dose escalation trial in non-small-cell lung cancer using three-dimensional conformal radiotherapy. *Int J Radiat Oncol Biol Phys* 2006;66:126-34.
10. van Loon J, De Ruyscher D, Wanders R, et al. Selective nodal irradiation on basis of (18)FDG-PET scans in limited-disease small-cell lung cancer: a prospective study. *Int J Radiat Oncol Biol Phys* 2010;77:329-36.
11. Steenbakkers RJ, Duppen JC, Fitton I, et al. Observer variation in target volume delineation of lung cancer related to radiation oncologist-computer interaction: a 'Big Brother' evaluation. *Radiother Oncol* 2005;77:182-90.
12. Caldwell CB, Mah K, Ung YC, et al. Observer variation in contouring gross tumor volume in patients with poorly defined non-small-cell lung tumors on CT: the impact of 18FDG-hybrid PET fusion. *Int J Radiat Oncol Biol Phys* 2001;51:923-31.
13. Werner-Wasik M, Nelson AD, Choi W, et al. What is the best way to contour lung tumors on PET scans? Multiobserver validation of a gradient-based method using a NSCLC digital PET phantom. *Int J Radiat Oncol Biol Phys* 2012;82:1164-71.
14. Thorwarth D, Beyer T, Boellaard R, et al. Integration of FDG-PET/CT into external beam radiation therapy planning: technical aspects and recommendations on methodological approaches. *Nuklearmedizin* 2012;51:140-53.
15. Nehmeh SA, Erdi YE, Ling CC, et al. Effect of respiratory gating on quantifying PET images of lung cancer. *J Nucl Med* 2002;43:876-81.
16. Aristophanous M, Berbeco RI, Killoran JH, et al. Clinical utility of 4D FDG-PET/CT scans in radiation treatment planning. *Int J Radiat Oncol Biol Phys* 2012;82:e99-105.
17. García Vicente AM, Soriano Castrejon AM, Talavera Rubio MP, et al. (18)F-FDG PET-CT respiratory gating in characterization of pulmonary lesions: approximation towards clinical indications. *Ann Nucl Med* 2010;24:207-14.
18. Dawood M, Buther F, Lang N, et al. Respiratory gating in positron emission tomography: a quantitative comparison of different gating schemes. *Med Phys* 2007;34:3067-76.
19. Liu C, Alessio A, Pierce L, et al. Quiescent period respiratory gating for PET/CT. *Med Phys* 2010;37:5037-43.
20. van Elmpt W, Hamill J, Jones J, et al. Optimal gating compared to 3D and 4D PET reconstruction for characterization of lung tumours. *Eur J Nucl Med Mol Imaging* 2011;38:843-55.
21. Dawood M, Lang N, Jiang X, et al. Lung motion correction on respiratory gated 3-D PET/CT images. *IEEE Trans Med Imaging* 2006;25:476-85.
22. van Baardwijk A, Bosmans G, Boersma L, et al. PET-CT-based auto-contouring in non-small-cell lung cancer correlates with pathology and

- reduces interobserver variability in the delineation of the primary tumor and involved nodal volumes. *Int J Radiat Oncol Biol Phys* 2007;68:771-8.
23. Bayne M, Hicks RJ, Everitt S, et al. Reproducibility of "intelligent" contouring of gross tumor volume in non-small-cell lung cancer on PET/CT images using a standardized visual method. *Int J Radiat Oncol Biol Phys* 2010;77:1151-7.
  24. van Loon J, Siedschlag C, Stroom J, et al. Microscopic disease extension in three dimensions for non-small-cell lung cancer: development of a prediction model using pathology-validated positron emission tomography and computed tomography features. *Int J Radiat Oncol Biol Phys* 2012;82:448-56.
  25. Schaefer A, Kim YJ, Kremp S, et al. PET-based delineation of tumour volumes in lung cancer: comparison with pathological findings. *Eur J Nucl Med Mol Imaging* 2013;40:1233-44.
  26. Cheebsumon P, Boellaard R, de Ruyscher D, et al. Assessment of tumour size in PET/CT lung cancer studies: PET- and CT-based methods compared to pathology. *EJNMMI Res* 2012;2:56.
  27. Hatt M, Cheze-le Rest C, van Baardwijk A, et al. Impact of tumor size and tracer uptake heterogeneity in (18)F-FDG PET and CT non-small cell lung cancer tumor delineation. *J Nucl Med* 2011;52:1690-7.
  28. Stroom J, Blaauwgeers H, van Baardwijk A, et al. Feasibility of pathology-correlated lung imaging for accurate target definition of lung tumors. *Int J Radiat Oncol Biol Phys* 2007;69:267-75.
  29. Zaidi H, El Naqa I. PET-guided delineation of radiation therapy treatment volumes: a survey of image segmentation techniques. *Eur J Nucl Med Mol Imaging* 2010;37:2165-87.
  30. Lee JA. Segmentation of positron emission tomography images: some recommendations for target delineation in radiation oncology. *Radiother Oncol* 2010;96:302-7.
  31. Wouters BG, van den Beucken T, Magagnin MG, et al. Targeting hypoxia tolerance in cancer. *Drug Resist Updat* 2004;7:25-40.
  32. Bollineni VR, Wiegman EM, Pruijm J, et al. Hypoxia imaging using Positron Emission Tomography in non-small cell lung cancer: implications for radiotherapy. *Cancer Treat Rev* 2012;38:1027-32.
  33. Mees G, Dierckx R, Vangestel C, et al. Molecular imaging of hypoxia with radiolabelled agents. *Eur J Nucl Med Mol Imaging* 2009;36:1674-86.
  34. Thorwarth D, Eschmann SM, Scheiderbauer J, et al. Kinetic analysis of dynamic 18F-fluoromisonidazole PET correlates with radiation treatment outcome in head-and-neck cancer. *BMC Cancer* 2005;5:152.
  35. Cherk MH, Foo SS, Poon AM, et al. Lack of correlation of hypoxic cell fraction and angiogenesis with glucose metabolic rate in non-small cell lung cancer assessed by 18F-Fluoromisonidazole and 18F-FDG PET. *J Nucl Med* 2006;47:1921-6.
  36. Bollineni VR, Kerner GS, Pruijm J, et al. PET imaging of tumor hypoxia using 18F-Fluoroazomycin arabinoside in stage III-IV non-small cell lung cancer patients. *J Nucl Med* 2013;54:1175-80.
  37. Li L, Hu M, Zhu H, et al. Comparison of 18F-Fluoroerythronitroimidazole and 18F-fluorodeoxyglucose positron emission tomography and prognostic value in locally advanced non-small-cell lung cancer. *Clin Lung Cancer* 2010;11:335-40.
  38. Gagel B, Reinartz P, Demirel C, et al. [18F] fluoromisonidazole and [18F] fluorodeoxyglucose positron emission tomography in response evaluation after chemo-/radiotherapy of non-small-cell lung cancer: a feasibility study. *BMC Cancer* 2006;6:51.
  39. Postema EJ, McEwan AJ, Riauka TA, et al. Initial results of hypoxia imaging using 1-alpha-D: -(5-deoxy-5-[18F]-fluoroarabinofuranosyl)-2-nitroimidazole (18F-FAZA). *Eur J Nucl Med Mol Imaging* 2009;36:1565-73.
  40. Koh WJ, Bergman KS, Rasey JS, et al. Evaluation of oxygenation status during fractionated radiotherapy in human nonsmall cell lung cancers using [F-18]fluoromisonidazole positron emission tomography. *Int J Radiat Oncol Biol Phys* 1995;33:391-8.
  41. Eschmann SM, Paulsen F, Reimold M, et al. Prognostic impact of hypoxia imaging with 18F-misonidazole PET in non-small cell lung cancer and head and neck cancer before radiotherapy. *J Nucl Med* 2005;46:253-60.
  42. Dehdashti F, Mintun MA, Lewis JS, et al. In vivo assessment of tumor hypoxia in lung cancer with 60Cu-ATSM. *Eur J Nucl Med Mol Imaging* 2003;30:844-50.
  43. Thorwarth D, Eschmann SM, Paulsen F, et al. Hypoxia dose painting by numbers: a planning study. *International journal of radiation oncology, biology, physics* 2007;68:291-300.
  44. Hendrickson K, Phillips M, Smith W, et al. Hypoxia imaging with [F-18] FMISO-PET in head and neck cancer: potential for guiding intensity modulated radiation therapy in overcoming hypoxia-induced treatment resistance. *Radiother Oncol* 2011;101:369-75.
  45. Thorwarth D, Alber M. Implementation of hypoxia imaging into treatment planning and delivery. *Radiother Oncol* 2010;97:172-5.
  46. Plathow C, Klopp M, Fink C, et al. Quantitative analysis of lung and tumour mobility: comparison of two time-resolved MRI sequences. *Br J Radiol* 2005;78:836-40.
  47. Blackall JM, Ahmad S, Miquel ME, et al. MRI-based measurements of respiratory motion variability and assessment of imaging strategies for radiotherapy planning. *Phys Med Biol* 2006;51:4147-69.
  48. Mori T, Nomori H, Ikeda K, et al. Diffusion-weighted magnetic resonance imaging for diagnosing malignant pulmonary nodules/masses: comparison with positron emission tomography. *J Thorac Oncol* 2008;3:358-64.
  49. Ng QS, Goh V, Fichte H, et al. Lung cancer perfusion at multi-detector row CT: reproducibility of whole tumor quantitative measurements. *Radiology* 2006;239:547-53.
  50. Ng QS, Goh V, Milner J, et al. Acute tumor vascular effects following fractionated radiotherapy in human lung cancer: in vivo whole tumor assessment using volumetric perfusion computed tomography. *Int J Radiat Oncol Biol Phys* 2007;67:417-24.
  51. Miles KA, Griffiths MR. Perfusion CT: a worthwhile enhancement? *Br J Radiol* 2003;76:220-31.
  52. Miles KA, Griffiths MR, Fuentes MA. Standardized perfusion value: universal CT contrast enhancement scale that correlates with FDG PET in

- lung nodules. *Radiology* 2001;220:548-53.
53. Wang J, Wu N, Cham MD, et al. Tumor response in patients with advanced non-small cell lung cancer: perfusion CT evaluation of chemotherapy and radiation therapy. *AJR Am J Roentgenol* 2009;193:1090-6.
  54. Lazanyi KS, Abramyuk A, Wolf G, et al. Usefulness of dynamic contrast enhanced computed tomography in patients with non-small-cell lung cancer scheduled for radiation therapy. *Lung Cancer* 2010;70:280-5.
  55. Shastry M, Miles KA, Win T, et al. Integrated 18F-fluorodeoxyglucose-positron emission tomography/dynamic contrast-enhanced computed tomography to phenotype non-small cell lung carcinoma. *Mol Imaging* 2012;11:353-60.
  56. Mandeville HC, Ng QS, Daley FM, et al. Operable non-small cell lung cancer: correlation of volumetric helical dynamic contrast-enhanced CT parameters with immunohistochemical markers of tumor hypoxia. *Radiology* 2012;264:581-9.
  57. Lee SM, Lee HJ, Kim JJ, et al. Adaptive 4D volume perfusion CT of lung cancer: effects of computerized motion correction and the range of volume coverage on measurement reproducibility. *AJR Am J Roentgenol* 2013;200:W603-9.
  58. Hwang SH, Yoo MR, Park CH, et al. Dynamic contrast-enhanced CT to assess metabolic response in patients with advanced non-small cell lung cancer and stable disease after chemotherapy or chemoradiotherapy. *Eur Radiol* 2013;23:1573-81.
  59. Koh TS, Ng QS, Thng CH, et al. Primary colorectal cancer: use of kinetic modeling of dynamic contrast-enhanced CT data to predict clinical outcome. *Radiology* 2013;267:145-54.
  60. Spira D, Neumeister H, Spira SM, et al. Assessment of tumor vascularity in lung cancer using volume perfusion CT (VPCT) with histopathologic comparison: a further step toward an individualized tumor characterization. *J Comput Assist Tomogr* 2013;37:15-21.
  61. Fraioli F, Anzidei M, Zaccagna F, et al. Whole-tumor perfusion CT in patients with advanced lung adenocarcinoma treated with conventional and antiangiogenic chemotherapy: initial experience. *Radiology* 2011;259:574-82.
  62. Schmid-Bindert G, Henzler T, Chu TQ, et al. Functional imaging of lung cancer using dual energy CT: how does iodine related attenuation correlate with standardized uptake value of 18FDG-PET-CT? *Eur Radiol* 2012;22:93-103.
  63. Kim YN, Lee HY, Lee KS, et al. Dual-energy CT in patients treated with anti-angiogenic agents for non-small cell lung cancer: new method of monitoring tumor response? *Korean J Radiol* 2012;13:702-10.
  64. Zhang LJ, Yang GF, Wu SY, et al. Dual-energy CT imaging of thoracic malignancies. *Cancer Imaging* 2013;13:81-91.
  65. Chae EJ, Song JW, Krauss B, et al. Dual-energy computed tomography characterization of solitary pulmonary nodules. *J Thorac Imaging* 2010;25:301-10.
  66. Goodsitt MM, Chan HP, Way TW, et al. Quantitative CT of lung nodules: dependence of calibration on patient body size, anatomic region, and calibration nodule size for single- and dual-energy techniques. *Med Phys* 2009;36:3107-21.
  67. Chae EJ, Song JW, Seo JB, et al. Clinical utility of dual-energy CT in the evaluation of solitary pulmonary nodules: initial experience. *Radiology* 2008;249:671-81.
  68. Scheenstra AE, Rossi MM, Belderbos JS, et al. Local dose-effect relations for lung perfusion post stereotactic body radiotherapy. *Radiother Oncol* 2013;107:398-402.
  69. De Jaeger K, Seppenwoolde Y, Boersma LJ, et al. Pulmonary function following high-dose radiotherapy of non-small-cell lung cancer. *Int J Radiat Oncol Biol Phys* 2003;55:1331-40.
  70. Zhang J, Ma J, Zhou S, et al. Radiation-induced reductions in regional lung perfusion: 0.1-12 year data from a prospective clinical study. *Int J Radiat Oncol Biol Phys* 2010;76:425-32.
  71. St-Hilaire J, Lavoie C, Dagnault A, et al. Functional avoidance of lung in plan optimization with an aperture-based inverse planning system. *Radiother Oncol* 2011;100:390-5.
  72. Munawar I, Yaremko BP, Craig J, et al. Intensity modulated radiotherapy of non-small-cell lung cancer incorporating SPECT ventilation imaging. *Med Phys* 2010;37:1863-72.
  73. McGuire SM, Marks LB, Yin FF, et al. A methodology for selecting the beam arrangement to reduce the intensity-modulated radiation therapy (IMRT) dose to the SPECT-defined functioning lung. *Phys Med Biol* 2010;55:403-16.
  74. Lavrenkov K, Singh S, Christian JA, et al. Effective avoidance of a functional spect-perfused lung using intensity modulated radiotherapy (IMRT) for non-small cell lung cancer (NSCLC): an update of a planning study. *Radiother Oncol* 2009;91:349-52.
  75. De Ruyscher D, Sharifi H, Defraene G, et al. Quantification of radiation-induced lung damage with CT scans: the possible benefit for radiogenomics. *Acta Oncol* 2013;52:1405-10.
  76. Ghobadi G, Hogeweg LE, Faber H, et al. Quantifying local radiation-induced lung damage from computed tomography. *Int J Radiat Oncol Biol Phys* 2010;76:548-56.
  77. Petit SF, van Elmpt WJ, Oberije CJ, et al. [18F]fluorodeoxyglucose uptake patterns in lung before radiotherapy identify areas more susceptible to radiation-induced lung toxicity in non-small-cell lung cancer patients. *Int J Radiat Oncol Biol Phys* 2011;81:698-705.
  78. Ireland RH, Bragg CM, McJury M, et al. Feasibility of image registration and intensity-modulated radiotherapy planning with hyperpolarized helium-3 magnetic resonance imaging for non-small-cell lung cancer. *Int J Radiat Oncol Biol Phys* 2007;68:273-81.
  79. Zhang LJ, Zhou CS, Schoepf UJ, et al. Dual-energy CT lung ventilation/perfusion imaging for diagnosing pulmonary embolism. *Eur Radiol* 2013;23:2666-75.
  80. Tang CX, Zhang LJ, Han ZH, et al. Dual-energy CT based vascular iodine analysis improves sensitivity for peripheral pulmonary artery thrombus detection: An experimental study in canines. *Eur J Radiol* 2013;82:2270-8.

81. Hansmann J, Fink C, Jost G, et al. Impact of iodine delivery rate with varying flow rates on image quality in dual-energy CT of patients with suspected pulmonary embolism. *Acad Radiol* 2013;20:962-71.
82. Nagayama H, Sueyoshi E, Hayashida T, et al. Quantification of lung perfusion blood volume (lung PBV) by dual-energy CT in pulmonary embolism before and after treatment: preliminary results. *Clin Imaging* 2013;37:493-7.
83. Yuan R, Shuman WP, Earls JP, et al. Reduced iodine load at CT pulmonary angiography with dual-energy monochromatic imaging: comparison with standard CT pulmonary angiography--a prospective randomized trial. *Radiology* 2012;262:290-7.
84. Apfaltrer P, Bachmann V, Meyer M, et al. Prognostic value of perfusion defect volume at dual energy CTA in patients with pulmonary embolism: correlation with CTA obstruction scores, CT parameters of right ventricular dysfunction and adverse clinical outcome. *Eur J Radiol* 2012;81:3592-7.
85. Kim WW, Lee CH, Goo JM, et al. Xenon-enhanced dual-energy CT of patients with asthma: dynamic ventilation changes after methacholine and salbutamol inhalation. *AJR Am J Roentgenol* 2012;199:975-81.
86. Honda N, Osada H, Watanabe W, et al. Imaging of ventilation with dual-energy CT during breath hold after single vital-capacity inspiration of stable xenon. *Radiology* 2012;262:262-8.
87. Hoegl S, Meinel FG, Thieme SF, et al. Worsening respiratory function in mechanically ventilated intensive care patients: feasibility and value of xenon-enhanced dual energy CT. *Eur J Radiol* 2013;82:557-62.
88. Yanagita H, Honda N, Nakayama M, et al. Prediction of postoperative pulmonary function: preliminary comparison of single-breath dual-energy xenon CT with three conventional methods. *Jpn J Radiol* 2013;31:377-85.
89. Goo HW, Yu J. Redistributed regional ventilation after the administration of a bronchodilator demonstrated on xenon-inhaled dual-energy CT in a patient with asthma. *Korean J Radiol* 2011;12:386-9.
90. Goo HW, Yang DH, Hong SJ, et al. Xenon ventilation CT using dual-source and dual-energy technique in children with bronchiolitis obliterans: correlation of xenon and CT density values with pulmonary function test results. *Pediatr Radiol* 2010;40:1490-7.
91. Chae EJ, Seo JB, Lee J, et al. Xenon ventilation imaging using dual-energy computed tomography in asthmatics: initial experience. *Invest Radiol* 2010;45:354-61.
92. Chae EJ, Seo JB, Goo HW, et al. Xenon ventilation CT with a dual-energy technique of dual-source CT: initial experience. *Radiology* 2008;248:615-24.
93. Goo HW, Chae EJ, Seo JB, et al. Xenon ventilation CT using a dual-source dual-energy technique: dynamic ventilation abnormality in a child with bronchial atresia. *Pediatr Radiol* 2008;38:1113-6.
94. Bentzen SM. Theragnostic imaging for radiation oncology: dose-painting by numbers. *Lancet Oncol* 2005;6:112-7.
95. Ling CC, Humm J, Larson S, et al. Towards multidimensional radiotherapy (MD-CRT): biological imaging and biological conformality. *Int J Radiat Oncol Biol Phys* 2000;47:551-60.
96. Lambin P, van Stiphout RG, Starmans MH, et al. Predicting outcomes in radiation oncology--multifactorial decision support systems. *Nat Rev Clin Oncol* 2013;10:27-40.
97. Lambin P, Petit SF, Aerts HJ, et al. The ESTRO Breur Lecture 2009. From population to voxel-based radiotherapy: exploiting intra-tumour and intra-organ heterogeneity for advanced treatment of non-small cell lung cancer. *Radiother Oncol* 2010;96:145-52.
98. van Elmpt W, De Ruyscher D, van der Salm A, et al. The PET-boost randomised phase II dose-escalation trial in non-small cell lung cancer. *Radiother Oncol* 2012;104:67-71.
99. Everitt S, Hicks RJ, Ball D, et al. Imaging cellular proliferation during chemo-radiotherapy: a pilot study of serial 18F-FLT positron emission tomography/computed tomography imaging for non-small-cell lung cancer. *Int J Radiat Oncol Biol Phys* 2009;75:1098-104.
100. van Elmpt W, Ollers M, Dingemans AM, et al. Response assessment using 18F-FDG PET early in the course of radiotherapy correlates with survival in advanced-stage non-small cell lung cancer. *J Nucl Med* 2012;53:1514-20.
101. Tsuchida T, Morikawa M, Demura Y, et al. Imaging the early response to chemotherapy in advanced lung cancer with diffusion-weighted magnetic resonance imaging compared to fluorine-18 fluorodeoxyglucose positron emission tomography and computed tomography. *J Magn Reson Imaging* 2013;38:80-8.



**Cite this article as:** van Elmpt W, Zegers CM, Das M, De Ruyscher D. Imaging techniques for tumour delineation and heterogeneity quantification of lung cancer: overview of current possibilities. *J Thorac Dis* 2014;6(4):319-327. doi: 10.3978/j.issn.2072-1439.2013.08.62

## Hyperfractionated and accelerated radiotherapy in non-small cell lung cancer

Kate Haslett<sup>1</sup>, Christoph Pöttgen<sup>2</sup>, Martin Stuschke<sup>2</sup>, Corinne Faivre-Finn<sup>1,3</sup>

<sup>1</sup>Radiotherapy Related Research, The Christie NHS Foundation Trust, Manchester, UK; <sup>2</sup>University of Duisburg-Essen, Department of Radiotherapy, Essen, Germany; <sup>3</sup>The University of Manchester, Oxford Road, Greater Manchester, UK

### ABSTRACT

Radical radiotherapy plays a major role in the treatment of non-small cell lung cancer (NSCLC) due to the fact that many patients are medically or surgically inoperable. Advances in technology and radiotherapy delivery allow targeted treatment of the disease, whilst minimizing the dose to organs at risk. This in turn creates an opportunity for dose escalation and the prospect of tailoring radiotherapy treatment to each patient. This is especially important in patients deemed unsuitable for chemotherapy or surgery, where there is a need to increase the therapeutic gain from radical radiotherapy alone. Recent research into fractionation schedules, with hyperfractionated and accelerated radiotherapy regimes has been promising. How to combine these new fractionated schedules with dose escalation and chemotherapy remains open to debate and there is local, national and international variation in management with a lack of overall consensus. An overview of the current literature on hyperfractionated and accelerated radiotherapy in NSCLC is provided.

### KEYWORDS

Accelerated radiotherapy; hyperfractionated radiotherapy; non-small cell lung cancer (NSCLC)

*J Thorac Dis 2014;6(4):328-335. doi: 10.3978/j.issn.2072-1439.2013.11.06*

### Introduction

Lung cancer is a major public health concern worldwide. Progress in improving 5-year survival is lagging behind comparable survival rates in other common cancers. Population-based lung cancer registry data analysis shows only a minimal increase in survival from 7-16% between 1995-1999 to 8-18% between 2005-2007 (1).

The majority of patients with locally advanced non-small cell lung cancer (NSCLC) are not suitable for surgical resection, often due to pre-existing co-morbidities and poor performance status. The international standard of care is concurrent chemo-radiotherapy which is associated with a 5-year survival of 20-30% and a median survival of 17-28 months (2-6). Due to the potential toxicity of concurrent chemo-radiotherapy patient

selection is important. Patients with a good performance status, without major co-morbidities and assuming an acceptable radiation dose to normal tissues are eligible for this intensive treatment (7,8). Alternative treatment options are sequential chemo-radiotherapy or radiotherapy alone. Radiotherapy alone is associated with a 5-year survival of less than 5% due to local, regional and distant relapse. Local control with standard 3D conformal radiotherapy remains poor, with reported two years loco-regional control rates of 20-44% (9-11).

However, recent studies have shown that better local control of lung cancer can lead to an improvement in overall survival (10), prompting interest in altering radiotherapy delivery regimes. High dose stereotactic ablative body radiotherapy typically delivering >100 Gy biologically effective dose (BED) in 3-8 fractions is associated with very high in-field local control rates, but such doses cannot be delivered safely to locally advanced tumours due to the proximity of organs at risk such as the proximal bronchial tree, heart and spinal cord. A gap between radiation fractions allows recovery of damage in normal tissues and may also increase the sensitivity of the tumour cells to radiation by processes such as reoxygenation (12). If the individual fraction size is reduced and the fractions delivered closer together (e.g., twice daily), it may be possible to increase

Correspondence to: Dr. Corinne Faivre-Finn, Radiotherapy Related Research, The Christie NHS Foundation Trust, Manchester. M20 4BX, UK. Email: corinne.finn@christie.nhs.uk.

Submitted Nov 04, 2013. Accepted for publication Nov 07, 2013.  
Available at [www.jthoracdis.com](http://www.jthoracdis.com)

ISSN: 2072-1439

© Pioneer Bioscience Publishing Company. All rights reserved.

**Table 1.** Description of included trials using hyperfractionation radiotherapy schedule in non-small cell lung cancer.

| Trial                       | No. patients randomised | Inclusion period | RT dose/no. of fractions     | Dose per fraction        | Duration (weeks) | Chemotherapy |
|-----------------------------|-------------------------|------------------|------------------------------|--------------------------|------------------|--------------|
| RTOG 8808-ECOG 4588 (15,16) | 326                     | 1989-1992        | Control arm: 60 Gy/30        | 2 Gy OD                  | 6                | None         |
|                             |                         |                  | Experimental arm: 69.6 Gy/58 | 1.2 Gy BID               | 6                | None         |
| RTOG 9410 (17)              | 610                     | 1994-1998        | Study 1: 63 Gy/34            | 1.8 Gy ×25, 2.0 Gy ×9 OD | 7                | Sequential   |
|                             |                         |                  | Study 2: 63 Gy/34            | 1.8 Gy ×25, 2.0 Gy ×9 OD | 7                | Concurrent   |
|                             |                         |                  | Study 3: 69.6 Gy/58          | 1.2 Gy BID               | 6                | Concurrent   |

Abbreviations: RT, radiotherapy; BID, RT given twice a day; ECOG, Eastern Cooperative Oncology Group; No, number; OD, RT given once a day; RTOG, Radiation Therapy Oncology Group.

the dose without detriment to normal tissues.

One of the strategies to improve local control is dose escalation. Evidence gathered from the standard radiation schedules utilised in NSCLC over the past 40 years have confirmed the importance of total dose as a factor in tumour response (13). These schedules often use a single treatment of 1.8-2 Gy fractions per day over 5 days per week for a period of 5-7 weeks.

The RTOG 0617 study has evaluated dose escalation in the context of standard fractionation (2 Gy/day) and concurrent chemo-radiotherapy (5). Unfortunately the study was closed early due to futility indicating the absence of a survival benefit to high dose radiotherapy (74 Gy in 37 fractions delivered over 7.5 weeks) compared to standard dose (60 Gy in 30 fractions delivered over 6 weeks) (5).

An alternative approach to increasing the biological tumour dose in NSCLC is to develop new fractionation regimes, most commonly by hyperfractionation or acceleration. Hyperfractionation is a radiation treatment in which the total dose of radiation delivered is divided into smaller doses and treatments are given more than once a day (typically 2-3 a day). Acceleration means radiation treatment in which the total dose of radiation is given over a shorter period of time (fewer days) compared to standard radiation therapy. A recent meta-analysis by Mauguen and co-workers, evaluated ten trials including 2,000 patients and concluded that modifying the radiotherapy schedule by hyperfractionation, acceleration or both resulted in an increase in overall survival (14). The use of modified radiotherapy led to a 12% reduction in the risk of death ( $P=0.009$ ). The absolute increase in overall survival in the NSCLC patients was by 3.8% at three years and 2.5% at five years, improving the survival rate from 15.9% to 19.7% at three years and from 8.3% to 10.8% at five years (14). Modified radiotherapy increased the risk of acute severe oesophagitis from 9% to 19% ( $P<0.001$ ), and as expected the most accelerated regimes were associated with the most severe toxicity. However,

at least 90% of patients completed the planned radiotherapy, with compliance in the experimental arms similar to the control arms. A summary of both hyperfractionation and acceleration is presented below.

## Hyperfractionation

Early clinical trials evaluating hyperfractionation in the late 1980's and early 1990's investigated the benefit of adding chemotherapy to radiotherapy. The RTOG 8808-ECOG 4588 randomised 458 patients to two months of induction chemotherapy with cisplatin and vinblastine, followed by conventional radiotherapy (60 Gy in 2 Gy per fraction), or radiotherapy alone, with either the same radiotherapy regime or a hyperfractionated regime of 1.2 Gy per fraction delivered twice daily to a total dose of 69.6 Gy (15,16). This study showed that patients receiving induction chemotherapy did best, with a median survival of 13.2 months and a 5-year overall survival of 8% ( $P=0.04$ ). Although the twice-daily radiation arm performed slightly better compared with the conventional radiation arm, the difference was not statistically significant (median survival 12 *vs.* 11.4 months, 5-year overall survival 6% *vs.* 5%).

The trials evaluating hyperfractionated radiotherapy are summarised in Table 1. One of these pivotal trials in demonstrating the advantage of concurrent over sequential chemo-radiotherapy was the RTOG 9410 study (17). It also addressed the important question of overall treatment time in the management of stage III NSCLC. This 3-arm study randomised patients to sequential chemo-radiotherapy with cisplatin/vinblastine followed by radiotherapy (60 Gy in 30 fractions of 2 Gy over six weeks) beginning on day 50 (arm 1); concurrent chemo-radiotherapy with combination cisplatin/vinblastine and the same radiotherapy beginning on day 1 (arm 2); *vs.* concurrent chemo-radiotherapy using combination cisplatin/etoposide with hyperfractionated radiotherapy beginning on day 1 (69.6 Gy in 58 fractions of 1.2 Gy twice daily, over six weeks) (arm 3).

Phase II data suggested that the hyperfractionated regimen in arm 3 would be superior (17). However survival in the RTOG 9410 study was actually higher for patients treated with the concurrent regimen with once-daily radiotherapy (arm 2) compared with the concurrent regimen using twice-daily radiotherapy (arm 3) ( $P=0.046$ ) (17). Median survival times were 14.6%, 17% and 15.6 %, with five years survival of 10%, 16% and 13% for arms 1-3, respectively ( $P=0.046$ ). This trial highlighted that dose escalation by a hyperfractionation regime delivered over a standard overall treatment time does not improve survival. In addition the results supported the use of concurrent chemo-radiotherapy with conventional fractionation, which has since become the gold standard treatment in good performance status stage III patients (3).

### Accelerated hyperfractionation

#### *Three fractions per day regime*

Treatment using continuous hyperfractionated accelerated radiotherapy (CHART) was shown to be of significant benefit by improving local control and overall survival (18,19). The randomised trial recruited 563 patients, PS 0-1, medically inoperable, and compared CHART (54 Gy in 36 fractions of 1.5 Gy 3 times per day over 12 consecutive days) to conventionally fractionated radiotherapy (60 Gy in 30 once daily fractions of 2 Gy over six weeks). As anticipated the main toxicity during treatment was dysphagia, which was more severe in the CHART patients, with 19% experiencing severe dysphagia, compared with 3% in the conventional group. Overall there was a 24% reduction in the relative risk of death in the CHART arm and the overall survival rates were significantly higher: 30% *vs.* 21% at two years and 12% *vs.* 7% at five years respectively for the CHART and conventional radiotherapy arm ( $P=0.004$ ) (18,19). On subgroup analysis, CHART demonstrated an even greater improvement for squamous cell carcinomas, with an overall survival at three years of 21% compared with 11% for the conventional regime ( $P=0.0007$ ). This evidence suggests that reducing overall treatment time in an effort to reduce tumour repopulation plays a key role in tumour control and treatment of NSCLC. Meanwhile, it should be noted that (I) the control arm of CHART would not be considered current standard of care as chemotherapy is not delivered with radiotherapy (either sequentially or concurrently) and (II) a large percentage of patients had stage I-II disease (36%) who would nowadays be considered for a surgical approach or in some cases stereotactic ablative body radiotherapy. Despite the overall benefit seen with hyperfractionated accelerated radiotherapy in the CHART trial,

this has not become standard practice. Recently published data gathered from a survey of UK clinical oncologists (20), revealed 55 Gy in 20 daily fractions as the commonest fractionation schedule for NSCLC in the UK, followed by 66 Gy in 33 daily fractions. Only 14/50 centres offered CHART despite the National Institute for Health and Clinical Excellence (NICE) recommending CHART as highly cost-effective (21). It is widely recognised that the schedule is demanding for patients and requires flexible and ad hoc radiotherapy department staffing willing to work extended day. If patients are unable to travel this treatment often necessitates a 12-day inpatient stay.

Between 1991 and 1994, Fu *et al.* conducted a phase I/II trial evaluating hyperfractionated accelerated radiation therapy (HART) which was published as a comparative cohort study. HART was delivered by 1.1 Gy per fraction, three fractions per day at intervals of four hours with five treatment days per week (22). The clinical disease was irradiated to 74.3 Gy delivered in 66-69 fractions over 33 days (not corrected for lung density), and the subclinical disease to 50.0 Gy delivered in 44-46 fractions over 33 days. There were 60 patients in the HART group and their survival and local control results were compared to those of 50 patients treated by conventional fractionated irradiation during the same period. Survival and local control were improved in the HART group. Three-year survival was 28% *vs.* 6% ( $P<0.001$ ). Three-year local control was 29% *vs.* 5% ( $P=0.008$ ). Median survival for HART was 22.6 months compared with 14.0 months for standard radiotherapy patients ( $P<0.05$ ).

The evolving evidence in favour of concurrent chemo-radiotherapy led to the premature closure of a number of clinical trials evaluating accelerated and hyperfractionated regimen. The trials which evaluated both these fractionation schedules as the primary treatment modality are summarised in Table 2. The ECOG 2,597 trial was closed in June 2001 when 141 patients had been recruited, reaching 42% of the overall target (25). This trial randomly assigned stage III NSCLC patients to induction chemotherapy followed by standard thoracic radiotherapy (64 Gy, 2 Gy once daily over 6.5 weeks), *vs.* induction chemotherapy followed by HART (57.6 Gy, 1.5 Gy in three daily fractions over 2.5 weeks, with weekend breaks). Although not statistically significant there was an improvement in survival with HART (20.3 *vs.* 14.9 months;  $P=0.28$ ).

The CHART schedule was logistically difficult for radiotherapy departments to implement due to the additional weekend and evening treatments. This led to the CHARTWEL-trial evaluating hyper-fractionated accelerated radiotherapy which omitted weekend treatments (24). The CHARTWEL-trial compared 60 Gy in 1.5 Gy fractions, delivered 3 times per day, on the 5 weekdays, over an average of 17 days *vs.* conventional

**Table 2.** Description of included trials using acceleration or hyperfractionation radiotherapy schedules in non-small cell lung cancer.

| Trial                          | No. patients randomised | Inclusion period | RT dose/no. of fractions        | Dose per fraction     | Duration (weeks) | Chemotherapy           |
|--------------------------------|-------------------------|------------------|---------------------------------|-----------------------|------------------|------------------------|
| Ball 1999 (23)                 | 204                     | 1989-1995        | Control arm: 60 Gy/30           | 2 Gy OD               | 6                | +/- concurrent         |
|                                |                         |                  | Experimental arm: 60 Gy/30      | 2 Gy BID              | 3                | +/- concurrent         |
| CHART (18,19)                  | 563                     | 1990-1995        | Control arm: 60 Gy/30           | 2 Gy OD               | 6                | None                   |
|                                |                         |                  | Experimental arm: 54 Gy/36      | 1.5 Gy TID            | 1.5              | None                   |
| Fu 1997 (22)                   | 69                      | 1991-1994        | Control arm: 60-64 Gy/32-34     | 1.8-2.0 Gy OD         | 7                | Adjuvant or none       |
|                                |                         |                  | Experimental arm: 74.3 Gy/66-69 | 1.1 Gy TID            | 6.5              | Adjuvant or none       |
| CHARTWEL-trial (ARO 97-1) (24) | 406                     | 1997-2005        | Control arm: 66 Gy/33           | 2 Gy OD               | 6.5              | Induction or none      |
|                                |                         |                  | Experimental arm: 60 Gy/40      | 1.5 Gy TID            | 2.5              | Induction or none      |
| ECOG 2597 (25)                 | 119                     | 1998-2001        | Control arm: 64 Gy/32           | 2 Gy OD               | 6.5              | Induction              |
|                                |                         |                  | Experimental arm: 57.6 Gy/36    | 1.6 Gy TID            | 2.5              | Induction              |
| Nyman 2009 (26)                | 152                     | 2002-2005        | Control arm: 60 Gy/30           | 2 Gy OD               | 6                | Induction & concurrent |
|                                |                         |                  | Control arm: 60 Gy/30           | 2 Gy OD               | 6                | Induction & concurrent |
|                                |                         |                  | Experimental arm: 64.6 Gy/38    | 1.7 Gy BID            | 4.5              | Induction & concurrent |
| Van Baardwijk 2012 (27)        | 137                     | 2006-2009        | Total dose 51-69 Gy             |                       | Total 6-7        | Concurrent             |
|                                |                         |                  | Study dose: phase 1 45 Gy/30    | 1.5 Gy BID            | 3                |                        |
|                                |                         |                  | Study dose: phase 2 isotoxic    | 2 Gy OD for remainder | 3-4              |                        |

Abbreviations: CHART, Continuous Hyperfractionated Accelerated Radiation Therapy; CHARTWEL, CHART Week-End Less; ECOG, Eastern Cooperative Oncology Group; No, Number; RT, Radiotherapy; OD, RT given once a day; RTOG, Radiation Therapy Oncology Group; BID, RT given twice a day; TID, RT given three times a day.

treatment of 66 Gy in 33 fractions delivered once daily over 45 days. The study found no significant difference between the two arms, with two years survival rates of 32% in the conventional arm and 31% in the CHARTWEL arm ( $P=0.43$ ). However, this study confirmed the importance of a time factor in this disease as the lower total dose in the CHARTWEL arm was compensated by the shorter overall treatment time.

Another strategy is to dose escalate CHART. Continuous hyperfractionated accelerated radiotherapy escalated dose (CHART-ED) was a multi-centre phase I feasibility study which completed recruitment in September 2012. It compared dose-escalated CHART, adding twice daily fractions after completion of 54 Gy in 36 fractions over 12 days (28). Patients were treated on day 15 in group 1 (total dose 57.6 Gy in 38 fractions), days 15-16 in group 2 (total dose 61.2 Gy in 40 fractions) and days 15-17 in group 3 (total dose 64.8 Gy in 42 fractions). The incidence and grade of potentially dose-limiting toxicities will be

assessed to determine whether dose escalation of around 6-10 Gy using this approach is safe, and the data is currently awaited.

### *Two fractions per day regime*

An Australian study by Ball *et al.* used a 2×2 factorial design to evaluate shortening of the overall treatment time and the addition of carboplatin in patients with inoperable NSCLC (23). The trial randomised 204 patients between conventional radiotherapy (60 Gy in 30 fractions, once daily over six weeks) or accelerated radiotherapy (60 Gy in 30 fractions, twice daily, over three weeks) with or without concurrent carboplatin chemotherapy. Oesophageal toxicity was significantly higher in the three week radiotherapy arms and no significant survival difference between the groups was found.

Between June 2002 and May 2005 152 patients with stage III NSCLC, PS 0-1 were randomised in a Swedish 3-arm

**Table 3.** Neoadjuvant chemo-radiotherapy trials prior to surgery using accelerated hyperfractionation radiotherapy schedules in non-small cell lung cancer.

| Trial             | No. patients randomised | Inclusion period | RT dose/no. of fractions                   | Dose per fraction | Duration (weeks) | Chemotherapy           |
|-------------------|-------------------------|------------------|--|-------------------|------------------|------------------------|
| Thomas (29)       | 558                     | 1993-2003        | Control arm: post-op RT 54-68.4 Gy/30-38   | 1.8 Gy OD         | 6-7.5            | Induction              |
|                   |                         |                  | Experimental arm: pre-op 45 Gy/30          | 1.5 Gy BID        | 3                | Induction & concurrent |
|                   |                         |                  | Experimental arm post-op: none or 24 Gy/16 | 1.5 Gy BID        | 1.5              | No adjuvant            |
| Pöttgen 2013 (30) | 239                     | 2000-2012        | Control arm: 46 Gy/23                      | 2 Gy OD           | 4.5              | Induction & concurrent |
|                   |                         |                  | Experimental arm: 45/30                    | 1.5 Gy BID        | 3                | Induction & concurrent |
| Pöttgen 2010 (31) | 135                     | 2004-2008        | Experimental arm 45 Gy/30                  | 1.5 Gy BID        | 3                | Induction & concurrent |

Abbreviations: No, number; RT, Radiotherapy; OD, RT given once a day; BID, RT given twice a day.

(A, B and C) phase II study by Nyman *et al.* (26). All arms started with two cycles of induction chemotherapy (carboplatin/paclitaxel), a third cycle was given concomitant with the start of accelerated radiotherapy in arm A (64.6 Gy in 1.7 Gy twice-daily fractions over 4.5 weeks), while in the remaining arms (B and C) conventional radiotherapy (60 Gy in 2 Gy daily fractions over 6 weeks) was combined with daily or weekly chemotherapy. Toxicity for all arms was similar and manageable with 12% grades 3-4 esophagitis, 1% grades 3-4 pneumonitis (all arms combined). Median survival was 17.8 (14.4-23.7) months (17.7, 17.7 and 20.6 months for A, B and C respectively). The 1-, 3- and 5-year overall survival was 63%, 31% and 24%. This study demonstrated that similar survival results could be achieved by intensifying treatment with either accelerated fractionated radiotherapy or concomitant chemo-radiotherapy.

Between 1995 and 2003 the German Lung Cancer Co-operative Group (GLCCG) evaluated the role of accelerated hyperfractionated chemo-radiotherapy regimes in the pre-operative setting (29). The trials which included this fractionation schedule in the neoadjuvant setting are summarised in Table 3. 558 patients with stage IIIA-IIIIB NSCLC were randomised between pre-operative chemo-radiotherapy and chemotherapy alone. In the control arm three cycles of cisplatin and etoposide chemotherapy were delivered followed by surgical resection, then adjuvant radiotherapy at 1.8 Gy daily fractions, the total dose dependent on surgical resection margins (54 Gy for negative margins, 68.4 Gy for positive margins). In the experimental arm the same induction chemotherapy was delivered, but followed by concurrent chemo-radiotherapy 45 Gy at 1.5 Gy twice daily fractions with carboplatin and vindesine, prior to surgical

resection. If the margins were negative no further radiotherapy was given. But in the presence of positive margins, additional radiotherapy of 24 Gy at 1.5 Gy twice daily fractions was delivered. Pneumonectomies were performed in 35% of the patients in each group, with an increase in treatment-associated mortality seen in the experimental arm. Overall a similar number of patients underwent surgery, with a slightly higher complete resection rate in the experimental arm of 37% compared with 32% in the control arm. However there was no difference in progression free survival, the primary endpoint of this trial (29).

Pöttgen *et al.* also evaluated neo-adjuvant accelerated hyperfractionated chemo-radiotherapy. In an observational study, 239 patients with stage III NSCLC were treated with neoadjuvant radiochemotherapy using either accelerated hyperfractionation (45 Gy in 1.5 Gy twice-daily fractions over three weeks) or conventional fractionation (46 Gy in 2 Gy once daily fractions over 4.5 weeks) prior to thoracotomy (30). The crude pathological complete response (pCR) rates of 37% and 24% were seen in the accelerated hyperfractionated group and conventional fractionated group respectively, with a significant relationship between pCR rates and the BED suggesting an improvement in local effectiveness of accelerated hyperfractionation in lung cancer.

This accelerated regimen was further evaluated in a prospective trial by the same group in stage III NSCLC patients not deemed resectable, mainly stage IIIIB (31). After three cycles of induction chemotherapy (cisplatin/paclitaxel) concurrent chemo-radiotherapy was delivered (accelerated hyperfractionated, 45 Gy in 1.5 Gy twice daily fractions over three weeks, with cisplatin/vinorelbine). Once 45 Gy was reached, a multidisciplinary

panel decision was made regarding operability. Inoperable patients received definitive radiotherapy (total dose 65 or 71 Gy, depending on the mean lung dose) with additional concurrent chemotherapy (cisplatin/vinorelbine). The majority (21 of 28 patients) received 71 Gy. Oesophagitis Grade 3+ was observed in 18% and pneumonitis Grade 3+ in 4% of the patients. At three years, the loco-regional control rate was 52% (95% CI, 29-75%). In an exploratory analysis, those patients receiving 71 Gy had a loco-regional control at two and three years of 74% (95% CI: 51.2-96.3%) and 63% (95% CI: 36.1-90.4%), while in those patients receiving the lower total dose (65 Gy), loco-regional control at two and three years was 18% (95% CI: 0-49.2%;  $P=0.001$ , Wilcoxon test), respectively. Overall survival at three years was 31% (95% CI: 12-50%) for all patients. This study led to the ESPATÜ trial, a phase III multicentre study that compared induction chemotherapy followed by definitive concurrent chemo-radiotherapy to trimodality treatment (induction chemotherapy followed by concurrent chemo-radiotherapy followed by surgery). The study recently closed and results are awaited.

Given the evidence in favour of hyperfractionation and acceleration, this has been taken a step further with specifically tailored regimes. The MAASTRO group have pioneered the concept of "isotoxic" radiotherapy allowing for individualised dose escalation in stage I-III patients based on dose delivered to organs at risk (such as lung and spinal cord), using hyperfractionated accelerated radiotherapy (32). In the first MAASTRO study 166 NSCLC patients (59% stage III) not suitable for concurrent chemo-radiotherapy received an individualised dose of radiotherapy alone or after induction chemotherapy (55% of patients). Using 3D conformal therapy, the total dose delivered was between 50.4-79.2 Gy (delivered within an accelerated schedule of 1.5 Gy twice daily). With a median follow-up of 31.6 months, the median overall survival was 21.0 months—95% CI, 15.8 to 26.2 months, (stage IIIA 16.2 months—95% CI, 7.6 to 24.8 months; stage IIIB, 17.2 months—95% CI, 8.4 to 26.0 months) with a 2-year overall survival of 45.0%. Only eight patients (4.8%) developed acute grade 3 dysphagia. Less than 10% of patients with stage III received the maximum dose as per protocol of 79.2 Gy.

A further MAASTRO study, evaluated the same strategy in the concurrent setting (27), only in stage III NSCLC patients. One hundred and thirty seven patients were included in this phase II study and treated with 3D conformal radiotherapy. The individually prescribed dose was based on mean lung dose of 19 Gy, spinal cord dose of 54 Gy, brachial plexus dose of 66 Gy and central mediastinal structure dose of 74 Gy. A total dose between 51 and 69 Gy was delivered in 1.5 Gy twice daily up to

45 Gy, followed by 2 Gy once daily and radiotherapy was started at the 2nd or 3rd course of chemotherapy. The median dose was  $65.0\pm 6.0$  Gy delivered in  $35\pm 5.7$  days. With a median follow-up of 30.9 months, the median overall survival was 25.0 months (95% CI: 19.8-30.3 months) and 2-year overall survival 52.4%. Thirty five patients (25.5%) developed G3+ dysphagia.

It should be noted that patients in the two MAASTRO group studies were treated with 3DCRT, probably limiting individualised dose escalation. The use of Intensity Modulated Radiotherapy (IMRT) could potentially allow for further dose escalation. IMRT modulates the intensity profile of radiation delivered to the patient, permitting improved targeting of the radiation dose, and in the thorax leads to a reduction in dose to organs at risk. This could therefore lead to increased tumour control probability yet with the same normal tissue complication probability (33). A planning study by The Christie using IMRT and twice daily fractionation for stage II/III NSCLC showed that this had potential to allow a further individual dose escalation in this group of patients (34). The starting point for dose escalation in this study was 55.8 Gy in 1.8 Gy per fraction delivered twice daily. The number of fractions was then increased until one or more organ at risk (OAR) tolerance dose was exceeded or a maximum dose of 79.2 Gy (i.e., 44 fraction of 1.8 Gy BD) was reached. IMRT allowed a significant dose increase in comparison to other methods ( $P<0.0001$ ) while no difference was found between 3D conformal planning and inverse planning ( $P=0.06$ ).

This regime will be assessed in a UK feasibility multicentre study of isotoxic hyperfractionated accelerated radiotherapy in stage III NSCLC patients not suitable for concurrent chemo-radiotherapy (ClinicalTrials.gov Identifier: NCT01836692). If isotoxic IMRT is proven to be feasible this regimen will be compared to standard sequential chemo-radiotherapy in a national phase II "pick-the-winner" trial alongside three other dose-escalated regimens currently being evaluated in the UK.

The use of concurrent chemo-radiotherapy with accelerated hyperfractionated schedules is compromised by high rates of acute mucosal toxicity which can be challenging for both patient and clinicians, however these side effects are usually transient and resolve within a few weeks of completion of radiotherapy. The Bortfeld group have raised the interesting issue that the optimal fractionation schedule (hypofractionated *vs.* hyperfractionated) may depend on the OAR doses (35). For larger tumours, their model which minimizes maximum BED within a serial organ suggests hyperfractionation. Thus, accelerated hyperfractionation may eventually turn out as an ideal alternative to pure dose-escalation in locally advanced NSCLC and should deserve further evaluation within properly designed randomised trials.

## Conclusions

There is significant evidence that prolonging the overall treatment time, can allow cancer stem cells to repopulate, and thus be detrimental to disease outcome (36). CHART has shown improved survival over standard radiotherapy, in patients with unresectable stage I-III NSCLC. Selected patients (with ECOG performance status 1 who do not fit the criteria for sequential or concurrent chemotherapy or patients who prefer radiotherapy only) may be considered for CHART (7,8).

Within the field of thoracic oncology evidence is emerging to suggest that an accelerated hyperfractionated radiotherapy schedule may be superior to conventional treatment. We believe that such treatment should be closely combined with other strategies in order to improve local control and survival. Dose escalation and individualised radiation doses facilitated by the use of IMRT should be combined in order to increase local control and survival. This is an exciting time for thoracic radiotherapy with these developments leading towards the goal of personalised treatment.

## Acknowledgements

*Disclosure:* The authors declare no conflict of interest.

## References

- Coleman MP, Forman D, Bryant H, et al. Cancer survival in Australia, Canada, Denmark, Norway, Sweden, and the UK, 1995-2007 (the International Cancer Benchmarking Partnership): an analysis of population-based cancer registry data. *Lancet* 2011;377:127-38.
- Rigas JR, Kelly K. Current treatment paradigms for locally advanced non-small cell lung cancer. *J Thorac Oncol* 2007;2 Suppl 2:S77-85.
- Aupérin A, Le Péchoux C, Pignon JP, et al. Concomitant radio-chemotherapy based on platin compounds in patients with locally advanced non-small cell lung cancer (NSCLC): a meta-analysis of individual data from 1764 patients. *Ann Oncol* 2006;17:473-83.
- Rowell NP, O'rouke NP. Concurrent chemoradiotherapy in non-small cell lung cancer. *Cochrane Database Syst Rev* 2004;(4):CD002140.
- Bradley DJ, Paulus R, Komaki R, et al. A randomized phase III comparison of standard-dose (60 Gy) versus high-dose (74 Gy) conformal chemoradiotherapy with or without cetuximab for stage III non-small cell lung cancer. Results on radiation dose in RTOG 0617. *J Clin Oncol* 2013;31:abstr 7501.
- De Ruyscher D, Botterweck A, Dirx M, et al. Eligibility for concurrent chemotherapy and radiotherapy of locally advanced lung cancer patients: a prospective, population-based study. *Ann Oncol* 2009;20:98-102.
- Lim E, Baldwin D, Beckles M, et al. Guidelines on the radical management of patients with lung cancer. *Thorax* 2010;65 Suppl 3:iii1-27.
- De Ruyscher D, Faivre-Finn C, Nestle U, et al. European Organisation for Research and Treatment of Cancer recommendations for planning and delivery of high-dose, high-precision radiotherapy for lung cancer. *J Clin Oncol* 2010;28:5301-10.
- Le Chevalier T, Arriagada R, Quoix E, et al. Radiotherapy alone versus combined chemotherapy and radiotherapy in nonresectable non-small-cell lung cancer: first analysis of a randomized trial in 353 patients. *J Natl Cancer Inst* 1991;83:417-23.
- Aupérin A, Le Péchoux C, Rolland E, et al. Meta-analysis of concomitant versus sequential radiochemotherapy in locally advanced non-small-cell lung cancer. *J Clin Oncol* 2010;28:2181-90.
- Machtay M, Paulus R, Moughan J, et al. Defining local-regional control and its importance in locally advanced non-small cell lung carcinoma: a Radiation Therapy Oncology Group analysis. *J Thorac Oncol* 2012;7:716-22.
- Stewart FA, Dörr W. Milestones in normal tissue radiation biology over the past 50 years: from clonogenic cell survival to cytokine networks and back to stem cell recovery. *Int J Radiat Biol* 2009;85:574-86.
- Perez CA, Stanley K, Grundy G, et al. Impact of irradiation technique and tumor extent in tumor control and survival of patients with unresectable non-oat cell carcinoma of the lung: report by the Radiation Therapy Oncology Group. *Cancer* 1982;50:1091-9.
- Mauguen A, Le Péchoux C, Saunders MI, et al. Hyperfractionated or accelerated radiotherapy in lung cancer: an individual patient data meta-analysis. *J Clin Oncol* 2012;30:2788-97.
- Sause W, Kolesar P, Taylor S IV, et al. Final results of phase III trial in regionally advanced unresectable non-small cell lung cancer: Radiation Therapy Oncology Group, Eastern Cooperative Oncology Group, and Southwest Oncology Group. *Chest* 2000;117:358-64.
- Sause WT, Scott C, Taylor S, et al. Radiation Therapy Oncology Group (RTOG) 88-08 and Eastern Cooperative Oncology Group (ECOG) 4588: preliminary results of a phase III trial in regionally advanced, unresectable non-small-cell lung cancer. *J Natl Cancer Inst* 1995;87:198-205.
- Curran WJ Jr, Paulus R, Langer CJ, et al. Sequential vs. concurrent chemoradiation for stage III non-small cell lung cancer: randomized phase III trial RTOG 9410. *J Natl Cancer Inst* 2011;103:1452-60.
- Saunders M, Dische S, Barrett A, et al. Continuous hyperfractionated accelerated radiotherapy (CHART) versus conventional radiotherapy in non-small-cell lung cancer: a randomised multicentre trial. CHART Steering Committee. *Lancet* 1997;350:161-5.
- Saunders M, Dische S, Barrett A, et al. Continuous, hyperfractionated, accelerated radiotherapy (CHART) versus conventional radiotherapy in non-small cell lung cancer: mature data from the randomised multicentre trial. CHART Steering committee. *Radiother Oncol* 1999;52:137-48.
- Prewett SL, Aslam S, Williams MV, et al. The management of lung cancer: a UK survey of oncologists. *Clin Oncol (R Coll Radiol)* 2012;24:402-9.
- Available online: <http://publications.nice.org.uk/lung-cancer-cg121>

22. Fu XL, Jiang GL, Wang LJ, et al. Hyperfractionated accelerated radiation therapy for non-small cell lung cancer: clinical phase I/II trial. *Int J Radiat Oncol Biol Phys* 1997;39:545-52.
23. Ball D, Bishop J, Smith J, et al. A randomized phase III study of accelerated or standard fraction radiotherapy with or without concurrent carboplatin in inoperable non-small cell lung cancer: final report of an Australian multi-centre trial. *Radiother Oncol* 1999;52:129-36.
24. Baumann M, Herrmann T, Koch R, et al. Final results of the randomized phase III CHARTWEL-trial (ARO 97-1) comparing hyperfractionated-accelerated versus conventionally fractionated radiotherapy in non-small cell lung cancer (NSCLC). *Radiother Oncol* 2011;100:76-85.
25. Belani CP, Wang W, Johnson DH, et al. Phase III study of the Eastern Cooperative Oncology Group (ECOG 2597): induction chemotherapy followed by either standard thoracic radiotherapy or hyperfractionated accelerated radiotherapy for patients with unresectable stage IIIA and B non-small-cell lung cancer. *J Clin Oncol* 2005;23:3760-7.
26. Nyman J, Friesland S, Hallqvist A, et al. How to improve loco-regional control in stages IIIa-b NSCLC? Results of a three-armed randomized trial from the Swedish Lung Cancer Study Group. *Lung Cancer* 2009;65:62-7.
27. van Baardwijk A, Reymen B, Wanders S, et al. Mature results of a phase II trial on individualised accelerated radiotherapy based on normal tissue constraints in concurrent chemo-radiation for stage III non-small cell lung cancer. *Eur J Cancer* 2012;48:2339-46.
28. Available online: <http://public.ukcrn.org.uk/search/StudyDetail.aspx?StudyID=6959>
29. Thomas M, Rube C, Hoffknecht P, et al. Effect of preoperative chemoradiation in addition to preoperative chemotherapy: a randomised trial in stage III non-small-cell lung cancer. *Lancet Oncol* 2008;9:636-48.
30. Pöttgen C, Eberhardt W, Graupner B, et al. Accelerated hyperfractionated radiotherapy within trimodality therapy concepts for stage IIIA/B non-small cell lung cancer: Markedly higher rate of pathologic complete remissions than with conventional fractionation. *Eur J Cancer* 2013;49:2107-15.
31. Pöttgen C, Eberhardt WE, Gauler T, et al. Intensified high-dose chemoradiotherapy with induction chemotherapy in patients with locally advanced non-small-cell lung cancer-safety and toxicity results within a prospective trial. *Int J Radiat Oncol Biol Phys* 2010;76:809-15.
32. van Baardwijk A, Wanders S, Boersma L, et al. Mature results of an individualized radiation dose prescription study based on normal tissue constraints in stages I to III non-small-cell lung cancer. *J Clin Oncol* 2010;28:1380-6.
33. Lievens Y, Nulens A, Gaber MA, et al. Intensity-modulated radiotherapy for locally advanced non-small-cell lung cancer: a dose-escalation planning study. *Int J Radiat Oncol Biol Phys* 2011;80:306-13.
34. Warren M, Webster G, Rowbottom C, et al. PO-0961 isotoxic radiotherapy for non-small cell lung cancer: is imrt the answer? *Radiother Oncol* 2012;103:S378-9.
35. Unkelbach J, Craft D, Salari E, et al. The dependence of optimal fractionation schemes on the spatial dose distribution. *Phys Med Biol* 2013;58:159-67.
36. Koukourakis MI, Giatromanolaki A, Tsakmaki V, et al. Cancer stem cell phenotype relates to radio-chemotherapy outcome in locally advanced squamous cell head-neck cancer. *Br J Cancer* 2012;106:846-53.



**Cite this article as:** Haslett K, Pöttgen C, Stuschke M, Faivre-Finn C. Hyperfractionated and accelerated radiotherapy in non-small cell lung cancer. *J Thorac Dis* 2014;6(4):328-335. doi: 10.3978/j.issn.2072-1439.2013.11.06

## Radiation dose effect in locally advanced non-small cell lung cancer

Feng-Ming (Spring) Kong<sup>1</sup>, Jing Zhao<sup>1,2</sup>, Jingbo Wang<sup>3</sup>, Corrine Faivre-Finn<sup>4</sup>

<sup>1</sup>Department of Radiation Oncology, GRU Cancer Center, Georgia Regents University, Augusta, Georgia, USA; <sup>2</sup>Department of Oncology, Tongji Hospital, Tongji Medical College, Huazhong University of Science and Technology, Wuhan 430030, China; <sup>3</sup>Cancer Hospital/Institutes of Peking Union Medical College, Beijing 100730, China; <sup>4</sup>Faculty Institute of Cancer Sciences, Manchester Academic Health Sciences Centre, University of Manchester, UK

### ABSTRACT

Radiation is the foundation of treatment for locally advanced non-small cell lung cancer (NSCLC), and as such, optimal radiation dose is essential for successful treatment. This article will briefly review biological considerations of radiation dose and their effect in the context of three-dimensional conformal radiation therapy (3D-CRT) including intensity modulated radiation therapy (IMRT) and stereotactic body radiation therapy (SBRT) for NSCLC. It will focus on literature review and discussions regarding radiation dose effect in locally advanced NSCLC including potential severe and lethal toxicities of high dose radiation given with concurrent chemotherapy. Potential new approaches for delivering safe and effective doses by individualizing treatment based on functional imaging are being applied in studies such as the PET boost trial and RTOG1106. The RTOG concept of delivering high dose radiation to the more resistant tumors with the use of isotoxic dose prescription and adaptive planning will also be discussed in detail.

### KEYWORDS

Non-small cell lung cancer (NSCLC); radiation dose; concurrent chemotherapy

*J Thorac Dis 2014;6(4):336-347. doi: 10.3978/j.issn.2072-1439.2014.01.23*

### Introduction

Radiotherapy (RT) is needed in over 60% of patients with lung cancer at least once during the course of disease, adequate dose is an essential element for successful treatment of patients with non-small cell lung cancer (NSCLC). This article will briefly review biological considerations of radiation dose and their effect in the context of three-dimensional conformal radiation therapy (3D-CRT) including intensity modulated radiation therapy (IMRT) and stereotactic body radiation therapy (SBRT) for NSCLC. It will focus on literature review and discussions regarding radiation dose effect in locally advanced NSCLC including potential severe and lethal toxicities of

high dose radiation given with concurrent chemotherapy. Potential approaches for delivering safe and effective doses by individualizing treatment are being applied in studies such as RTOG1106. The concept of delivering high dose radiation to the most resistant tumors with the use of isotoxic dose prescription and adaptive approaches will also be discussed in this paper.

### Radiation dose effect: biology consideration

In the laboratory, from a biological effectiveness perspective, efficacy of radiation cell killing is directly correlated with the dose delivered. According to the basic principle of the linear-quadratic model, lethal radiation damage is created in one of two ways: as a consequence of a single ionizing event of double-strand breaks in the DNA or as a consequence of two, separate, sub-lethal ionizing events which interact pairwise to create lethal damage. As a result, the biological effect (E) of RT depends on the dose in a linear and quadratic fashion:  $E = n(\alpha d + \beta d^2)$  with n being the number of fractions, d being the dose per fraction, and  $\alpha$  and  $\beta$  being parameters that determine the initial slope and curvature of the underlying cell-survival curve. From this equation, the biological effect dose (BED) can be calculated as:  $BED = nd$

Correspondence to: Feng-Ming (Spring) Kong, MD, PhD. Department of Radiation Oncology, GRU Cancer Center, Georgia Regents University, Augusta, Georgia, USA. Email: fkong@gru.edu.

Submitted Dec 17, 2013. Accepted for publication Jan 20, 2014.  
Available at [www.jthoracdis.com](http://www.jthoracdis.com)

ISSN: 2072-1439

© Pioneer Bioscience Publishing Company. All rights reserved.

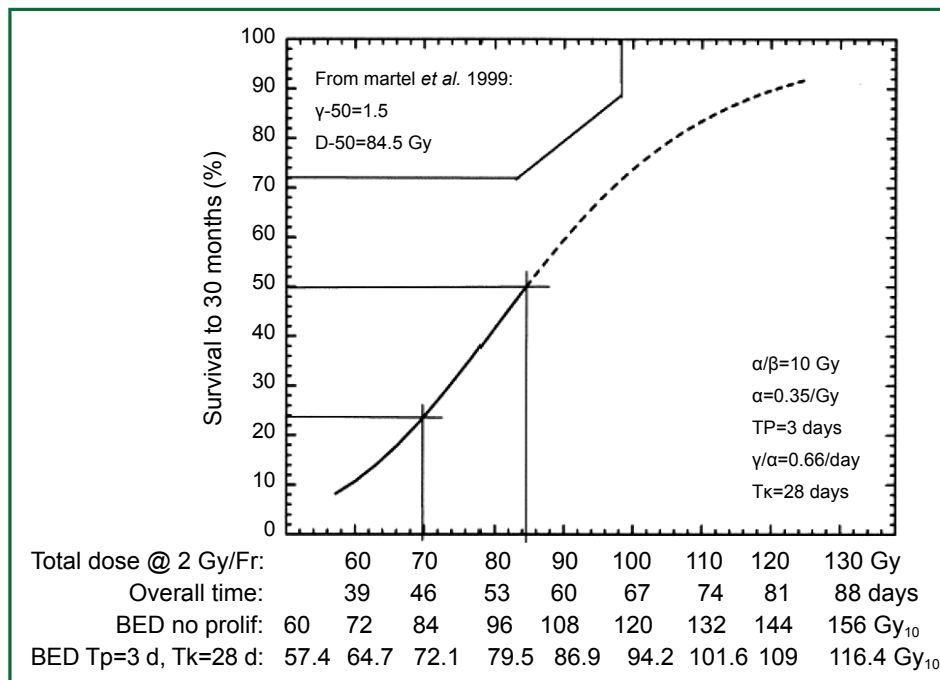


**Figure 1.** Tumor control probability and biological effective dose. The dose response relationship is sigmoidal in one of the early dose escalation studies of non-small cell lung cancer (NSCLC) performed in University of Michigan.

$[1+d/(\alpha/\beta)]$  (1). BED varies according to dose per fraction, number of fractions and characteristics of the tissue contributing to the  $\alpha/\beta$  ratio. BED is used to estimate the effect or risk of radiation in current practice of radiation oncology. When effects of equivalent total doses with different fractionation schemes are compared, they produce unequal biological effects (1). In lung cancer, early evidence suggests that the tumor control rate increases with escalation of BED (Figure 1) (2).

### RT dose effect in NSCLC treated with conventionally fractionated 3D-CRT

While traditional radiation was previously more limited by technology for normal tissue sparing, modern 3D-CRT is able to deliver high-dose radiation to the tumor target areas while minimizing dose to surrounding tissues, allowing greater RT dose for early stage inoperable NSCLC patients (3-7). Dose has been escalated to up to 102.9 Gy while limiting lung dosimetry with most patients tolerating treatment, and post treatment radiation injuries considered to be acceptable (8). Increasing the dose of radiation improves local control and overall survival in most studies reported. In RTOG protocol 73-01 (9) it was found that the in-field failure rate decreased from 58% to 35% as the dose was increased from 40 to 60 Gy.

In a phase I dose-escalation study reported by Rosenzweig *et al.* (10) the 2-year overall survival (OS) rate for patients with stage I-II disease who received <80 Gy was 60%, compared with 66% for patients who received >80 Gy ( $P<0.05$ ), with a median survival time of 25.0 months versus 53.6 months, respectively. A prospective study reported by Kong *et al.* (3) found that the 5-year local-regional progression-free survival (PFS) rates were 12%, 35%, and 49% for groups treated with 67, 80, and 97 Gy, respectively. Median survival (5-year OS) in this study was 12 months (4%), 27 months (22%), and 22 months (28%) for dose levels of 63-69 Gy (mean =67 Gy), 74-84 Gy (mean =80 Gy) and 92-102 Gy (mean =97 Gy), respectively ( $P<0.0002$ ) (Figure 2) (8). The dose response curve for local tumor control was steeper for five years than that of three or four years. Kong *et al.* from University of Michigan (8) demonstrated that high-dose radiation is more vital for patients with larger tumors and may be effective in reducing the adverse outcome associated with a large GTV in early stage NSCLC treated with conventionally fractionated radiation.

### RT dose effect in early stage NSCLC treated with hypo-fractionated SBRT

A promising new technique, SBRT normally delivers much higher

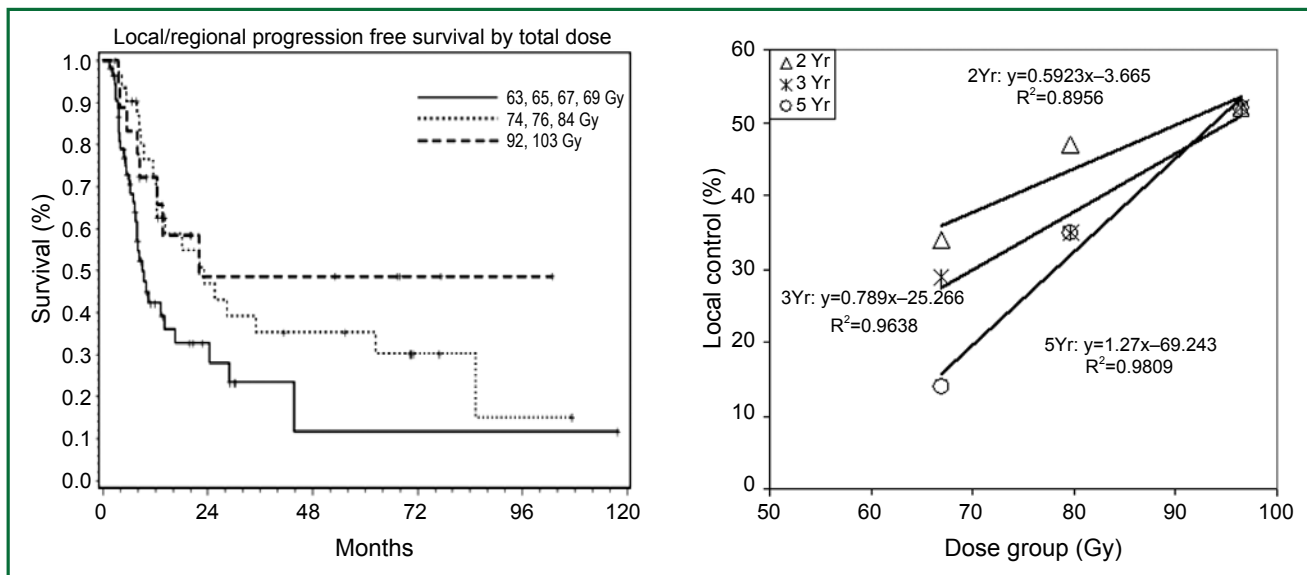


**Figure 2.** Local tumor control increases with higher dose radiation. Radiation dose is associated with long-term tumor control. Dose response relationship is steeper for longer follow-up.

BED than conventionally fractionated 3D-CRT (typically BED of 70-85 Gy), and has generated outstanding tumor control in early stage NSCLC. High BED often contributes to long survival and good local tumor control. Studies from Japan, Germany and China all reported that SBRT with BED  $\geq 100$  Gy was associated with significantly better local control and long-term survival. In patients who received a BED  $\geq 100$  Gy, local tumor control was over 90%. A multicenter study (11) reviewed 257 patients treated at 14 institutions in Japan using a number of different treatment doses and delivery approaches. At median follow up of 38 months, local recurrence rate was 8.4% in patients who were treated to a BED  $\geq 100$  Gy. A recent German study also reported that BED  $\geq 100$  Gy is critical for achieving good local control (12). A Chinese study applied daily fractionated SBRT with a total BED of up to 115 Gy and reported 3- and 5-year OS rates for T1-3 patients of 57.3% and 35.1%, respectively, and 60.2 and 36.5% 3- and 5-year OS rates for stage T1-2 patients respectively (13). Studies from the U.S. suggest that patients who receive 16 Gy  $\times$  3 (BED =124 Gy) have significantly better local control than those who receive lower doses (14). Dose response analysis showed that the outcome plateaued around 120 Gy BED. In Guckenberger's study (12), a PTV-encompassing dose of  $\geq 100$  Gy BED was estimated to be required for local tumor control rates  $>90\%$ . RTOG 0236 (15), using 18 Gy  $\times$  3, equating to a BED of 180 Gy to tumor, represented the First National Cancer Institute cooperative group trial using SBRT for early NSCLC. The study reported 98% tumor control rate at three years. Updated Japanese (16) and German (17)

studies of BED above 100 Gy confirmed over 90% local tumor control for T1 tumors. However, there is no randomized trial to compare different dose regimens for SBRT. In a meta-analysis containing 34 published SBRT datasets (18), observed 5-year OS and cancer specific survival (CSS) was best in those treated to medium BED (around 100 Gy).

Modern technology also allows SBRT delivery of very high radiation dose to the target volume, in as few as one single fraction. However, the effects of radiation after SBRT in a single fraction are not well known. In lung metastases patients receiving a dose of 30 Gy in a single fraction therapy It was reported that LC rates at one and two years were 89.1% and 82.1%, OS rates were 76.4% and 31.2%, CCS rates were 78.5% and 35.4%, and PFS rates were 53.9% and 22%, respectively (19). Interestingly, Guckenberger *et al.* (20) reported that the dose-response relationship was limited in fractionated SBRT: LC was independent from the irradiation dose in the subgroup of patients treated with single-fraction SBRT. Nevertheless, adequate radiation dose is important for good tumor control and survival in early stage NSCLC and the success of hypofractionated high dose SBRT is a strong testimony for radiation dose effect in patients treated with hypofractionated techniques (3 to 8 fractions).

### RT dose effect in locally advanced NSCLC treated with chemoradiation

In locally advanced NSCLC, there are two important aspects to consider: (I) does local regional tumor control impact survival

in patients with locally advanced disease, with high risk of distant disease spread? (II) with extensive tumor involvement in the chest which hosts critical structures, would high dose radiation cause significant toxicity adversely impacting patients? Ultimately, it is important to address whether high dose radiation improves overall survival and quality of life.

### **Local-regional tumor control and overall survival in locally advanced NSCLC**

Local tumor progression is common, and remains a major problem after radiation-based non-surgical treatment in locally advanced NSCLC, despite of advances in radiation technology. Using modern techniques, current radiation therapy applying a uniform dose prescription of 60 Gy or slightly higher generates local control rates of less than 50% and a 5-year overall survival rate of about 10-15% (8,21,22). After RT with or without neoadjuvant chemotherapy, Kong *et al.* in a University of Michigan trial reported ultimate local failure in 70% of patients (8). After neoadjuvant chemoradiotherapy in CALGB 9431 (23), 90% of patients ultimately failed locally, with 45% having local failure alone. After neoadjuvant and concurrent chemotherapy with radiation doses of 60-74 Gy, Socinski *et al.* (24) reported that 46% of patients initially had local failure. Evaluation by bronchoscopy and biopsy one year after treatment completion revealed pathologic local control rates of only 15-17% after 65 Gy of radiation with neoadjuvant therapy (25). After chemoradiation with RT doses of 60 Gy in 2 Gy daily fractions or 69.6 Gy in 1.2 Gy twice daily fractions, a secondary analysis of 11 RTOG trials (9/11 had concurrent chemoradiation) with 1,356 patients reported 2- and 5-year survival rates of 38% and 15%, with 2- and 5-year local-regional failure (LRF) rates of 46% and 52%, respectively (26).

Local-regional disease not only leads to death due to local effects within the chest, but also can serve as a source for metastatic dissemination. In patients with locally advanced disease, Arriagada (27) concluded that the main cause of failure is the absence of local control, and local progression or relapse correlated with poorer survival. In RTOG 73-01 (9), the death rate in patients with intra-thoracic failure was similar to that of patients with distant metastases, and increased survival was observed in patients with complete tumor response (28). In the CHART trial, local control rates of 20% and 29% were associated with median survivals of 9.9 and 27.9 months, respectively (29). In an EORTC trial, Schaake-Koning *et al.* (30) demonstrated a similar correlation between LRC and survival. Reviewing mature results of ten randomized phase III trials with inclusion of concurrent chemoradiation, Auperin *et al.* (31) reported local or local regional control along with overall survival; there seemed significant correlation between LRC and survival rates (Figure 3) (32-37).

### **RT dose, fraction and survival in locally advanced NSCLC**

In locally advanced NSCLC, 5-year OS rate is only about 15% after conventionally fractionated 60 Gy radiation. Dose escalation trials using involved field radiation therapy have demonstrated improved outcomes for patients treated to higher radiation doses, however only a few studies have investigated efficacy and tolerance. The Memorial Sloan Kettering Cancer Center (MSKCC) conducted a phase I dose escalation study of stage IIIA/B patients who received radiation dose of 70.2 to 84 Gy in 1.8 Gy fractions; the OS was significantly superior in patients who received  $\geq 80$  Gy (38). In a randomized trial from China, 5-year LC and 2-year OS improved significantly in stage III patients treated with total dose of 68-74 Gy compared with those treated to 60-64 Gy (51% vs. 36%,  $P=0.032$ ; 39.4% vs. 25.6%,  $P=0.048$ ) (39). Hypo-fractionated RT regimens can also increase the dose to the tumor volume based on the concept that a higher dose per fraction can increase BED, though there are no randomized trials comparing benefits and tolerance among Hypo-fractionated RT and standard schedules. A study by Zhu *et al.* (40) performed dose escalation up to 65-68 Gy in 22 to 23 fractions in 34 NSCLC patients with stage III at diagnosis. 2-year OS, PFS, and LPFS rates were 38%, 30%, and 61%, respectively. In a recent study (41) reported by Osti *et al.*, 24 stage IIIA/B patients had a median OS of 13 months (16 months for IIIA; 13 months for IIIB), with a range of 4 to 56 months.  $BED > 55$  Gy was significantly associated with survival benefit ( $P < 0.001$ ). Another hypo-fractionated RT study (42) included 37 stage III patients without administration of concurrent chemotherapy. All patients were treated with 25 fractions, with dose per fraction ranging from 2.28 to 3.22 Gy. The outcome data showed that 17% of patients achieved complete response, the actuarial 2-year OS calculated to be  $46.8\% \pm 9.7\%$ , with median survival of 18 months. Hyper-fractionated accelerated RT is another method to elevate BED to the tumor. In order to increase total dose to tumor while shortening treatment duration and decreasing late effects, hyper-fractionated-accelerated RT has been attempted in IIIA/B NSCLC patients. In 127 patients receiving hyper-fractionated-accelerated RT, Jeremić *et al.* (43) reported 5-year OS, local PFS and distant metastasis-free survival of 7%, 16%, and 36%, respectively. After two cycles of chemotherapy, stage III NSCLC patients in the DART-bid trial (44) had median OS of 24.3 months, and 2-/5-year OS rates to 51% and 18%, respectively. In a randomized phase III trial reported by Baumann *et al.* (45), survival after conventional RT and Hyper-fractionated-accelerated RT was not different, while local control after Hyper-fractionated-accelerated RT was significantly better than control after conventional RT in patients who had received

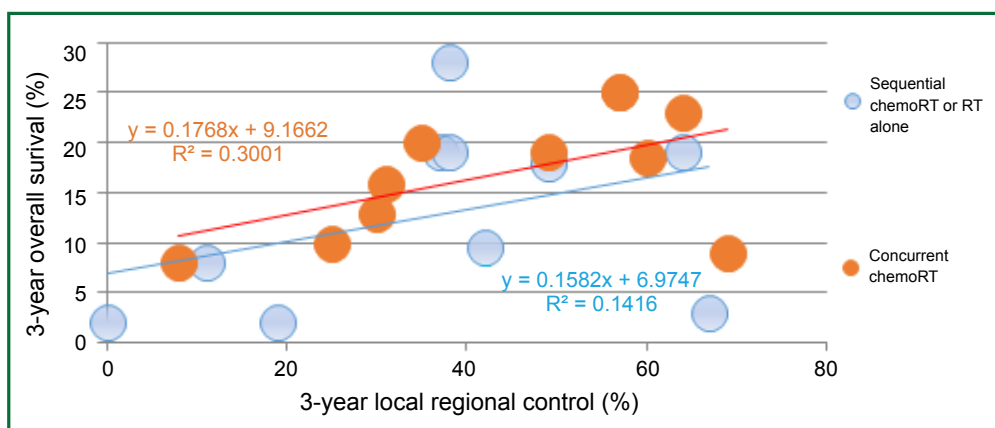


**Figure 3.** Correlation between local regional tumor control and overall survival in locally advanced non-small cell lung cancer (NSCLC). Data presented are reported individual results from 10 phase III trials comparing sequential chemoradiation with concurrent chemoradiation.

chemotherapy before RT ( $P=0.019$ ).

#### **RT dose effect in locally advanced NSCLC treated with concurrent chemoradiation**

In the standard care for locally advanced NSCLC: platinum based chemotherapy concurrent with RT, local tumor control and overall survival remain poor. After neo-adjuvant and concurrent chemotherapy with radiation doses of 60-74 Gy, Socinski *et al.* (46) reported that 46% of patients initially had local failure. A secondary analysis of 11 RTOG trials (9/11 had concurrent chemoradiation) with 1,356 patients treated with chemoradiation with RT doses of 60 Gy in 2 Gy daily fractions or 69.6 Gy in 1.2 Gy twice daily fractions reported 2- and 5-year OS rates of 38% and 15%, with 2- and 5-year LRF rates of 46% and 52%, respectively (25). With concurrent chemotherapy, RTOG 92-04 reported that 2- and 4-year in-field progression (ITPs) were 26% and 30% in the patients receiving radiation dose of 69.6 Gy, compared to 45% and 49% in the 63 Gy arms (47).

RT dose may be an important factor for local tumor control and perhaps survival in this patient population. A good example is a report of 237 patients with stage III NSCLC treated with radiation +/- chemotherapy between 1992 and 2002 at the University of Michigan which showed that BED was the most significant prognostic factor associated with the risk of death (HR =0.96 for each Gy, 95% CI: 0.95-0.97,  $P<0.001$ ). For patients who received concurrent chemotherapy, the hazard ratio of BED for the risk of death was 0.97 per Gy (95% CI: 0.95-0.99,  $P=0.013$ ). One Gy of dose escalation was associated with a 3% reduction in the risk of death. BED remained a significant independent prognostic factor in

patients treated with chemoradiation in the dose range of 60-66 Gy (HR =0.91, 95% CI: 0.84-0.99,  $P=0.041$ ) (48). The RTOG secondary analysis of 1,356 patients treated with chemoradiation between 1988 to 2002 serves as a good example of this as well. This study analyzed for BED effect (1,348 for treatment time adjusted BED~tBED) in the range of 60 Gy in 2 Gy fractions and 69.6 Gy in 1.2 Gy fractions. The 2- and 5-year OS rates were 38% and 15%, respectively. The 2- and 5-year LRF rates were 46% and 52%, respectively. BED (and tBED) was significantly associated with both OS and LRF, with or without adjustment for other covariates on multivariate analysis ( $P<0.0001$ ). A 1-Gy BED increase in RT dose intensity was significantly associated with approximately 4% relative improvement in survival (HR for death =0.96) and 3% relative improvement (HR =0.97) in local-regional control (26).

Overall, radiation dose escalation may improve local regional control and overall survival in patients with stage III NSCLC, based on the results of non-randomized trials (8,48-50) and an RTOG secondary analysis (26) of over 1,300 cases treated with chemoradiation. Regarding the dose effect of >70 Gy with concurrent chemoradiation, investigators from University of Michigan reported results on patients treated in the dose range of 60-100 Gy with concurrent and adjuvant carboplatin and paclitaxel (51). The median local-regional PFS was 10.7 (range: 8.4-13.0) months and has not yet been reached (14.1 to date) ( $P=0.001$ ) for physical doses <70 and >70 Gy, respectively. The median survival was 15.5 (range: 6.5-24.4) months and 41.9 (range: 18.3-65.5) months ( $P=0.003$ ), for physical doses less than and greater than 70 Gy, respectively. The RT dose effect was statistically significant for patients treated with or without concurrent chemotherapy (Figure 4).

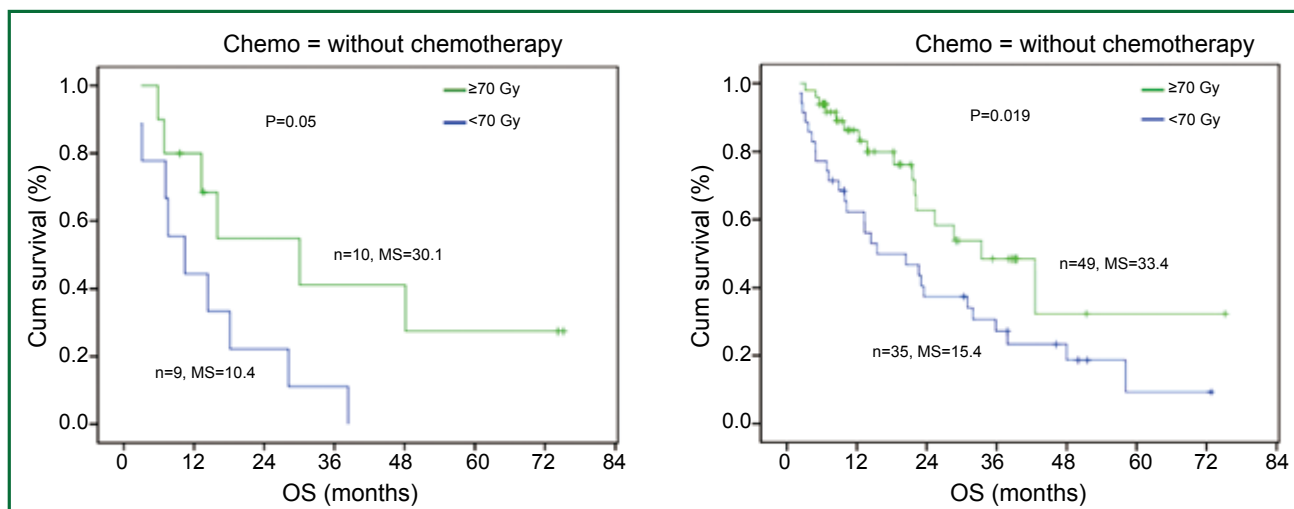


**Figure 4.** Radiation dose and survival in non-small cell lung cancer (NSCLC) in patients treated with or without concurrent chemotherapy. High dose group has better overall survival in both Chemo+ and Chemo- groups.

### Challenges in delivering high dose radiation in locally advanced NSCLC

#### Treatment effect and toxicity after dose escalated RT

It is a remarkable challenge to deliver high dose radiation in patients with advanced NSCLC. A dose escalation study of 79 patients with locally advanced NSCLC treated without chemotherapy reported a maximum tolerance dose of 63.25 Gy in 25 daily fractions over five weeks using intensity-modulated RT to limit severe toxicity to 20%. Grade 4 to 5 late toxicities were attributable to damage to central and perihilar structures and correlated with dose to the proximal bronchial tree (52-54). A trial from University of Michigan with concurrent carboplatin and paclitaxel (UMCC 2003-073) was stopped prematurely due to lack of dose escalation in 60% of patients limited by clinical lung toxicity at 15%. RTOG 0117, a phase I/II dose escalation study with concurrent and adjuvant carboplatin and paclitaxel, reported two acute, treatment-related dose limiting toxicities (DLTs) in the 1st cohort of 17 patients and 6/8 (75%) grade  $\geq 3$  events during long-term follow up. The protocol was revised to de-escalate the radiation therapy dose (74 Gy in 37 fractions). In the new cohort of seven patients, treated with 74 Gy, there was 1 DLT in the first five patients and no DLTs in the next two patients. The maximum tolerable dose was thus determined to be 74 Gy in 37 fractions (2 Gy per fraction) using 3D-CRT with concurrent paclitaxel and carboplatin therapy (55). The CALBG 30105 trial (11) studied induction

chemotherapy followed by concurrent chemoradiotherapy in stage III NSCLC patients randomised between two different chemotherapy regimens delivered concurrently with dose-escalated thoracic conformal RT (74 Gy, once daily, 2 Gy per fraction) in both arms. The carboplatin/gemcitabine arm closed prematurely due to a high rate of grade 4 to 5 pulmonary toxicity. However the carboplatin/paclitaxel arm demonstrated a median survival of 24 months with a 12% rate of grade 3 or higher pulmonary toxicity.

These trial results compared favorably to the historical standard concurrent chemoradiotherapy doses of 60-66 Gy in 2 Gy fractions and formed the basis for the experimental arm in the recently closed phase III RTOG 0617 trial. In this 2x2 factorial design trial patients with stage III NSCLC were treated with weekly carboplatin-paclitaxel chemotherapy and concurrent RT in 2 Gy fractions. Patients were randomised to receive 60 or 74 Gy RT, with or without cetuximab. After RT, all patients received a further two cycles of consolidation chemotherapy, with or without cetuximab. A planned interim analysis after 85 documented events demonstrated a non-superior median survival in the high dose arms which were closed due to a low likelihood of survival benefit from high dose RT with additional accrual and follow up. An updated analysis of the data after 207 events demonstrated a significant increased risk of death in the high dose arms [median survival 28.7 (60 Gy arm) *vs.* 19.5 months (74 Gy),  $P=0.0007$ ; HR =1.56, 95% CI: 1.19-2.06], with a 37% increased risk of local failure in the high dose arms (HR =1.37, 95% CI: 0.99 to 1.89,  $P=0.0319$ ). There were more

treatment related deaths in the high dose arms (10 vs. 2) but this did not reach statistical significance. The worse local control and survival of the high dose arms of RTOG 0617 trial has challenged the assumption that RT dose escalation using conventional dose/fractionation regimens with concurrent chemotherapy will improve outcome in stage III NSCLC. At the time of writing this article, the reasons for the underperformance of the 74 Gy arm are still unclear and the analysis of the individual RT plans by RTOG is ongoing. Hypotheses for the worse local control in the 74 Gy arms include issues with the assessment of local progression versus fibrosis, chemotherapy and RT dose delivery and compliance, issues with RT planning and quality assurance (particularly since IMRT was only used in 46% of centers) and accelerated repopulation due to the prolongation of the overall treatment time. This is supported by an early analysis estimating that tumor control probability of NSCLC decreases 1.6% per day after a six-week duration of RT, and according to a secondary analysis of three RTOG trials for stage III NSCLC patients treated with concurrent chemoradiotherapy, showing that prolonged treatment time translated into a 2% increase in the risk of death for each day of prolongation in therapy (56). A combination of factors probably account for the survival results of RTOG 0617, including inferior local control in the 74 Gy arms; but unreported treatment-related deaths (cardiac and pulmonary) are likely to be one of the major causes for the inferior survival in the 74 Gy arms. Indeed the multivariate survival analysis reported that V5 and V50 heart were both associated with worse survival. This study highlights the need for stricter constraints to adjacent critical organs at risk such as heart, lung, proximal bronchial tree and RT quality assurance programs in future studies and institutional protocols. The current view in the radiation oncology community is that radiation dose escalation with conventional fractionation and concurrent CT is not the way forward, but treatment intensification should be pursued, including studies of altered fractionation and individualization of dose (57-59).

Currently, there are investigative efforts to increase daily fraction size to escalate total radiation dose without extending the treatment duration. One approach involves dose escalation using 2.25 Gy daily fractions (once or twice daily) while limiting treatment duration to six weeks (60). This approach was used to escalate to 87.8 Gy in patients with limited lung volumes without concurrent chemotherapy. Another approach is to use a higher dose fraction every day while limiting the treatment duration to five weeks without concurrent chemotherapy (61). UMCC 200373 and UMCC2007123 limited treating duration to six weeks while delivering RT dose escalation with concurrent chemotherapy, and achieved promising results (51).

### **Treatment related death after RT based treatment**

Treatment related severe toxicities can be fatal. For example, a recent meta-analysis reported 1.9% grade 5 pneumonitis after concurrent chemoradiotherapy (62). Radiation pneumonitis attributed death occurred in up to 10% (35,63,64) of patients treated with concurrent chemoradiation, and up to 4.3% of patients treated with radiation alone (35,65,66). Critical organs at risk include the heart, lung and esophagus. Grade 5 adverse events were reported in 1.7% (range, 1-3%) (67,68), and 2.5% (range, 1.2-8.2%) (69,70), for patients treated with concurrent chemotherapy with conventional doses (60-63 Gy) and concurrent chemotherapy with escalated doses (>63 Gy). It is possible that these increased events were due to treatment toxicity, though some of them were not identified as such. Another ongoing issue with the reporting of treatment related deaths is that many patients die at home or at local community hospitals, leading to probable underreporting of grade 5 events. These treatment toxicities often arise as a consequence of the challenges of delivering high dose radiation to locally advanced disease without incidentally delivering high dose to the OARs (Table 1).

### **Potential strategies to improve therapeutic gain in NSCLC**

It is imperative to pursue new strategies to increase the dose ratio of tumor target over critical structures. Radiation physics and technology advancements such as IMRT, IGRT, and volume based planning are important for delivery of radiation precisely to the target, though this will not be discussed in this review. Knowledge of tumor target gained from tools such as Positron Emission Tomography helps define the target more accurately. Individualized radiation with isototoxicity prescription is a promising strategy. For traditional adaptive radiation plan, prescription dose is required to cover the whole GTV and CTV determined according to images simulated before therapy. To obtain the best LRC and OS from radiation, higher total dose while limiting total treatment duration less than six weeks and dosimetric factors such as V20 and MLD should be seriously considered especially for larger tumors ( diameter >5 cm). An ongoing European phase II PET-boost trial (ClinicalTrials.gov Identifier: NCT01024829) randomises patients with stage IB-III NSCLC to dose-escalation starting from 66 Gy given in 24 fractions of 2.75 Gy with an integrated boost to either the entire primary tumour or to >50% of the maximum Standardised Uptake Volume (SUV<sub>max</sub>) area of the primary tumor, while limiting MLD to 20 Gy. Preliminary results from

**Table 1.** Grade 5 events in reported clinical trials.

| Trials   | RT total dose (Gy) | Number of Fx | Number of patients | Grade 5 events (%) | Chemoregimens                       |
|--|--------------------|--------------|--------------------|--------------------|-------------------------------------|
| <b>Dose escalation radiation with concurrent chemotherapy</b>    |                    |              |                    |                    |                                     |
| RTOG 0617, Bradley <i>et al.</i> , 2013 (56)                     | 74                 | 37           | 208                | 8.2                | TC                                  |
|  | 60                 | 30           | 216                | 3.2                | TC                                  |
| RTOG 9410, Curran <i>et al.</i> , 2011 (71)                      | 63                 | 34           | 195                | 3.6                | Vinblastine, cisplatin              |
|  | 69.6               | 58           | 382                | 1.8                | EP                                  |
| Salama <i>et al.</i> , 2011 (11)                                 | 74                 | 37           | 26                 | 7.7                | Gemcitabine, carboplatin            |
| Uitterhoeve, 2007 (72)   | 66                 | 24           | 56                 | 1.8                | cisplatin                           |
| Berghmans <i>et al.</i> , 2009 (73)                              | 66                 | 33           | 48                 | 6.3                | Gemcitabine, cisplatin, vinorelbine |
| Movsas <i>et al.</i> , 2005 (74)                                 | 69.6               | 58           | 242                | 1.2                | TC                                  |
| LAMP trial, Belani <i>et al.</i> , 2005 (75)                     | 63                 | 34           | 166                | 1.8                | TC                                  |
| NPC 95-01, Fournel <i>et al.</i> , 2005 (35)                     | 66                 | 33           | 100                | 10                 | EP                                  |
| <b>Conventional dose radiation concurrent with chemotherapy</b>  |                    |              |                    |                    |                                     |
| RTOG 0617, Bradley <i>et al.</i> , 2013 (56)                     | 60                 | 30           | 216                | 3.2                | TC                                  |
| Albain <i>et al.</i> , 2009 (76)                                 | 61                 | NR           | 194                | 1.5                | EP                                  |
| SWOG S0023, Kelly <i>et al.</i> , 2008 (34)                      | 61                 | 33           | 543                | 1.1                | EP                                  |
| NCCTG 90-24-51, NCCTG 94-24-52, Schild <i>et al.</i> , 2007 (65) | 60                 | 20 or 40     | 129                | 1.6                | EP                                  |
| <b>Radiation alone</b>   |                    |              |                    |                    |                                     |
| NCCTG 90-24-51, NCCTG 94-24-52, Schild <i>et al.</i> , 2007 (65) | 60                 | 20 or 40     | 37                 | 2.7                | —                                   |
| JCOG9812, Atagi <i>et al.</i> , 2005 (36)                        | 60                 | 30           | 23                 | 4.3                | —                                   |
| ECOG, Clamon <i>et al.</i> , 1999 (66)                           | 60                 | 30           | 120                | 1.7                | —                                   |

RT, radiotherapy; EP, etoposide and cisplatin; TC, paclitaxel and carboplatin.

the first 20 randomised patients showed that this was feasible and did not exceed pre-defined normal tissue constraints. Recent studies from Kong *et al.* at University of Michigan (3) demonstrated that there is a significant decrease in tumor size and FDG activity after radiation dose of 45 Gy. According to this result, we could adapt targeting to the decreased tumor defined on FDG-PET/CT after 45 Gy with a fixed composite MLD limit of 20 Gy while allowing remarkable escalation of total dose to the tumor. Kong *et al.* have demonstrated that tumor volume reduces significantly more on FDG PET than on CT at 40-50 Gy (4-5 weeks during the course of fractionated RT) (77). Using the reduced volume identified on during-RT PET, dose to active and resistant tumor was significantly escalated while dose to the normal tissues were either reduced (due to adaptive shrinking fields) or unchanged (78). The ongoing RTOG1106

trial (<http://www.rtog.org/ClinicalTrials/ProtocolTable/StudyDetails.aspx?study=1106>) adopted this concept, and will use this approach to obtain FDG-PET/CT during the course of chemoradiation to adapt their plan to a tumor target smaller than that from before therapy to escalate dose to as high as 80.4 Gy delivered in six weeks without increasing doses to the OARs. The total dose for each patient in the experimental arm will be determined by the dose corresponding to a MLD of 20 Gy (equivalent to a 15-17% probability of grade >2 lung toxicity based on the current NTCP model). The study hypothesized that the during-treatment PET/CT-based adaptive therapy will allow us to dose escalate (i.e., raise the daily dose to the reduced target volume for the remainder of the treatment) in the majority of patients and meet the dose limits of normal structures, thus improving LRC without increasing normal tissue toxicity. This

will also allow us to use the lung dose limits to individualize adaptive dose escalation to residual active tumor regions and limit the incidence of pneumonitis and other toxicities simultaneously.

## Conclusions

In summary, there is a clear radiation dose effect in NSCLC patients. Although the benefit of high dose radiation has been demonstrated in early stage patients, the clinical benefit of high dose radiation in patients has been challenged by preliminary results from RTOG0617. Treatment related toxicity can be a major reason for failure of high dose radiation. Future study of radiation therapy may benefit from individualized radiation dose prescription based on the sensitivity of tumor and critical organs of each individual patient. Studies from Europe will individualize doses based on FDG intensity at baseline while limiting treatment duration to five weeks. RTOG1106, an ongoing randomized phase II study, will examine the effect of individualized adaptive radiation therapy (over an uniform 60 Gy) by targeting high dose radiation to most resistant tumor while keeping doses to critical structures strictly controlled in locally advanced NSCLC patients.

## Acknowledgements

*Disclosure:* The authors declare no conflict of interest.

## References

- O'Rourke SF, McAnaney H, Hillen T. Linear quadratic and tumour control probability modelling in external beam radiotherapy. *J Math Biol* 2009;58:799-817.
- Martel MK, Ten Haken RK, Hazuka MB et al. Estimation of tumor control probability model parameters from 3-D dose distributions of non-small cell lung cancer patients. *Lung Cancer* 1999;24:31-7.
- Kong FM, Hayman JA, Griffith KA, et al. Final toxicity results of a radiation-dose escalation study in patients with non-small-cell lung cancer (NSCLC): predictors for radiation pneumonitis and fibrosis. *Int J Radiat Oncol Biol Phys* 2006;65:1075-86.
- Socinski MA, Marks LB, Garst J, et al. Carboplatin/paclitaxel or carboplatin/vinorelbine followed by accelerated hyperfractionated conformal radiation therapy: a preliminary report of a phase I dose escalation trial from the Carolina Conformal Therapy Consortium. *Oncologist* 2001;6 Suppl 1:20-4.
- Bradley J, Graham MV, Winter K, et al. Toxicity and outcome results of RTOG 9311: a phase I-II dose-escalation study using three-dimensional conformal radiotherapy in patients with inoperable non-small-cell lung carcinoma. *Int J Radiat Oncol Biol Phys* 2005;61:318-28.
- Song Y, Mueller B, Obcemea C, et al. Feasibility of implementing stereotactic body radiation therapy using a non-commercial volumetric modulated arc therapy treatment planning system for early stage lung cancer. *Conf Proc IEEE Eng Med Biol Soc* 2011;2011:409-12.
- Sonke JJ, Rossi M, Wolthaus J, et al. Frameless stereotactic body radiotherapy for lung cancer using four-dimensional cone beam CT guidance. *Int J Radiat Oncol Biol Phys* 2009;74:567-74.
- Kong FM, Ten Haken RK, Schipper MJ, et al. High-dose radiation improved local tumor control and overall survival in patients with inoperable/unresectable non-small-cell lung cancer: long-term results of a radiation dose escalation study. *Int J Radiat Oncol Biol Phys* 2005;63:324-33.
- Perez CA, Pajak TF, Rubin P, et al. Long-term observations of the patterns of failure in patients with unresectable non-oat cell carcinoma of the lung treated with definitive radiotherapy. Report by the Radiation Therapy Oncology Group. *Cancer* 1987;59:1874-81.
- Rosenzweig KE, Fox JL, Yorke E, et al. Results of a phase I dose-escalation study using three-dimensional conformal radiotherapy in the treatment of inoperable nonsmall cell lung carcinoma. *Cancer* 2005;103:2118-27.
- Salama JK, Stinchcombe TE, Gu L, et al. Pulmonary toxicity in Stage III non-small cell lung cancer patients treated with high-dose (74 Gy) 3-dimensional conformal thoracic radiotherapy and concurrent chemotherapy following induction chemotherapy: a secondary analysis of Cancer and Leukemia Group B (CALGB) trial 30105. *Int J Radiat Oncol Biol Phys* 2011;81:e269-74.
- Guckenberger M, Wulf J, Mueller G, et al. Dose-response relationship for image-guided stereotactic body radiotherapy of pulmonary tumors: relevance of 4D dose calculation. *Int J Radiat Oncol Biol Phys* 2009;74:47-54.
- Chen Y, Guo W, Lu Y, et al. Dose-individualized stereotactic body radiotherapy for T1-3N0 non-small cell lung cancer: long-term results and efficacy of adjuvant chemotherapy. *Radiother Oncol* 2008;88:351-8.
- Chang BK, Timmerman RD. Stereotactic body radiation therapy: a comprehensive review. *Am J Clin Oncol* 2007;30:637-44.
- Taremi M, Hope A, Dahele M, et al. Stereotactic body radiotherapy for medically inoperable lung cancer: prospective, single-center study of 108 consecutive patients. *Int J Radiat Oncol Biol Phys* 2012;82:967-73.
- Onishi H, Shirato H, Nagata Y, et al. Stereotactic body radiotherapy (SBRT) for operable stage I non-small-cell lung cancer: can SBRT be comparable to surgery? *Int J Radiat Oncol Biol Phys* 2011;81:1352-8.
- Wulf J, Baier K, Mueller G, et al. Dose-response in stereotactic irradiation of lung tumors. *Radiother Oncol* 2005;77:83-7.
- Zhang J, Yang F, Li B, et al. Which Is the Optimal Biologically Effective Dose of Stereotactic Body Radiotherapy for Stage I Non-Small-Cell Lung Cancer? A Meta-Analysis. *Int J Radiat Oncol Biol Phys* 2011;81:e305-16.
- Osti MF, Carnevale A, Valeriani M, et al. Clinical outcomes of single dose stereotactic radiotherapy for lung metastases. *Clin Lung Cancer* 2013;14:699-703.
- Guckenberger M, Klement RJ, Allgauer M, et al. Applicability of the linear-quadratic formalism for modeling local tumor control probability in high dose per fraction stereotactic body radiotherapy for early stage non-small

- cell lung cancer. *Radiother Oncol* 2013;109:13-20.
21. Dillman RO, Herndon J, Seagren SL, et al. Improved survival in stage III non-small-cell lung cancer: seven-year follow-up of cancer and leukemia group B (CALGB) 8433 trial. *J Natl Cancer Inst* 1996;88:1210-5.
  22. Sause W, Kolesar P, Taylor S IV, et al. Final results of phase III trial in regionally advanced unresectable non-small cell lung cancer: Radiation Therapy Oncology Group, Eastern Cooperative Oncology Group, and Southwest Oncology Group. *Chest* 2000;117:358-64.
  23. Vokes EE, Herndon JE 2nd, Crawford J, et al. Randomized phase II study of cisplatin with gemcitabine or paclitaxel or vinorelbine as induction chemotherapy followed by concomitant chemoradiotherapy for stage IIIB non-small-cell lung cancer: cancer and leukemia group B study 9431. *J Clin Oncol* 2002;20:4191-8.
  24. Socinski MA, Rosenman JG, Halle J, et al. Dose-escalating conformal thoracic radiation therapy with induction and concurrent carboplatin/paclitaxel in unresectable stage IIIA/B nonsmall cell lung carcinoma: a modified phase I/II trial. *Cancer* 2001;92:1213-23.
  25. Tursz T, Cesne AL, Baldeyrou P, et al. Phase I study of a recombinant adenovirus-mediated gene transfer in lung cancer patients. *J Natl Cancer Inst* 1996;88:1857-63.
  26. Machtay M, Bae K, Movsas B, et al. Higher Biologically Effective Dose of Radiotherapy Is Associated with Improved Outcomes for Locally Advanced Non-Small Cell Lung Carcinoma Treated with Chemoradiation: An Analysis of the Radiation Therapy Oncology Group. *Int J Radiat Oncol Biol Phys* 2012;82:425-34.
  27. Arriagada R. Current strategies for radiation therapy in non-small cell lung cancer. *Chest* 1997;112:209S-213S.
  28. Schaake-Koning C, van den Bogaert W, Dalesio O, et al. Effects of concomitant cisplatin and radiotherapy on inoperable non-small-cell lung cancer. *N Engl J Med* 1992;326:524-30.
  29. Saunders M, Dische S, Barrett A, et al. Continuous, hyperfractionated, accelerated radiotherapy (CHART) versus conventional radiotherapy in non-small cell lung cancer: mature data from the randomised multicentre trial. CHART Steering committee. *Radiother Oncol* 1999;52:137-48.
  30. Schaake-Koning C, van den Bogaert W, Dalesio O, et al. Radiosensitization by cytotoxic drugs. The EORTC experience by the Radiotherapy and Lung Cancer Cooperative Groups. *Lung Cancer* 1994;10 Suppl 1:S263-70.
  31. Aupérin A, Le Péchoux C, Rolland E, et al. Meta-analysis of concomitant versus sequential radiochemotherapy in locally advanced non-small-cell lung cancer. *J Clin Oncol* 2010;28:2181-90.
  32. Lu C, Lee JJ, Komaki R, et al. Chemoradiotherapy with or without AE-941 in stage III non-small cell lung cancer: a randomized phase III trial. *J Natl Cancer Inst* 2010;102:859-65.
  33. Hanna N, Neubauer M, Yiannoutsos C, et al. Phase III study of cisplatin, etoposide, and concurrent chest radiation with or without consolidation docetaxel in patients with inoperable stage III non-small-cell lung cancer: the Hoosier Oncology Group and U.S. Oncology. *J Clin Oncol* 2008;26:5755-60.
  34. Kelly K, Chansky K, Gaspar LE, et al. Phase III trial of maintenance gefitinib or placebo after concurrent chemoradiotherapy and docetaxel consolidation in inoperable stage III non-small-cell lung cancer: SWOG S0023. *J Clin Oncol* 2008;26:2450-6.
  35. Fournel P, Robinet G, Thomas P, et al. Randomized phase III trial of sequential chemoradiotherapy compared with concurrent chemoradiotherapy in locally advanced non-small-cell lung cancer: Groupe Lyon-Saint-Etienne d'Oncologie Thoracique-Groupe Français de Pneumo-Cancerologie NPC 95-01 Study. *J Clin Oncol* 2005;23:5910-7.
  36. Atagi S, Kawahara M, Tamura T, et al. Standard thoracic radiotherapy with or without concurrent daily low-dose carboplatin in elderly patients with locally advanced non-small cell lung cancer: a phase III trial of the Japan Clinical Oncology Group (JCOG9812). *Jpn J Clin Oncol* 2005;35:195-201.
  37. Belani CP, Wang W, Johnson DH, et al. Phase III study of the Eastern Cooperative Oncology Group (ECOG 2597): induction chemotherapy followed by either standard thoracic radiotherapy or hyperfractionated accelerated radiotherapy for patients with unresectable stage IIIA and B non-small-cell lung cancer. *J Clin Oncol* 2005;23:3760-7.
  38. Le QT, Loo BW, Ho A, et al. Results of a phase I dose-escalation study using single-fraction stereotactic radiotherapy for lung tumors. *J Thorac Oncol* 2006;1:802-9.
  39. Yuan S, Sun X, Li M, et al. A randomized study of involved-field irradiation versus elective nodal irradiation in combination with concurrent chemotherapy for inoperable stage III nonsmall cell lung cancer. *Am J Clin Oncol* 2007;30:239-44.
  40. Zhu ZF, Fan M, Wu KL, et al. A phase II trial of accelerated hypofractionated three-dimensional conformal radiation therapy in locally advanced non-small cell lung cancer. *Radiother Oncol* 2011;98:304-8.
  41. Osti MF, Agolli L, Valeriani M, et al. Image guided hypofractionated 3-dimensional radiation therapy in patients with inoperable advanced stage non-small cell lung cancer. *Int J Radiat Oncol Biol Phys* 2013;85:e157-63.
  42. Adkison JB, Khuntia D, Bentzen SM, et al. Dose escalated, hypofractionated radiotherapy using helical tomotherapy for inoperable non-small cell lung cancer: preliminary results of a risk-stratified phase I dose escalation study. *Technol Cancer Res Treat* 2008;7:441-7.
  43. Jeremić B, Miličić B, Milisavljević S. Concurrent hyperfractionated radiation therapy and chemotherapy in locally advanced (Stage III) non-small-cell lung cancer: single institution experience with 600 patients. *Int J Radiat Oncol Biol Phys* 2012;82:1157-63.
  44. Wurstbauer K, Deutschmann H, Dagn K, et al. DART-bid (Dose-differentiated accelerated radiation therapy, 1.8 Gy twice daily)--a novel approach for non-resected NSCLC: final results of a prospective study, correlating radiation dose to tumor volume. *Radiat Oncol* 2013;8:49.
  45. Baumann M, Herrmann T, Koch R, et al. Final results of the randomized phase III CHARTWEL-trial (ARO 97-1) comparing hyperfractionated-accelerated versus conventionally fractionated radiotherapy in non-small cell lung cancer (NSCLC). *Radiother Oncol* 2011;100:76-85.
  46. Socinski MA, Morris DE, Halle JS, et al. Induction and concurrent

- chemotherapy with high-dose thoracic conformal radiation therapy in unresectable stage IIIA and IIIB non-small-cell lung cancer: a dose-escalation phase I trial. *J Clin Oncol* 2004;22:4341-50.
47. Komaki R, Seiferheld W, Ettinger D, et al. Randomized phase II chemotherapy and radiotherapy trial for patients with locally advanced inoperable non-small-cell lung cancer: long-term follow-up of RTOG 92-04. *Int J Radiat Oncol Biol Phys* 2002;53:548-57.
  48. Wang L, Correa CR, Zhao L, et al. The effect of radiation dose and chemotherapy on overall survival in 237 patients with Stage III non-small-cell lung cancer. *Int J Radiat Oncol Biol Phys* 2009;73:1383-90.
  49. Bradley JD, Ieumwananonthachai N, Purdy JA, et al. Gross tumor volume, critical prognostic factor in patients treated with three-dimensional conformal radiation therapy for non-small-cell lung carcinoma. *Int J Radiat Oncol Biol Phys* 2002;52:49-57.
  50. Rengan R, Rosenzweig KE, Venkatraman E, et al. Improved local control with higher doses of radiation in large-volume stage III non-small-cell lung cancer. *Int J Radiat Oncol Biol Phys* 2004;60:741-7.
  51. Kong FM, Ten Haken R, Hayman J, et al. Personalized High Dose Radiation (> 70 Gy) Is Significantly Associated with Better Local Regional Control and Overall Survival in Non-small Cell Lung Cancer Treated with Concurrent Chemoradiation. *Int J Radiat Oncol Biol Phys* 2011;81:S594.
  52. Cannon DM, Mehta MP, Adkison JB, et al. Dose-limiting toxicity after hypofractionated dose-escalated radiotherapy in non-small-cell lung cancer. *J Clin Oncol* 2013;31:4343-8.
  53. Han C, Wang W, Quint L, et al. Relationship Between Pulmonary Artery Invasion and High-dose Radiation and Overall Survival in Patients With Non-small Cell Lung Cancer. *Int J Radiat Oncol Biol Phys* 2012;84:S612.
  54. Xue J, Han C, Matuszak M, et al. High Dose to Large Volumes of Pericardium May Be Associated With Radiation-related Pericardial Effusion and Survival in Patients With NSCLC. *Int J Radiat Oncol Biol Phys* 2012;84:S592-3.
  55. Bradley JD, Moughan J, Graham MV, et al. A phase I/II radiation dose escalation study with concurrent chemotherapy for patients with inoperable stages I to III non-small-cell lung cancer: phase I results of RTOG 0117. *Int J Radiat Oncol Biol Phys* 2010;77:367-72.
  56. Bradley JD, Komaki R, Masters GA, et al. A randomized phase III comparison of standard-dose (60 Gy) versus high-dose (74 Gy) conformal chemoradiotherapy with or without cetuximab for stage III non-small cell lung cancer: Results on radiation dose in RTOG 0617. *J Clin Oncol* 2013;31:abstr 7501.
  57. Ben-Dor I, Waksman R, Hanna NN, et al. Utility of radiologic review for noncardiac findings on multislice computed tomography in patients with severe aortic stenosis evaluated for transcatheter aortic valve implantation. *Am J Cardiol* 2010;105:1461-4.
  58. Zhao KL, Ma JB, Liu G, et al. Three-dimensional conformal radiation therapy for esophageal squamous cell carcinoma: is elective nodal irradiation necessary? *Int J Radiat Oncol Biol Phys* 2010;76:446-51.
  59. Cheng Y, Anick P, Hong P, et al. Temporal relation discovery between events and temporal expressions identified in clinical narrative. *J Biomed Inform* 2013;46 Suppl:S48-53.
  60. Belderbos JS, De Jaeger K, Heemsbergen WD, et al. First results of a phase I/II dose escalation trial in non-small cell lung cancer using three-dimensional conformal radiotherapy. *Radiother Oncol* 2003;66:119-26.
  61. Mehta M, Scrimger R, Mackie R, et al. A new approach to dose escalation in non-small-cell lung cancer. *Int J Radiat Oncol Biol Phys* 2001;49:23-33.
  62. Palma DA, Senan S, Tsujino K, et al. Predicting radiation pneumonitis after chemoradiation therapy for lung cancer: an international individual patient data meta-analysis. *Int J Radiat Oncol Biol Phys* 2013;85:444-50.
  63. Bral S, Duchateau M, Versmissen H, et al. Toxicity report of a phase 1/2 dose-escalation study in patients with inoperable, locally advanced nonsmall cell lung cancer with helical tomotherapy and concurrent chemotherapy. *Cancer* 2010;116:241-50.
  64. Naito Y, Kubota K, Nihei K, et al. Concurrent chemoradiotherapy with cisplatin and vinorelbine for stage III non-small cell lung cancer. *J Thorac Oncol* 2008;3:617-22.
  65. Schild SE, Mandrekar SJ, Jatoi A, et al. The value of combined-modality therapy in elderly patients with stage III nonsmall cell lung cancer. *Cancer* 2007;110:363-8.
  66. Clamon G, Herndon J, Cooper R, et al. Radiosensitization with carboplatin for patients with unresectable stage III non-small-cell lung cancer: a phase III trial of the Cancer and Leukemia Group B and the Eastern Cooperative Oncology Group. *J Clin Oncol* 1999;17:4-11.
  67. Saitoh J, Saito Y, Kazumoto T, et al. Concurrent chemoradiotherapy followed by consolidation chemotherapy with bi-weekly docetaxel and carboplatin for stage III unresectable, non-small-cell lung cancer: clinical application of a protocol used in a previous phase II study. *Int J Radiat Oncol Biol Phys* 2012;82:1791-6.
  68. Phernambucq EC, Hartemink KJ, Smit EF, et al. Tumor cavitation in patients with stage III non-small-cell lung cancer undergoing concurrent chemoradiotherapy: incidence and outcomes. *J Thorac Oncol* 2012;7:1271-5.
  69. Byhardt RW, Vaickus L, Witt PL, et al. Recombinant human interferon-beta (rHuIFN-beta) and radiation therapy for inoperable non-small cell lung cancer. *J Interferon Cytokine Res* 1996;16:891-902.
  70. Graham PH, Clark C, Abell F, et al. Concurrent end-phase boost high-dose radiation therapy for non-small-cell lung cancer with or without cisplatin chemotherapy. *Australas Radiol* 2006;50:342-8.
  71. Curran WJ Jr, Paulus R, Langer CJ, et al. Sequential vs. concurrent chemoradiation for stage III non-small cell lung cancer: randomized phase III trial RTOG 9410. *J Natl Cancer Inst* 2011;103:1452-60.
  72. Uitterhoeve AL, Koolen MG, van Os RM, et al. Accelerated high-dose radiotherapy alone or combined with either concomitant or sequential chemotherapy; treatments of choice in patients with Non-Small Cell Lung Cancer. *Radiat Oncol* 2007;2:27.
  73. Berghmans T, Van Houtte P, Paesmans M, et al. A phase III randomised study comparing concomitant radiochemotherapy as induction versus

- consolidation treatment in patients with locally advanced unresectable non-small cell lung cancer. *Lung Cancer* 2009;64:187-93.
74. Movsas B, Scott C, Langer C, et al. Randomized trial of amifostine in locally advanced non-small-cell lung cancer patients receiving chemotherapy and hyperfractionated radiation: radiation therapy oncology group trial 98-01. *J Clin Oncol* 2005;23:2145-54.
75. Belani CP, Choy H, Bonomi P, et al. Combined chemoradiotherapy regimens of paclitaxel and carboplatin for locally advanced non-small-cell lung cancer: a randomized phase II locally advanced multi-modality protocol. *J Clin Oncol* 2005;23:5883-91.
76. Albain KS, Swann RS, Rusch VW, et al. Radiotherapy plus chemotherapy with or without surgical resection for stage III non-small-cell lung cancer: a phase III randomised controlled trial. *Lancet* 2009;374:379-86.
77. Kong FM, Frey KA, Quint LE, et al. A pilot study of [<sup>18</sup>F] fluorodeoxyglucose positron emission tomography scans during and after radiation-based therapy in patients with non small-cell lung cancer. *J Clin Oncol* 2007;25:3116-23.
78. Mahasittiwat P, Yuan S, Xie C, et al. Metabolic Tumor Volume on PET Reduced More than Gross Tumor Volume on CT during Radiotherapy in Patients with Non-Small Cell Lung Cancer Treated with 3DCRT or SBRT. *J Radiat Oncol* 2013;2:191-202.



**Cite this article as:** Kong FM, Zhao J, Wang J, Faivre-Fin C. Radiation dose effect in locally advanced non-small cell lung cancer. *J Thorac Dis* 2014;6(4):336-347. doi: 10.3978/j.issn.2072-1439.2014.01.23

## Accelerated dose escalation with proton beam therapy for non-small cell lung cancer

Daniel R. Gomez, Joe Y. Chang

Department of Radiation Oncology, University of Texas MD Anderson Cancer Center, Houston, TX, USA

### ABSTRACT

Local tumor control remains challenging in many cases of non-small cell lung cancer (NSCLC), particularly those that involve large or centrally located tumors. Concurrent chemotherapy and radiation can maximize tumor control and survival for patients with locally advanced disease, but a substantial proportion of such patients cannot tolerate this therapy, and sequential chemoradiation regimens or radiation given alone at conventionally fractionated doses produces suboptimal results. An alternative approach is the use of hypofractionated proton beam therapy (PBT). The energy distribution of protons can be exploited to reduce involuntary irradiation of normal tissues, particularly the low-dose irradiation problematic in intensity-modulated (photon) radiation therapy (IMRT). Here we summarize current evidence on the use of hypofractionated PBT for both early-stage and locally advanced NSCLC, and the possibility of using hypofractionated regimens for patients who are not candidates for concurrent chemotherapy.

### KEYWORDS

Hypofractionation; early-stage disease; locally advanced disease; proton beam therapy (PBT); stereotactic ablative body radiation (SABR); intensity-modulated proton therapy (IMPT); passive scattering; dosimetric comparisons; clinical studies

*J Thorac Dis 2014;6(4):348-355. doi: 10.3978/j.issn.2072-1439.2013.11.07*

### Introduction

Local tumor control remains a substantial challenge in many cases of non-small cell lung cancer (NSCLC). For patients with early-stage disease, the advent of stereotactic ablative body radiation (SABR) for definitive therapy has drastically reduced the rate of locoregional recurrence (1), but some tumors, particularly those that are large or centrally located, remain challenging to treat because of the risk of severe toxicity (2). For patients with locally advanced disease, concurrent chemotherapy and radiation have been shown to maximize control and survival outcomes, but many patients are not candidates for this approach because of age, the presence of comorbid conditions, or poor performance status (3,4), and for such patients sequential chemoradiation regimens or radiation

given alone at conventionally fractionated doses produces suboptimal results.

Thus, more effective and safe radiation therapy regimens are needed for subsets of patients with early-stage or locally advanced NSCLC. An approach that has been increasingly explored over the past decade has been the use of hypofractionated proton beam therapy (PBT). The energy distribution of protons [as opposed to photon (X-ray- or gamma-ray-) based irradiation] has theoretical advantages over that of photons because of the Bragg peak characteristic of proton particles, which can be exploited to reduce exposure of normal tissues to radiation, particularly at low doses. Under this premise, emerging dosimetric and clinical studies are being undertaken to assess the role of PBT, including hypofractionated regimens as appropriate, for carefully chosen patients.

This review summarizes current evidence regarding the use of hypofractionated PBT for early-stage NSCLC, including use of PBT as an alternative to SABR for patients with T1-T2 node-negative tumors, followed by a discussion of PBT for locally advanced disease, including tumors that involve the mediastinum, and the possibility of using hypofractionated regimens for patients who are not candidates for concurrent chemotherapy. We have endeavored to convey a level-of-

Correspondence to: Daniel Gomez, MD. The University of Texas MD Anderson Cancer Center, 1840 Old Spanish Trail, Houston, TX, USA. Email: dgomez@mdanderson.org

Submitted Aug 21, 2013. Accepted for publication Nov 07, 2013.  
Available at [www.jthoracdis.com](http://www.jthoracdis.com)

ISSN: 2072-1439

© Pioneer Bioscience Publishing Company. All rights reserved.

evidence-based approach to applying these concepts for specific cases and to outline future paths for research to better determine which patients would derive the greatest benefit from hypofractionated PBT.

### Hypofractionated proton beam therapy for early-stage NSCLC

#### *Dosimetric analyses*

Several treatment-planning studies have been done to compare the radiation dose that would be delivered to tumors and surrounding normal structures with PBT *vs.* with photon techniques for early-stage tumors. In one of the earliest analyses, investigators from the University of Florida and the Mayo Clinic assessed eight patients with medically inoperable, peripherally located lesions that had initially been treated with SABR to 48 Gy in 12 fractions. An additional set of treatment plans at the equivalent dose was then generated to identify possible differences in dose distribution to normal structures if the treatment had been passive-scattering PBT instead of SABR. The median relative difference in lung dose between the two modalities was 2-10% depending on the parameter of interest, with low-dose regions being affected more than higher doses [median difference in the volume receiving at least 5 Gy ( $V_5$ ) = 10.4%; in  $V_{20}$  = 2.1%; and in  $V_{40}$  = 1.5%]; the median difference in mean lung dose was 2.2 Gy. Depending on the location of the lesion, PBT was also beneficial in other dose-volume parameters of the heart, esophagus, and bronchus. The investigators concluded from these findings that normal structure dosing was superior with PBT compared with SABR for early-stage, peripheral tumors (5).

A similar analysis done by authors from the University of Nagoya in Japan involved 21 patients with peripheral stage I NSCLC for whom plans were generated for both SABR and stereotactic body proton therapy (SBPT) to 66 Gy (RBE) in ten fractions. Again, the investigators found differences in several lung, heart, spinal cord, and esophagus doses, with the advantage from PBT again being more pronounced in the lower-dose than in the higher-dose regions in the lung. They further found that incremental increases in the tumor/target volume led to sharper rates of increase in  $V_5$  for SABR versus SBPT, but these differences were attenuated for  $V_{15}$ - $V_{20}$ . Overall, because the differences in low-dose regions were more substantial when planning target volumes were larger, this group concluded that SBPT seemed to be more advantageous for larger tumors (6).

Finally, researchers at The University of Texas MD Anderson Cancer Center examined the role of SBPT for particularly

challenging cases of early-stage disease, specifically tumors that were centrally or superiorly located. They compared plans for SABR, given as either passive scattering SBPT or intensity-modulated proton therapy (IMPT), for 15 patients with tumors located within 2 cm of a critical structure. They found that SABR plans could be created that would meet dose constraints for normal structures in 6 of the 15 patients, passive scattering SBPT for 12 patients, and IMPT for 14 of the 15 patients. Moreover, the proton techniques were associated with considerable improvements in target coverage when tumors were within 2 cm of the following structures: aorta, brachial plexus, heart, pulmonary vessels, and spinal cord (7) (Figure 1). Collectively, these studies demonstrated that hypofractionated PBT was dosimetrically superior to SABR for most patients with early-stage NSCLC, and that this superiority was substantially enhanced (as was the potential clinical benefit) for patients with larger, superiorly or centrally located tumors within 2 cm of a critical structure.

#### *Clinical analyses*

Although the sum total of clinical experience with hypofractionated PBT is still relatively limited at this time, several institutions have reported their experiences with this technique, and all showed similarly promising outcomes. These studies are summarized in Table 1. The experience with the longest follow-up comes from Loma Linda University, which has published several studies on toxicity and survival among patients with node-negative disease who underwent definitive treatment with PBT (8,13,14). In the most recent analysis, these investigators published their 12-year findings on the use of PBT to treat patients with T1-T2N0M0 peripheral NSCLC tumors (60%) or centrally located NSCLC tumors who could not undergo surgery for medical reasons or who declined resection. All patients received PBT in a dose-escalating fashion starting at 50 Gy (RBE) and increasing to 70 Gy (RBE) in ten fractions. At a median follow-up time of 48 months for the 111 patients so treated (mean tumor size, 3.6 cm), overall survival was significantly improved in patients who received 70 Gy (RBE) compared with those treated to 51 or 60 Gy (RBE) in ten fractions. Moreover, although local control rates were excellent at about 85-90% for patients with T1 tumors, the difference in control was much more significant for those with T2 lesions (4-year local control rates of 45% for those receiving 60 Gy *vs.* 74% for 70 Gy). Analysis of outcomes among patients who were also thought to be candidates for SABR revealed excellent rates of local control rate (96%) and overall survival (80%) at four years. Finally, treatment-related toxicity with PBT

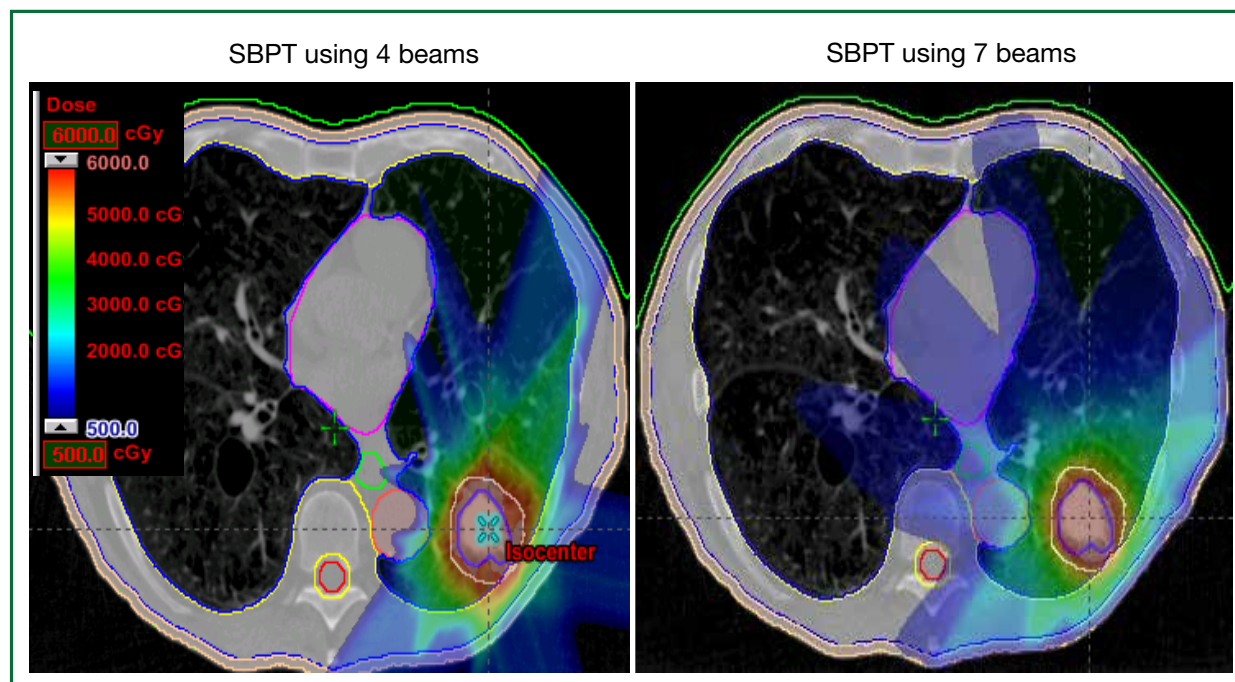


**Figure 1.** Comparison of stereotactic body proton therapy (SBPT) and stereotactic ablative body radiation (SABR) plans for early-stage lung cancer.

**Table 1.** Selected studies of accelerated proton beam therapy for early-stage non-small cell lung cancer.

| Study and reference         | Year | No. of patients             | Regimen                                    | Toxicity   | Control and survival rates  |
|-----------------------------|------|-----------------------------|--|--|---|
| Bush <i>et al.</i> (8)      | 2013 | 111                         | Dose escalation (50-70 Gy in 10 fractions) | No patients with grade $\geq 2$ RP; 4 patients with rib fractures  | 4-year outcomes for 70 Gy: OS 51%; DSS 74%; LC 86-91% for T1 tumors, 45-74% for T2 tumors |
| Hata <i>et al.</i> (9)      | 2007 | 21                          | 50-60 Gy in 10 fractions                   | 1 patient with grade 2 RP; 1 patient with painful subcutaneous induration; 1 patient with chest wall myositis                      | 2-year outcomes: OS 74%; DSS 86%; LC 95%  |
| Iwata <i>et al.</i> (10)    | 2010 | 57 (23 with carbon therapy) | 60 Gy in 10 fractions                      | 13% grade $\geq 2$ RP; 16% grade 2 dermatitis; 4% grade 3 dermatitis; 23% grade 2 rib fracture; 6% grade 2 fibrosis of soft tissue | 3-year outcomes: OS 75%; DSS 86%; LC 82%  |
| Chang <i>et al.</i> (11)    | 2011 | 13                          | 87.5 Gy in 35 fractions                    | 11% grade 2 RP; 1 patient with grade 2 esophagitis; 67% grade 2 dermatitis; 17% grade 3 dermatitis                                 | 2-year outcomes: OS 55%; DFS 46%  |
| Westover <i>et al.</i> (12) | 2012 | 15 (20 tumors)              | 42-50 Gy in 3-5 fractions                  | 1 patient with grade 2 fatigue; 1 patient with grade 2 dermatitis; 3 patients with rib fracture; 1 patient with grade 3 RP         | 2-year outcomes: OS 64%; LC 64%   |

Abbreviations: RP, radiation pneumonitis; OS, overall survival; DSS, disease-specific survival; LC, local control; DFS, disease-free survival.

was minimal, with no patients experiencing radiation pneumonitis requiring intervention, and pulmonary function, as measured by forced expiratory volume in one second ( $FEV_1$ ), was largely maintained. These investigators concluded that PBT was feasible, safe, and effective for either peripheral or centrally located lesions, and that use of higher radiation doses was beneficial in terms of local control, particularly for larger tumors (8).

Other institutions have also reported outcomes with use of PBT, although the follow-up time in most studies has been shorter. Investigators from the University of Tsukuba in Japan published an initial analysis (9) and then follow-up data (15) on patients with medically inoperable stage I NSCLC treated to either 66 Gy (RBE) in ten fractions for peripherally located lesions or 72 Gy (RBE) in 22 fractions for central lesions. In the most recent report, at a median follow-up time of 17 months, the progression-free survival rates were 88.7% at two years and 78.9% at three years, with no differences found between T1 vs. T2 tumors or between central vs. peripheral lesions. Of the seven recurrences in this group of 55 patients, one was local, three were in the mediastinum or lymph nodes, and three were at other locations within the lung. Two patients experienced grade 3 pneumonitis, two grade 2, and one grade 1. One patient was noted to have a rib fracture. These investigators concluded, as did those in the Loma Linda study, that PBT was safe and feasible for patients with medically inoperable stage I disease (15).

Investigators from several institutions in Japan have reported their results PBT or carbon therapy to treat stage I NSCLC. Patients treated with PBT initially received 80 Gy (RBE) in 20 fractions, and this regimen was subsequently changed to a more aggressive alternative of 60 Gy (RBE) in ten fractions. As initially reported, at a median follow-up of approximately three years for living patients, the 3-year local control rate was 82%, with an overall survival rate at three years of 75%. Of the 80 treated patients, only one experienced grade 3 pulmonary toxicity (10). A subsequent report of outcomes among 70 patients with T2 tumors (43 treated with PBT), with the hypothesis being that control rates and toxicity would be better for this subset of patients with PBT than with SABR revealed that, at a median follow-up time of 51 months, the 4-year rates of overall survival, local control, and progression-free survival for the 70 patients were 58%, 75%, and 46%. Notably, 11 of 70 patients had mediastinal or hilar recurrences; another 12 patients with T2a or T2b tumors had similar control rates, and 2 of 70 patients experienced grade  $\geq 3$  radiation pneumonitis. Five patients had grade 3 or 4 dermatitis, and one rib fracture was reported. These investigators concluded that PBT or carbon ion therapy was well tolerated by patients with T2 disease but given the relatively high rate of distant and regional metastases, the

addition of systemic therapy should be considered as well (16).

An analysis of patients treated with SBPT at Massachusetts General Hospital from 2008 through 2010 revealed a 2-year overall survival rates of 64% but a local control rate of 100% (12). Finally, in a phase I/II trial at MD Anderson Cancer Center, patients with early-stage disease who were not candidates for SABR (i.e., those with central or superior lesions or tumors  $>3$  cm) were treated with a hypofractionated regimen of 87.5 Gy (RBE) in 35 fractions. In the first report from this trial, 18 patients had been treated at a median follow-up time of 16.3 months; no patient had experienced grade 4 or 5 toxicity, and the most common grade  $\geq 3$  adverse event was dermatitis (17%). No patient experienced grade 3 or higher pneumonitis or esophagitis. The local control rate was 89%, with 11% of patients experiencing local-regional recurrence and 28% distant metastasis. Conclusions from this study were that this regimen was well tolerated and was promising in terms of local control. Notably, the dermatitis was probably related, at least in part, to the use of two or three beams in the treatment plan (vs. using more than three beams to distribute the dose to the skin and chest wall over a larger area) (11), and thus the current practice at MD Anderson for hypofractionated regimens is to use four to six beams to minimize hot spots in that region.

### Hypofractionated PBT for locally advanced NSCLC

#### *Dosimetric analyses*

Few studies to date have explored dosimetric differences between tumor targets and normal structures when hypofractionated dosing regimens are used for locally advanced disease. Therefore, such comparisons must be extrapolated from the literature on use of PBT at conventionally fractionated doses. For instance, investigators from MD Anderson Cancer Center compared dose-volume histograms in patients with stage III NSCLC treated with either PBT or (photon) IMRT and found that lung tissue parameters such as mean lung dose,  $V_5$ ,  $V_{10}$ , and  $V_{20}$  were all improved with PBT as compared with IMRT. Doses to the lung, spinal cord, heart, and esophagus were also improved with PBT relative to IMRT (17). Similarly, a study from the University of Florida examined whether PBT could reduce the radiation dose to the lung and bone marrow [compared with 3-dimensional conformal radiation therapy (3D-CRT) or IMRT] in patients with stage III NSCLC. In plan comparisons for eight patients, PBT was associated with a median reduction of 29% in lung  $V_{20}$  and a 30% reduction in bone marrow  $V_{10}$  compared with 3D-CRT. These advantages were maintained when PBT was compared with

IMRT, with PBT showing an improvement of 26% in lung  $V_{20}$  and 27% in bone marrow  $V_{10}$ . In a correlative study, the same authors found that PBT could cover “high-risk” lymph nodes (mediastinal, hilar, or supraclavicular nodal regions anatomically adjacent to involved regions according to positron emission tomography) with a lung dose approximating that of photon plans that covered only involved lymph nodes, leading the authors to include that PBT could be used to expand coverage to at-risk regions without substantially increasing lung dose (18). Presumably the dosimetric advantages demonstrated in studies of locally advanced disease such as these can be extrapolated to hypofractionated therapy as well, because the proportional differences should hold with the change in fraction size.

### **Clinical analyses**

Use of hypofractionated 3D-CRT or IMRT regimens for locally advanced disease has been evaluated by several groups; these regimens tend to involve moderate hypofractionation, with smaller fractions used than for early-stage disease because of the risks of irradiating mediastinal structures and the greater degree of lung involvement in many patients. For example, investigators from the University of Wisconsin conducted a dose-escalation study in radiation was given in 25 fractions ranging from 2.28 to 3.22 Gy. Toxicity was acceptable, with no incidences of grade  $\geq 3$  pneumonitis and 15% of patients developing grade 2 radiation pneumonitis (19). Similarly, investigators at Fudan University in Shanghai treated 34 patients with stage III NSCLC with 3D-CRT in accelerated hypofractionation, with an initial dose of 50 Gy in 20 fractions ultimately escalated to a total dose of 68 Gy after two cycles of induction chemotherapy. At three years, the median progression-free survival rate was 32% and the overall survival rate 30%, but the local-regional control rate at that time was a remarkable 61%, demonstrating that induction chemotherapy followed by hypofractionated RT is promising for such cases (20).

Another group at MD Anderson published their findings from the use of 45 Gy, delivered in 3-Gy fractions, for 26 patients with stage I-IIIB disease with involved nodes and borderline performance status, defined as a Karnofsky Performance Status (KPS) score of 60-70 or weight loss of  $>5\%$ . These authors found that this regimen produced comparable survival outcomes (local control, freedom from progression) and toxicity for these patients relative to patients with higher performance status (KPS  $>70$  and with weight loss of  $\leq 5\%$ ) who were treated to 60-66 Gy in a standard fractionation regimen over 6 to 6.5 weeks, leading them to conclude that the accelerated treatment regimen was a reasonable alternative to conventionally fractionated doses

for patients who could not tolerate concurrent chemotherapy (21). This analysis was updated after its initial publication to include 119 patients in the accelerated-treatment group and again showed no differences with regard to local or distant control compared with patients given standard fractionation regimens (22).

With these prior results, investigators at MD Anderson undertook the first dedicated study of hypofractionated PBT that included patients with locally advanced disease. In this phase I trial, 25 patients were treated in a dose-escalating manner with fifteen 3-, 3.5-, and 4-Gy fractions, yielding total doses of 45-60 Gy, with the dose being escalated in a 3+3 design. Thus 3 patients were treated to 45 Gy, 4 patients to 52.5 Gy, and 18 patients to 60 Gy. At a median follow-up time of 13 months for patients who were alive at the time of analysis, the authors found that only two patients had experienced dose-limiting toxicity, one with grade 3 infectious pneumonia after receiving a dose of 60 Gy in 4 Gy fractions and the other with a grade 5 tracheoesophageal fistula developing nine months after PBT to 52.5 Gy in 3.5-Gy fractions (23). However, the latter patient had also received bevacizumab, which has been shown to cause fistulas (24,25), at one month before developing the fistula. These investigators concluded that hypofractionated PBT to the thorax was well tolerated even when significant doses were delivered to the lung and central structures such as the bronchus and esophagus. This analysis also involved the development of unique dose constraints, based on extrapolations of those used in standard fractionated regimens and adjusted for biologically equivalent dose, which can be used as a foundation for future trials examining analogous regimens for mediastinal disease. Representative dose distributions for a patient treated to 60 Gy in 4 Gy fractions in that study are shown in Figure 2.

### **Conclusions and future directions**

The feasibility of hypofractionated dose-escalated PBT for NSCLC has been demonstrated by several groups at a variety of institutions. The evidence is stronger for early-stage disease, as more studies have focused solely on PBT. The clinical benefit of PBT remains to be seen; SABR, particularly for small, peripherally located lesions, appears to produce excellent results, with local control rates often exceeding 95% and modest toxicity (1). The benefit of hypofractionated SABR in this context may be limited to patients with larger or centrally or superiorly located lesions or patients with recurrent disease. To address this possibility, investigators from MD Anderson and Massachusetts General Hospital have begun a randomized phase II study comparing SABR with SPBT for patients with centrally located

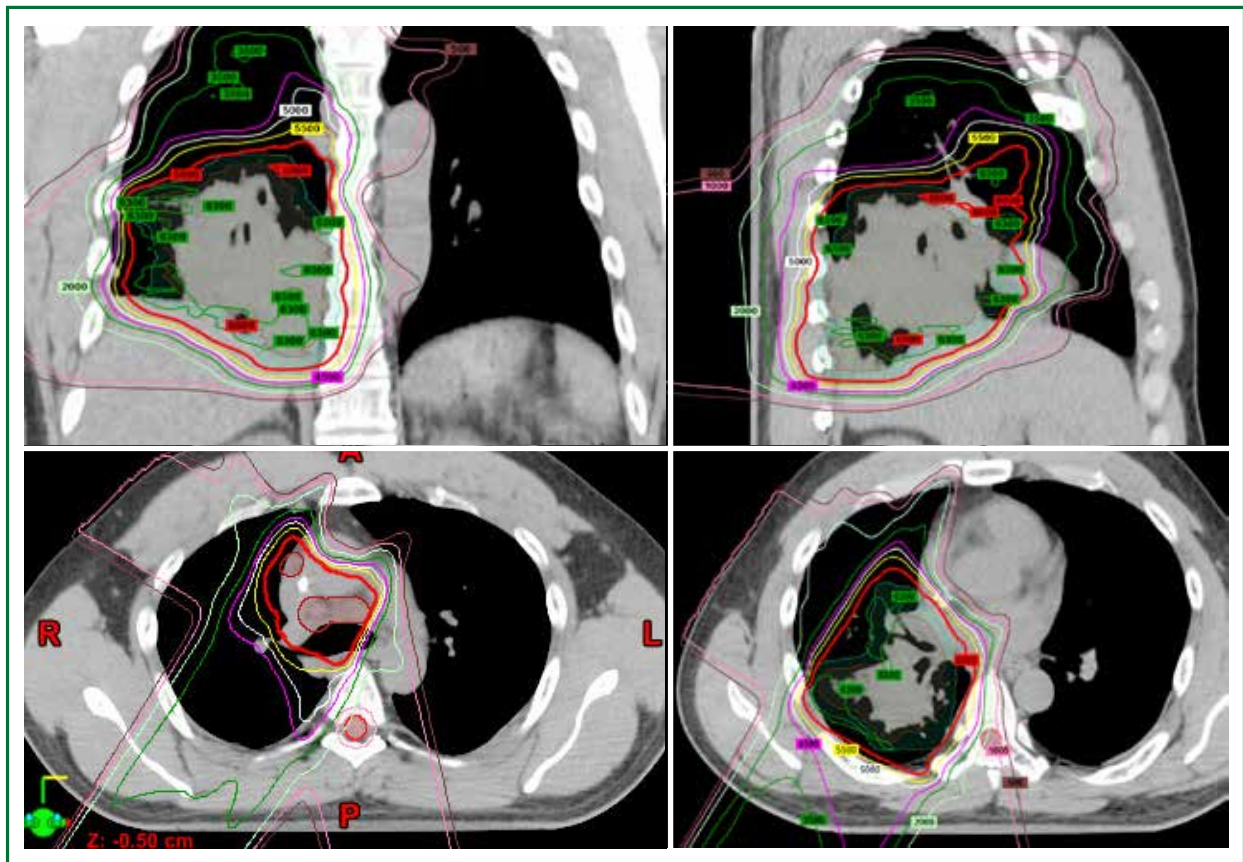


**Figure 2.** Dose distributions for a patient who received proton-beam therapy for a T3N2 adenocarcinoma of the right lower lobe in a prospective phase I trial. The contralateral lung is almost completely spared.

|   |   |           |  |   | 50 Gy (RBE) in 4 consecutive fractions |
|---|---|-----------|--|---|--|
| R | S |           |  | R |  |
| E | T | Cohort 1  |  | A | Cohort 1 A                             |
| G | R | Central   |  | N | SBPT                                   |
| I | A |           |  | D | Cohort 1 B                             |
| S | T |           |  | O | SBRT                                   |
| T | I |           |  | M |  |
| E | F | Cohort 2  |  | I | Cohort 2 A                             |
| R | Y | Recurrent |  | Z | SBPT                                   |
|   |   |           |  | E | Cohort 2 B                             |
|   |   |           |  |   | SBRT                                   |

**Figure 3.** Schema for ongoing trial of stereotactic ablative body radiotherapy (SABR) vs. stereotactic body proton therapy (SBPT) for centrally located or recurrent NSCLC. The primary outcome is 2-year toxicity, with a target accrual of 120 patients.

stage I, selected stage II, or recurrent NSCLC (Figure 3). Candidates for this study must have primary tumors located within 2 cm of the bronchial tree, major vessels, or mediastinal structures; or T2/T3 lesions with involvement of the mediastinal pleura or pericardium; or recurrent disease. Patients are randomly assigned to receive SBRT or SBPT to a total dose of 50 Gy in four fractions, and the primary outcome is a reduction in the 2-year toxicity rate. This study will provide valuable information to address the question of whether patients with more challenging tumors would benefit more from SBRT or PBT.

Regarding hypofractionated PBT for locally advanced disease, dosimetric analyses have shown a benefit for PBT over 3D-CRT or IMRT in select cases, and this advantage can reasonably be extrapolated to the hypofractionated context. Several phase I and phase II trials have also demonstrated the feasibility of hypofractionated regimens for patients with stage II-III disease who are not candidates for concurrent chemoradiation, with promising local control rates and acceptable toxicity. However, dose-escalation regimens in such cases have been somewhat

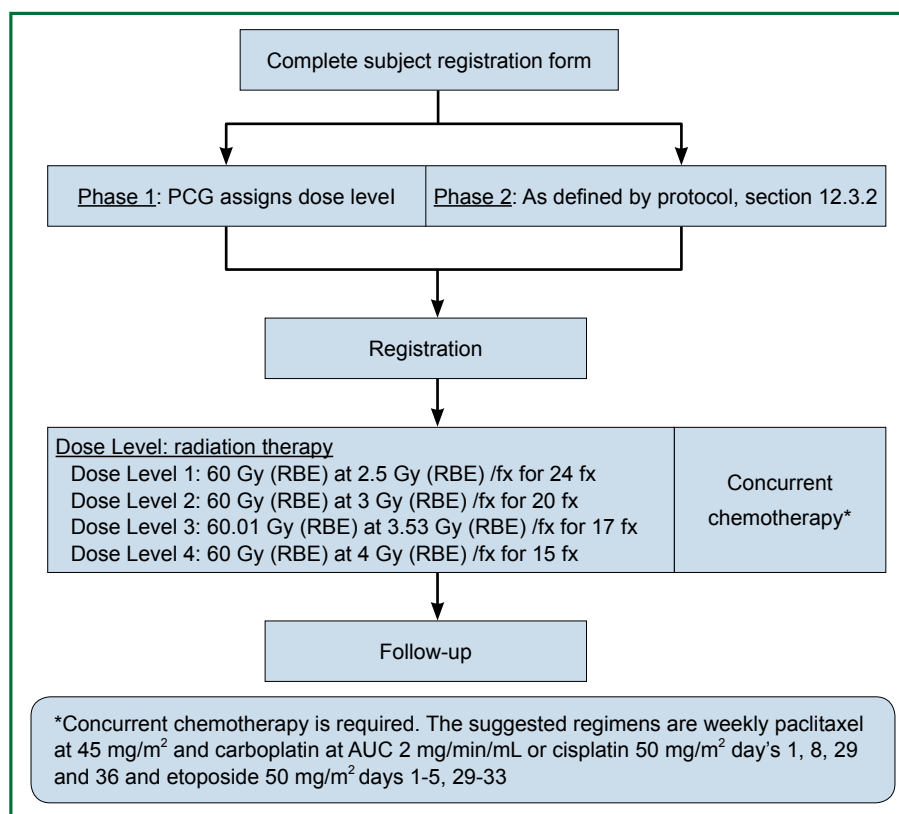


**Figure 4.** Schema for prospective phase I/II study of hypofractionated PBT, with concurrent chemotherapy, for stage II-III non-small cell lung cancer. This dose-escalation study will enroll 28 patients in the phase I component and 61 in the phase II component. Abbreviations: PCG, Proton Cooperative Group; fx, fractions.

limited by normal tissue constraints and the degree to which mediastinal structures can be spared. Ideally, the dosimetric advantages of PBT would translate into the ability to prescribe increasing fraction sizes, which would maintain reasonable rates of adverse events while improving local control. To date, only one published study has focused solely on hypofractionated PBT for NSCLC, and this analysis showed limited toxicity. However, much more information is needed regarding the safety of hypofractionated PBT before it can be widely adopted, and long-term follow-up is urgently needed to assess chronic toxicities (those appearing more than 12 months after treatment) and rates of disease control and survival compared with conventionally fractionated regimens and prior studies using photon techniques. In a phase I/II study recently opened through the Proton Cooperative Group (Figure 4), patients are to receive concurrent chemotherapy at escalating doses of hypofractionation; this regimen is intended for patients with higher performance status who are also candidates for systemic therapy. The concept is that the increased sparing of normal tissues afforded by PBT will

allow more aggressive approaches to be used. Over the next several years, given the growing number of PBT facilities, collaborative efforts in prospective, ideally randomized studies will be crucial for developing appropriately individualized treatments that can take advantage of PBT, a valuable yet limited, resource-intensive, and costly modality, in the hypofractionated setting.

## Acknowledgements

*Disclosure:* The authors declare no conflict of interest.

## References

1. Timmerman R, Paulus R, Galvin J, et al. Stereotactic body radiation therapy for inoperable early stage lung cancer. *JAMA* 2010;303:1070-6.
2. Timmerman R, McGarry R, Yiannoutsos C, et al. Excessive toxicity when treating central tumors in a phase II study of stereotactic body radiation therapy for medically inoperable early-stage lung cancer. *J Clin Oncol* 2006;24:4833-9.

3. Langer CJ, Manola J, Bernardo P, et al. Cisplatin-based therapy for elderly patients with advanced non-small-cell lung cancer: implications of Eastern Cooperative Oncology Group 5592, a randomized trial. *J Natl Cancer Inst* 2002;94:173-81.
4. Sweeney CJ, Zhu J, Sandler AB, et al. Outcome of patients with a performance status of 2 in Eastern Cooperative Oncology Group Study E1594: a Phase II trial in patients with metastatic nonsmall cell lung carcinoma. *Cancer* 2001;92:2639-47.
5. Hoppe BS, Huh S, Flampouri S, et al. Double-scattered proton-based stereotactic body radiotherapy for stage I lung cancer: a dosimetric comparison with photon-based stereotactic body radiotherapy. *Radiother Oncol* 2010;97:425-30.
6. Kadoya N, Obata Y, Kato T, et al. Dose-volume comparison of proton radiotherapy and stereotactic body radiotherapy for non-small-cell lung cancer. *Int J Radiat Oncol Biol Phys* 2011;79:1225-31.
7. Register SP, Zhang X, Mohan R, et al. Proton stereotactic body radiation therapy for clinically challenging cases of centrally and superiorly located stage I non-small-cell lung cancer. *Int J Radiat Oncol Biol Phys* 2011;80:1015-22.
8. Bush DA, Cheek G, Zaheer S, et al. High-dose hypofractionated proton beam radiation therapy is safe and effective for central and peripheral early-stage non-small cell lung cancer: results of a 12-year experience at Loma Linda University Medical Center. *Int J Radiat Oncol Biol Phys* 2013;86:964-8.
9. Hata M, Tokuyue K, Kagei K, et al. Hypofractionated high-dose proton beam therapy for stage I non-small-cell lung cancer: preliminary results of a phase I/II clinical study. *Int J Radiat Oncol Biol Phys* 2007;68:786-93.
10. Iwata H, Murakami M, Demizu Y, et al. High-dose proton therapy and carbon-ion therapy for stage I nonsmall cell lung cancer. *Cancer* 2010;116:2476-85.
11. Chang JY, Komaki R, Wen HY, et al. Toxicity and patterns of failure of adaptive/ablative proton therapy for early-stage, medically inoperable non-small cell lung cancer. *Int J Radiat Oncol Biol Phys* 2011;80:1350-7.
12. Westover KD, Seco J, Adams JA, et al. Proton SBRT for medically inoperable stage I NSCLC. *J Thorac Oncol* 2012;7:1021-5.
13. Bush DA, Hillebrand DJ, Slater JM, et al. High-dose proton beam radiotherapy of hepatocellular carcinoma: preliminary results of a phase II trial. *Gastroenterology* 2004;127:S189-93.
14. Bush DA, Slater JD, Bonnet R, et al. Proton-beam radiotherapy for early-stage lung cancer. *Chest* 1999;116:1313-9.
15. Nakayama H, Sugahara S, Tokita M, et al. Proton beam therapy for patients with medically inoperable stage I non-small-cell lung cancer at the university of tsukuba. *Int J Radiat Oncol Biol Phys* 2010;78:467-71.
16. Iwata H, Demizu Y, Fujii O, et al. Long-term outcome of proton therapy and carbon-ion therapy for large (T2a-T2bN0M0) non-small-cell lung cancer. *J Thorac Oncol* 2013;8:726-35.
17. Chang JY, Zhang X, Wang X, et al. Significant reduction of normal tissue dose by proton radiotherapy compared with three-dimensional conformal or intensity-modulated radiation therapy in Stage I or Stage III non-small-cell lung cancer. *Int J Radiat Oncol Biol Phys* 2006;65:1087-96.
18. Nichols RC, Huh SH, Hoppe BS, et al. Protons safely allow coverage of high-risk nodes for patients with regionally advanced non-small-cell lung cancer. *Technol Cancer Res Treat* 2011;10:317-22.
19. Adkison JB, Khuntia D, Bentzen SM, et al. Dose escalated, hypofractionated radiotherapy using helical tomotherapy for inoperable non-small cell lung cancer: preliminary results of a risk-stratified phase I dose escalation study. *Technol Cancer Res Treat* 2008;7:441-7.
20. Zhu ZF, Fan M, Wu KL, et al. A phase II trial of accelerated hypofractionated three-dimensional conformal radiation therapy in locally advanced non-small cell lung cancer. *Radiother Oncol* 2011;98:304-8.
21. Nguyen LN, Komaki R, Allen P, et al. Effectiveness of accelerated radiotherapy for patients with inoperable non-small cell lung cancer (NSCLC) and borderline prognostic factors without distant metastasis: a retrospective review. *Int J Radiat Oncol Biol Phys* 1999;44:1053-6.
22. Amini A, Lin SH, Wei C, et al. Accelerated hypofractionated radiation therapy compared to conventionally fractionated radiation therapy for the treatment of inoperable non-small cell lung cancer. *Radiat Oncol* 2012;7:33.
23. Gomez DR, Gillin M, Liao Z, et al. Phase 1 study of dose escalation in hypofractionated proton beam therapy for non-small cell lung cancer. *Int J Radiat Oncol Biol Phys* 2013;86:665-70.
24. Gore E, Currey A, Choong N. Tracheoesophageal fistula associated with bevacizumab 21 months after completion of radiation therapy. *J Thorac Oncol* 2009;4:1590-1.
25. Spigel DR, Hainsworth JD, Yardley DA, et al. Tracheoesophageal fistula formation in patients with lung cancer treated with chemoradiation and bevacizumab. *J Clin Oncol* 2010;28:43-8.



**Cite this article as:** Gomez DR, Chang JY. Accelerated dose escalation with proton beam therapy for non-small cell lung cancer. *J Thorac Dis* 2014;6(4):348-355. doi: 10.3978/j.issn.2072-1439.2013.11.07

## Combining targeted agents and hypo- and hyper-fractionated radiotherapy in NSCLC

Fiona McDonald, Sanjay Papat

The Royal Marsden NHS Foundation Trust, UK

### ABSTRACT

Radical radiotherapy remains the cornerstone of treatment for patients with unresectable locally advanced non small cell lung cancer (NSCLC) either as single modality treatment for poor performance status patients or with sequential or concomitant chemotherapy for good performance status patients. Advances in understanding of tumour molecular biology, targeted drug development and experiences of novel agents in the advanced disease setting have brought targeted agents into the NSCLC clinic. In parallel experience using modified accelerated fractionation schedules in locally advanced disease have demonstrated improved outcomes compared to conventional fractionation in the single modality and sequential chemo-radiotherapy settings. Early studies of targeted agents combined with (chemo-) radiotherapy in locally advanced disease in different clinical settings are discussed below and important areas for future studies are highlighted.

### KEYWORDS

Non small cell lung cancer (NSCLC); radical radiotherapy; modified fractionation; targeted agents

*J Thorac Dis 2014;6(4):356-368. doi: 10.3978/j.issn.2072-1439.2013.12.05*

### Introduction

Arguably one of the most important objectives for cancer researchers remains the reduction in the millions of years of healthy life lost to lung cancer worldwide each year [estimated at 24.5 million in 2008 (1)] with little impact made on the poor relative survival in recent years (2) and improvements in survival trailing behind other cancers (3). Non-small cell lung cancer (NSCLC) accounts for approximately 85% of all lung cancers. Approximately one third of these patients have early stage disease (stages I and II) at the time of presentation and are usually treated surgically, with radiotherapy being reserved for those who are medically inoperable. Another one third of patients present with advanced disease and radiotherapy is reserved for palliation of symptoms. The remainder of patients present with locally advanced disease (stage III) with the majority being unresectable and the mainstay of treatment is radical intent radiotherapy.

In good performance status patients, the addition of sequentially or concomitant platinum-based chemotherapy is considered as the standard of care in patients with locally advanced disease due to the associated improved outcome (4,5). Importantly, a meta-analysis of over 1,200 patients from six trials comparing concomitant to sequential chemo-radiotherapy reveals the concomitant approach is associated with lower loco-regional disease progression (absolute decrease of 6.1% at five years, from 35.0% to 28.9%) but similar distant disease progression (40.6% and 39.5%, respectively) compared to sequential (6). This suggests an important temporal relationship between the two treatment modalities. The consequent 4.5% increase in 5-year overall survival from 10.6% with sequential to 15.1% with concomitant chemotherapy highlights the opportunity for radio-sensitisation with systemic agents and the relevance of improved local disease control on long term outcome.

However, an estimated 60% of patients with locally advanced disease are not fit enough for concomitant chemo-radiotherapy due to poor performance status and co-morbidities (7). In addition to the less toxic alternative of sequential chemo-radiotherapy, radiotherapy dose escalation has been explored, given conventional doses achieve sub-optimal rates of local disease control with estimates of pathologically persistent tumour following treatment in 60% of patients (8). Tumour control probability modelling suggests that using conventional

Correspondence to: Dr. Fiona McDonald. The Royal Marsden NHS Foundation Trust, Downs Road, Sutton, Surrey, SM2 5PT, UK. Email: Fiona.mcdonald@rmh.nhs.uk.

Submitted Sep 02, 2013. Accepted for publication Dec 03, 2013.  
Available at [www.jthoracdis.com](http://www.jthoracdis.com)

ISSN: 2072-1439

© Pioneer Bioscience Publishing Company. All rights reserved.

fractionation (1.8 to 2 Gy daily), a dose of 84 Gy is required to achieve 50% probability of tumour control at three years (9), some 18-24 Gy higher than the standard dose radiotherapy. Unfortunately, preliminary clinical data from the RTOG 0617 randomised phase III trial of conventionally fractionated radiotherapy (with concurrent and consolidation platinum-based chemotherapy +/- cetuximab) comparing standard dose (60 Gy) to high dose (74 Gy) has revealed the conventionally fractionated high dose arm is associated with a higher rate of local disease progression (34% compared to 25%) and shorter median survival (19.5 months compared to 28.7 months) compared to standard dose (10). It is as yet unclear the reason for the detrimental effect of the higher dose arm, but the extended duration of treatment by dose escalating using conventionally fractionated may be an important factor.

The alternative strategy is to intensify radiotherapy dose using modified fractionation schedules and reduced overall length of the treatment course with the aim of reducing the effect of accelerated tumour cell repopulation during treatment (11,12). The number of fractions given each day can be increased from one to two or three with at least a 6-hour gap in-between (hyper-fractionation) or the number of daily fractions given can be decreased by increasing the dose per fraction (hypo-fractionation). Such schedules increase the biologically effective dose (BED) (13) delivered to the tumour. Experience with extreme hypo-fractionation in stereotactic ablative radiotherapy for early stage disease demonstrates that a BED of over 100 Gy (using a ratio of 10 for tumour linear to quadratic radio-sensitivity) is required to achieve local disease control rates in excess of 90% (14,15). A recent meta-analysis of over 2,000 patients, of which >80% had stage III disease, from eight trials comparing modified to conventional fractionation radiotherapy schedules reveals modified fractionation is associated with improved overall survival at five years (absolute increase of 2.5%, from 8.3% to 10.8%) compared to standard fractionation schedules and importantly, good compliance with the modified regimens (16). Additionally accelerated radiotherapy is associated with higher pathological complete resection rates than conventional fractionation in patients with stage III NSCLC treated with tri-modality therapy (17). The optimal modified fractionation schedule is yet to be clarified, however accelerated schedules to a total dose of 60-66 Gy are considered optimal for patients considered unsuitable for concomitant chemo-radiotherapy (18).

With the recent increase in understanding of the molecular biology of NSCLC and experience of the use of targeted agents in the advanced disease setting, a number of published studies report on combining targeted agents into radical treatment schedules for locally advanced disease, from addition to concomitant chemo-radiotherapy in good performance status

patients to combination with radiotherapy alone in elderly or poor performance status patients. Published studies in the various clinical settings are discussed below.

### Molecular biology of NSCLC and epidermal growth factor receptor (EGFR) inhibitors

EGFR is one of a family of four structurally similar tyrosine kinase-associated receptors which comprise the human epidermal growth factor receptor (HER) family. EGFR (HER1 or ERBB1) was the first to be described in humans, and identified to be a protein comprising an extracellular ligand-binding domains, trans-membrane domain and an intracellular tyrosine kinase domain (19). Each receptor must homo- or hetero-dimerise to activate the intrinsic kinase activity and phosphorylate tyrosine residues on the C-terminal tail, activating intracellular signalling pathways. Epidermal growth factor expression has long been regarded as a poor prognostic factor in NSCLC, suggesting its potential as a therapeutic target (20,21).

Since then, a number of small molecule reversible and more recently irreversible EGFR tyrosine kinase motif inhibitors (TKIs) have been developed, with gefitinib and erlotinib both demonstrating modest activity in EGFR wild-type advanced NSCLC (22,23), leading to licensing for erlotinib. The discovery of constitutionally activating somatic *EGFR* mutations mapping to the kinase domain in 2004 (24,25) changed drug development strategies, with gefitinib, erlotinib and afatinib now licensed for EGFR TKI naïve advanced NSCLC, with an overwhelming consistent evidence from eight randomized trials demonstrating their superior efficacy over chemotherapy in advanced NSCLC. In this setting, toxicities of EGFR TKIs are more manageable than chemotherapy, and toxic fatalities rare usually at up to 3%. Moreover, there seems to be no obvious difference in proportion of grade 3-5 toxicities between the three agents. The most significant serious adverse event reported in EGFR-TKI development was initially pneumonitis. However, with greater experience of use of these agents in the advanced disease setting, rates of grade 3-5 pneumonitis are routinely observed at up to 3% of most trial series, with no clear differences between the agents, but a possible geographical distribution, with increased events reported from East Asian series (26). Whether this reflects pharmacogenomic differences or differing clinical diagnostic interpretation remains unresolved.

Unlike the success of the EGFR-TKIs, targeting through antibody inhibition has proven more problematic in advanced NSCLC. Whilst preclinical models demonstrated the activity of anti-EGFR monoclonal antibodies (MAbs) against several carcinoma cell lines, with synergistic activity in combination with

cisplatin (27), despite encouraging phase II studies (28) two large randomized phase III trials in advanced NSCLC (29,30) demonstrated little or no survival advantage for the addition of cetuximab to standard platinum-doublet chemotherapy, although subsequent post-hoc analyses suggested potential activity contingent on extent of EGFR expression (31). EGFR MABs are therefore not standard in advanced NSCLC.

For stage III NSCLC, the combination of EGFR inhibitors and radiotherapy has considerable scientific rationale, despite some of the efficacy concerns identified through advanced disease trials. A positive correlation has been demonstrated between EGFR expression and tumour radio-resistance (32) and the magnitude of over-expression has been correlated with the degree of resistance (33). Radiation damage results in increased EGFR expression and subsequent augmentation of down-stream pathways (34,35). Pre-clinical evidence suggests EGFR blockade potentiates tumour radio-sensitivity. Cetuximab has demonstrated the ability to modulate tumour proliferation, apoptosis and inhibit deoxyribonucleic acid (DNA) repair following irradiation (36-39). Gefitinib has been shown to inhibit the radiation-induced activation of DNA-dependent protein kinase and potentiate radiation response (40,41). Erlotinib similarly causes radio-sensitization potentially through a number of effects including increased apoptosis, cell cycle arrest, and DNA damage repair changes (42). Other mechanisms postulated include micro-environmental changes mediated through decreased vascular endothelial growth factor messenger ribonucleic acid (VEGF mRNA) and protein expression, and blunted hypoxia-inducible factor 1-alpha (HIF-1 $\alpha$ ) induction (43), with studies of gefitinib (44) and cetuximab (45) demonstrating improved oxygenation.

### EGFR inhibitors with conventional fractionation radical radiotherapy alone

In the clinical setting, subsequent to the encouraging improved outcomes with minimal additional toxicity in locally advanced head and neck cancer patients treated with radical radiotherapy combined with cetuximab compared to radiotherapy alone (46), similar studies have been carried out in patients with locally advanced NSCLC. Given the patient population offered radiotherapy alone tend to be elderly and/or with poor performance status, the N0422 phase II single arm study of radical radiotherapy (60 Gy) combined with concomitant cetuximab is interesting (47) (Table 1). The cohort of 57 patients with stage III NSCLC who were considered unfit for combined chemo-radiotherapy included either patients aged 65 years or older with an ECOG performance status of 0-1 or patients of any age

with a performance status of 2. Fifty patients (86%) completed the entire treatment and there were no treatment related deaths. Grade 3/4 toxicities were experienced by 31 (54%) patients, with the most common side effects being fatigue (9%) and dyspnoea (9%). The median survival of the cohort was 15.1 (95% CI: 31.1-19.3) months. Of note, patients in this study were not staged with positron emission tomography (PET) scans and outdated radiotherapy techniques were used. A similar smaller single arm phase II study, the Near trial, treated 30 patients with stage III NSCLC, who were considered unfit for or who had refused combined chemo-radiotherapy, with radical radiotherapy (66 Gy) combined with concomitant cetuximab followed by maintenance cetuximab (48) (Table 1). The median age of this cohort was younger at 71 years and all patients had a Karnofsky performance status of  $\geq 70\%$ , however, the median survival was encouraging at 19.6 (95% CI: 11.5-24.7) months. Treatment completion rate and grade 3/4 toxicity rates were similar at 90% (27 patients) and 40% (12 patients), respectively, with the most common side effect being pneumonia (10%). There were however three deaths (myocardial infarction, bacterial endocarditis related sepsis, pulmonary embolus following deep vein thrombosis) reported as unlikely related to the treatment. Both studies included elective nodal irradiation up to 40-50 Gy, however in contrast to the first study, patients in the Near trial were staged with PET scans and modern radiotherapy techniques were used, including intensity modulated radiotherapy (IMRT) and cone beam CT image guided delivery. It is also noted that while the median percentage of normal lung planned to receive 20 Gy ( $V_{20}$ ) in this cohort of patients was 26%, the range extended up to 60% and therefore included patients at high risk for pulmonary complications due to the radiotherapy (51). Given the skin toxicity rates associated with cetuximab, there is interest in newer EGFR MABs that demonstrate a lower incidence of skin complications, with phase I studies of nimotuzumab in the palliative radiotherapy setting for NSCLC patients demonstrating feasibility and tolerance (52,53).

Studies of erlotinib and gefitinib in combination with radical radiotherapy alone in locally advanced NSCLC have raised concerns about pulmonary toxicity. In particular, a phase II study from Japan (49) (Table 1) on good performance status patients with a median age of 54 years was closed early due to toxicity concerns. Of the nine patients with stage III NSCLC recruited to the study, seven received gefitinib concurrently with thoracic radiotherapy (60 Gy). Three dimensional (3D) conformal planning was used and all plans had a lung  $V_{20} \leq 35\%$ . Despite this, two of these patients experienced acute pulmonary toxicity (grade 1 and 3) after approximately 30 Gy had been delivered. In contrast, another phase II study from China (50) (Table 1)

**Table 1.** Published studies of EGFR inhibitors with conventional fractionation radical radiotherapy alone.

| Ref        | Patients   | Disease  | Induction              | Target dose/fractionation  | RT planning/delivery  | Concomitant               | Consolidation/maintenance         | Compliance/toxicity   | Median survival (months) |
|------------|--|--|------------------------|--|---|---------------------------|-----------------------------------|---|--------------------------|
| (47) Ph II | Number: 57;<br>Age: 77 [60-87];<br>M/F: 60/40;<br>PS: 22/57/21         | Path: 38/43/19;<br>Stage: 0/59/41/0;<br>PET: N                 | -                      | 60 Gy 30#;<br>Once daily;<br>ENI to 44 Gy  | Planning: 2D;<br>Verification: IGRT N   | Cetuximab                 | -                                 | Compliance 86% overall;<br>G3/4 54%; Overall G5 0%;<br>Oesoph G3/4 7%; Pulmon G3/4 9%   | 15.1                     |
| (48) Ph II | Number: 30;<br>Age: 71 [57-82];<br>M/F: 77/23;<br>PS: (Karnofsky ≥70%) | Path: 33/57/10;<br>Stage: 6/57/37/0;<br>PET: Y                 | -                      | 66 Gy 33#;<br>Once daily;<br>ENI to 40-50 Gy   | Planning: 4D IMRT;<br>PTV: 254 [46-529];<br>Lung V <sub>20</sub> : 26% [15-60];<br>Verification: IGRT Y     | Cetuximab                 | Cetuximab                         | Compliance 90% overall;<br>G3/4 40%; Overall G5 10%; Oesoph G3/4 3%;<br>Pulmon G3/4 23% | 19.6                     |
| (49) Ph I  | Number: 9;<br>Age: 63 [56-71];<br>M/F: 89/11;<br>PS: (All 0-1)         | Path: 72/14/14;<br>Stage: 0/55/44/0;<br>PET: N                 | -                      | 60 Gy 30#;<br>Once daily;<br>ENI to 40 Gy  | Planning: 3D;<br>Lung V <sub>20</sub> : All ≤35%;<br>Verification: IGRT N                                   | Gefitinib                 | -                                 | Compliance 44% overall;<br>G3/4 44%; Overall G5 0%;<br>Oesoph G3/4 0%; Pulmon G3/4 11%  | -                        |
| (50) Ph I  | Number: 26;<br>Age: 56 [30-84];<br>M/F: 42/58;<br>PS: 4/85/11          | Path: 73/15/12;<br>Stage: 0/8/11/81; systemic<br>PET: Optional | 54% prior chemotherapy | 'Individualised'<br>GTV 70 Gy 30#;<br>PTV 50 Gy 30#<br>Once daily;<br>± SABR to 1-3 metastatic sites | Planning: 3DCRT/<br>IMRT;<br>GTV: 56 [5-420];<br>Lung V <sub>20</sub> : 14% [3-28];<br>Verification: IGRT Y | Gefitinib<br>or Erlotinib | 69% maintenance median 7.3 months | Compliance 96% overall;<br>G3/4 NR; Overall G5 0%;<br>Oesoph G3/4 4%; Pulmon G3/4 4%    | 21.8                     |

Abbreviations: Ref, Reference; Ph, phase; Number, number of patients; Age, median age of patients in years [range]; M/F, percentage of males to females; PS, percentage of patients with performance status of 0/1/2; Path, percentage of patients with histological adenocarcinoma/squamous cell carcinoma/other subtypes of NSCLC; Stage, percentage of patients with stage II/IIIA/IIIB/IV disease; PET Y/N, Yes or No to mandatory use of PET for staging; ENI, elective nodal irradiation; 2D, 2 dimensional; 3D, 3 dimensional; 4D, 4 dimensional; CRT, conformal radiotherapy; IMRT, intensity modulated radiotherapy; IGRT Y/N, Yes or No to use of image-guided radiotherapy delivery; GTV/PTV, gross or planning target volume median in cm<sup>3</sup> (range); Lung V<sub>20</sub>, median percentage of total lung volume receiving at least 20 Gy (range); Toxicity G3/4/5, rates of grades of toxicity; NR, not reported; Oesoph, oesophageal; Pulmon, pulmonary; DLT, dose limiting toxicity; Medial survival, overall median survival in months.

studied 26 patients with stage III or IV disease, treated with 'individualised' radical radiotherapy in combination with either erlotinib or gefitinib. The patients were a heterogeneous group with only 5 (19%) patients having stage III disease. The 21 (81%) patients with stage IV disease had up to three organs treated with stereotactic ablative radiotherapy in addition to radical thoracic radiotherapy given concurrently with the EGFR tyrosine kinase inhibitor. However, treatment was completed as planned in 96% of patients and grade 3/4 pulmonary toxicity rates were acceptable at 4%. The whole cohort had a promising median survival of 21.8 (95% CI: 8.5-35.1) months. Additional toxicity concerns with erlotinib, published in abstract only, come from a small phase I/II Canadian study of erlotinib given concurrently with radical radiotherapy (60 Gy) in poor risk patients with PS 2 or weight loss >5% (54). This study was terminated early due to grade 3-5 pulmonary toxicity in two of five patients.

### EGFR inhibitors with conventional fractionation sequential chemo-radiotherapy

An early phase I study demonstrated the safety of combining cetuximab with radical radiotherapy (64 Gy) following induction platinum-based chemotherapy in 12 patients with stage III NSCLC (55) (Table 2). One patient died of bronchopneumonia during treatment and two others experienced grade 3 toxicity (a fatigue and a pneumonitis). All patients radiotherapy plans had a lung  $V_{20} < 30\%$  (median 22%).

Subsequently a single arm phase II study, the Satellite trial, treated 71 patients with stage III NSCLC using a combination of cetuximab and radical radiotherapy (68 Gy) following induction chemotherapy (56) (Table 2). The patients were of good performance status [0-1] with a relatively low median age of 62 years, however 37% had significant weight loss prior to treatment, a documented poor prognostic factor (60,61). Interestingly, this study omitted elective nodal irradiation, yet despite this PTV volumes up to 1,543 cm<sup>3</sup> (median 586 cm<sup>3</sup>) were treated and lung  $V_{20}$  parameters up to 54% (median 33%) were documented. Importantly, the study reports high compliance rates, low severe toxicity and a median overall survival of 17 (95% CI: 14.0-23.0) months in the whole cohort and a median survival of 24 months in the patients with <5% weight loss prior to treatment. Impact on health related quality of life with the combination also appears reasonable (62). Of note, the one patient with grade 5 toxicity developed pneumonitis soon after treatment and had a lung  $V_{20}$  of 41%, higher than the recommended QUANTEC constraint of 35% (51). Recently a further phase II study of 40 patients with stage II NSCLC reported on experience of cetuximab with concurrent

radiotherapy (73.5 Gy) followed by cetuximab and consolidation chemotherapy with paclitaxel and carboplatin (57) (Table 2). The radiotherapy volumes and normal tissue constraints are not reported however one patient died from pneumonitis after 56 Gy of radiotherapy. Overall median survival was 19.4 (95% CI: 15.4-26) months and interestingly no oesophageal toxicity > grade 2 was observed.

Again concerns over pulmonary toxicity have been raised in studies of EGFR TKIs in combination with radical radiotherapy given sequentially with systemic chemotherapy. A Japanese phase II study, JCOG 0402 trial, in 38 good performance status patients with stage III NSCLC and median age of 60 years received gefitinib concurrently with radical radiotherapy (60 Gy) following two cycles of platinum-based induction chemotherapy (58) (Table 2). Compliance with completing the planned concomitant phase of treatment was low at 63% and a patient (3%) developed grade 3 pneumonitis. However, a promising median survival rate of 28.5 (95% CI: 22.5-38.2) months was reported. The CALEB 30106 phase II study evaluated the addition of gefitinib concurrently with radical sequential or concomitant chemo-radiotherapy to patients with stage III NSCLC, based on initial assessment of prognostic factors (59). Patients considered as 'poor risk' in the study were those with a PS of 2 and/or weight loss of  $\geq 5\%$ . These patients were treated similarly to in the Japanese study, with two cycles of platinum-based chemotherapy followed by gefitinib given concurrently with radical radiotherapy (66 Gy). The grade 3/4 pulmonary toxicity rate was 10% with grade 5 pulmonary toxicity rate of 5%. The median survival was 19 (95% CI: 9.9-28.4) months. In both studies PET staging was not mandated and 2D radiotherapy planning was permitted with comparable elective nodal irradiation included to 40-44 Gy. An additional confounding factor for the studies is that in both protocols patients were additionally offered maintenance gefitinib. These studies were designed prior to the reporting of the randomised phase III SWOG S0023 trial of concurrent chemo-radiotherapy and consolidation docetaxel with or without maintenance gefitinib in stage III NSCLC, demonstrating inferior survival for the maintenance gefitinib arm (63).

### EGFR inhibitors with conventional fractionation concomitant chemo-radiotherapy

The addition of cetuximab to concomitant chemo-radiotherapy has also been studied in patients with locally advanced NSCLC. The phase II RTOG 0324 study treated 87 good performance status patients radical radiotherapy (63 Gy) and concomitant and consolidation carboplatin, paclitaxel and cetuximab (64)

**Table 2.** Published studies of EGFR inhibitors with conventional fractionation radical sequential chemo-radiotherapy.

| Ref          | Patients  | Disease                                    | Induction                             | Target dose/<br>fractionation             | RT planning/delivery  | Concomitant | Consolidation/<br>maintenance          | Compliance/<br>toxicity   | Median survival<br>(months) |
|--------------|---|--|---------------------------------------|---|---|-------------|--|---|-----------------------------|
| (55) Ph I    | Number: 12;<br>Age: 68 [58-76];<br>M/F: 74/25;<br>PS: 42/58/0   | Path: 33/50/17;<br>Stage: 40/60;<br>PET: N | ≤4 cycles<br>platinum<br>doublet      | 64 Gy 32#;<br>Once daily;<br>ENI to 50 Gy | Planning: 3D;<br>Verification: IGRT N;<br>Lung V <sub>20</sub> : 22% [14-29]  | Cetuximab;  | —                                      | Compliance 75%;<br>Overall G3/4 17%;<br>Overall G5 8%;<br>Oesoph G3/4 0%;<br>Pulmon G3/4 8%       | —                           |
| (56) Ph II   | Number: 71;<br>Age: 62 [42-81];<br>M/F: 50/50;<br>PS: 62/38/0;<br>>5% wt lo: 37%                      | Path: 49/39/12;<br>Stage: 37/63;<br>PET: N | 2 cycles<br>cisplatin<br>docetaxel    | 68 Gy 34#;<br>Once daily;<br>No ENI       | Planning: 3D;<br>Verification: IGRT N;<br>GTV: 91 [9-499];<br>PTV: 586 [135-1,543];<br>Lung V <sub>20</sub> : 33% [12-54] | Cetuximab   | —                                      | Compliance 82%;<br>Overall G3/4 NR;<br>Overall G5 1%;<br>Oesoph G3/4 1%;<br>Pulmon G3/4 4%        | 17.0                        |
| (57) Ph II   | Number: 40;<br>Age: 67 [40-82];<br>M/F: 65/35;<br>PS: All 0-1   | Path: 37/27/35;<br>Stage: 32/64;<br>PET: N | —<br>Once daily;<br>No ENI            | 73.5 Gy 35#;<br>Once daily;<br>No ENI     | Planning: 2D/3D;<br>Verification: IGRT N;   | Cetuximab   | Paclitaxel<br>carboplatin<br>cetuximab | Compliance 84%;<br>Overall G3/4 NR;<br>Overall G5 3%;<br>Oesoph G3/4 0%;<br>Pulmon G3/4 11%       | 19.4                        |
| (58) Ph I/II | Number: 38;<br>Age: 60 [30-69];<br>M/F: 37/63;<br>PS: 76/24/0;<br>>5% wt lo: 5%                       | Path: 97/0/3;<br>Stage: 58/42;<br>PET: N   | 2 cycles<br>cisplatin<br>vinorelbine  | 60 Gy 30#;<br>Once daily;<br>ENI to 40 Gy | Planning: 2D/3D;<br>Verification: IGRT N  | Gefitinib   | Gefitinib                              | Compliance<br>63%/24%;<br>Overall G3/4 NR;<br>Overall G5 0%;<br>Oesoph G3/4 0%;<br>Pulmon G3/4 3% | 28.5                        |
| (59) Ph II   | 'Poor risk' arm;<br>Number: 21;<br>Age: 68 [41-82];<br>M/F: 76/24;<br>PS: 0/62/38;<br>>5% wt lo: ≥62% | Path: 32/48/20;<br>Stage: 43/57;<br>PET: N | 2 cycles<br>carboplatin<br>Paclitaxel | 66 Gy 33#;<br>Once daily;<br>ENI to 44 Gy | Planning: 2D/3D;<br>Verification: IGRT N  | Gefitinib   | Gefitinib                              | Compliance NR;<br>Overall G3/4 71%;<br>Overall G5 5%;<br>Oesoph G3/4 19%;<br>Pulmon G3/4 10%      | 19.0                        |

Abbreviations: Ref, reference; Ph, phase; Number, number of patients; Age, median age of patients in years (range); M/F, percentage of males to females; PS, percentage of patients with performance status of 0/1/2; >5% wt lo, percentage of patients with >5% weight loss; Path, percentage of patients with histological adenocarcinoma/squamous cell carcinoma/other subtypes of NSCLC; Stage, percentage of patients with stage IIIA/IIIB disease; PET Y/N, Yes or No to mandatory use of PET for staging; ENI, elective nodal irradiation; 2D, 2 dimensional; 3D, 3 dimensional; 4D, 4 dimensional; CRT, conformal radiotherapy; IMRT, intensity modulated radiotherapy; IGRT Y/N, Yes or No to use of image-guided radiotherapy delivery; GTV/PTV, gross or planning target volume median in cm<sup>3</sup> (range); Lung V<sub>20</sub>, median percentage of total lung volume receiving at least 20 Gy (range); Toxicity G3/4/5, rates of grades of toxicity; NR, not reported; Oesoph, oesophageal; Pulmon, pulmonary; DLT, dose limiting toxicity; Medial survival, overall median survival in months.

Table 3. Published studies of EGFR inhibitors with conventional fractionation radical concomitant chemo-radiotherapy.

| Ref        | Patients   | Disease   | Induction   | Target dose/<br>fractionation             | RT planning/delivery                     | Concomitant  | Consolidation/<br>maintenance                        | Compliance/toxicity  | Median survival<br>(months)    |
|------------|--|---|---|---|--|--|--|--|--------------------------------|
| (64) Ph II | Number: 87;<br>Age: 64 [42-85];<br>M/F: 57/43;<br>PS: 47/53/0;<br>>5% wt lo: 0%  | Path: NR;<br>Stage: 46/54;<br>PET: 64%  | —   | 63 Gy 35#;<br>Once daily;<br>ENI to 45 Gy | Planning: 3D;<br>Verification: IGRT N    | Carboplatin<br>paclitaxel<br>weekly +<br>Cetuximab   | 2 cycles<br>Carboplatin<br>paclitaxel +<br>Cetuximab | Compliance 68%;<br>NH G3/4 68%;<br>Overall G5 7%;<br>Oesoph G3/4 7%;<br>Pulmon G3/4 9%   | 22.7                           |
| (65) Ph II | Arm A<br>Number: 48;<br>Age: 65 [41-79];<br>M/F: 56/44;<br>PS: 58/42/0<br>Arm B<br>Number: 53;<br>Age: 66 [32-81];<br>M/F: 64/36;<br>PS: 34/66/0 | Arm A<br>Path: 46/35/19;<br>Stage: 60/38<br>Arm B<br>Path: 42/34/24;<br>Stage: 51/45;<br>PET: Y | —   | 70 Gy 35 #;<br>Once daily;<br>No ENI      | Planning: 3D/4D;<br>Verification: IGRT N | 4 cycles<br>Carboplatin<br>Pemetrexed<br>Arm A;<br>Carboplatin<br>Pemetrexed +<br>Cetuximab<br>Arm B | ≤4 cycles<br>Pemetrexed                              | Arm A<br>Compliance: 54%;<br>NH G3/4 52%;<br>Overall G5 4%;<br>Oesoph G3/4<br>16%;<br>Pulmon G3/4 12%<br>Arm B<br>Compliance: 53%;<br>NH G3/4 62%;<br>Overall G5 6%;<br>Oesoph G3/4<br>13%;<br>Pulmon G3/4 11% | Arm A<br>21.2<br>Arm B<br>25.2 |
| (59) Ph II | 'Good risk' arm<br>Number: 39;<br>Age: 64 [44-82];<br>M/F: 72/28;<br>PS: 46/54/0;<br>>5% wt lo: 0%   | Path: 33/41/26;<br>Stage: 54/46;<br>PET: N  | 2 cycles<br>carboplatin<br>paclitaxel               | 66 Gy 33#;<br>Once daily;<br>ENI to 44 Gy | Planning: 2D/3D;<br>Verification: IGRT N | Carboplatin<br>paclitaxel<br>gefitinib   | Gefitinib  | Compliance NR;<br>Overall G3/4 86%;<br>Overall G5 5%;<br>Oesoph G3/4<br>31%;<br>Pulmon G3/4 11%  | 13.0                           |
| (66) Ph I  | Number: 23;<br>Age: 62 [44-82];<br>M/F: 48/52;<br>PS: 60/40/0;<br>>5% wt lo: 17%   | Path: 52/44/4;<br>Stage: 60/40;<br>PET: 91%   | 2 cycles<br>carboplatin<br>paclitaxel<br>irinotecan | 74 Gy 37#;<br>Once daily;<br>ENI to 44 Gy | Planning: 2D/3D;<br>Verification: IGRT N | Carboplatin<br>paclitaxel<br>gefitinib   | —  | Compliance 86%;<br>Overall G5 0%;<br>Oesoph G3/4 5%;<br>Pulmon G3/4 10%  | 16.0                           |

Table 3 (continued)

Table 3 (continued)

| Ref       | Patients  | Disease   | Induction                          | Target dose/<br>fractionation             | RT planning/delivery                     | Concomitant  | Consolidation/<br>maintenance        | Compliance/toxicity  | Median survival<br>(months) |
|-----------|---|---|------------------------------------|---|--|--|--------------------------------------|--|-----------------------------|
| (67) Ph I | Number: 16;<br>Age: 64 [43-79];<br>M/F: 56/44;<br>PS: 6/94/0  | Path: NR;<br>Stage: NR;<br>PET: N                       | —                                  | 70 Gy 35#;<br>Once daily;<br>ENI to 40 Gy | Planning: 3D;<br>Verification: IGRT N    | Gefitinib +<br>Dose-escalating<br>docetaxel  | 2 cycles<br>Docetaxel +<br>Gefitinib | Compliance 88%;<br>Overall G5 19%;<br>Oesoph G3/4<br>19%;<br>Pulmon G3/4 6%  | 21.0                        |
| (68) Ph I | Step 1<br>Number: 5;<br>Step 2<br>Number: 9<br>Steps 1 + 2<br>Age: 60 [38-74];<br>M/F: 79/21;<br>PS: 93/7/0 | Path: NR;<br>Stage: NR;<br>PET: 'optimal'               | Variable                           | 63 Gy 34#;<br>Once daily;<br>ENI to 45 Gy | Planning: 3D;<br>Verification: IGRT N    | Step 1 gefitinib<br>Step 2 Cisplatin<br>+ Gefitinib  | Gefitinib                            | Step 1<br>Overall G5 0%;<br>Oesoph G3/4 0%;<br>Pulmon G3/4 0%<br>Step 2<br>Overall G5 0%;<br>Oesoph G3/4<br>22%;<br>Pulmon G3/4 11%  | Steps 1 + 2<br>12.5         |
| (69) Ph I | Arm A<br>Number: 17<br>Arm B<br>Number: 17<br>Arms A+B<br>Age: 63 [39-78];<br>M/F: 59/41;<br>PS: 71/29      | Arms A+B<br>Path:<br>21/29/50<br>Stage: 29/71<br>PET: N | Arm B<br>Carboplatin<br>paclitaxel | 66 Gy 33#;<br>Once daily;<br>ENI to 44 Gy | Planning: 2D/3D;<br>Verification: IGRT N | Arm A<br>Cisplatin<br>etoposide<br>erlotinib;<br>Arm B<br>carboplatin<br>paclitaxel<br>erlotinib | Arm A<br>docetaxel                   | Arm A<br>Overall G5 0%;<br>Oesoph G3/4<br>18%;<br>Pulmon G3/4 6%<br>Arm B<br>Overall G5 0%;<br>Oesoph G3/4<br>35%;<br>Pulmon G3/4 0% | Arm A 10.2<br>Arm B 13.7    |

Abbreviations: Ref, reference; Ph, phase; Number, number of patients; Age, median age of patients in years (range); M/F, percentage of males to females; PS, percentage of patients with performance status of 0/1/2; >5% wt lo, percentage of patients with >5% weight loss; Path, percentage of patients with histological adenocarcinoma/squamous cell carcinoma/other subtypes of NSCLC; Stage, percentage of patients with stage IIIA/IIIB disease; PET Y/N, Yes or No to mandatory use of PET for staging; ENI, elective nodal irradiation; 2D, 2 dimensional; 3D, 3 dimensional; 4D, 4 dimensional; CRT, conformal radiotherapy; IMRT, intensity modulated radiotherapy; IGRT Y/N, Yes or No to use of image-guided radiotherapy delivery; GTV/PTV, gross or planning target volume median in cm<sup>3</sup> (range); Lung V<sub>30</sub>, median percentage of total lung volume receiving at least 20 Gy (range); Toxicity G3/4/5, rates of grades of toxicity; NR, not reported; NH, non-haematological toxicity; Oesoph, oesophageal; Pulmon, pulmonary; DLT, dose limiting toxicity; Medial survival, overall median survival in months.

(Table 3). The majority of patients were staged with PET and all had 3D conformal radiotherapy. Compliance with treatment was 68% and grade 3/4 toxicity rates were acceptable, however there were six deaths (7%) considered as related to the treatment and at least three of these were pulmonary in nature. The median survival was encouraging at 22.7 (95% CI: 15.3-30.4) months. Another phase II study in 101 good performance status patients with locally advanced NSCLC compared high-dose radical radiotherapy (70 Gy) given with concomitant carboplatin and pemetrexed chemotherapy with or without cetuximab, followed by maintenance pemetrexed. PET staging was mandated and 3D or 4D radiotherapy was used without elective nodal irradiation. Compliance was similarly just over 50% in both arms with acceptable grade 3/4 toxicity rates. There were two (4%) patients with grade 5 toxicities in the arm without cetuximab and three (6%) patients in the cetuximab arm, all pulmonary related. The median survival rates were 21.2 and 25.2 months in the non-cetuximab versus cetuximab arms, respectively. The patients were highly selected which may account in part for the higher than anticipated median survival in the non-cetuximab arm. It is important to note this study was designed before lack of efficacy of pemetrexed in squamous histology was known (70). Also there is concern about the effect of the high-dose of radiotherapy used in this study, given in standard 2 Gy daily fractions, due to the recent preliminary results from the subsequent phase III RTOG 0617 study. The RTOG 0617 trial treated 544 patients with locally advanced NSCLC using radical radiotherapy with concomitant carboplatin and paclitaxel chemotherapy followed by consolidation chemotherapy and randomised patients in a 2x2 factorial design between an escalated dose of 74 Gy compared to 60 Gy in 2 Gy daily fractions and between concomitant cetuximab or not. The initial results of the radiotherapy dose analyses demonstrated a worse prognosis in the high-dose compared to standard-dose radiotherapy arm (10), with an 18-month overall survival of 53.9% versus 66.9%, respectively. Recently, the initial results of the cetuximab analyses were also presented (10) and unfortunately no significant difference was observed in median survival or 18 month overall survival between the cetuximab and non-cetuximab arms (23.1 versus 23.5 months and 60.8% versus 60.2%, respectively). The addition of cetuximab was however associated with increase toxicity compared to the non-cetuximab arm ( $\geq$  grade 3 non-haematological 70.5% versus 50.7% and  $\geq$  grade 4 35.8% versus 28.2%, respectively).

Phase I studies of erlotinib and gefitinib given with concomitant chemo-radiotherapy for locally advanced disease have demonstrated feasibility of the combination with both standard (68,69) and high-dose (66,67) conventionally fractionated radiotherapy, although the associated medial

survivals reported in these studies have been disappointing (~12-16 months) (Table 3). Again confounding factors are noted including for example, lack of PET staging and use of maintenance gefitinib (63) in some studies. In addition, the CALEB 30106 phase II study discussed above in relation to combination of gefitinib given with sequential chemo-radiotherapy, treated the 'good-risk' patients, defined as PS 0-1 with <5% weight loss, with two cycles of induction carboplatin and paclitaxel chemotherapy followed by concomitant gefitinib and chemo-radiotherapy to 66 Gy in standard fractionation, followed by maintenance gefitinib. The median overall survival was poor at 13 (95% CI: 8.5-17.2) months and worse than the median survival of 19 (95% CI: 9.9-28.4) months observed in the 'poor-risk' patients treated sequentially.

### Other targeted agents and radiotherapy for NSCLC

Considerable pre-clinical rationale exists to combine other targeted therapeutics with radiotherapy. The phosphoinositol 3-kinase (PI3K)/Akt/mTOR pathway is transforming for some NSCLC and a number of inhibitors of components of this pathway are in development for advanced NSCLC. Some of these have been shown to be radio-sensitizers in non-NSCLC models (71). Perhaps the best investigated includes abrogation of the tumour microvasculature by vascular disrupting agents (e.g., ZD6126) or anti-angiogenic agents (e.g., bevacizumab). VEGF is known to be upregulated by irradiation and VEGF inhibition is associated with increased tumour control after irradiation in pre-clinical models (72). However, early phase studies have raised toxicity concerns about combinations of agents targeting tumour vasculature or angiogenesis with radiotherapy in NSCLC patients (73) whereas early phase studies of radiotherapy combined with agents targeting tumour cell proliferation and survival pathways demonstrate feasibility (74,75). A recent review highlights the number of pre-clinical and ongoing early phase clinical studies assessing targeting agents in NSCLC patients (76). With the rapidly expanding availability of novel targeted agents and growing experience of these agents in the advanced disease setting, careful consideration of the optimal agents to combine with radiation and study design remains paramount to maximise therapeutic gain and avoid undue toxicity. Guidelines have been published to provide a framework for assessment of novel radio-sensitizers in the pre-clinical and early phase clinical setting (77).

Of the different exploitable mechanisms (78) by which a drug may interact with radiotherapy to improve the therapeutic ratio, it may be that NSCLC patients identified as harbouring

an oncogenic driver mutation that confers sensitivity to a specific targeted agent [e.g., echinoderm microtubule-associated protein-like 4 and anaplastic lymphoma kinase gene translocation (EML4-ALK) and ALK TKI crizotinib] will benefit from treatment schedule aimed at maximising spatial co-operation of treatment modalities whereas those without an identifiable mutation may derive benefit from a schedule aimed at maximising the concomitant radio-sensitising approach of combining novel agent with radiotherapy. The central role of DNA damage response to radiotherapy and whether this effect can be modulated by targeted agents remains an important area of research (79). Modulation of the effect of radiation rather than targeting specific driver mutations is also of research interest given the emerging issues of tumour heterogeneity (80).

### Targeted agents with altered fractionation radiotherapy in NSCLC

Whilst the majority of studies of targeted agents with radiotherapy in NSCLC have also included concomitant chemotherapy, it is important to maintain a focus on studies of radiotherapy and targeted agent without additional chemotherapy or with sequential chemotherapy for the important group of patients with locally advanced NSCLC who are elderly, have poor performance status or multiple co-morbidities (7). With evidence that modified fractionation schedules are associated with improved outcome compared to conventional fractionation in NSCLC (16) and the experience to date of combining cetuximab with conventionally fractionated radiotherapy alone or sequential chemo-radiotherapy suggesting feasibility with acceptable toxicity, studies of cetuximab with modified fractionation radiotherapy in these settings are warranted. Patient selection remains important with accurate staging and reporting of important prognostic factors in addition to patient demographics to assist the reproducibility of treatment results in the wider population.

Given the initial results from the phase III RTOG 0617 study, there does not appear to be a role for the additional of cetuximab in combination with standard dose concurrent chemo-radiotherapy using conventional fractionation. Interestingly, no significant interaction between the radiotherapy dose and the addition of cetuximab were observed. The question remains as to whether cetuximab can be safely added to modified fractionation schedule chemo-radiotherapy and whether this provides any benefit.

### Additional considerations

When considering the total dose of radiation prescribed for a given schedule, it is important to consider that locally advanced

NSCLC encompasses a heterogenous population of individuals with differing volume, location and extent of disease. Recently the concept of isotoxic dose escalation was introduced, moving away from a fixed radiotherapy dose prescription for all patients to a tailored prescription based on the surrounding normal tissue dose constraints, predicting a certain acceptable probability of toxicity (81). Use of this approach in modified fractionation radiotherapy with sequential or concomitant chemotherapy demonstrates promising results in phase II setting (82-84). The study of the addition of targeted agents to isotoxic dose escalated accelerated radiotherapy schedules is an interesting area of ongoing research.

For trial design, patient selection remains important and patients need to be optimally staged and stratified based on prognostic variables to ensure the results are repeatable in the wider patient population. State-of-the-art radiotherapy techniques for planning and delivery, including IMRT and image-guided radiotherapy (IGRT), stand to optimise the therapeutic window. Detailed reporting of radiotherapy planning and delivery parameters will reduce the heterogeneity in studies discussed above and permit optimal comparison between studies and reproducibility of outcomes.

Further work is required to improve understanding of the mechanisms of response and toxicity using targeted agents with radiation and to assess for early predictors of response and toxicity, particularly with respect to fraction-size sensitivity with the increasing use of altered fractionation radiotherapy schedules.

### Conclusions

Advances in the molecular understanding of NSCLC have accelerated in recent years and the era of personalised medicine in systemic treatment, particularly in advanced disease, has become a reality. At the same time, advances in technology and imaging have led to improvements in patient selection and in accuracy of radical radiotherapy planning and delivery for locally advanced NSCLC. The combination of individualised biological optimisation using novel targeted agents with physical optimisation using state-of-the-art radical (chemo-) radiotherapy, including accelerated-fractionation schedules and individualised radiotherapy dose-prescriptions, stands to improve outcomes in the heterogeneous population of patients with unresectable locally advanced NSCLC.

### Acknowledgements

This review work was supported by The Royal Marsden NHS Foundation Trust which received a proportion of its funding from the NHS Executive; the views expressed in this publication

are those of the authors and not necessarily those of the NHS Executive. We acknowledge NHS funding to the NIHR Biomedical Research Centre.

*Disclosure:* FM reports no actual or potential conflicts of interest. SP has been a non-reimbursed consultant to Astra Zeneca, Boehringer Ingelheim and Roche.

## References

- Soerjomataram I, Lortet-Tieulent J, Parkin DM, et al. Global burden of cancer in 2008: a systematic analysis of disability-adjusted life-years in 12 world regions. *Lancet* 2012;380:1840-50.
- Cancer Research UK; 2013 (updated 2013; cited 2013); Available online: <http://info.cancerresearchuk.org/cancerstats/survival>
- Coleman MP, Forman D, Bryant H, et al. Cancer survival in Australia, Canada, Denmark, Norway, Sweden, and the UK, 1995-2007 (the International Cancer Benchmarking Partnership): an analysis of population-based cancer registry data. *Lancet* 2011;377:127-38.
- Chemotherapy in non-small cell lung cancer: a meta-analysis using updated data on individual patients from 52 randomised clinical trials. Non-small Cell Lung Cancer Collaborative Group. *BMJ* 1995;311:899-909.
- Aupérin A, Le Péchoux C, Pignon JP, et al. Concomitant radio-chemotherapy based on platin compounds in patients with locally advanced non-small cell lung cancer (NSCLC): a meta-analysis of individual data from 1764 patients. *Ann Oncol* 2006;17:473-83.
- Aupérin A, Le Péchoux C, Rolland E, et al. Meta-analysis of concomitant versus sequential radiochemotherapy in locally advanced non-small-cell lung cancer. *J Clin Oncol* 2010;28:2181-90.
- De Ruyscher D, Botterweck A, Dirx M, et al. Eligibility for concurrent chemotherapy and radiotherapy of locally advanced lung cancer patients: a prospective, population-based study. *Ann Oncol* 2009;20:98-102.
- Groen HJ, van der Leest AH, Fokkema E, et al. Continuously infused carboplatin used as radiosensitizer in locally unresectable non-small-cell lung cancer: a multicenter phase III study. *Ann Oncol* 2004;15:427-32.
- Martel MK, Ten Haken RK, Hazuka MB, et al. Estimation of tumor control probability model parameters from 3-D dose distributions of non-small cell lung cancer patients. *Lung Cancer* 1999;24:31-7.
- Bradley JD, Paulus R, Komaki R, et al. A randomised phase III comparison of standard-dose (60 Gy) versus high-dose (74 Gy) conformal chemoradiotherapy with or without cetuximab for stage III NSCLC: Results on radiation dose in RTOG 0617. *J Clin Oncol* 2013;31:abstr 7501.
- Withers HR, Taylor JM, Maciejewski B. The hazard of accelerated tumor clonogen repopulation during radiotherapy. *Acta Oncol* 1988;27:131-46.
- Suwinski R, Withers HR. Time factor and treatment strategies in subclinical disease. *Int J Radiat Biol* 2003;79:495-502.
- Fowler JF. 21 years of biologically effective dose. *Br J Radiol* 2010;83:554-68.
- Onishi H, Shirato H, Nagata Y, et al. Hypofractionated stereotactic radiotherapy (HypoFXSRT) for stage I non-small cell lung cancer: updated results of 257 patients in a Japanese multi-institutional study. *J Thorac Oncol* 2007;2:S94-100.
- Ohri N, Werner-Wasik M, Grills IS, et al. Modeling local control after hypofractionated stereotactic body radiation therapy for stage I non-small cell lung cancer: a report from the elekta collaborative lung research group. *Int J Radiat Oncol Biol Phys* 2012;84:e379-84.
- Mauguen A, Le Pechoux C, Saunders MI, et al. Hyperfractionated or accelerated radiotherapy in lung cancer: an individual patient data meta-analysis. *J Clin Oncol* 2012;30:2788-97.
- Pöttgen C, Eberhardt W, Graupner B, et al. Accelerated hyperfractionated radiotherapy within trimodality therapy concepts for stage IIIA/B non-small cell lung cancer: Markedly higher rate of pathologic complete remissions than with conventional fractionation. *Eur J Cancer* 2013. [Epub ahead of print].
- Vansteenkiste J, De Ruyscher D, Eberhardt WE, et al. Early and locally advanced non-small-cell lung cancer (NSCLC): ESMO Clinical Practice Guidelines for diagnosis, treatment and follow-up. *Ann Oncol* 2013;24 Suppl 6:vi89-98.
- Buhrow SA, Cohen S, Garbers DL, et al. Characterization of the interaction of 5'-p-fluorosulfonylbenzoyl adenosine with the epidermal growth factor receptor/protein kinase in A431 cell membranes. *J Biol Chem* 1983;258:7824-7.
- Veale D, Ashcroft T, Marsh C, et al. Epidermal growth factor receptors in non-small cell lung cancer. *Br J Cancer* 1987;55:513-6.
- Veale D, Kerr N, Gibson GJ, et al. The relationship of quantitative epidermal growth factor receptor expression in non-small cell lung cancer to long term survival. *Br J Cancer* 1993;68:162-5.
- Kim ES, Hirsh V, Mok T, et al. Gefitinib versus docetaxel in previously treated non-small-cell lung cancer (INTEREST): a randomised phase III trial. *Lancet* 2008;372:1809-18.
- Shepherd FA, Rodrigues Pereira J, Ciuleanu T, et al. Erlotinib in previously treated non-small-cell lung cancer. *N Engl J Med* 2005;353:123-32.
- Lynch TJ, Bell DW, Sordella R, et al. Activating mutations in the epidermal growth factor receptor underlying responsiveness of non-small-cell lung cancer to gefitinib. *N Engl J Med* 2004;350:2129-39.
- Paez JG, Janne PA, Lee JC, et al. EGFR mutations in lung cancer: correlation with clinical response to gefitinib therapy. *Science* 2004;304:1497-500.
- Hirsch FR, Vannice PA, Eberhardt WE, et al. Epidermal growth factor receptor inhibition in lung cancer: status 2012. *J Thorac Oncol* 2013;8:373-84.
- Fan Z, Baselga J, Masui H, et al. Antitumor effect of anti-epidermal growth factor receptor monoclonal antibodies plus cis-diamminedichloroplatinum on well established A431 cell xenografts. *Cancer Res* 1993;53:4637-42.
- Rosell R, Robinet G, Szczesna A, et al. Randomized phase II study of cetuximab plus cisplatin/vinorelbine compared with cisplatin/vinorelbine alone as first-line therapy in EGFR-expressing advanced non-small-cell lung cancer. *Ann Oncol* 2008;19:362-9.
- Lynch TJ, Patel T, Dreisbach L, et al. Cetuximab and first-line taxane/carboplatin chemotherapy in advanced non-small-cell lung cancer: results of the randomized multicenter phase III trial BMS099. *J Clin Oncol* 2010;28:911-7.

30. Pirker R, Pereira JR, Szczesna A, et al. Cetuximab plus chemotherapy in patients with advanced non-small-cell lung cancer (FLEX): an open-label randomised phase III trial. *Lancet* 2009;373:1525-31.
31. Pirker R, Pereira JR, von Pawel J, et al. EGFR expression as a predictor of survival for first-line chemotherapy plus cetuximab in patients with advanced non-small-cell lung cancer: analysis of data from the phase 3 FLEX study. *Lancet Oncol* 2012;13:33-42.
32. Contessa JN, Reardon DB, Todd D, et al. The inducible expression of dominant-negative epidermal growth factor receptor-CD533 results in radiosensitization of human mammary carcinoma cells. *Clin Cancer Res* 1999;5:405-11.
33. Akimoto T, Hunter NR, Buchmiller L, et al. Inverse relationship between epidermal growth factor receptor expression and radiocurability of murine carcinomas. *Clin Cancer Res* 1999;5:2884-90.
34. Schmidt-Ullrich RK, Valerie K, Fogleman PB, et al. Radiation-induced autophosphorylation of epidermal growth factor receptor in human malignant mammary and squamous epithelial cells. *Radiat Res* 1996;145:81-5.
35. Schmidt-Ullrich RK, Valerie KC, Chan W, et al. Altered expression of epidermal growth factor receptor and estrogen receptor in MCF-7 cells after single and repeated radiation exposures. *Int J Radiat Oncol Biol Phys* 1994;29:813-9.
36. Huang SM, Bock JM, Harari PM. Epidermal growth factor receptor blockade with C225 modulates proliferation, apoptosis, and radiosensitivity in squamous cell carcinomas of the head and neck. *Cancer Res* 1999;59:1935-40.
37. Huang SM, Harari PM. Modulation of radiation response after epidermal growth factor receptor blockade in squamous cell carcinomas: inhibition of damage repair, cell cycle kinetics, and tumor angiogenesis. *Clin Cancer Res* 2000;6:2166-74.
38. Milas L, Mason K, Hunter N, et al. In vivo enhancement of tumor radioresponse by C225 anti-epidermal growth factor receptor antibody. *Clin Cancer Res* 2000;6:701-8.
39. Raben D, Helfrich B, Chan DC, et al. The effects of cetuximab alone and in combination with radiation and/or chemotherapy in lung cancer. *Clin Cancer Res* 2005;11:795-805.
40. Li L, Wang H, Yang ES, et al. Erlotinib attenuates homologous recombinational repair of chromosomal breaks in human breast cancer cells. *Cancer Res* 2008;68:9141-6.
41. She Y, Lee F, Chen J, et al. The epidermal growth factor receptor tyrosine kinase inhibitor ZD1839 selectively potentiates radiation response of human tumors in nude mice, with a marked improvement in therapeutic index. *Clin Cancer Res* 2003;9:3773-8.
42. Chinnaiyan P, Huang S, Vallabhaneni G, et al. Mechanisms of enhanced radiation response following epidermal growth factor receptor signaling inhibition by erlotinib (Tarceva). *Cancer Res* 2005;65:3328-35.
43. Pore N, Jiang Z, Gupta A, et al. EGFR tyrosine kinase inhibitors decrease VEGF expression by both hypoxia-inducible factor (HIF)-1-independent and HIF-1-dependent mechanisms. *Cancer Res* 2006;66:3197-204.
44. Solomon B, Binns D, Roselt P, et al. Modulation of intratumoral hypoxia by the epidermal growth factor receptor inhibitor gefitinib detected using small animal PET imaging. *Mol Cancer Ther* 2005;4:1417-22.
45. Krause M, Ostermann G, Petersen C, et al. Decreased repopulation as well as increased reoxygenation contribute to the improvement in local control after targeting of the EGFR by C225 during fractionated irradiation. *Radiother Oncol* 2005;76:162-7.
46. Bonner JA, Harari PM, Giralt J, et al. Radiotherapy plus cetuximab for squamous-cell carcinoma of the head and neck. *N Engl J Med* 2006;354:567-78.
47. Jatoi A, Schild SE, Foster N, et al. A phase II study of cetuximab and radiation in elderly and/or poor performance status patients with locally advanced non-small-cell lung cancer (N0422). *Ann Oncol* 2010;21:2040-4.
48. Jensen AD, Munter MW, Bischoff HG, et al. Combined treatment of nonsmall cell lung cancer NSCLC stage III with intensity-modulated RT radiotherapy and cetuximab: the NEAR trial. *Cancer* 2011;117:2986-94.
49. Okamoto I, Takahashi T, Okamoto H, et al. Single-agent gefitinib with concurrent radiotherapy for locally advanced non-small cell lung cancer harboring mutations of the epidermal growth factor receptor. *Lung Cancer* 2011;72:199-204.
50. Wang J, Xia TY, Wang YJ, et al. Prospective study of epidermal growth factor receptor tyrosine kinase inhibitors concurrent with individualized radiotherapy for patients with locally advanced or metastatic non-small-cell lung cancer. *Int J Radiat Oncol Biol Phys* 2011;81:e59-65.
51. Marks LB, Bentzen SM, Deasy JO, et al. Radiation dose-volume effects in the lung. *Int J Radiat Oncol Biol Phys* 2010;76:S70-6.
52. Bebb G, Smith C, Rorke S, et al. Phase I clinical trial of the anti-EGFR monoclonal antibody nimotuzumab with concurrent external thoracic radiotherapy in Canadian patients diagnosed with stage IIB, III or IV non-small cell lung cancer unsuitable for radical therapy. *Cancer Chemother Pharmacol* 2011;67:837-45.
53. Choi HJ, Sohn JH, Lee CG, et al. A phase I study of nimotuzumab in combination with radiotherapy in stages IIB-IV non-small cell lung cancer unsuitable for radical therapy: Korean results. *Lung Cancer* 2011;71:55-9.
54. Wan J, Cohen J, Agulnik J, et al. Unexpected high lung toxicity from radiation pneumonitis in phase I/II trial of concurrent erlotinib with limited field radiation for intermediate prognosis patients with stage III or inoperable stage IIB NSCLC. *Int J Rad Onc Biol Phys* 2009;75:abstr 235.
55. Hughes S, Liang J, Miah A, et al. A brief report on the safety study of induction chemotherapy followed by synchronous radiotherapy and cetuximab in stage III non-small cell lung cancer (NSCLC): SCRATCH study. *J Thorac Oncol* 2008;3:648-51.
56. Hallqvist A, Wagenius G, Rylander H, et al. Concurrent cetuximab and radiotherapy after docetaxel-cisplatin induction chemotherapy in stage III NSCLC: satellite--a phase II study from the Swedish Lung Cancer Study Group. *Lung Cancer* 2011;71:166-72.
57. Ramalingam SS, Kotsakis A, Tarhini AA, et al. A multicenter phase II study of cetuximab in combination with chest radiotherapy and consolidation chemotherapy in patients with stage III NSCLC. *Lung Cancer* 2013;81:416-21.
58. Niho S, Ohe Y, Ishikura S, et al. Induction chemotherapy followed by gefitinib and concurrent thoracic radiotherapy for unresectable locally advanced adenocarcinoma of the lung: a multicenter feasibility study

- (JCOG 0402). *Ann Oncol* 2012;23:2253-8.
59. Ready N, Janne PA, Bogart J, et al. Chemoradiotherapy and gefitinib in stage III non-small cell lung cancer with epidermal growth factor receptor and KRAS mutation analysis: cancer and leukemia group B (CALEB) 30106, a CALGB-stratified phase II trial. *J Thorac Oncol* 2010;5:1382-90.
  60. Werner-Wasik M, Scott C, Cox JD, et al. Recursive partitioning analysis of 1999 Radiation Therapy Oncology Group (RTOG) patients with locally-advanced non-small-cell lung cancer (LA-NSCLC): identification of five groups with different survival. *Int J Radiat Oncol Biol Phys* 2000;48:1475-82.
  61. Vokes EE, Herndon JE 2nd, Kelley MJ, et al. Induction chemotherapy followed by chemoradiotherapy compared with chemoradiotherapy alone for regionally advanced unresectable stage III Non-small-cell lung cancer: Cancer and Leukemia Group B. *J Clin Oncol* 2007;25:1698-704.
  62. Hallqvist A, Bergman B, Nyman J. Health related quality of life in locally advanced NSCLC treated with high dose radiotherapy and concurrent chemotherapy or cetuximab--pooled results from two prospective clinical trials. *Radiother Oncol* 2012;104:39-44.
  63. Kelly K, Chansky K, Gaspar LE, et al. Phase III trial of maintenance gefitinib or placebo after concurrent chemoradiotherapy and docetaxel consolidation in inoperable stage III non-small-cell lung cancer: SWOG S0023. *J Clin Oncol* 2008;26:2450-6.
  64. Blumenschein GR Jr, Paulus R, Curran WJ, et al. Phase II study of cetuximab in combination with chemoradiation in patients with stage IIIA/B non-small-cell lung cancer: RTOG 0324. *J Clin Oncol* 2011;29:2312-8.
  65. Govindan R, Bogart J, Stinchcombe T, et al. Randomized phase II study of pemetrexed, carboplatin, and thoracic radiation with or without cetuximab in patients with locally advanced unresectable non-small-cell lung cancer: Cancer and Leukemia Group B trial 30407. *J Clin Oncol* 2011;29:3120-5.
  66. Stinchcombe TE, Morris DE, Lee CB, et al. Induction chemotherapy with carboplatin, irinotecan, and paclitaxel followed by high dose three-dimension conformal thoracic radiotherapy (74 Gy) with concurrent carboplatin, paclitaxel, and gefitinib in unresectable stage IIIA and stage IIIB non-small cell lung cancer. *J Thorac Oncol* 2008;3:250-7.
  67. Center B, Petty WJ, Ayala D, et al. A phase I study of gefitinib with concurrent dose-escalated weekly docetaxel and conformal three-dimensional thoracic radiation followed by consolidative docetaxel and maintenance gefitinib for patients with stage III non-small cell lung cancer. *J Thorac Oncol* 2010;5:69-74.
  68. Rothschild S, Bucher SE, Bernier J, et al. Gefitinib in combination with irradiation with or without cisplatin in patients with inoperable stage III non-small cell lung cancer: a phase I trial. *Int J Radiat Oncol Biol Phys* 2011;80:126-32.
  69. Choong NW, Mauer AM, Haraf DJ, et al. Phase I trial of erlotinib-based multimodality therapy for inoperable stage III non-small cell lung cancer. *J Thorac Oncol* 2008;3:1003-11.
  70. Scagliotti GV, Parikh P, von Pawel J, et al. Phase III study comparing cisplatin plus gemcitabine with cisplatin plus pemetrexed in chemotherapy-naive patients with advanced-stage non-small-cell lung cancer. *J Clin Oncol* 2008;26:3543-51.
  71. Karar J, Maity A. Modulating the tumour microenvironment to increase radiation responsiveness. *Cancer Biol Ther* 2009;8:1994-2001.
  72. Gorski DH, Beckett MA, Jaskowiak NT, et al. Blockage of the vascular endothelial growth factor stress response increases the anti-tumour effects of ionising radiation. *Cancer Res* 1999;59:3374-8.
  73. Spigel DR, Hainsworth JD, Yardley DA, et al. Tracheoesophageal fistula formation in patients with lung cancer treated with chemoradiation and bevacizumab. *J Clin Oncol* 2010;28:43-8.
  74. Sarkaria JN, Schwingler P, Schild SE, et al. Phase I trial of sirolimus combined with radiation and cisplatin in non-small cell lung cancer. *J Thorac Oncol* 2007;2:751-7.
  75. Schild S, Molina J, Dy G. A Phase I study of bortezomib, paclitaxel, carboplatin (CBDCA) and radiotherapy (RT) for locally advanced non-small cell lung cancer (NSCLC). *J Clin Oncol* 2010;28:abstr 7085.
  76. Koh PK, Favier-Finn C, Blackhall FH, et al. Targeted agents in non-small cell lung cancer (NSCLC): clinical developments and rationale for the combination with thoracic radiotherapy. *Cancer Treat Rev* 2012;38:626-40.
  77. Harrington KJ, Billingham LJ, Brunner TB, et al. Guidelines for preclinical and early phase clinical assessment of novel radiosensitisers. *Br J Cancer* 2011;105:628-39.
  78. Bentzen SM, Harari PM, Bernier J. Exploitable mechanisms for combining drugs with radiation: concepts, achievements and future directions. *Nat Clin Pract Oncol* 2007;4:172-80.
  79. Powell C, Mikropoulos C, Kaye SB, et al. Pre-clinical and clinical evaluation of PARP inhibitors as tumour-specific radiosensitisers. *Cancer Treat Rev* 2010;36:566-75.
  80. Gerlinger M, Rowan AJ, Horswell S, et al. Intratumor heterogeneity and branched evolution revealed by multiregion sequencing. *N Engl J Med* 2012;366:883-92.
  81. van Baardwijk A, Bosmans G, Boersma L, et al. Individualized radical radiotherapy of non-small-cell lung cancer based on normal tissue dose constraints: a feasibility study. *Int J Radiat Oncol Biol Phys* 2008;71:1394-401.
  82. De Ruyscher D, van Baardwijk A, Steevens J, et al. Individualised isotoxic accelerated radiotherapy and chemotherapy are associated with improved long-term survival of patients with stage III NSCLC: a prospective population-based study. *Radiother Oncol* 2012;102:228-33.
  83. van Baardwijk A, Reymen B, Wanders S, et al. Mature results of a phase II trial on individualised accelerated radiotherapy based on normal tissue constraints in concurrent chemo-radiation for stage III non-small cell lung cancer. *Eur J Cancer* 2012;48:2339-46.
  84. van Baardwijk A, Wanders S, Boersma L, et al. Mature results of an individualized radiation dose prescription study based on normal tissue constraints in stages I to III non-small-cell lung cancer. *J Clin Oncol* 2010;28:1380-6.



**Cite this article as:** McDonald F, Popat S. Combining targeted agents and hypo- and hyper-fractionated radiotherapy in NSCLC. *J Thorac Dis* 2014;6(4):356-368. doi: 10.3978/j.issn.2072-1439.2013.12.05

## Local control rates with five-fraction stereotactic body radiotherapy for oligometastatic cancer to the lung

Deepinder Singh, Yuhchayou Chen, Mary Z. Hare, Kenneth Y. Usuki, Hong Zhang, Thomas Lundquist, Neil Joyce, Michael C. Schell, Michael T. Milano

Department of Radiation Oncology, University of Rochester School of Medicine and Dentistry, Rochester, NY 14642, USA

### ABSTRACT

**Objective:** To report our institutional experience with five fractions of daily 8-12 Gy stereotactic body radiotherapy (SBRT) for the treatment of oligometastatic cancer to the lung.

**Methods:** Thirty-four consecutive patients with oligometastatic cancers to the lung were treated with image-guided SBRT between 2008 and 2011. Patient age ranged from 38 to 81 years. There were 17 males and 17 females. Lung metastases were from the following primary cancer types: colon cancer (n=13 patients), head and neck cancer (n=6), breast cancer (n=4), melanoma (n=4), sarcoma (n=4) and renal cell carcinoma (n=3). The median prescription dose was 50 Gy in five fractions (range, 40-60 Gy) to the isocenter, with the 80% isodose line encompassing the planning target volume (PTV) [defined as gross tumor volume (GTV) + 7-11 mm volumetric expansion]. The follow-up interval ranged from 2.4-54 months, with a median of 16.7 months.

**Results:** The 1-, 2-, and 3-year patient local control (LC) rates for all patients were 93%, 88%, and 80% respectively. The 1-, 2-, and 3-year overall survival (OS) rates were 62%, 44%, and 23% respectively. The 1- and 2-year patient LC rates were 95% and 88% for tumor size 1-2 cm (n=25), and 86% for tumor size 2-3 cm (n=7). The majority (n=4) of local failures occurred within 12 months. No patient experienced local failure after 12 months except for one patient with colon cancer whose tumors progressed locally at 26 months. All five patients with local recurrences had colorectal cancer. Statistical analyses showed that age, gender, previous chemotherapy, previous surgery or radiation had no significant effect on LC rates. No patient was reported to have any symptomatic pneumonitis at any time point.

**Conclusions:** SBRT for oligometastatic disease to the lung using 8-12 Gy daily fractions over five treatments resulted in excellent 1- and 2-year LC rates. Most local failures occurred within the first 12 months, with five local failures associated with colorectal cancer. The treatment is safe using this radiation fractionation schedule with no therapy-related pneumonitis.

### KEYWORDS

Stereotactic body radiotherapy (SBRT); lung cancer; oligometastases

*J Thorac Dis 2014;6(4):369-374. doi: 10.3978/j.issn.2072-1439.2013.12.03*

### Introduction

Metastases to lungs from various malignancies have generally been regarded as incurable and ultimately fatal (1,2). Systemic

chemotherapy has played a major palliative role in keeping cancer-related symptoms and disease progression under control for a limited time, after which these tumors generally become refractory to chemotherapy. Long-term survival with chemotherapy for metastatic lung disease is extremely rare (2). A select group of patients develop lung metastases that are limited in number and extent, and are amenable to surgical or locally ablative techniques such as stereotactic body radiotherapy (SBRT) (2-4). In others with widespread disease, effective chemotherapy with near complete response could result in limited lung metastases (2,3). This state of limited metastases was coined "oligometastasis" in the 1990s when radiation planning and delivery were experiencing major technical

Correspondence to: Deepinder Singh, MD. Department of Radiation Oncology, University of Rochester, 601 Elmwood Ave, Box 647, Rochester, NY 14642, USA. Email: deepinder\_singh@urmc.rochester.edu.

Submitted Aug 08, 2013. Accepted for publication Dec 03, 2013. Available at [www.jthoracdis.com](http://www.jthoracdis.com)

ISSN: 2072-1439

© Pioneer Bioscience Publishing Company. All rights reserved.

**Table 1.** Patient and treatment characteristics.

| Characteristics                            | N  |
|--|----|
| Age, 38-81 (median 51) years               |    |
| Gender                                     |    |
| Male                                       | 17 |
| Female                                     | 17 |
| Primary site                               |    |
| Colorectal                                 | 13 |
| Head and neck                              | 6  |
| Breast                                     | 4  |
| Melanoma                                   | 4  |
| Sarcoma                                    | 4  |
| Renal carcinoma                            | 3  |
| Follow-up                                  |    |
| Range, 2.4 to 54 months                    |    |
| Median FU period, 16.7 months              |    |
| Isocenter dose (Gy)                        |    |
| 40   | 11 |
| 45   | 4  |
| 50   | 18 |
| 60   | 1  |
| Number of lung lesions treated per patient |    |
| N=1  | 19 |
| N=2  | 7  |
| N=3  | 5  |
| N=5  | 3  |

advances (5). Patients with oligometastasis have been considered candidates for curative treatments because prolonging survival can be expected (6-8).

With the advent of improved 3-dimensional computed tomography (CT) based radiation treatment planning and more precise dose delivery methods, treatments using radiation have taken a leap forward in offering a more curative and less toxic approach in the management of cancers overall. The dose escalation coupled with high doses of radiation delivered per fraction in a short overall treatment time using high degrees of anatomic targeting accuracy results in an improved therapeutic ratio while minimizing radiation-associated early and late pulmonary toxicity. SBRT utilizes a large number of non-opposing beams with anatomic targeting using stereotactic localization and/or image guidance. Improved reproducibility in patient set-up and targeting accuracy facilitates the use of large

fraction, ablative radiation doses resulting in high local control (LC) rates.

Many reports are now available on the use of SBRT for oligometastatic lung disease, although patient cohorts in these studies are heterogeneous with respect to cancer types and selection criteria (2-4,9-11). SBRT can either be done for patients with new overt oligometastatic disease (patients not suitable for chemotherapy/surgery), or after the chemotherapy options have been exhausted. Furthermore, the extent of oligometastatic disease varies in patients included in different studies. For example, an early study by the University of Rochester included patients with five or fewer lesions, not necessarily confined to the thorax (2). Kyoto University uses criteria of one or two pulmonary metastases, tumor diameter <4 cm, locally controlled primary tumor, and no other metastatic sites (12). Duke University's criteria are stage IV cancer (any histology) with 1 to 5 metastases, with each metastasis  $\leq 10$  cm or  $\leq 500$  mL in volume on standard imaging (4).

The University of Rochester started using SBRT for oligometastasis in 2001 and has previously published survival and tumor control data showing 2-4 years overall survival (OS) rates of 50% and 28% and progression-free survival (PFS) rates of 26% and 26% respectively. Most of these patients were treated with a 10-fraction regimen using 4-6 Gy daily. As the outcomes of SBRT with less protracted regimes of five or fewer fractions were published by other institutions, our policy changed from ten-fraction SBRT to five-fraction SBRT using larger daily fraction sizes of 8-12 Gy. The present retrospective study was carried out to analyze the survival and tumor control and failure patterns for oligometastatic lung metastases treated with five fractions of SBRT among patients with chemorefractory disease or who were not candidates for chemotherapy or surgical resection.

## Methods

Between January 2008 and December 2011, thirty-four patients with oligometastatic cancer to the lungs who were considered refractory to (n=28) or ineligible for (n=6) chemotherapy were treated with SBRT. The 17 male and 17 female patients' ages ranged from 38 to 81 years with a median age of 51 years (Table 1). The study was approved by the University of Rochester Medical Center Research Subjects Review Board.

The inclusion criteria of this study included patients with one to five lung metastases, age >18, KPS >70%, tumor diameter (on CT) <5 cm, locally controlled primary tumor, and no other active metastatic sites. Patients with primary non-small cell lung cancer were not included [as patients with separate nodules within the same lung are defined as T3 (same lobe) to T4 disease

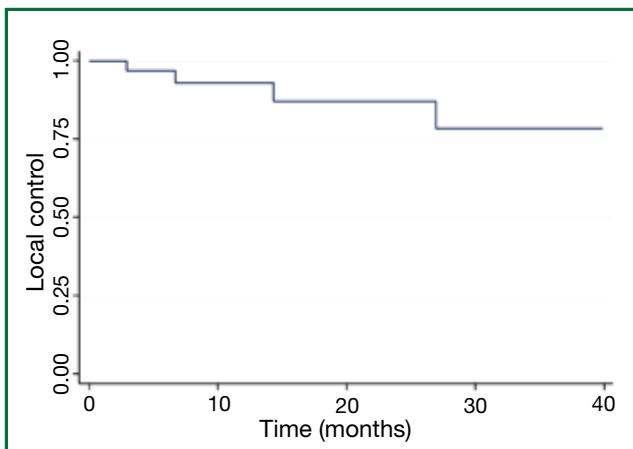


**Figure 1.** Overall local control among 34 patients.

(same lung, different lobes)]. The work up included contrast enhanced CT of the thorax and upper abdomen and FDG-PET. Patients were followed with CT or PET-CT every 3-6 months. Patients with no progression of treated lesions who developed new radiographically apparent oligometastatic lesions on follow-up imaging were allowed to undergo repeat cycle(s) of SBRT for new lesions (13).

### **SBRT technique**

The SBRT techniques that have been described in detail in previous publications from our group are briefly summarized here (2). All patients undergoing initial CT simulation required immobilization with a vacuum cushion device. All patients were treated with the Novalis ExacTrac system (BrainLab Inc.). The ExacTrac patient positioning platform using infrared reflecting body fiducial markers monitored by two ceiling mounted infrared cameras was used for patient positioning and real-time monitoring. Respiratory motion was minimized by using relaxed expiratory breath hold techniques (in most patients) or shallow breathing (in patients with poor lung function). Patients also underwent a CT in the set-up position, which was fused to the planning CT, prior to treatment and after the second fraction to ensure three-dimensional set-up accuracy. The gross tumor volume (GTV) was delineated using CT and fused PET imaging when needed. The use of arcs and non co-planner beams was encouraged. Dose volume histograms (DVH) were calculated for the lung (defined as total lung minus GTV), heart, esophagus, spinal cord, and liver. The planning target volume (PTV) was defined as a 7 mm circumferential and 11 mm superior-inferior expansion of the GTV (with no expansion for CTV) (2,3,13). The 80% isodose line encompassed the PTV, with isocenter dose

defined as 100% of the prescribed dose. The prescribed target dose was determined based on the DVH of normal (uninvolved) lung and surrounding organs. The median prescription dose was 50 Gy in five fractions (range, 40-60 Gy) to isocenter with 80-100% isodose covering 95% of PTV. Patients were required to have 1,000 mL of tumor free lung, with a volume of lung receiving >20 Gy ( $V_{20}$ ) less than 25%. The spinal cord maximum was required to be <4.5 Gy/fraction. Care was taken so that hot spots (i.e., >80% isodose) occurred solely within the GTV. The dose for smaller peripheral tumors was mostly 50-60 Gy and the dose for larger central tumors was mostly 40-50 Gy.

### **Outcomes/statistics**

The primary end point was tumor LC and secondary end points included regional control as well as OS. Actuarial tumor control and survival were calculated using the Kaplan-Meier actuarial survival analyses. OS was defined from date of completion of SBRT until death or last follow-up. Patient LC was scored as an event if any treated lesion grew by  $\geq 20\%$ , based on the Response Evaluation Criteria In Solid Tumors (RECIST) criteria or a local failure was confirmed pathologically. LC was analyzed per patient, meaning that if a patient had more than one lesion treated, progression of any of the treated lesions was considered a local failure. LC was analyzed by tumor size; among patients with more than one lesion, treated tumor size represents the largest lesion treated. Among patients who underwent repeat courses of SBRT for new lesions(s), only the LC of the index lesion(s) was considered in this study. STATA version 9.2 was used for all data analysis.

## **Results**

The primary cancer sites among the 34 patients included colorectal (n=13), head and neck (n=6), breast (n=4), melanoma (n=4), sarcoma (n=4) and renal carcinoma (n=3). Follow-up ranged from 2.4 to 54 months (median 16.7 months) (Table 1). Nineteen patients had one lesion treated, seven patients had two lesions, five patients had three lesions, and three patients had five lesions treated with SBRT.

The 1-, 2-, and 3-year patient LC rates for all comers were 93%, 88%, and 80% respectively (Figure 1) with 1-, 2-, and 3-year OS of 62%, 44%, and 23% respectively. Four patients had lung metastases recur locally within 12 months; only one patient developed a local recurrence beyond 24 months (at 26 months), although only 12 patients were alive with follow-up beyond two years.

Among the 25 patients with maximal lesion size of 1- <2 cm, the 1- and 2-year patient LC rates were 95% and 88%. Among the

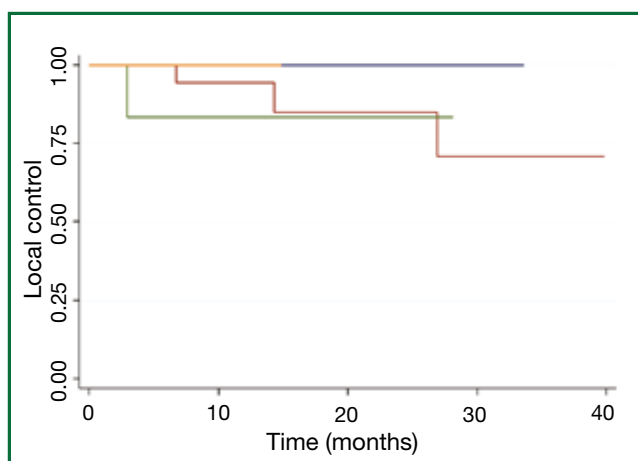


**Figure 2.** Overall local control based on lesion size at one year and at two years.

seven patients with maximal lesion size of 2- <3 cm, the 1- and 2-year patient LC rates were 86% and 86%, and not significantly different than for patients with smaller lesions (Figure 2). Only one patient was treated with a maximal lesion size of >3 cm and only one patient was treated with a maximal lesion size <1 cm (neither of whom experienced a local recurrence. All five patients with local recurrences had colorectal cancer. Gender ( $P=0.30$ ), previous treatment with chemotherapy ( $P=0.95$ ), radiation dose (0.26), and nodule size ( $P=0.97$ ) were not statistically significant on univariate analysis. A multivariate analysis was not done because of the small number of events. Symptomatic pneumonitis (grade  $\geq 2$ ) was not seen in any patient. Post-radiation fibrotic changes and consolidation occurred in 26 of the 34 patients.

## Discussion

Metastatic disease to lung is one of the most common life threatening complications of cancer (2) and has been regarded as an incurable condition (1). However, patients with oligometastatic lung metastases have been considered candidates for curative treatment because of prolonged tumor LC rates and OS. Improved imaging now allows detection of tumor metastases at a smaller size and effective systemic therapy allows for potential 'downstaging' widely metastatic disease to an oligometastatic state, and thus provides an opportunity for local therapy as consolidation for patients with minimal bulk metastases (2). Surgical pulmonary metastatectomy in suitable patients with oligometastases is recognized as a potential curative treatment, and published data reveal a 5-year survival rate in these patients to be 20-40% (14). Alternatively, SBRT has also been used as a curative treatment

of oligometastasis especially in patients who are not eligible candidates for surgery, either because of medical comorbidities, or because central lesions and/or multiple lesions would require a more extensive surgery than the patient could tolerate. The International Registry of Lung Metastases (IRLM) (14) reported the results of pulmonary complete resection in a large number of patients with lung metastases showing a 2-, 5-, and 10-year survival rate of 70%, 36%, and 26% respectively. In one of the largest published series on SBRT comprising of 175 patients (311 lesions), Siva *et al.* (15) has shown encouraging results with an OS rate of 54.5%. The IRLM study (14) also reported that a disease-free interval of more than 36 months and single metastasis were good prognostic factors. In our current study, gender ( $P=0.30$ ), previous treatment with chemotherapy ( $P=0.95$ ), radiation dose (0.11), and nodule size ( $P=0.97$ ) were not statistically significant on univariate analysis. Symptomatic pneumonitis requiring treatment or hospitalization was not seen in any of the patients treated with SBRT.

Several reports have been published regarding the outcomes of SBRT for metastatic lung tumors, but no standard treatment regimens have been defined with respect to the optimal dose and fractionation schedules. From published studies, the dose-fractionation of SBRT varies from 40-60 Gy in 3-10 fractions. Our institution had been using 5 Gy  $\times$  10 from the inception of SBRT at the University of Rochester in 2001, but we recently changed the dose to 8-12 Gy in five fractions (2). Japanese studies have shown the correlation of dose effect with improved LC rates. With regards to the biologic effective dose, assuming an alpha/beta ratio of ten, ( $BED_{10}$ ), Hamamoto *et al.* (16) have reported rather poor LC of 25% at two years using 48 Gy in four fractions ( $105.6 \text{ Gy}_{10}$ ) where as another report by Norihisa *et al.* (12) showed that LC rate of 43 metastatic lung tumors was 90% at two years with 60 Gy in five fractions ( $132 \text{ Gy}_{10}$ ). A recent multi-institutional phase I/II study by Rusthoven *et al.* (17) reported a 2-year LC of 96% by 48-60 Gy in three fractions ( $124-180 \text{ Gy}_{10}$ ) for 63 metastatic lung lesions. Similarly, McCammon *et al.* (18) showed the dose-LC relationship of SBRT for 246 lesions (primary or metastatic) by using a regimen of 54-60 Gy in three fractions ( $151-180 \text{ Gy}_{10}$ ) achieving LC of 89% at three years.

Our earlier institutional report (2) showed a LC of 83% with 5 Gy fractions for total doses of 50 to 60 Gy, whereas a subsequent report showed LC of 87% at two and six years (3). In the current study, SBRT was delivered to a median dose of 50 Gy (range, 40-60 Gy) in five fractions with 1- and 2-year LC rates of 93% and 87% for all patients. Local progression occurred in four patients within 12 months and the other 30 patients had excellent LC and remained locally NED to date except one patient with primary colon cancer who failed locally at 26 months.

Onishi *et al.* (19) concluded that  $BED_{10}$  of >100 Gy at isocenter is preferable for treatment of primary lung cancer to achieve an optimal OS rate. For SBRT for pulmonary metastases, the  $BED_{10}$  of published dose-fractionation schedules ranges from 70-162 Gy, with the 2-year survival ranging from 33% to 84% in various studies (11,12,20,21). Norihisa *et al.* (12) have reported a 2-year survival rate of 84% in their study, whereas Lee *et al.* (11) have reported a 2-year survival rate of 68% from their study. Onimaru *et al.* (20) and Wulf *et al.* (21) reported survival rates of 49% and 33% at two years. The median and OS in present series was 16 months and 62%, 44%, and 23% at one, two, and three years, respectively.

When comparing dose fractionation schemes, it is important to recognize that different institutions prescribe dose differently and use different methodologies to plan and deliver SBRT. The dose can be prescribed to a point (i.e., isocenter), volume (i.e., GTV or PTV), or isodose line. Also, the PTV margins vary from institute to institute depending upon set up accuracy. Furthermore, defining the PTV reflects a difference in CT scanning with regards to free breathing *vs.* breath holding and fast *vs.* slow scan times (12). Also, some utilize 4-D scanning and definition of an ITV. Difference in dose calculation by taking in to account tissue heterogeneity corrections would affect margin dose in lung tumors (12). Lastly, differences in planning approaches (fixed *vs.* arcing beams; 3-D conformal *vs.* IMRT *vs.* VMAT) may also be relevant.

The primary cancer site seems to have a significant effect on outcomes of patients treated with SBRT. Milano *et al.* (22) reported earlier results from our institution using 50 Gy in ten fractions with 2-year LC of all lesions being 77%, concluding that metastatic tumors originating from the pancreas, biliary, liver, or colon were associated with poorer LC. Hamamoto *et al.* (16) also reported LC of 25% at two years and attributed the poor outcome to a large proportion of metastatic tumors from the colon (67%). Similarly Kim *et al.* (23) have also reported a poor outcome with 3-year LC of 52.7% using 39-51 Gy in three fractions. Takeda *et al.* (24) compared outcomes of primary lung tumors with metastases treated by SBRT showing a LC of 94% *vs.* 72% at two years ( $P < 0.05$ ). The present study also showed poor outcome with colorectal cancers, as all of the local failures were seen in this group.

In many studies, tumor size plays a significant role in predicting the LC, as various studies have shown a trend for improved LC with smaller size of the tumor and interval tumor volume (ITV <17 mL, i.e., approximately 3 cm in diameter) (23). A study by McCammon *et al.* (18) showed better LC in smaller tumors with GTV <8.9 mL ( $P = 0.003$ ). Kim *et al.* (25) reported that tumors <2.5 cm were associated with higher LC than tumors >2.5 cm;

100% *vs.* 82.3% in patients with primary or metastases lung tumors. Oh *et al.* (1) also reported that tumors <2.5 cm have better LC 98.3% *vs.* 77.8% ( $P < 0.01$ ). Our current study did not show a statistically significant effect of tumor size on patient LC, albeit with a relatively narrow range of size for most patients and a heterogeneous patient population.

Weaknesses of our study include the small retrospective nature, with a diverse population, in terms of primary site and histology. Because the majority of patients were treated with the same dose (50 Gy in five fractions), and the dose range was not large, we could not adequately analyze a dose-response relationship. Nevertheless, we are able to report promising LC and survival outcomes in this cohort of patients with oligometastatic disease of the lung. Our conclusion is that SBRT for oligometastatic cancer to the lungs is effective and well tolerated for nonsurgical/chemorefractory patients.

## Acknowledgements

The authors thank Ms. Laura Finger for editorial assistance.

**Disclosure:** The authors declare no sources of funding or conflicts of interest.

## References

1. Oh D, Ahn YC, Seo JM, et al. Potentially curative stereotactic body radiation therapy (SBRT) for single or oligometastases to the lung. *Acta Oncol* 2012;51:596-602.
2. Okunieff P, Petersen AL, Philip A, et al. Stereotactic Body Radiation Therapy (SBRT) for lung metastases. *Acta Oncol* 2006;45:808-17.
3. Milano MT, Katz AW, Zhang H, et al. Oligometastases treated with stereotactic body radiotherapy: long-term follow-up of prospective study. *Int J Radiat Oncol Biol Phys* 2012;83:878-86.
4. Salama JK, Hasselle MD, Chmura SJ, et al. Stereotactic body radiotherapy for multisite extracranial oligometastases: final report of a dose escalation trial in patients with 1 to 5 sites of metastatic disease. *Cancer* 2012;118:2962-70.
5. Hellman S, Weichselbaum RR. Oligometastases. *J Clin Oncol* 1995;13:8-10.
6. Singh D, Yi WS, Brasacchio RA, et al. Is there a favorable subset of patients with prostate cancer who develop oligometastases? *Int J Radiat Oncol Biol Phys* 2004;58:3-10.
7. Kavanagh BD, McGarry RC, Timmerman RD. Extracranial radiosurgery (stereotactic body radiation therapy) for oligometastases. *Semin Radiat Oncol* 2006;16:77-84.
8. Yang JC, Abad J, Sherry R. Treatment of oligometastases after successful immunotherapy. *Semin Radiat Oncol* 2006;16:131-5.
9. Nagata Y, Negoro Y, Aoki T, et al. Clinical outcomes of 3D conformal hypofractionated single high-dose radiotherapy for one or two lung tumors

- using a stereotactic body frame. *Int J Radiat Oncol Biol Phys* 2002;52:1041-6.
10. Hof H, Herfarth KK, Munter M, et al. Stereotactic single-dose radiotherapy of stage I non-small-cell lung cancer (NSCLC). *Int J Radiat Oncol Biol Phys* 2003;56:335-41.
  11. Lee SW, Choi EK, Park HJ, et al. Stereotactic body frame based fractionated radiosurgery on consecutive days for primary or metastatic tumors in the lung. *Lung Cancer* 2003;40:309-15.
  12. Norihisa Y, Nagata Y, Takayama K, et al. Stereotactic body radiotherapy for oligometastatic lung tumors. *Int J Radiat Oncol Biol Phys* 2008;72:398-403.
  13. Milano MT, Philip A, Okunieff P. Analysis of patients with oligometastases undergoing two or more curative-intent stereotactic radiotherapy courses. *Int J Radiat Oncol Biol Phys* 2009;73:832-7.
  14. Long-term results of lung metastasectomy: prognostic analyses based on 5206 cases. The International Registry of Lung Metastases. *J Thorac Cardiovasc Surg* 1997;113:37-49.
  15. Siva S, MacManus M, Ball D. Stereotactic radiotherapy for pulmonary oligometastases: a systematic review. *J Thorac Oncol* 2010;5:1091-9.
  16. Hamamoto Y, Kataoka M, Yamashita M, et al. Local control of metastatic lung tumors treated with SBRT of 48 Gy in four fractions: in comparison with primary lung cancer. *Jpn J Clin Oncol* 2010;40:125-9.
  17. Rusthoven KE, Kavanagh BD, Burri SH, et al. Multi-institutional phase I/II trial of stereotactic body radiation therapy for lung metastases. *J Clin Oncol* 2009;27:1579-84.
  18. McCammon R, Schefter TE, Gaspar LE, et al. Observation of a dose-control relationship for lung and liver tumors after stereotactic body radiation therapy. *Int J Radiat Oncol Biol Phys* 2009;73:112-8.
  19. Onishi H, Araki T, Shirato H, et al. Stereotactic hypofractionated high-dose irradiation for stage I nonsmall cell lung carcinoma: clinical outcomes in 245 subjects in a Japanese multiinstitutional study. *Cancer* 2004;101:1623-31.
  20. Onimaru R, Shirato H, Shimizu S, et al. Tolerance of organs at risk in small-volume, hypofractionated, image-guided radiotherapy for primary and metastatic lung cancers. *Int J Radiat Oncol Biol Phys* 2003;56:126-35.
  21. Wulf J, Haedinger U, Oppitz U, et al. Stereotactic radiotherapy for primary lung cancer and pulmonary metastases: a noninvasive treatment approach in medically inoperable patients. *Int J Radiat Oncol Biol Phys* 2004;60:186-96.
  22. Milano MT, Katz AW, Schell MC, et al. Descriptive analysis of oligometastatic lesions treated with curative-intent stereotactic body radiotherapy. *Int J Radiat Oncol Biol Phys* 2008;72:1516-22.
  23. Kim MS, Yoo SY, Cho CK, et al. Stereotactic body radiation therapy using three fractions for isolated lung recurrence from colorectal cancer. *Oncology* 2009;76:212-9.
  24. Takeda A, Kunieda E, Ohashi T, et al. Stereotactic body radiotherapy (SBRT) for oligometastatic lung tumors from colorectal cancer and other primary cancers in comparison with primary lung cancer. *Radiother Oncol* 2011;101:255-9.
  25. Kim H, Ahn YC, Park HC, et al. Results and prognostic factors of hypofractionated stereotactic radiation therapy for primary or metastatic lung cancer. *J Thorac Oncol* 2010;5:526-32.



**Cite this article as:** Singh D, Chen Y, Hare MZ, Usuki KY, Zhang H, Lundquist T, Joyce N, Schell MC, Milano MT. Local control rates with five-fraction stereotactic body radiotherapy for oligometastatic cancer to the lung. *J Thorac Dis* 2014;6(4):369-374. doi: 10.3978/j.issn.2072-1439.2013.12.03

## New techniques for assessing response after hypofractionated radiotherapy for lung cancer

Sarah A. Mattonen<sup>1</sup>, Kitty Huang<sup>2,3</sup>, Aaron D. Ward<sup>1,2</sup>, Suresh Senan<sup>4</sup>, David A. Palma<sup>2,3</sup>

<sup>1</sup>Department of Medical Biophysics, <sup>2</sup>Department of Oncology, The University of Western Ontario, London, ON, Canada; <sup>3</sup>Division of Radiation Oncology, London Regional Cancer Program, London, ON, Canada; <sup>4</sup>Department of Radiation Oncology, VU University Medical Center, Amsterdam, Netherlands

### ABSTRACT

Hypofractionated radiotherapy (HFRT) is an effective and increasingly-used treatment for early stage non-small cell lung cancer (NSCLC). Stereotactic ablative radiotherapy (SABR) is a form of HFRT and delivers biologically effective doses (BEDs) in excess of 100 Gy<sub>10</sub> in 3-8 fractions. Excellent long-term outcomes have been reported; however, response assessment following SABR is complicated as radiation induced lung injury can appear similar to a recurring tumor on CT. Current approaches to scoring treatment responses include Response Evaluation Criteria in Solid Tumors (RECIST) and positron emission tomography (PET), both of which appear to have a limited role in detecting recurrences following SABR. Novel approaches to assess response are required, but new techniques should be easily standardized across centers, cost effective, with sensitivity and specificity that improves on current CT and PET approaches. This review examines potential novel approaches, focusing on the emerging field of quantitative image feature analysis, to distinguish recurrence from fibrosis after SABR.

### KEYWORDS

Lung cancer; stereotactic radiotherapy; hypofractionated radiotherapy (HFRT); image feature analysis; positron emission tomography (PET)

*J Thorac Dis 2014;6(4):375-386. doi: 10.3978/j.issn.2072-1439.2013.11.09*

### Hypofractionated radiotherapy (HFRT) for early-stage lung cancer

HFRT is an effective and well-tolerated treatment for early stage non-small cell lung cancer (NSCLC) (1,2). Although several HFRT schemes have been used historically in the treatment of T1N0 or T2N0 NSCLC, ranging from mildly hypofractionated regimens [e.g., 55 Gy in 20 fractions (3)], to more potent stereotactic regimens (e.g., 54 Gy in 3 fractions), evidence suggests that a biologically effective dose (BED) in excess of 100 Gy<sub>10</sub> is required for optimal local control (4). Such stereotactic regimens, referred to as stereotactic ablative

radiotherapy (SABR) or stereotactic body radiotherapy (SBRT), have been rapidly adopted into clinical use in the last decade (5). SABR is a guideline-recommended treatment for T1/T2 N0 NSCLC when surgery, the gold standard treatment, is not an option due to patient comorbidities or refusal (6-8). SABR is arguably one of the largest medical breakthroughs in the curative treatment of early stage NSCLC in the last two decades, with improved population-based survival rates demonstrated after the implementation of SABR (9-11).

Excellent long-term outcomes support this increasing popularity of SABR as a treatment option for lung cancer. SABR outcomes appear not only superior to more fractionated HFRT regimens (12), but are comparable to standard surgical resection, as supported by retrospective, single- or multi-institution, and modeling studies, with the largest single-institution retrospective study reporting a 5-year local control rate of 89.5% (13-15). Although three randomized studies comparing surgery to SABR have failed to accrue, propensity score matched analyses are available, and have shown comparable, if not superior outcomes post-SABR (16,17). In high-risk patients with severe pulmonary

Correspondence to: Dr. David A. Palma. London Regional Cancer Program, 790 Commissioners Rd E, London, Ontario, Canada. Email: david.palma@lhsc.on.ca.

Submitted Aug 23, 2013. Accepted for publication Nov 07, 2013.  
Available at [www.jthoracdis.com](http://www.jthoracdis.com)

ISSN: 2072-1439

© Pioneer Bioscience Publishing Company. All rights reserved.

comorbidities, SABR offers comparable rates of local control without the attendant short-term mortality risks of surgery (18). In the operable patient population, promising outcomes are reported by two prospective clinical trials: RTOG 0618, reporting a primary tumor failure rate of 7.7% (19), and JCOG 0403, reporting a preliminary 3-year tumor control rate of 86% (20). For institutions without the capability to deliver SABR, other HFRT regimens can also achieve reasonable local control at early time-points: a recent Canadian multicenter study of HFRT delivering 60 Gy in 15 fractions (BED of 75 Gy<sub>10</sub>) achieved a two-year local control rate of 88% (21).

### Response assessment: lung injury after SABR

Response assessment following SABR is complicated by the frequent presence of benign lung injury on follow-up CT. Ablative doses of radiation delivered to the tumor and surrounding lung parenchyma nearly always result in radiologic lung injury (pneumonitis and fibrosis), appearing as an increased density and opacity on CT in the area of the high-dose region, and occasionally a corresponding increase in metabolic activity on functional imaging in the months following SABR (22,23). Such CT changes correlate closely with local delivered dose (24). Such findings are not unique to lung SABR; they have also been described in other organs treated with stereotactic radiotherapy including brain and liver (25,26). From histopathological studies obtained after resection for false-positive imaging studies, these areas of lung injury are made up of a benign mixture of inflammatory cells, fibrocytes and other benign features (27). The appearance of fibrosis is very common, occurring in 62% of patients within six months of treatment (acute) and 91% thereafter (late), as classified by a common classification scheme (22,23). This scheme classifies acute radiation pneumonitis into consolidative or ground-glass opacity changes, which can further be subdivided into diffuse (>5 cm) or patchy (≤5 cm). Late radiation fibrosis can be categorized into modified conventional, mass-like, or scar-like patterns. Although this classification scheme is used to categorize radiological changes following SABR, it is not used to distinguish recurrence from fibrosis. Morphologic patterns of fibrosis can also vary with treatment type; patients that underwent arc-based SABR had a predicted probability of a modified conventional pattern of 96.3% versus 68.9% for those who underwent fixed-beam treatment (28). Although such radiologic lung injury occurs in nearly all patients by two years (22), only a small minority of patients develop clinical symptoms.

Against this background of asymptomatic radiation-induced lung injury, accurate assessment of local recurrence is

of paramount importance. Misclassification of a recurrence as “benign fibrosis” can result in a missed window of opportunity for curative-intent salvage treatment. Conversely, misclassification of fibrosis as a recurrence may lead to unnecessary interventions, such as biopsy, imaging, chemotherapy, and even surgery, exposing patients to unnecessary risks and morbidity (27,29-32). The ability to accurately assess response is particularly important in light of the changing practice patterns for early stage NSCLC. As a growing number of patients are being treated by SABR (5), this clinical scenario will become more common. The treatment of a fitter patient population may result in a larger proportion of patients who are candidates for salvage treatment in the case of recurrence. Finally, since recent data on potentially operable SABR patients suggest that failure may be higher than in the inoperable SABR cohort [with two-year lobar failure rates in one recent multicenter study (defined as recurrence anywhere in the irradiated lobe) as high as 19.2% (19)], accurate distinction between recurrence and fibrosis to permit early salvage is a pressing clinical problem.

Distinguishing a recurrent tumor from fibrotic lung changes on CT can be challenging for several reasons (Figure 1). Both radiation-induced lung injury and recurrent disease follow a similar temporal course, with lung fibrosis continuing to evolve two years after treatment, during which time, the majority of local recurrences occur (22,33). In contrast to lung injury following traditional 3D-CRT, which was often characterized by straight edges that conform to treatment portals (34) (Figure 2), the pattern of lung injury on CT following SABR can be mass-like, due to the conformal nature of SABR (22,31,35). Fibrosis may even appear on CT as an enlarging density and therefore can mimic the growth of a local recurrence (31).

### Current clinical approach for assessing response

Current recommendations for imaging follow-up after SABR are generally based on retrospective evidence and expert opinion, rather than randomized data. Such follow-up serves three major goals: detection of local recurrence, detection of regional recurrence that may be amenable to salvage, and detection of new primary lung tumors, which occur at a rate of 2-10% per person-year (33,36). Based on the results of the National Lung Screening Trial (37), the American Association for Thoracic Surgery guidelines recommends four years of CT follow-up for patients who have undergone treatment for lung cancer and are eligible for additional treatment (38).

Tumor response assessment following definitive treatment is typically categorized according to Response Evaluation Criteria in Solid Tumors (RECIST) 1.1 criteria (39) as complete

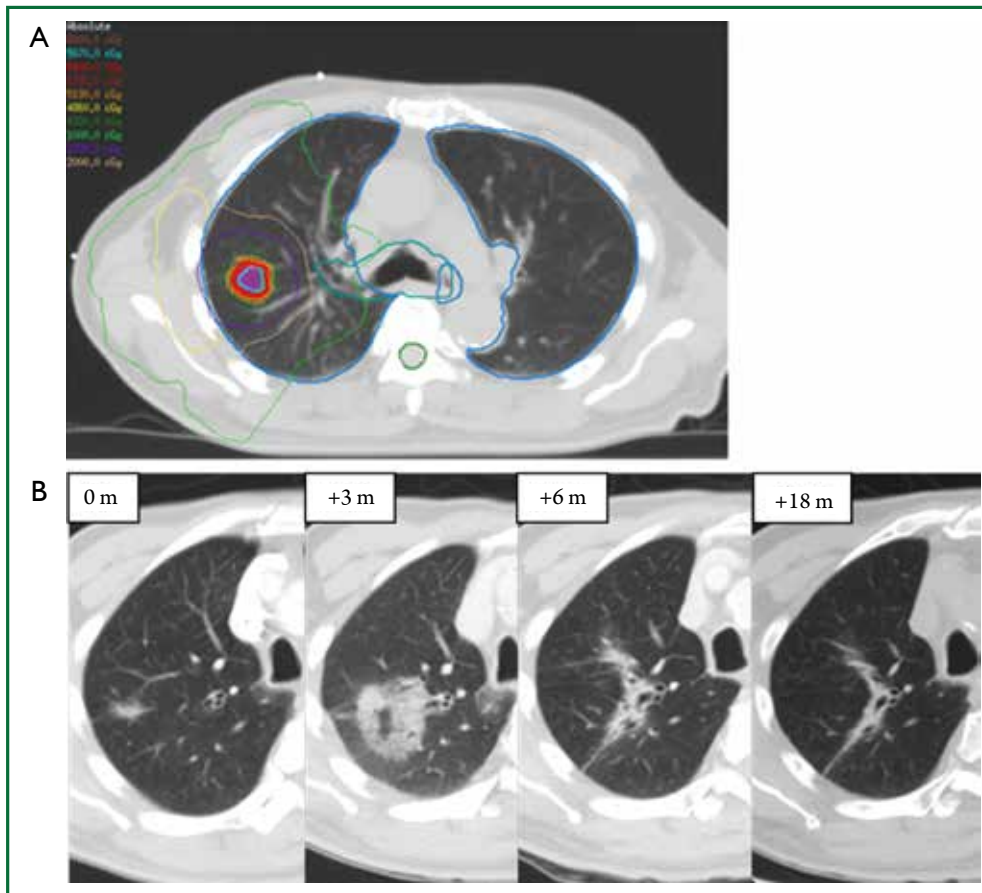


**Figure 1.** Radiological changes following SABR for an 85-year-old gentleman with biopsy proven adenocarcinoma. This patient received 54 Gy in 3 fractions with the treatment plan shown in (A). Radiological changes are seen (B) where 0 m indicates the pre-treatment lesion measuring 2.0 cm. At 3 months post-SABR, further enlargement of a ground-glass semi-solid opacity measuring 4.3 cm and at 6 months there is interval reduction in size and a decrease in ground-glass opacity, with ongoing reduction in size by 18 months.

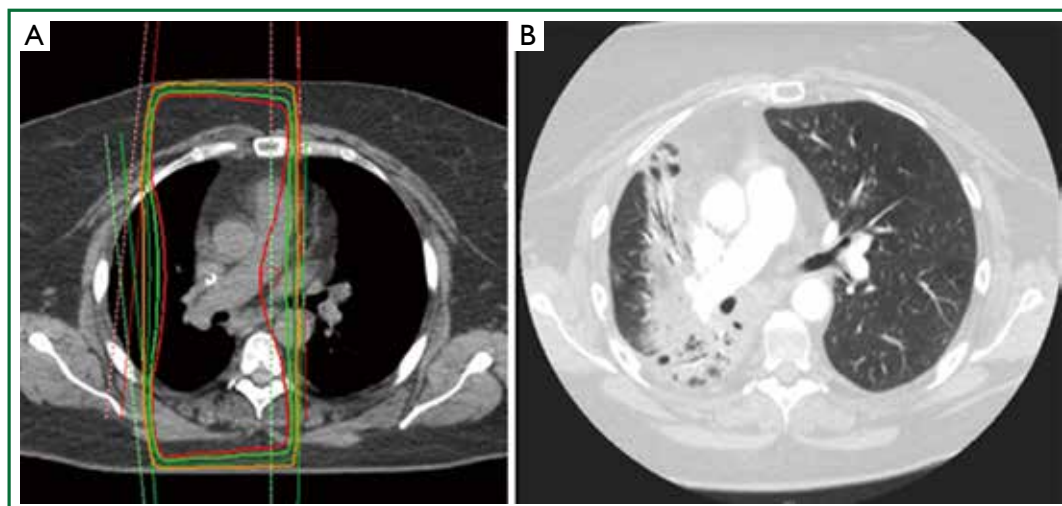


**Figure 2.** Radiation induced lung injury following a traditional anterior/posterior parallel opposed pair (treatment plan shown in Box A); (B) The resulting benign injury conforms to the treatment portals and is easily distinguished by a straight line.

**Table 1.** Selected studies using FDG-PET for detecting recurrence following SABR.

| Study                  | Number of patients | Number of recurrences [proportion pathology proven %] | SUV <sub>max</sub> cutoff | Sensitivity (%) | Specificity (%) | Definition of local recurrence if not biopsied   |
|------------------------|--------------------|---|---------------------------|-----------------|-----------------|--|
| Essler, et al. (50)    | 29                 | 6 [NR]  | 5.48                      | NR              | NR              | Increase in tumor volume of more than 25% on CT, accompanied by metabolic activity in FDG-PET                        |
| Bollineni, et al. (49) | 132                | 6 [50]  | 5.0                       | NR              | NR              | Based on growth by more than 20% of the tumor diameter compared with the pretreatment                                |
| Zhang, et al. (47)     | 128                | 9 [78]  | 5.0                       | 100             | 91              | PET/CT   |
| Takeda et al. (48)     | 154                | 17 [18]   | 3.2 (early)<br>4.2 (late) | 100             | 96-98           | Increase in the cross-sectional tumor size of >25% on successive CT scans at least three times over a 6-month period |

NR, not reported.

**Table 2.** High-risk features for recurrence on CT. Data from reference (51).

| High-risk feature                                   | Sensitivity (%) | Specificity (%) |
|---|-----------------|-----------------|
| Enlarging opacity                                   | 92              | 67              |
| Sequential enlargement                              | 67              | 100             |
| Enlargement after 12 months                         | 100             | 83              |
| Bulging margin                                      | 83              | 83              |
| Linear margin disappearance                         | 42              | 100             |
| Loss air bronchogram                                | 67              | 96              |
| Cranio-caudal growth of $\geq 5$ mm and $\geq 20\%$ | 92              | 83              |

(disappearance of the target), partial ( $\geq 30\%$  decrease), stable disease, or progression ( $\geq 20\%$  increase) according to the diameter of the target tumor. However, RECIST 1.1 has limited use in the post-SABR lung setting, since the target lesion may actually represent lung fibrosis, and response may be mis-categorised (11,40). Re-evaluation of RECIST 1.1 has been proposed (41).

Although FDG-PET scans are recommended in lung cancer diagnosis and re-staging (42), functional imaging currently has a limited role in the evaluation of tumor response and detection of local recurrence. Lung injury following ablative radiation doses can commonly result in a metabolically active FDG-avid lesion, which may rise transiently immediately post-SABR and persist after 12 months (43-45). False-positive PET SUV<sub>max</sub> readings as high as 7.0 have been reported (27,46). Most evidence supports a SUV<sub>max</sub> of approximately 5.0 as a clinically useful threshold for the distinction between recurrence and fibrosis (47-50). Table 1 summarizes selected studies using FDG-PET to assess treatment response post-SABR.

Following SABR, recommended surveillance for patients eligible for salvage treatment is routine CT imaging, often at 3-6-month intervals in the first year, then annually thereafter (8,38). A systematic review of the literature on the role of imaging in discriminating recurrence from fibrosis provides structured recommendations based on the available evidence, citing high-risk features (HRFs, Table 2) on CT (31,35,52) and specific SUV<sub>max</sub> thresholds to estimate the probability of recurrence and appropriate investigations into “no-risk” “low-risk” and “high-risk” categories (23). The clinical performance of the HRFs was validated by a blinded assessment of matched CT datasets from pathology-proven recurrences and non-recurrences (51). The concurrent presence of  $\geq 3$  HRFs provides a useful cutoff (sensitivity and specificity both  $>90\%$ ) for detection of recurrence.

There are several advantages to the use of CT, rather than routine functional imaging, in assessment of response post-SABR. In contrast to FDG-PET imaging, CT is more accessible and inexpensive, does not rely on isotopes with short half-lives, and

is already part of standard-of-care follow-up for patients who have received curative treatment for early-stage lung cancer, and who are eligible for salvage. Importantly, standardization of CT across centres is much less complex than standardization of PET/CT. Lack of PET/CT standardization can be an important confounder: measured SUVs can be affected by multiple factors, including technical, physical, and biologic (53). In order to generalize PET/CT findings, minimum performance or harmonizing standards are needed for many factors including uptake period, patient motion, inflammation, blood glucose level correction, as well as scan acquisition and reconstruction parameters. Standard machine settings and reconstruction algorithms are widely available for CT imaging of the chest, increasing the generalizability of any follow-up recommendations. As such, new algorithms for early detection of recurrence based on standard-of-care CT imaging could be easily integrated into current clinical practice. However, novel imaging techniques must move beyond qualitative image analysis and simple RECIST measurements.

### Quantitative image feature analysis

In contrast to qualitative image assessment described above, quantitative image feature analysis extracts measurable information from within an image, such as intensities or densities, shape or morphology, or texture. Intensity refers the brightness of an individual voxel; in CT imaging this can also be described as density and is quantified in Hounsfield Units (HUs). HUs measure the attenuation of a material relative to water (HU =0). The shape or morphology of a region describes the geometry of the external boundary. "CT image texture" is a set of more complex measurements which describe local brightness variation or the spatial arrangement of intensities in an image (54,55).

Image feature analysis has emerging roles in general medicine and oncology. Numerous imaging modalities can be used for quantitative image analysis at different body sites, including CT, magnetic resonance imaging (MRI), ultrasound, and mammography (56,57). Applications in oncology include the computer-aided detection or diagnosis of diseases such as breast and bladder cancer (56,57). Texture analysis of the liver has suggested that texture parameters may distinguish high-risk from low-risk colorectal cancer patients (58). Texture analysis on MRI, CT, and PET has been able to diagnose and characterize tumor heterogeneity for several tumor types and is showing promise in response assessment and as a predictive biomarker (59,60). In the thorax, the use of quantitative image feature analysis on CT has been widely investigated in many benign diseases, including characterizing pulmonary infections as well

as varying benign lung disease patterns (61-63). Texture analysis, specifically the product of tumor uniformity and gray-level, has also been correlated with tumor response following chemotherapy in advanced stage NSCLC (64).

### Quantitative image analysis workflow

Figure 3 demonstrates the typical workflow for quantitative image feature analysis. In general, image acquisition should be standardized to minimize any variability between scanners, imaging parameters, or reconstruction techniques. Standardization includes the use of the same scan protocol for imaging acquisition, with consistencies in settings such as kV, mAs, slice collimation, and slice thickness. Breathing instructions and the use of intravenous contrast should also be consistent across all patients, although patients with contra-indications to contrast injection must be noted and studies analyzing the effect of contrast on image feature analysis should be performed. Reconstruction kernels or filters are used to determine image quality of a CT scan and are chosen based on the intended clinical application of the scan. Such decisions are a compromise between spatial resolution and noise, and depending on the organ being scanned, may require a smoother image with less noise or a sharper image with higher noise. Reconstruction kernels should also be consistent across all images and a higher sharpness thorax kernel should be used when available. However, optimal scan parameters and reconstruction kernels must be investigated for the effect of variations among these settings on quantitative image feature analysis.

Image feature analysis can be performed on any region of interest (ROI), such as tumor, normal lung, or fibrotic regions; such ROIs can be selected by means of manual, semi-automated, or fully-automated methods. A manual method involves delineation of an ROI by an investigator on each individual slice using imaging software. Manual methods do not require specialized algorithms, but can be tedious and time consuming, and are subject to intra- and inter-observer variability (65). A semi-automated method requires a smaller amount of user input, and may require a user to initialize the segmentation by selecting a point or ROI. A fully automated approach requires no user interaction or input and the image is automatically segmented based on a series of predetermined parameters. This makes a fully automated approach quick and reproducible; however the lack of user input or knowledge can be an issue in terms of reliability. Therefore, semi-automated approaches to segmentation have become increasingly popular as they are reproducible, fast, and require minimal user input or knowledge (66).

After ROIs are delineated, quantitative measures can then

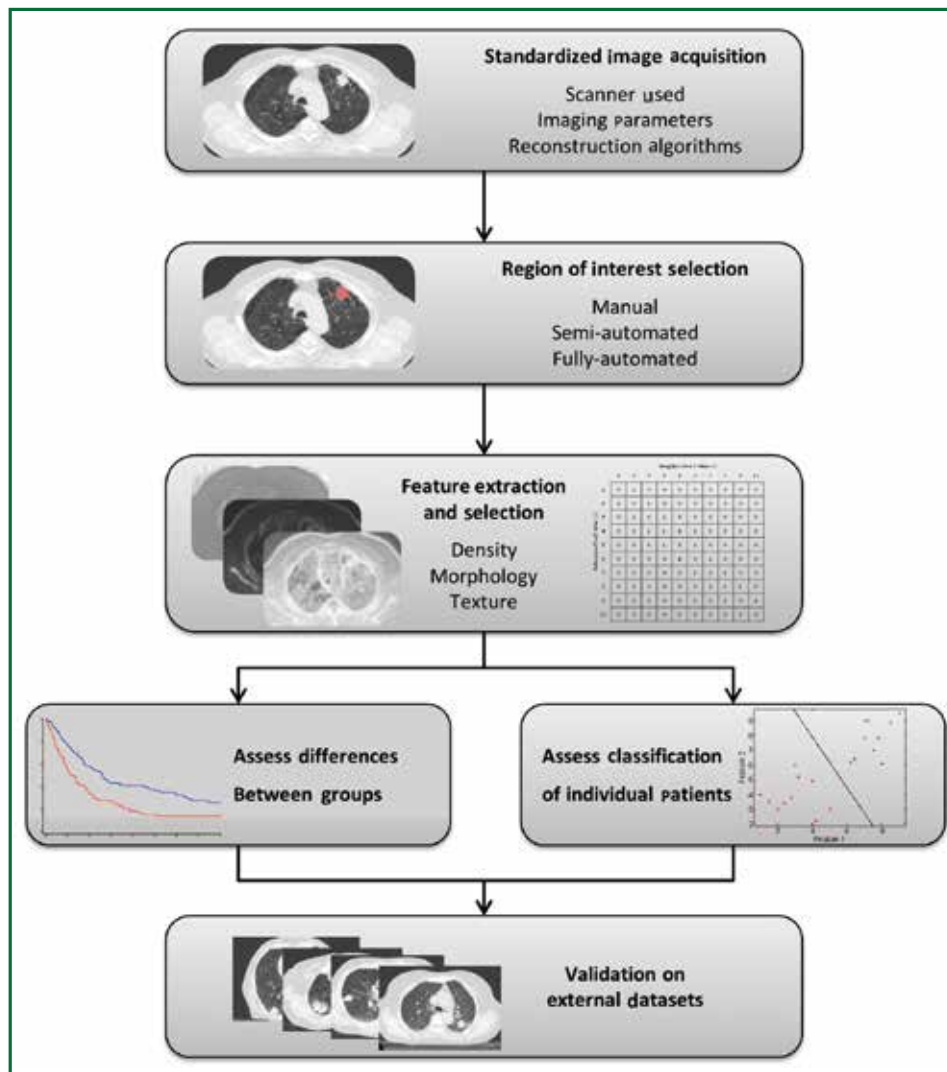


**Figure 3.** Typical workflow for image feature analysis.

be extracted including measures such as density, morphology, or texture, and these measures can be evaluated as predictive or prognostic biomarkers. Extracted measures can be calculated with a variety of input parameters and settings specific to each case. Such measures range from simple first-order assessments such as the mean HU density within a region, to complex measures of the spatial relationship of voxel intensities, for example analyzing neighboring voxels of varying distances apart.

Optimal features or sets of features for predictive or prognostic biomarkers must be determined and validated through training and testing on multiple data sets. This can include analyzing individual features alone or a combination of these features together. Due to the large number of metrics available as well as the large number of possible combinations of these metrics, the

high-risk of type I error must be recognized when comparisons and cross-validations are performed. As a result, initial exploratory studies must be considered hypothesis-generating, and validation on external datasets is crucial.

#### **Common metrics used for image feature analysis**

Image feature analysis metrics can be defined as first-order, second-order, and third-order. First-order image appearance features measure the global appearance of a ROI and do not take into consideration relationships between adjacent voxels. A common example includes the mean density based on CT HU. The standard deviation of density can be used as a first-order texture feature, which shows the global variability of densities

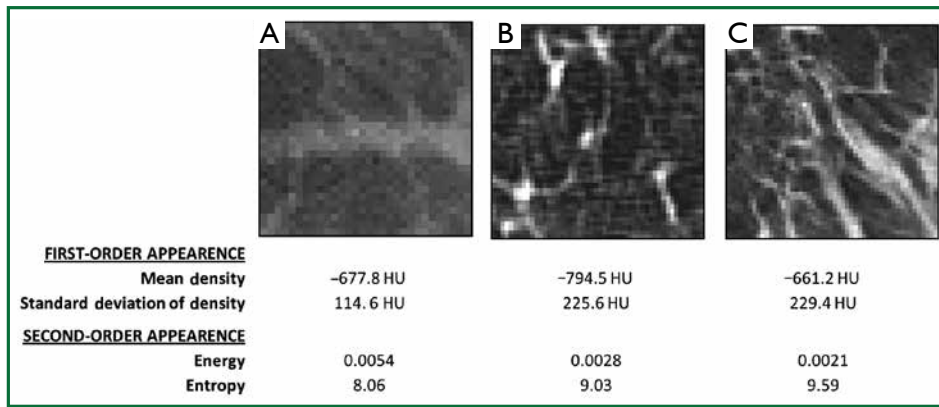


**Figure 4.** Sample lung images showing the variations in two first-order appearance measures [mean density and standard deviation of density (first-order texture analysis)] and two second-order appearance measures, energy and entropy. (A) and (C) have similar mean densities, but are better differentiated by the first- and second-order texture measures. (B) and (C) have similar first-order texture values, but are better differentiated by the second-order measures.

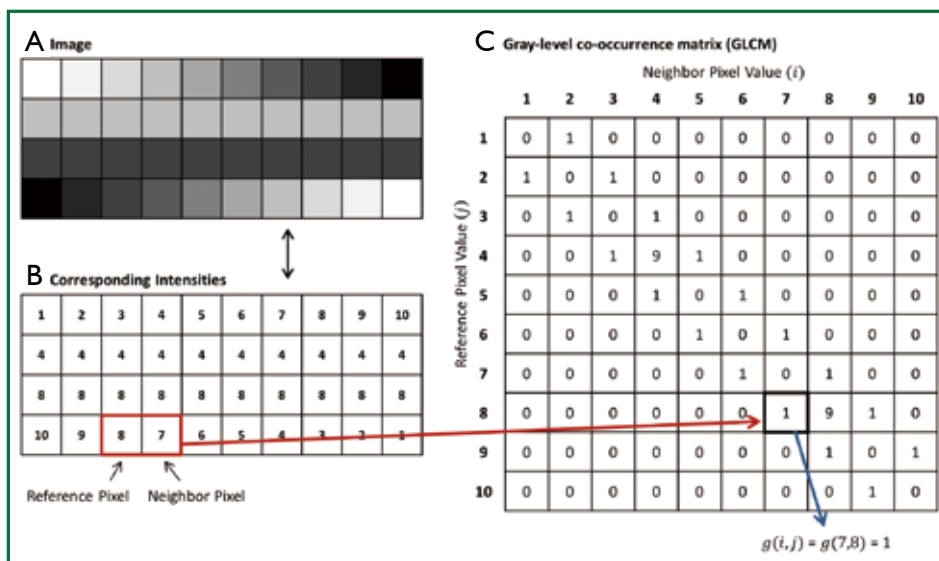


**Figure 5.** A sample image (A) with its corresponding numerical intensity values (B). The gray-level co-occurrence matrix (GLCM) for this image can be seen in (C), with the pixel relationship for analysis being one voxel to the right, as indicated by the reference and neighbor pixel.

within a region (Figure 4). Second-order appearance measures characterize the intensity relationships between voxels pairs in an image, whereas third-order measures (which are less commonly used) consider the spatial relationship of three or more voxels in an image. Extraction of second and third-order texture features can be performed in many ways, including statistical methods, structural methods, model-based methods, and transform-based methods (67).

Statistical texture analysis is the most frequently cited method of texture analysis. This approach describes texture through high-order statistics of an image intensity histogram (67).

This analysis typically assesses neighboring voxel pairs; however it can be done with multiple spatial directions and distances. Second-order statistical texture features are typically computed with the use of a grey-level co-occurrence matrix (GLCM). As shown in Figure 5, A GLCM is a square two-dimensional matrix  $g$ , in which the row and columns correspond to image intensity values. Each element in the matrix  $g(i,j)$  contains a non-negative integer corresponding to the number of voxel pairs whose intensity values are  $i$  and  $j$ . A variety of texture measures can be calculated from the GLCM, such as energy, entropy, inverse difference moment



**Figure 6.** Post-SABR consolidative and ground-glass opacity findings throughout follow-up for a patient with radiation-induced lung injury (A) and recurrence (B). The zero-month (0 m) time point indicates the pre-treatment lesion. The solid lines enclose consolidative regions and the dashed lines enclose ground-glass opacity regions.

(IDM), inertia, cluster shade, and cluster prominence (68-70). In general, energy and entropy measure the orderliness of the GLCM, or the homogeneity of the image. IDM and inertia measure the contrast of the image, and cluster shade and cluster prominence measure the symmetry of an image.

An example of images with their corresponding first-order and second-order appearance measures is seen in Figure 4. The variation in the number and distribution of vessels in the image results in differences in feature measurements. For example, Figure 4A and C have similar mean densities but are better differentiated by the texture measures, both first-order and second-order. Figure 4B and C have similar first-order texture feature measurements but are differentiated by the second-order measures of energy and entropy. Each measure can extract specific information from the image, and overall first-order measures are less sensitive to spatial variations in intensities whereas second-order appearance measures are taking neighboring voxels into account and are therefore sensitive to the relationship of voxels.

### Image feature analysis post-SABR

Several studies have examined simple dose-response relationships of HU changes following SABR. Increasing densities on CT post-SABR are seen with larger planning target volumes and longer time post-SABR, and these are most evident in regions receiving doses greater than 20 Gy (24). Density changes post-SABR have also been shown to linearly increase to doses of 35-40 Gy and then plateau thereafter (24,71). The spatial location of fibrosis following SABR is on average 2.6 cm from the gross tumor volume (GTV) position, although displacement of the fibrotic changes of >5 cm can also be observed (72).

Quantitative image analysis has been investigated for distinguishing RILI and recurrence following SABR (Figure 6). A preliminary study of 13 RILI lesions and 11 recurrent lesions (8 biopsy proven) suggested that first-order appearance measures could significantly distinguish RILI and recurrence patient groups at 9 months following treatment, with recurrence patients having significantly brighter consolidative changes (73).

The standard deviation of densities within regions of GGO (first-order texture analysis) could also distinguish the groups at nine months, with recurrence patients having a larger standard deviation (variability) of densities. This indicates that these patients have a more variegated texture within the GGO, as seen in Figure 4. In contrast, size measures (RECIST or 3D volume) could not differentiate the groups until 15 months post-treatment. A preliminary study of predictive abilities of these measures has shown that the first-order texture analysis within the GGO was the best predictor of recurrence at nine months post-SABR with accuracies of 74% (74).

Further investigation has evaluated texture changes in the immediate post-SABR period. At 2-5 months post-SABR, preliminary analysis suggests that the basic measure of ground-glass texture alone can predict recurrence with 81% accuracy (75). Several second-order texture features have also shown promise, including energy and entropy, with leave-one-out cross validation accuracies of 81% and AUCs of 0.79-0.81 (75). Patients with recurrence had significantly higher entropy and lower energy values. In contrast, traditional measures of response such as RECIST performed inferiorly, with accuracy of 61% and an AUC of 0.72. These results suggest that early quantitative appearance changes may precede any changes in size, and as such may serve as early biomarkers of recurrence in individual patients. Quantitative image analysis allows for maximal information to be obtained from images already being performed in clinical practice, and can easily be translated into a useful clinical tool to aid in treatment response assessment. Further quantitative metrics, including additional second-order textural features and shape analysis, should be investigated and validated for early prediction of recurrence following SABR.

### Future directions and potential pitfalls

Novel imaging modalities may allow for better assessment of treatment responses following SABR or HFRT. In addition to standard FDG-PET reporting  $SUV_{max}$  values, functional imaging with additional metrics such as metabolic tumor burden markers may show improvement for assessing response. Preliminary studies have investigated using pre-treatment measures such as metabolic tumor volume and total lesion glycolysis for assessing clinical outcomes after SABR, however further studies with larger samples and follow-up periods are needed (76). Additional PET tracers such as 18-fluoroazomycin-araboside (FAZA) and 18F-fluoromisonidazole (F-MISO) are used for imaging hypoxia in head and neck cancers (77,78) and could also be investigated for assessing response following HFRT.

Perfusion imaging, such as dynamic-contrast-enhanced-CT

(DCE-CT) or MRI (DCE-MRI) characterizes vascular properties of a tissue and can quantitatively map their spatial distributions. Measures such as blood volume, blood flow, permeability, and mean transit time can be calculated after administration of a contrast agent. Both DCE-CT and DCE-MRI have shown promise as prognostic or predictive biomarkers in oncology, and their value in assessing response after SABR warrants investigation (79,80).

Several potential pitfalls must be considered when evaluating novel imaging modalities for response assessment. First, the gold-standard definition of "recurrence" varies across studies, and many studies use imaging-based definitions of recurrence, rather than pathologic confirmation. Such imaging-based definitions of the endpoint may introduce substantial bias and create a self-fulfilling prophecy: if imaging features are used to define "recurrence" (e.g., sequential growth of lesion) and then the same features are assessed to predict these "recurrences", their performance may be artificially inflated. The majority of studies include only a small number of biopsy-proven recurrences, with remainder of patients defined as recurrence based on an increase in tumor size on successive CT scans (48,49,81). Many also use a modified progression criterion of two consecutive enlargements on CT to define recurrence, which hampers response assessment at an early time point, and suggesting that and that the usefulness of PET is limited. Since recurrences are uncommon after SABR, large databases are required to have sufficient events for analysis, and any new promising markers require robust external validation, since the chances of type I error are high when multiple features are being assessed. Variations in standardization of imaging protocols in both CT and PET studies must be assessed for their impact on predictive ability. Finally, post-SABR surgical studies, including registration of digitized histology to CT, would be valuable for correlating imaging findings at the voxel level with true pathologic outcome.

### Conclusions

Distinguishing recurrence from fibrosis following SABR for early-stage lung cancer is expected to become an increasingly common clinical problem. Although recommendations exist for CT- and PET/CT-based follow-up after SABR, better metrics are required for early detection of recurrence, to allow for salvage, and to avoid unnecessary investigations in patients with benign radiation-induced lung injury. Promising new techniques may involve more robust analysis of currently-obtained imaging, such as CT texture analysis, or introduction of novel imaging modalities into routine clinical practice. Large imaging datasets are required for assessment and subsequent independent

validation of novel new imaging biomarkers.

### Acknowledgements

This project is supported by a research grant from the National Sciences and Engineering Research Council. Dr. Palma is a recipient of research funding from the Ontario Institute for Cancer Research. Dr. Ward acknowledges the support of the Cancer Care Ontario Research Chairs program. The VU university medical center has a research agreement with Varian Medical Systems, Inc.

*Disclosure:* The authors DP, SM, SS and AW hold a provisional patent regarding advanced CT image analysis for assessment of response after lung cancer radiotherapy. The authors declare no additional conflict of interest.

### References

- Soliman H, Cheung P, Yeung L, et al. Accelerated hypofractionated radiotherapy for early-stage non-small-cell lung cancer: long-term results. *Int J Radiat Oncol Biol Phys* 2011;79:459-65.
- Bogart JA, Hodgson L, Seagren SL, et al. Phase I study of accelerated conformal radiotherapy for stage I non-small-cell lung cancer in patients with pulmonary dysfunction: CALGB 39904. *J Clin Oncol* 2010;28:202-6.
- Smith SL, Palma D, Parhar T, et al. Inoperable early stage non-small cell lung cancer: comorbidity, patterns of care and survival. *Lung Cancer* 2011;72:39-44.
- Onishi H, Shirato H, Nagata Y, et al. Hypofractionated stereotactic radiotherapy (HypoFXSRT) for stage I non-small cell lung cancer: updated results of 257 patients in a Japanese multi-institutional study. *J Thorac Oncol* 2007;2:S94-100.
- Pan H, Simpson DR, Mell LK, et al. A survey of stereotactic body radiotherapy use in the United States. *Cancer* 2011;117:4566-72.
- Palma DA, Senan S. Early-stage non-small cell lung cancer in elderly patients: should stereotactic radiation therapy be the standard of care? *Int J Radiat Oncol Biol Phys* 2012;84:1058-9.
- Palma D, Senan S. Stereotactic radiation therapy: changing treatment paradigms for stage I nonsmall cell lung cancer. *Curr Opin Oncol* 2011;23:133-9.
- Vansteenkiste J, De Ruysscher D, Eberhardt WE, et al. Early and locally advanced non-small-cell lung cancer (NSCLC): ESMO Clinical Practice Guidelines for diagnosis, treatment and follow-up. *Ann Oncol* 2013;24 Suppl 6:vi89-98.
- Palma D, Visser O, Lagerwaard FJ, et al. Impact of introducing stereotactic lung radiotherapy for elderly patients with stage I non-small-cell lung cancer: a population-based time-trend analysis. *J Clin Oncol* 2010;28:5153-9.
- Haasbeek CJ, Palma D, Visser O, et al. Early-stage lung cancer in elderly patients: a population-based study of changes in treatment patterns and survival in the Netherlands. *Ann Oncol* 2012;23:2743-7.
- Senan S, Palma DA, Lagerwaard FJ. Stereotactic ablative radiotherapy for stage I NSCLC: Recent advances and controversies. *J Thorac Dis* 2011;3:189-96.
- Shirvani SM, Jiang J, Chang JY, et al. Comparative effectiveness of 5 treatment strategies for early-stage non-small cell lung cancer in the elderly. *Int J Radiat Oncol Biol Phys* 2012;84:1060-70.
- Nguyen NP, Garland L, Welsh J, et al. Can stereotactic fractionated radiation therapy become the standard of care for early stage non-small cell lung carcinoma. *Cancer Treat Rev* 2008;34:719-27.
- Timmerman R, Paulus R, Galvin J, et al. Stereotactic body radiation therapy for inoperable early stage lung cancer. *JAMA* 2010;303:1070-6.
- Louie AV, Rodrigues G, Hannouf M, et al. Stereotactic body radiotherapy versus surgery for medically operable Stage I non-small-cell lung cancer: a Markov model-based decision analysis. *Int J Radiat Oncol Biol Phys* 2011;81:964-73.
- Varlotto J, Fakiris A, Flickinger J, et al. Matched-pair and propensity score comparisons of outcomes of patients with clinical stage I non-small cell lung cancer treated with resection or stereotactic radiosurgery. *Cancer* 2013;119:2683-91.
- Verstegen NE, Oosterhuis JW, Palma DA, et al. Stage I-II non-small-cell lung cancer treated using either stereotactic ablative radiotherapy (SABR) or lobectomy by video-assisted thoracoscopic surgery (VATS): outcomes of a propensity score-matched analysis. *Ann Oncol* 2013;24:1543-8.
- Palma D, Lagerwaard F, Rodrigues G, et al. Curative treatment of Stage I non-small-cell lung cancer in patients with severe COPD: stereotactic radiotherapy outcomes and systematic review. *Int J Radiat Oncol Biol Phys* 2012;82:1149-56.
- Timmerman RD, Paulus R, Pass HI, et al. RTOG 0618: Stereotactic body radiation therapy (SBRT) to treat operable early-stage lung cancer patients (Abstract 7523). American Society of Clinical Oncology 2013 meeting.
- Nagata Y, Hiraoka M, Shibata T, et al. A Phase II Trial of Stereotactic Body Radiation Therapy for Operable T1N0M0 Non-small Cell Lung Cancer. Japan Clinical Oncology Group (JCOG0403). *Int J Radiat Oncol Biol Phys* 2010;78:S27.
- Cheung P, Faria S, Ahmed S, et al. A phase II study of accelerated hypofractionated 3-dimensional conformal radiotherapy for inoperable T1-3 N0 M0 non-small cell lung cancer: NCIC CTG BR.25. *Canadian Assoc Rad Oncol* 2012:abstr 171.
- Dahele M, Palma D, Lagerwaard F, et al. Radiological changes after stereotactic radiotherapy for stage I lung cancer. *J Thorac Oncol* 2011;6:1221-8.
- Huang K, Dahele M, Senan S, et al. Radiographic changes after lung stereotactic ablative radiotherapy (SABR)--can we distinguish recurrence from fibrosis? A systematic review of the literature. *Radiother Oncol* 2012;102:335-42.
- Palma DA, van Sörnsen de Koste J, Verbakel WF, et al. Lung density changes after stereotactic radiotherapy: a quantitative analysis in 50 patients. *Int J Radiat Oncol Biol Phys* 2011;81:974-8.

25. Kickingereder P, Dorn F, Blau T, et al. Differentiation of local tumor recurrence from radiation-induced changes after stereotactic radiosurgery for treatment of brain metastasis: case report and review of the literature. *Radiat Oncol* 2013;8:52.
26. Pan CC, Kavanagh BD, Dawson LA, et al. Radiation-associated liver injury. *Int J Radiat Oncol Biol Phys* 2010;76:S94-100.
27. Singhvi M, Lee P. Illustrative cases of false positive biopsies after stereotactic body radiation therapy for lung cancer based on abnormal FDG-PET-CT imaging. *BMJ Case Rep* 2013;2013. pii: bcr2012007967.
28. Senthil S, Dahele M, van de Ven PM, et al. Late radiologic changes after stereotactic ablative radiotherapy for early stage lung cancer: A comparison of fixed-beam versus arc delivery techniques. *Radiother Oncol* 2013;109:77-81.
29. Wiener RS, Schwartz LM, Woloshin S, et al. Population-based risk for complications after transthoracic needle lung biopsy of a pulmonary nodule: an analysis of discharge records. *Ann Intern Med* 2011;155:137-44.
30. Gupta S, Wallace MJ, Cardella JF, et al. Quality improvement guidelines for percutaneous needle biopsy. *J Vasc Interv Radiol* 2010;21:969-75.
31. Takeda A, Kunieda E, Takeda T, et al. Possible misinterpretation of demarcated solid patterns of radiation fibrosis on CT scans as tumor recurrence in patients receiving hypofractionated stereotactic radiotherapy for lung cancer. *Int J Radiat Oncol Biol Phys* 2008;70:1057-65.
32. Stauder MC, Rooney JW, Neben-Wittich MA, et al. Late tumor pseudoprogression followed by complete remission after lung stereotactic ablative radiotherapy. *Radiat Oncol* 2013;8:167.
33. Senthil S, Lagerwaard FJ, Haasbeek CJ, et al. Patterns of disease recurrence after stereotactic ablative radiotherapy for early stage non-small-cell lung cancer: a retrospective analysis. *Lancet Oncol* 2012;13:802-9.
34. Libshitz HI, Shuman LS. Radiation-induced pulmonary change: CT findings. *J Comput Assist Tomogr* 1984;8:15-9.
35. Matsuo Y, Nagata Y, Mizowaki T, et al. Evaluation of mass-like consolidation after stereotactic body radiation therapy for lung tumors. *Int J Clin Oncol* 2007;12:356-62.
36. Lou F, Huang J, Sima CS, et al. Patterns of recurrence and second primary lung cancer in early-stage lung cancer survivors followed with routine computed tomography surveillance. *J Thorac Cardiovasc Surg* 2013;145:75-81; discussion 81-2.
37. National Lung Screening Trial Research Team, Aberle DR, Adams AM, et al. Reduced lung-cancer mortality with low-dose computed tomographic screening. *N Engl J Med* 2011;365:395-409.
38. Jaklitsch MT, Jacobson FL, Austin JH, et al. The American Association for Thoracic Surgery guidelines for lung cancer screening using low-dose computed tomography scans for lung cancer survivors and other high-risk groups. *J Thorac Cardiovasc Surg* 2012;144:33-8.
39. Eisenhauer EA, Therasse P, Bogaerts J, et al. New response evaluation criteria in solid tumours: revised RECIST guideline (version 1.1). *Eur J Cancer* 2009;45:228-47.
40. Dunlap NE, Yang W, McIntosh A, et al. Computed tomography-based anatomic assessment overestimates local tumor recurrence in patients with mass-like consolidation after stereotactic body radiotherapy for early-stage non-small cell lung cancer. *Int J Radiat Oncol Biol Phys* 2012;84:1071-7.
41. Oxnard GR, Morris MJ, Hodi FS, et al. When progressive disease does not mean treatment failure: reconsidering the criteria for progression. *J Natl Cancer Inst* 2012;104:1534-41.
42. Donington J, Ferguson M, Mazzone P, et al. American College of Chest Physicians and Society of Thoracic Surgeons consensus statement for evaluation and management for high-risk patients with stage I non-small cell lung cancer. *Chest* 2012;142:1620-35.
43. Fuss M. Strategies of assessing and quantifying radiation treatment metabolic tumor response using F18 FDG Positron Emission Tomography (PET). *Acta Oncol* 2010;49:948-55.
44. Henderson MA, Hoopes DJ, Fletcher JW, et al. A pilot trial of serial 18F-fluorodeoxyglucose positron emission tomography in patients with medically inoperable stage I non-small-cell lung cancer treated with hypofractionated stereotactic body radiotherapy. *Int J Radiat Oncol Biol Phys* 2010;76:789-95.
45. Matsuo Y, Nakamoto Y, Nagata Y, et al. Characterization of FDG-PET images after stereotactic body radiation therapy for lung cancer. *Radiother Oncol* 2010;97:200-4.
46. Feigenberg S, Yu JQM, Eade TN, et al. FDG PET response by 3 months following stereotactic body radiotherapy for non-small cell lung cancer may be an early surrogate of local failure [abstract]. *Int J Radiat Oncol Biol Phys* 2007;69:S479-80.
47. Zhang X, Liu H, Balter P, et al. Positron emission tomography for assessing local failure after stereotactic body radiotherapy for non-small-cell lung cancer. *Int J Radiat Oncol Biol Phys* 2012;83:1558-65.
48. Takeda A, Kunieda E, Fujii H, et al. Evaluation for local failure by 18F-FDG PET/CT in comparison with CT findings after stereotactic body radiotherapy (SBRT) for localized non-small-cell lung cancer. *Lung Cancer* 2013;79:248-53.
49. Bollineni VR, Widder J, Pruijm J, et al. Residual <sup>18</sup>F-FDG-PET uptake 12 weeks after stereotactic ablative radiotherapy for stage I non-small-cell lung cancer predicts local control. *Int J Radiat Oncol Biol Phys* 2012;83:e551-5.
50. Essler M, Wantke J, Mayer B, et al. Positron-emission tomography CT to identify local recurrence in stage I lung cancer patients 1 year after stereotactic body radiation therapy. *Strahlenther Onkol* 2013;189:495-501.
51. Huang K, Senthil S, Palma DA, et al. High-risk CT features for detection of local recurrence after stereotactic ablative radiotherapy for lung cancer. *Radiother Oncol* 2013;109:51-7.
52. Kato S, Nambu A, Onishi H, et al. Computed tomography appearances of local recurrence after stereotactic body radiation therapy for stage I non-small-cell lung carcinoma. *Jpn J Radiol* 2010;28:259-65.
53. Boellaard R. Need for standardization of 18F-FDG PET/CT for treatment response assessments. *J Nucl Med* 2011;52 Suppl 2:93S-100S.
54. Russ JC. *The Image Processing Handbook*. Fifth Edition. Taylor & Francis, 2006.

55. IEEE Standard Glossary of Image Processing and Pattern Recognition Terminology. IEEE Std 6104-1990 1990:0\_1.
56. Shi Z, Yang Z, Zhang G, et al. Characterization of texture features of bladder carcinoma and the bladder wall on MRI: initial experience. *Acad Radiol* 2013;20:930-8.
57. Jalalian A, Mashohor SB, Mahmud HR, et al. Computer-aided detection/diagnosis of breast cancer in mammography and ultrasound: a review. *Clin Imaging* 2013;37:420-6.
58. Ganeshan B, Burnand K, Young R, et al. Dynamic contrast-enhanced texture analysis of the liver: initial assessment in colorectal cancer. *Invest Radiol* 2011;46:160-8.
59. Davnall F, Yip CS, Ljungqvist G, et al. Assessment of tumor heterogeneity: an emerging imaging tool for clinical practice? *Insights Imaging* 2012;3:573-89.
60. Chicklore S, Goh V, Siddique M, et al. Quantifying tumour heterogeneity in 18F-FDG PET/CT imaging by texture analysis. *Eur J Nucl Med Mol Imaging* 2013;40:133-40.
61. Yao J, Dwyer A, Summers RM, et al. Computer-aided diagnosis of pulmonary infections using texture analysis and support vector machine classification. *Acad Radiol* 2011;18:306-14.
62. Yoon RG, Seo JB, Kim N, et al. Quantitative assessment of change in regional disease patterns on serial HRCT of fibrotic interstitial pneumonia with texture-based automated quantification system. *Eur Radiol* 2013;23:692-701.
63. Korfiatis PD, Karahaliou AN, Kazantzi AD, et al. Texture-based identification and characterization of interstitial pneumonia patterns in lung multidetector CT. *IEEE Trans Inf Technol Biomed* 2010;14:675-80.
64. Ravanelli M, Farina D, Morassi M, et al. Texture analysis of advanced non-small cell lung cancer (NSCLC) on contrast-enhanced computed tomography: prediction of the response to the first-line chemotherapy. *Eur Radiol* 2013;23:3450-5.
65. Louie AV, Rodrigues G, Olsthoorn J, et al. Inter-observer and intra-observer reliability for lung cancer target volume delineation in the 4D-CT era. *Radiother Oncol* 2010;95:166-71.
66. Poon M, Hamarneh G, Abugharbieh R. Efficient interactive 3D Livewire segmentation of complex objects with arbitrary topology. *Comput Med Imaging Graph* 2008;32:639-50.
67. Bharati MH, Liu JJ, MacGregor JF. Image texture analysis: methods and comparisons. *Chemometr Intell Lab Syst* 2004;72:57-71.
68. Connors RW, Trivedi MM, Harlow CA. Segmentation of a high-resolution urban scene using texture operators. *Comput Vision Graph* 1984;25:273-310.
69. Haralick RM. Statistical and Structural Approaches to Texture. *Proc IEEE* 1979;67:786-804.
70. Haralick RM, Shanmugam K, Dinstein I. Textural Features for Image Classification. *IEEE T Syst Man Cyb* 1973;SMC-3:610-21.
71. Diot Q, Kavanagh B, Scheffer T, et al. Regional normal lung tissue density changes in patients treated with stereotactic body radiation therapy for lung tumors. *Int J Radiat Oncol Biol Phys* 2012;84:1024-30.
72. Vinogradskiy Y, Diot Q, Kavanagh B, et al. Spatial and dose-response analysis of fibrotic lung changes after stereotactic body radiation therapy. *Med Phys* 2013;40:081712.
73. Mattonen SA, Palma DA, Haasbeek CJ, et al. Distinguishing radiation fibrosis from tumour recurrence after stereotactic ablative radiotherapy (SABR) for lung cancer: a quantitative analysis of CT density changes. *Acta Oncol* 2013;52:910-8.
74. Mattonen SA, Palma DA, Haasbeek CJ, et al. CT image feature analysis in distinguishing radiation fibrosis from tumour recurrence after stereotactic ablative radiotherapy (SABR) for lung cancer: a preliminary study. *SPIE Medical Imaging 2013: Biomedical Applications in Molecular, Structural, and Functional Imaging Proceedings* 2013;8672.
75. Mattonen SA, Palma DA, Haasbeek CJA, et al. editors. Assessment of response after stereotactic ablative radiotherapy (SABR) for lung cancer: can advanced CT image feature analysis predict recurrence? Canadian Cancer Research Conference; 2013; Toronto, Canada.
76. Vu CC, Matthews R, Kim B, et al. Prognostic value of metabolic tumor volume and total lesion glycolysis from 18F-FDG PET/CT in patients undergoing stereotactic body radiation therapy for stage I non-small-cell lung cancer. *Nucl Med Commun* 2013;34:959-63.
77. Grosu AL, Souvatzoglou M, Röper B, et al. Hypoxia imaging with FAZA-PET and theoretical considerations with regard to dose painting for individualization of radiotherapy in patients with head and neck cancer. *Int J Radiat Oncol Biol Phys* 2007;69:541-51.
78. Hendrickson K, Phillips M, Smith W, et al. Hypoxia imaging with [F-18] FMISO-PET in head and neck cancer: potential for guiding intensity modulated radiation therapy in overcoming hypoxia-induced treatment resistance. *Radiother Oncol* 2011;101:369-75.
79. Cao Y. The promise of dynamic contrast-enhanced imaging in radiation therapy. *Semin Radiat Oncol* 2011;21:147-56.
80. Cao Y, Pan C, Balter JM, et al. Liver function after irradiation based on computed tomographic portal vein perfusion imaging. *Int J Radiat Oncol Biol Phys* 2008;70:154-60.
81. Nakajima N, Sugawara Y, Kataoka M, et al. Differentiation of tumor recurrence from radiation-induced pulmonary fibrosis after stereotactic ablative radiotherapy for lung cancer: characterization of 18F-FDG PET/CT findings. *Ann Nucl Med* 2013;27:261-70.



**Cite this article as:** Mattonen SA, Huang K, Ward AD, Senan S, Palma DA. New techniques for assessing response after hypofractionated radiotherapy for lung cancer. *J Thorac Dis* 2014;6(4):375-386. doi: 10.3978/j.issn.2072-1439.2013.11.09

## Molecular markers to predict clinical outcome and radiation induced toxicity in lung cancer

Joshua D. Palmer<sup>1</sup>, Nicholas G. Zaorsky<sup>1,2</sup>, Matthew Witek<sup>1</sup>, Bo Lu<sup>1</sup>

<sup>1</sup>Department of Radiation Oncology, Kimmel Cancer Center and Jefferson Medical College of Thomas Jefferson University, Philadelphia, PA, USA; <sup>2</sup>Department of Radiation Oncology, Fox Chase Cancer Center, Philadelphia, PA, USA

### ABSTRACT

The elucidation of driver mutations involved in the molecular pathogenesis of cancer has led to a surge in the application of novel targeted therapeutics in lung cancer. Novel oncologic research continues to lead investigators towards targeting personalized tumor characteristics rather than applying targeted therapy to broad patient populations. Several driver genes, in particular epidermal growth factor receptor (EGFR) and ALK fusions, are the earliest to have made their way into clinical trials. The *avant-garde* role of genomic profiling has led to important clinical challenges when adapting current standard treatments to personalized oncologic care. This new frontier of medicine requires newer biomarkers for toxicity that will identify patients at risk, as well as, new molecular markers to predict and assess clinical outcomes. Thus far, several signature genes have been developed to predict outcome as well as genetic factors related to inflammation to predict toxicity.

### KEYWORDS

Lung cancer; biomarkers; toxicity; novel therapies

*J Thorac Dis* 2014;6(4):387-398. doi: 10.3978/j.issn.2072-1439.2013.12.04

### Introduction

In 2013, an estimated 228,000 new cases of lung cancer will be diagnosed in the United States and more than 70,000 will die from the disease. The risk of developing lung cancer for all American men and woman during their lifetimes is between 6-7%. This risk increases with age, genetic susceptibility and toxic exposures (e.g., smoking) (1). Lung cancer is a heterogeneous group of carcinomas comprised of several histologic subtypes: adenocarcinoma, squamous cell carcinoma, and large cell and small cell neuroendocrine tumors. The vast majority of molecular research focuses on the most prevalent histologic subtypes: adenocarcinoma and squamous cell carcinomas.

Since the initial heralding in the last decade of “the six

hallmarks of cancer”, advances in the study of molecular pathways, identification of biomarkers and novel targeted therapies have made their way to clinical applications and widened the scope of our understanding of the molecular pathogenesis of lung cancer (2,3). The appropriate introduction of targeted therapies into current standards of care remains an open area of clinical investigation.

The current understanding of the mechanisms of transformation from normal physiologic epithelial cells to malignant lung cancer has evolved alongside our increasing knowledge of many other cancer types and falls into a multi-step paradigm (4,5). A series of either chromosomal or nucleotide aberrations and epigenetic events in driver genes lead to immortality and the malignant phenotype of lung cancer (6). It is theorized that during this multi-step transformation, certain driver genes cause “addiction” and are required for tumor maintenance and targeting these biomarkers will lead to the eradication of selective cancer cells.

Various lung cancer biomarkers have been identified, including epidermal growth factor receptor (EGFR) mutations, EML4/ALK fusion genes, p53 mutations, RAS/MAP kinase mutations, Her-2 overexpression and PI3K/mTOR mutations.

A consequence of targeted radiotherapy in lung cancer is damage to the surrounding organs at risk which include the lung

Correspondence to: Joshua D. Palmer, M.D. Department of Radiation Oncology, Jefferson Medical College of Thomas Jefferson University, Kimmel Cancer Center, 111 South 11th Street, Philadelphia, PA 19107, USA. Email: [joshua.palmer@jeffersonhospital.org](mailto:joshua.palmer@jeffersonhospital.org).

Submitted Aug 26, 2013. Accepted for publication Dec 03, 2013.  
Available at [www.jthoracdis.com](http://www.jthoracdis.com)

ISSN: 2072-1439

© Pioneer Bioscience Publishing Company. All rights reserved.

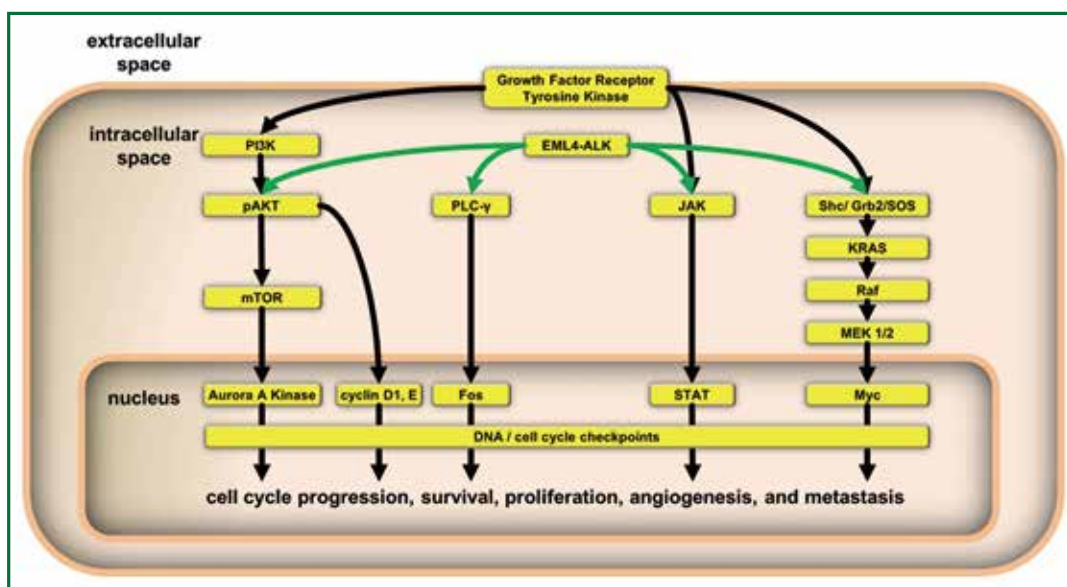


**Figure 1.** Summary of intracellular signaling pathways containing the crucial driver genes in lung cancer which promote tumor cell proliferation, survival, angiogenesis and metastatic potential.

and heart. The majority of molecular biomarkers of toxicity in lung cancer focus on lung damage or pneumonitis. Attempts have been made to combine dosimetric parameters in lung radiotherapy with various lung biomarkers to define a group of patients most at risk for severe lung toxicity.

### Lung cancer molecular markers

The search for a cancer biomarker or targetable genetic aberration requires years of preclinical studies *in vitro* and *in vivo*. Currently there are approximately a dozen biomarkers that have demonstrated clinical benefit and another dozen are currently under investigation (7). Of these, several are considered lung cancer driver genes by the NCI's lung cancer mutation consortium. These include EGFR, KRAS, HER2, PI3K, BRAF and ALK fusions (4). Of these EGFR, KRAS, HER2 and ALK fusions are predictive of response to targeted therapies (5,8-11). These driver genes play an important role in lung cancer tumorigenesis involving alterations in their proliferative potential, apoptotic signaling, angiogenesis and invasion/extravasation. Clinically relevant pathways are depicted in Figure 1 and include the RAS/MAP kinase, PI3K/AKT/mTOR, JAK/STAT pathways and cell cycle checkpoints. It is known that, in varying degrees, these biomarkers are mutated, amplified or overexpressed in non-small cell lung cancers. Table 1 outlines the relative frequency with which each driver gene occurs in lung cancer (5,8,12,13).

### EGFR

This family of receptor tyrosine kinases (RTKs) include the EGFR or HER1 and HER2-4 (14). They are a group of RTKs with approximately 75% homology that once bound to an extracellular ligand form homo- and heterodimers which leads to their intracellular signaling (5). The vast majority of mutations in this family occurs within the tyrosine kinase domain and correlate with drug sensitivity (15). Therapeutic targets for this family are summarized in Table 1 and include small molecule inhibitors, gefitinib and erlotinib, and monoclonal antibodies, cetuximab and trastuzumab. Interestingly mutations in EGFR seem to occur more frequently in never-smokers, people of Asian descent, and women with adenocarcinomas (5,15). These groups also seem to be more sensitive to molecular inhibition. Several studies have found both EGFR amplifications and most mutations correlate with improved clinical outcomes (8). There are, however, mutations that predict a negative response to EGFR inhibition which include the T790M mutation, a concomitant KRAS mutation or MET amplification. More recent studies suggest a D761Y mutation in exon 19 and insertion within exon 20 leads to further resistance to targeted therapy (16). HER2 mutations occur much less frequently although mutations seem to correlate with those in EGFR mutated patients. Targeting Her2-4, however, has not led to improved outcomes in unselected patients and large groups of patients harboring these mutations have not been identified (8,9,17,18).

**Table 1.** Lung cancer genetic aberrations and associated targeted therapy.

| Biomarker gene      | Aberration                     | Targeted therapeutic            | Frequency of aberration [%]        |
|---------------------|--------------------------------|---------------------------------|------------------------------------|
| <i>EGFR</i>         | Mutation or amplification      | Gefitinib, erlotinib, cetuximab | [10-25] (35% in Asian patients)    |
| <i>HER2 (ERBB2)</i> | Mutation or amplification      | Trastuzumab                     | [5-10]                             |
| <i>BRAF</i>         | Mutation                       | Sorafenib                       | [2-3]                              |
| <i>p53</i>          | Mutation or deletion           | Advexin a p53 adenoviral vector | [30-50]                            |
| <i>VEGF</i>         | Overexpression                 | Bevacizumab, afibercept         |                                    |
| <i>PI3K</i>         | Modified and activated         | BEZ235, LY294002                | [1-3]                              |
| <i>mTOR</i>         | Activated                      | Rapamycin, RAD001, CCL-779      | [70-75]                            |
| <i>RAS</i>          | Mutation leading to activation | Tipifarnib, lonafarnib          | [10-15] (20-30% in Adenocarcinoma) |
| <i>MEK</i>          | Activated                      | Trametinib, salmetinib          | [1-2]                              |
| <i>c-KIT</i>        | Overexpressed                  | Imatinib                        | [1-2]                              |
| <i>EML/ALK</i>      | Fusion                         | Crizotinib                      | [5-13]                             |

### RAS/RAF/MAP kinase pathway

In lung cancer, nearly all clinically relevant mutations in the RAS family occur in KRAS. Once mutated RAS is activated and may lead to cellular transformation and sustained proliferation making this family an ideal candidate for targeting. Several drugs, among them tipifarnib and lonafarnib, are known as farnesyl transferase inhibitors and have been developed to target RAS modification. In order to perform intracellular cell signaling (8), RAS requires modification with a farnesyl group. This allows proper attachment to the cell membrane. Without proper modification and cell membrane localization, RAS becomes ineffective.

BRAF is a part of a family of serine/threonine kinases downstream of RAS. BRAF is mutated in lung cancer but this occurs much less frequently than with melanoma (Table 1). Because the mutations in BRAF differ substantially between lung and melanoma, the translational use of vemurafenib for treatment of lung cancer is unlikely. However, the use of oral RAF kinase inhibitors like sorafenib is being studied. Sorafenib is unique in that it is an inhibitor of the RAF/MAP kinase pathway and has activity on multiple tyrosine kinases (VEGF and PDGF) allowing for multiple pathways involved in lung tumorigenesis to be targeted (8,11,19).

Once activated BRAF signals MEK1/2 which goes on to activate the MAP kinase pathway through ERK1/2. These downstream effectors are known to be constitutively activated in human lung cancer cell lines. Oral inhibitors such as CI-1040 and PD03244901 have been developed and studies are actively being pursued (8,20).

### ALK translocations (*ALK/EML4* and *ROS1*)

The echinoderm microtubule-associated protein-like 4-anaplastic lymphoma kinase fusion gene (*EML4/ALK*) is the most common form of translocation. The fusion protein results in a constitutively active tyrosine kinase (21). This fusion product is more common in the young, low volume or never-smokers with adenocarcinoma histology with signet ring features. ALK rearrangements are clinically detected with fluorescence *in situ* hybridization. A dual ALK translocation inhibitor called crizotinib is available to suppress the effects. Both preclinical and clinical testing has demonstrated radiosensitivity and remarkable response rates of EML/ALK positive tumors to therapy with crizotinib (9,22). Several second site mutations L1152R, L1196M and C1156Y have been and confer resistance to crizotinib treatment. ROS1 rearrangements have also been identified recently to remain sensitive to crizotinib (8).

### P53

The p53 protein is a transcription factor that is modified in various cellular stress situations. It functions to initiate apoptosis or to arrest the cell cycle. P53 is well known, as it is the most frequently mutated gene in human cancers (4). The majority of mutations in p53 are inactivating mutations, or deletions, although some missense mutations result in a gain-of-function phenotype that portends a poor prognosis in lung cancer (8). Classically, cigarette smoking is linked to transversion mutations in lung cancer. Clinical applications to subvert p53 have been made by using adenoviral gene replacement vectors to re-introduce

wildtype p53 (4,8,21). This is based on the preclinical work demonstrating that tumors that harbor a mutant p53 undergo apoptosis if wildtype p53 is re-expressed within the cell. Early phase clinical trials have determined this vector to be safe and effective in lung cancer and continued studies are planned (23).

### **The PI3K/mTOR pathway**

Phosphatidylinositol-3 kinase (PI3K) encoded from the oncogene PIK3CA belongs to a family of lipid kinases leading to mammalian target of rapamycin (mTOR) activation that is estimated to be activated in nearly 75% of lung cancers (8). PI3K leads to inhibition of apoptosis and a regulation of growth. PIK3CA is mutated in lung cancer (Table 1), leading to high levels of kinase activity and downstream signaling. When combined with radiotherapy, PI3K inhibitors such as LY294002 and wortmannin reduce downstream effects which stall the growth potential and cell killing of human cell lines. These drugs are, however, rather toxic as they are nonspecific and inhibit a broad range of this family of kinases. Most recently, pharmaceutical companies are attempting to isolate isoform specific inhibitors of PI3K for a variety of cancers, IC486068 and IC87114 (8,18,21).

mTOR is a serine/threonine protein kinase. This kinase is the main downstream effector of the pathway that leads to regulation of cell growth. Two complexes, mTORC1 and mTORC2, form a catalytic subunit allowing for both cellular activity and possible therapeutic targeting. Several available therapeutic drugs are available, including Sirolimus and derivatives such as CCI-779, RAD001 and AP23576. Both have shown activity in lung cancer and are under further current clinical study (8,21,22).

### **JAK/STAT**

The Janus kinase (JAK) and Signal Transducer and Activator of Transcription (STAT) pathway has been implicated in preclinical study to increase cell proliferation and inhibit apoptosis through downstream effects like BCL, Cyclin and MYC in lung cancer. JAK localizes toward and is activated by ligand bound receptor tyrosine kinases leading to phosphorylated sites recognized by the SH2 domain of various STATs. They become phosphorylated by JAKs and form homo- and heterodimers which localize to the cell nucleus and regulate gene transcription. Interestingly, several STATs may be phosphorylated directly by EGFR and other kinases. Most notably, STAT3 has been linked to lung cancer oncogenesis within cell lines that carry a mutated EGFR. In fact, in EGFR mutants, STAT3 activation is necessary for cell growth and survival. Downstream of STAT3 is an inhibitor of apoptosis named

survivin which functions to increase cell proliferation through the cell cycle and inhibition of apoptosis through caspases. This pathway of signaling is an attractive therapeutic target and preclinical work using TG101209 has demonstrated induced radiosensitivity, likely through inhibition of STAT3 (8,21,22).

### **TGF- $\beta$ and angiogenesis**

Transforming growth factor beta (TGF- $\beta$ ) is a cytokine that regulates multiple cellular processes, including cell survival, growth and immunomodulation. TGF- $\beta$  activates downstream effectors in the SMAD family. TGF- $\beta$  plays a dual role in lung cancer. During early tumorigenesis, TGF- $\beta$  induces apoptosis and is responsible for growth inhibition. And, as we will see later, it also plays a role in inflammation. However, in late stage lung cancers, TGF- $\beta$  induces angiogenesis (3,8,22).

Vascular density and angiogenesis correlate with advanced stage lung cancers and poor survival. A critical mediator in angiogenesis is the VEGF family. VEGF receptor inhibitors include the monoclonal antibody bevacizumab and the fusion protein aflibercept which bind circulating VEGF amongst others currently under investigation. Assessing response after treatment with bevacizumab has become a challenge. Pooling available anti-VEGF trials has allowed assessment of possible biomarkers to measure outcome. In fact, recent data suggests biomarkers such as circulating short VEGF-A, as well as modified expression of receptors neuropilin-1 and VEGF receptor 1, are potential candidates to predict outcome (8,24). A prospective biomarker study named MERiDiAN will stratify patients based on their short VEGF isoform and plans to address this issue.

### **Biomarkers of radioresistance**

The development of radiation resistance relies on innate tumor characteristics. Classically, the most important features in the response of tumors and normal tissues to fractionated radiotherapy are referred to as the "4 Rs": repair of DNA damage, redistribution of cells within the cell cycle, accelerated repopulation and reoxygenation of hypoxic tumor cells (25). During the accelerated repopulation phase, tumor cells begin to repair their damage and proliferate at a markedly faster rate. During this phase, several cellular mechanisms take place that lead to resistance to radiotherapy: cellular senescence, DNA repair and cell cycle checkpoints regulation. Unfortunately the pathways and mechanisms of resistance are complex, and to date, are poorly elucidated. However, several investigators have shed light on genes likely related to both innate and acquired radioresistance. Innate radioresistance refers to genes present prior to exposure to ionizing

therapeutic radiation and the acquired genes are those whose expression is changed after exposure to ionizing radiation. Using various methods of gene expression profiling a series of pathways involved in hypoxia, DNA repair and apoptosis have been studied in human lung cancer cell lines. Eighteen key genes linked to radioresistance were identified but of these genes only three have been validated to date. The three validated genes were MDM2, Livin  $\alpha$  and TP54I3 (18,26).

MDM2 involved in innate radiation resistance encodes a protein called E3 ubiquitin-protein ligase which is an important negative regulator of p53 both through ubiquitinylation leading to degradation and inhibition of transcriptional activation (27). It has been demonstrated that up-regulation of MDM2 expression leads to radioresistance and targeted down regulation with siRNA leads to a reversion back to radiosensitivity. The remaining two validated genes are associated with acquired radioresistance where Livin- $\alpha$  is up-regulated and TP54I3 is down-regulated. Livin is a novel inhibitor of apoptosis (IAP) which is normally not expressed at high levels. In 2011, it was found that levels of expression are highly up-regulated after exposure to radiation leading to acquired resistance, especially in isoform  $\alpha$ . The tumor protein p53 inducible protein 3 (TP53I3) gene is nearly turned off subsequent to fractionated radiotherapy leading to a depression of p53 cell death signaling (18).

Other potential mechanisms of resistance to radiation include mutations in EGFR and RAS. Preclinical studies have shown low levels of apoptosis in human cell lines with KRAS mutations in codon 12 (12V). It is theorized that this low level of apoptosis is mediated through modification of ERK. This may explain the resistance to radiotherapy. Various investigators have demonstrated a link between high levels of survivin expression and radioresistance (28,29). Radioresistance through mutations in EGFR has been studied and linked to various intracellular pathways yet no clear mechanism has been discovered.

### Immunotherapy in lung cancer

Over the past several years, the importance of immune responses in cancer stem from the update of “the hallmarks of cancer” which included several new mechanisms important to cancer cell proliferation and evasion of the body’s innate system of immunosurveillance (30). It was noted that cancer cells require the ability to thrive in a chronically inflamed environment and evade and suppress the immune system. With this knowledge researchers have begun to seek out mechanisms to effectively activate immune reactivity, counteract immune suppression and characterize cancer specific antigens that are present throughout the cell’s lineage.

The basis for immunotherapy lies in mounting an adaptive response to cancer specific antigens. This relies on the tumor microenvironment, myeloid suppressing cells like T-regulatory (Treg) cells and the discovery of conserved cancer cell antigens (30-33).

In fact, Suzuki *et al.* have begun to clarify the importance of the tumor microenvironment on the risk of recurrence (33). The tumor microenvironment was studied by separating eight tumors infiltrating immune cells from the tumor and surrounding stroma and studying the expression of several cytokines in nearly 1,000 early stage lung cancer patients. Several markers were found to be significantly strong predictors of the risk for a recurrence at five years. These markers included an elevated forkhead box P3 (FOXP3): CD3 ratio and high levels of interleukin-7 receptor. The interleukin-7 receptor was also linked to worse overall survival. It was also noted that high levels of interleukin-12 receptor  $\beta$ 2 was associated with a lower risk of recurrence. It turns out that FOXP3 is a marker for Treg cells. The expression of FOXP3 was also noted in the tumor stroma emphasizing the necessity of the tumors microenvironment in the relapse potential. IL-12 and its associated receptor acts as a tumor suppressor that is associated with less aggressive tumors. On the other hand, IL-7R has been shown to enhance angiogenesis by upregulating VEGF-D and acts through the JAK/STAT pathway. Several therapeutic targets have been suggested to counteract these newly found prognosticators in early lung cancer cells including cyclophosphamide which may deplete Treg cells and alter the FOXP3:CD3 ratio, reintroducing IL-12 or stimulating the IL-12R and blocking angiogenesis and the STAT family (33-35).

Several other mechanisms have been thoroughly studied to manipulate the immune environment including cytotoxic T lymphocyte antigen-4 (CTLA-4), programmed death 1 (PD-1), PD-1 ligands and damage associated molecular-pattern molecules (DAMPs) (33). CTLA-4 is expressed on CD4 cells and inhibits cytotoxic T lymphocytes. Ipilimumab is an antibody which targets CTLA-4. A clinical response relies on nonspecific alterations in immunogenicity through changes in total lymphocyte number and dendritic cells as well as altering expression of indoleamine dioxygenase. Ipilimumab has demonstrated a progression free survival in advanced stage, metastatic lung cancer in combination with chemotherapy. Other inhibitors of T cells include the PD-1 receptor which is a co-inhibitor present on T cells that is activated by PD ligands 1 and 2 (PD-L1 and PD-L2). Both PD-1 and PD-L1 have been targeted clinically in metastatic lung cancer demonstrating an objective response in 10-33% of patients with squamous cell carcinoma. Much lower response rates have been noted in adenocarcinomas (34,36). DAMPs such as heat-shock proteins (HSP) and high-mobility group box 1 (HMGB1)

enhance autophagy which is down regulated in cancer cells. It is theorized this may play a role in the abscopal effect and manipulation of DAMPS may increase the chances for systemic control of disease (34,35,37).

Lung cancer vaccines have been developed and demonstrated impressive results in several clinical trials. Targets range from conserved proteins, molecular biomarkers to nonspecific targets. Mucin 1 (MUC1) is a cellular adhesion molecule expressed on many epithelial cells and is largely conserved within malignant lung cancer cells. MUC1 targeting vaccines including BLP-25 and TG4010 have demonstrated improvements clinical outcomes in early phase trials. BLP-25 is the only MUC1 vaccine that has thus far demonstrated a significant improvement in overall survival. The phase IIB trial demonstrated a 31% 3-year overall survival compared to 17% with best supportive care (34,38). Although no benefit in survival was demonstrated in metastatic disease. Importantly, the administration of BLP-25 was administered with cyclophosphamide to inhibit T cell suppression. Several phase three trials including the START and INSPIRE trials are currently assessing BLP-25 in the phase III setting. The TG4010 vaccine acts by inducing MUC1 and IL-2 expression through transfection with a recombinant vaccine virus. There have been promising results in early phase studies yet no significant improvement in clinical outcomes. Clinical outcome with this technique relies on the expression and recognition of transfected targets and phase three studies are now excluding patients with increased NK cell activity as these patients tended to have worse outcomes and toxicity. The CIMAvax EGF vaccine has demonstrated an improved median survival through targeting the EGFR receptor but this effect is limited to those patients that produce a good antibody response to the vaccine. MAGE-A3 is another conserved protein that has been targeted for vaccine development which in phase II studies has led to a trend to improved overall survival. This has led to the MAGRIT phase III study. Belagenpumatucel-L is a vaccine targeting TGF- $\beta$ . The high-dose arm had a significantly improved median survival of nearly one year without significant toxicity. This has led to a phase II trial (NCT00676507) (34,38).

Combining immunotherapy with radiotherapy has been postulated to improve clinical outcome. Commonly after standard fractionated radiotherapy most cells undergo apoptosis as their mechanism for cell death which is non-immunogenic. But it is theorized that with hypofractionated therapy cells in combination with immunomodulators may make tumor cells more immunogenic. In fact, Shaue *et al.* demonstrated in a murine melanoma model a threshold where doses of 7.5 Gy were immunostimulatory yet less hypofractionated doses were not effective (39). The exact mechanism of enhancement of the innate

and adaptive immune systems is unclear but there have been several reports demonstrating marked reduction in systemic disease after local radiotherapy (39,40).

### Status of personalized care in lung cancer

Personalized medicine has become a hot topic due to the lower costs of genetic testing and the voluminous research each year that demonstrate new molecular biomarkers. Rather than treating tumors based on stage and anatomical location the ultimate goal of personalized oncology is to identify sub-classes of molecular tumor types, which will lead to improved treatment strategies and prognosis.

Biomarker driven clinical trials utilizing first generation EGFR tyrosine kinase inhibitors (erlotinib and gefitinib), as well as ALK inhibitors such as crizotinib have improved clinical outcomes with demonstrated response rates between 50-75% (16,41,42). In fact, these studies have led to a recent change in the National Comprehensive Cancer Network 2013 guidelines for non-small cell lung cancer which recommends molecular testing in the work-up of metastatic lung cancer patients. Now, many clinicians and several multi-disciplinary tumor boards are recommending molecular testing be done earlier and earlier in the clinical presentation of disease.

Although molecular testing is becoming a part of our clinical acumen in lung cancer serious limitations of our current targetable biomarkers exist. The largest limitation in applying these data to the general population lies in the fact that Americans only harbor between 10-30% of ALK and EGFR mutations and between 80-90% of all lung cancer patients do not harbor these mutations at all (8,16,43). In patients that harbor a targetable mutation between 25-50% of them do not respond to therapy. Efforts to determine the mechanisms of resistance amongst patient's harboring these mutations as well as emerging ALK inhibitors and second generation EGFR inhibitors will hopefully address this key issue.

Our understanding of the molecular pathways of driver mutations and their mechanisms of resistance will continue to improve. Many of the aforementioned molecular biomarker subtypes will likely be a part of our growing clinical armamentarium as the fight continues to tailor therapy to each tumor.

### Molecular markers: clinical applications and outcomes

The application of novel therapeutics to disrupt driver gene pathways has met with mixed results. Attempts to use these molecular biomarkers earlier in the pathogenesis of lung cancer

are under active investigation.

Erlotinib, crizotinib and bevacizumab have played a role in improving clinical outcomes in metastatic lung cancer (11,44-47). Yet, the use of concurrent or adjuvant EGFR inhibitors has led to inferior or equivocal results compared to current standard therapy (47). Also, the use of concurrent bevacizumab remains perilous. Many clinicians believe that the unselected nature of these trials has led to unexpected results. Logically, patients that harbor these mutations should have improved clinical outcomes (45,46,48). This has been noted with the addition of crizotinib in patients harboring the fusion gene with metastatic disease (49). Researchers await the results of the cetuximab data from the RTOG 0617 trial to determine if the addition of targeted therapy will lead to improved clinical outcomes in combined modality therapy. Excitingly, personalized targeted therapy is being explored in an upcoming RTOG trial assessing the efficacy of induction targeted therapy followed by standard therapy. Of course, the drawbacks in this design are that induction therapy will delay local therapy. But the safety of combining these therapies with combined modality therapy remains unclear and adjuvant therapy has demonstrated poor results.

Further genetic testing has been explored to identify sub-groups of patients with improved outcomes. In fact, a 5-gene signature was identified and validated by researchers in Taiwan (50). Using gene expression profiling, risk scores and decision-tree analysis, the researchers found DUSP6, MMD, STAT1, ERBB3 and LCK were independent predictors of relapse free and overall survival. They performed a microarray analysis of 16 genes in 125 patients and grouped patients into high risk and low risk groups. Using their 5-gene signature, the median overall survival in the low risk group was 40 months while the rate for those in the high risk group was 30 months with a  $P < 0.001$ . Relapse free survival was also significant; 29 months in low risk patients and 13 months in high risk patients. Importantly, these genes functions were observed in various realms of tumorigenesis, including apoptosis, cell differentiation and metastatic potential.

Preclinical studies have found other predictive biomarkers, including inhibitors of DNA binding ID1 and ID3. Immunohistochemical staining for ID1/3 was performed in 17 stage III lung cancer patient that received combined modality treatment. Interestingly, a dramatic improvement in progression free and overall survival was demonstrated. In patients without ID1/ID3 co-expression, the median progression free survival was 30 months compared to 1 month in those with co-expression. The median overall survival for patients without ID1/ID3 co-expression was 45 months and for those with co-expression was six months (51). It is theorized that these genes may correlate with the extent of hypoxia leading to resistance to radiotherapy (52).

Recently, there has been a remarkable uptrend of clinical trials addressing the use of targeted therapies earlier in the pathogenesis of disease (53). Importantly, the application of these novel therapeutics is being tailored to individual tumors which will hopefully improve clinical outcomes. The characterization of driver genes and prognostic biomarkers like the 5-gene signature and ID1/3 expression is an exciting revelation in lung cancer but we still require further study and validation in large randomized trials to determine if these biomarkers are clinically relevant.

### Radiation pneumonitis and novel biomarkers for toxicity

Radiation pneumonitis is characterized by inflammation of the lung after delivering therapeutic doses of radiation to the thorax. Clinically significant pneumonitis is considered any toxicity that will require medical intervention. Clinically significant radiation pneumonitis occurs in approximately 5-50% of patients with lung cancer and is one of the most common clinical toxicities. It is also one of the most dangerous (54). Approximately 80% of clinically significant pneumonitis manifests in the first 10 months following therapy. The frequency of different clinical endpoints varies among patients with radiation pneumonitis: 20-80% will have a radiologic abnormality, 5-50% will have shortness of breath and <3% will develop a bronchial stricture.

Quantitative analysis of normal tissue effects in the clinic (QUANTEC) is the guide radiation oncologists use to interpret dose volume histograms. The recommended dose-volume limits generally used (many caveats exist) in clinical practice include: the volume of lung receiving over 20 Gy ( $V_{20}$ ) of less than 30-35% and a mean lung dose of less than 20-23 Gy (55). These constraints portend a risk of less than 20% risk of pneumonitis. In patients after a pneumonectomy, more stringent limits include a  $V_5 < 60\%$ ,  $V_{20} < 10\%$  and a mean lung dose of <8 Gy. There are also factors that affect risk for pneumonitis. Classically, young age groups (<60-70 years old) and active smokers have a lower risk of developing pneumonitis. The use of concurrent chemotherapy increases the risk of radiation pneumonitis.

Acute radiation pneumonitis (within 12 weeks of radiotherapy) and subsequent pulmonary fibrosis which forms within the first 1-2 years results from a cascade of inflammatory cytokines and vasculature changes. Below is a depiction of several key markers of pneumonitis during the pathogenesis of fibrosis (Figure 2). The alveolar epithelium of the lung is made up of Type I (>90%) and Type II pneumocytes and upon exposure to radiotherapy there is a large loss of type I pneumocytes through apoptosis. The Type II alveolar cells begin to proliferate and produce surfactant apoproteins to repair

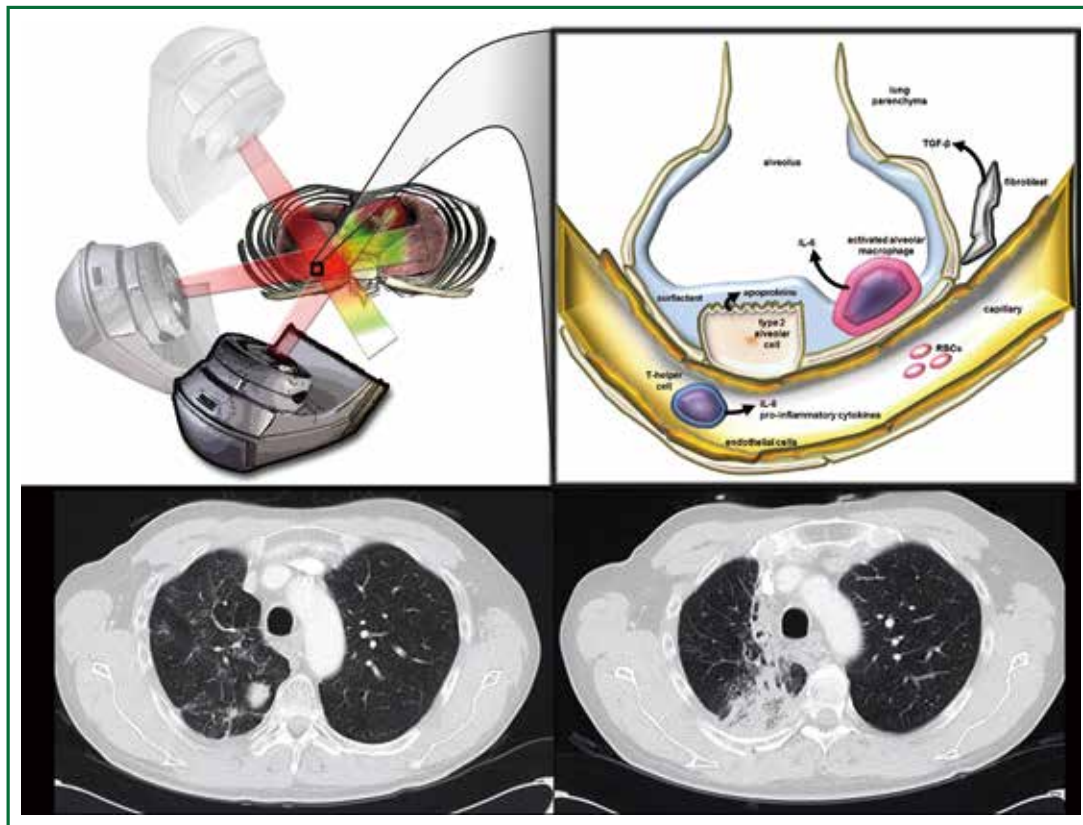


**Figure 2.** Mechanism of Pulmonary Toxicity. Radiation therapy is targeted at a right lower lobe lung mass (upper left panel). The irradiation of normal tissue during radiotherapy (black box, inset) causes certain patients to develop radiation pneumonitis, which is associated with release of IL-6 from neutrophils, TGF- $\beta$  from fibroblasts, and apoproteins in surfactant from type II alveolar cells (black box inset, magnification). Pre- and one year post-radiotherapy axial CT slices from a patient that developed radiation pneumonitis in the right lung is displayed (lower panel, left and right, respectively). Illustration created by Nicholas G. Zaorsky, M.D.

the surrounding damage. Cells within the extracellular matrix including macrophages, fibroblasts along with circulating T helper cells begin secreting cytokines including IL-6 and TGF- $\beta$  recruiting other inflammatory cells and beginning the cascade leading to collagen deposition and fibrosis within the lung parenchyma (56).

Recently, biomarkers and organ interactions have become important predictors of radiation pneumonitis. Inflammatory cytokines are known to participate in the pathogenesis of radiation pneumonitis and they pose a possible serum biomarker for toxicity. An early study linking serum markers to lung toxicity was the ROTG 91-03 trial studying stage II and III lung cancer patients undergoing 60-66 Gy of radiotherapy but were not surgical candidates (57). Some patients in this trial were able to receive concurrent or sequential chemotherapy but during the initial phases of the trial patients received radiotherapy alone. They found that after 10 Gy, elevated serum IL-6 ( $>0$ ) predicted for acute grade 2 or higher radiation pneumonitis. At the same

time, elevated levels of surfactant apoproteins ( $>797$ ) after 20 Gy were correlated with late radiation pneumonitis. They also noted that a diffusion capacity of  $<54$  and age  $>60$  portends a higher risk of radiation pneumonitis. The remainder of the serum markers studied failed to correlate well with pneumonitis, including TNF and TGF- $\beta$ .

TGF- $\beta$  is the most heavily studied and scrutinized inflammatory biomarker for lung toxicity because it has conflicting data regarding its predictive ability for radiation pneumonitis (58,59). Several studies have linked elevations in TGF- $\beta$  levels to radiation pneumonitis. They reported that levels of TGF- $\beta$  differ significantly during radiotherapy and that sampling time determines the level of serum concentration. Other studies found that technical factors related to testing blood samples may explain the elevations in TGF- $\beta$  levels. Still others found that normal tissue production of TGF- $\beta$  during radiotherapy was influenced by the genetic background of the tumor and the patient (52,59).

Nonetheless, a combined analysis from Michigan and China

found that elevation of serum TGF- $\beta$ 1 levels during radiotherapy (at four weeks) compared to pre-treatment TGF- $\beta$  levels predicted for pneumonitis. The addition of mean lung dose helps stratify patients at the highest risk. Using a TGF- $\beta$  ratio of  $>1$  and mean lung dose of  $>20$  Gy as risk factors, they categorized patients into three groups: no risk factors (low risk), one risk factor (intermediate risk) and both risk factors (high risk group). The risk of pneumonitis for each group was  $<5\%$  for low risk,  $50\%$  for intermediate risk and  $66\%$  for the high risk group. A similar study was performed using TGF- $\beta$  levels at the end of therapy and V30 (58). They were also able to adequately stratify each set of patients based on these two factors. Several investigators have found the combination of inflammatory markers with dose-volume characteristics seems to be the best predictor for pneumonitis, rather than being compared to any factor alone. Unfortunately, these studies found a marker that must be drawn during therapy and in some cases this was too late to make any significant change in the outcome.

A recent sophisticated study that searched for single nucleotide polymorphisms (SNPs) of *TGF $\beta$ 1* gene found genotypes at lower risk for radiation pneumonitis. This study randomly acquired DNA from 164 lung cancer patient's resected tumor specimen and genotyped each sample to reveal SNPs in the *TGF- $\beta$*  gene. The CT/CC genotypes in rs1982073:T869C *TGF $\beta$ 1* allele had a lower risk of developing radiation pneumonitis after radiotherapy independent of dosimetric factors such as mean lung dose and V20 (41). This may allow pre-treatment assessment of pneumonitis risk and further allow personalized radiotherapy treatment planning.

Strikingly, there is data linking parameters of radiation dose administered to the heart to lung toxicity. A single institutional review of hundreds of dose volume parameters found several variables, heart D10, lung D35 and maximum dose of the lung, were significant predictors for radiation pneumonitis in their cohort of patients (60). Due to the confounding variables within this type of analysis, further assessment and generalization to other patient populations are needed prior to using these variables in everyday practice. Additionally, heart toxicity has been linked to several biomarkers including pro-BNP and troponins (61). Though, no studies have linked these biomarkers to heart toxicity after completing radiotherapy to the lungs.

Other mechanism based biomarkers have been developed to determine improved outcomes in patients taking targeted therapies. These mechanism based biomarkers are well known side-effects, such as an acneiform rash with EGFR inhibitors, hypertension for VEGF inhibitors, hypothyroidism with multitargeted tyrosine kinase inhibitors and hyperglycemia with mTOR or PI3K inhibitors. Through analysis of the most recent targeted therapy trials in lung cancer, as well as analysis of other anatomic sites, trends were identified linking improved

clinical outcomes in those patient's that experienced mechanism based toxicities (62). Conversely, it is postulated that a lack of mechanism based toxicity is a surrogate for lack of effective tumor response. These data are interesting, yet they remain preliminary.

Lately researchers have begun combining targeted therapies in lung cancer with standard chemoradiotherapy. This raises a question: How will the addition of targeted therapies alter the therapeutic window?

Several early phase clinical trials assessing the safety and efficacy of adding bevacizumab to standard chemoradiotherapy in lung cancer have found an alarming rate of tracheoesophageal fistulas. Tracheoesophageal fistulas are normally an exceedingly rare occurrence in the treatment of lung cancer. However, in a small pooled analysis, investigators found more than  $10\%$  incidence of tracheoesophageal fistula formation prompting the early termination of these investigations (44,63,64). Another early phase trial assessed the incidence of clinically significant pneumonitis. When combined with chemoradiotherapy in advanced lung cancer, they found a clinically significant pneumonitis rate of  $67\%$  (44,63). Although these studies are relatively small, they demonstrate an alarmingly high rate of significant lung and esophageal toxicity occurs with the addition of bevacizumab in standard chemoradiotherapy. This finding has prompted many researchers to abandon the addition of current generation VEGF inhibitors in combined modality lung cancer treatment. Additional studies using next generation anti-angiogenic factors are needed to further characterize the safety and efficacy of this modality of treatment.

The controversial multi-institutional RTOG trial 0617 also assessed whether the addition of targeted therapy to combined modality therapy may improve outcomes. They used a  $2 \times 2$  factorial design comparing standard dose (60 Gy) versus high dose radiotherapy (74 Gy), with and without the addition of cetuximab. Paradoxically, there were significantly more local failures in the high dose arm,  $34\%$  versus  $25\%$  in the standard dose arm. Also noted was a startling stratification in survival, with a median survival in the standard dose arm of 28.7 months and 19.5 months in the high dose arm. The only significant difference in toxicity was esophagitis was three times higher (65). Many questions about these results remain unanswered. Some postulate that overall treatment time plays a role. Using tighter treatment margins without using 4D CT scans to determine tumor motion or awaiting the additional dosimetric data.

The appropriate timing of targeted therapies to use in combined modality therapy remains unclear. To address this issue, a trial in the pre-activation stage RTOG 1306 will add targeted therapies as an induction therapy for advanced stage lung cancer. Patients with stage III non-squamous, non-small cell lung cancer with N2 or N3 disease will be enrolled. All patients will have surgical staging

and tissue sent for molecular testing that searches for EGFR mutations and ALK translocations. Patients will be randomized based on their mutation analysis to receive either standard chemoradiotherapy or induction therapy with either erlotinib or crizotinib based on their mutation status.

The era of personalized medicine continues to bloom by allowing tailored treatments in addition to standard therapy. However, there are many unknown variables to consider when adding novel therapeutics to other cytotoxic therapies, as we have not completely defined the various therapeutic ratios. We have begun to define newer markers of toxicity. These latest findings will help next generation trials assess and prevent toxicity in lung cancer patients.

### Hypofractionated radiotherapy and pneumonitis

Hypofractionated radiotherapy is employed as a means of either dose escalation or shortening overall treatment times for both early and late stage lung cancer (66). However, the optimal dose, fractionation and schedule remain under investigation. There are several early phase clinical trials with data maturing which have combined hypofractionated radiotherapy with targeted agents including erlotinib (NCT00983307) and ZD1839 (NCT00328562). As of November of 2013, there are no active clinical trials assessing targeted therapies and hypofractionated radiotherapy registered to clinicaltrials.gov, which highlights a need for continued investigation. Patient factors and dosimetric information related to pneumonitis in the setting of hypofractionated radiotherapy is derived from early phase clinical trials and large retrospective analysis. A recent phase I study assessing hypofractionated attempting to raise the biologic effective dose (BED) over 100 Gy for patients of all stages revealed 16% grade 2 and no grade 3 radiation pneumonitis. However, six patients experienced grade 4 or 5 radiation toxicity including hemoptysis, lung abscess and bronchocavitary fistula. Univariate analysis demonstrated a significant association of high grade toxicity and total irradiation dose over 75 Gy with a 2-year incidence of toxicity of 31% vs. 1.8%. The maximal tolerated dose in this trial was 63.25 Gy in 25 fractions. The dose parameters which significantly predicted for 5% toxicity at two years were a D3cc of 75 Gy and a Dmax of 83 Gy (66). The high grade toxicities were attributed, by the investigators, to high doses as mentioned above being delivered to central structures including the proximal bronchial tree. The rate of pneumonitis for stereotactic body radiotherapy (SBRT), a form of ultra-hypofractionated therapy which employs image guidance and smaller treatment margins, has demonstrated rates of pneumonitis between 5-21% (67).

As the use of these techniques has increased, more attention has been paid to the size of the tumor volume treated and the dose

to the uninvolved lung. Several studies revealed larger primary tumor volume, mean lung dose, and maximum dose to the tumor predicted for higher rates of pneumonitis (67,68). Reasonable dosimetric guidelines include a mean lung dose less than 6 Gy, a contralateral mean lung dose less than 3.6 Gy, and a V20 <10%. Factors which may predict for increased risk for pneumonitis include concurrent systemic therapy, active smoker, advanced age (>65), central location, and size of treatment volume (>145 cc) (66-69). Since the available toxicity data is more robust in the setting of hypofractionated or SBRT alone, it is prudent that combination targeted therapy and hypofractionated or SBRT be conducted on prospective clinical trials to allow detailed assessment of possible toxicities as available dosimetric and patient factors may underestimate the rates of high-grade toxicity.

### Conclusions

Lung cancer is a heterogeneous group of tumor sub-types. Each type carries individualized mutations in multiple driver gene pathways. Classically, cancer therapies have been applied based on anatomic site, stage and other limited prognostic information. With the explosion of data that demonstrates targetable biomarkers in cancer, we are faced with new challenges to balance toxicity with clinical outcomes.

Genetic signatures have been discovered that influence outcome and one day may identify groups of patients that benefit from more aggressive therapy. Novel organ specific toxicity-related biomarkers in combination with radiotherapy derived parameters will improve treatment decisions and allow real-time treatment modifications to prevent long-term toxicity.

New approaches based on tumor and normal tissue characteristics are necessary to continue improving clinical outcomes. New multi-disciplinary tumor boards should be formed based on genetic tumor characteristics rather than tumor sites. Medicine requires an ever-increasing level of sophistication to interpret studies and design clinical trials. Technology, data management and analysis and novel therapies will improve more rapidly than ever before impacting our ability to predict and change clinical outcomes.

### Acknowledgements

*Disclosure:* The authors declare no conflict of interest.

### References

1. Siegel R, Naishadham D, Jemal A. Cancer Statistics, 2013. *CA Cancer J Clin* 2013;63:11-30.
2. Hanahan D, Weinberg RA. The hallmarks of cancer. *Cell* 2000;100:57-70.

3. Herbst RS, Onn A, Sandler A. Angiogenesis and lung cancer: prognostic and therapeutic implications. *J Clin Oncol* 2005;23:3243-56.
4. Kris MG, Johnson BE, Kwiatkowski DJ, et al. Identification of driver mutations in tumor specimens from 1,000 patients with lung adenocarcinoma: the NCI's lung cancer mutation consortium (LCMC). *J Clin Oncol* 2011;29:CRA7506.
5. Rowinsky EK. The erB family: targets for therapeutic development against cancer and therapeutic strategies using monoclonal antibodies and tyrosine kinase inhibitors. *Annu Rev Med* 2004;55:433-57.
6. Decker RH, Lynch TJ. Unmet challenges in the use of novel agents in locally advanced non-small-cell lung cancer. *J Clin Oncol* 2012;30:582-4.
7. Li T, Kung HJ, Mack PC, et al. Genotyping and genomic profiling of non-small-cell lung cancer: implications for current and future therapies. *J Clin Oncol* 2013;31:1039-49.
8. Sato M, Shames DS, Gasdar AF, et al. A translational view of the molecular pathogenesis of lung cancer. *J Thorac Oncol* 2007;2:327-43.
9. Oldenhuis CN, Oosting SF, Gietema JA, et al. Prognostic versus predictive value of biomarkers in oncology. *Eur J Cancer* 2008;44:946-53.
10. Sidransky D. Emerging molecular markers of cancer. *Nat Rev Cancer* 2002;2:210-9.
11. Shepherd FA, Domerg C, Hainaut P, et al. Pooled analysis of the prognostic and predictive effects of KRAS mutation status and KRAS mutation subtype in early-stage resected non-small-cell lung cancer in four trials of adjuvant chemotherapy. *J Clin Oncol* 2013;31:2173-81.
12. Oxnard GR, Binder A, Jänne PA. New targetable oncogenes in non-small-cell lung cancer. *J Clin Oncol* 2013;31:1097-104.
13. Sekido Y, Fong KM, Minna JD. Molecular genetics of lung cancer. *Annu Rev Med* 2003;54:73-87.
14. Shigematsu H, Gazdar AF. Somatic mutations of epidermal growth factor receptor signaling pathway in lung cancers. *Int J Cancer* 2006; 118:257-62.
15. Shigematsu H, Lin L, Takahashi T, et al. Clinical and biological features associated with epidermal growth factor receptor gene mutations in lung cancers. *J Natl Cancer Inst* 2005;97:339-46.
16. Wu K, House L, Liu W, et al. Personalized targeted therapy for lung cancer. *Int J Mol Sci* 2012;13:11471-96.
17. Verweij J, de Jonge M. Multitarget tyrosine kinase inhibition: [and the winner is ...]. *J Clin Oncol* 2007;25:2340-2.
18. Aréchaga-Ocampo E, Villegas-Sepulveda N, Lopez-Urrutia E, et al. (2013). Biomarkers in Lung Cancer: Integration with Radiogenomics Data, Oncogenomics and Cancer Proteomics - Novel Approaches in Biomarkers Discovery and Therapeutic Targets in Cancer, Dr. Cesar Lopez (Ed.), ISBN: 978-953-51-1041-5, InTech, DOI: 10.5772/53426.
19. Zhu CQ, da Cunha Santos G, Ding K, et al. Role of KRAS and EGFR as biomarkers of response to erlotinib in National Cancer Institute of Canada clinical trials group study BR.21. *J Clin Oncol* 2008;26:4268-75.
20. Roberts PJ, Stinchcombe TE, Der CJ, et al. Personalized medicine in non-small-cell lung cancer: is DRAS a useful marker in selecting patients for epidermal growth factor receptor-targeted therapy? *J Clin Oncol* 2010;28:4769-77.
21. Ausborn NL, Le QT, Bradley JD, et al. Molecular profiling to optimize treatment in non-small cell lung cancer: a review of potential molecular targets for radiation therapy by the translational research program of the radiation therapy oncology group. *Int J Radiat Oncol Biol Phys* 2012;83:e453-64.
22. Rose-James A, Sreelekha TT. Molecular markers with predictive and prognostic relevance in lung cancer. *Lung Cancer Int* 2012;2012:12.
23. Fujiwara T, Tanaka N, Kanazawa S, et al. Multicenter phase I study of repeated intratumoral delivery of adenoviral p53 in patients with advanced non-small-cell lung cancer. *J Clin Oncol* 2006;24:1689-99.
24. Lambrechts D, Lenz HJ, de Haas S, et al. Markers of response for the antiangiogenic agent bevacizumab. *J Clin Oncol* 2013;31:1219-30.
25. Withers HR. The four Rs of radiotherapy. *Adv Radiat Biol* 1975;5:241-7.
26. Li T, Kung HJ, Mack PC, et al. Genotyping and genomic profiling of non-small-cell lung cancer: implications for current and future therapies. *J Clin Oncol* 2013;31:1039-49.
27. Heist RS, Zhou W, Chirieac LR, et al. MDM2 polymorphism, survival, and histology in early-stage non-small-cell lung cancer. *J Clin Oncol* 2007;25:2243-7.
28. Sun Y, Moretti L, Giacalone NJ, et al. Inhibition of JAK2 signaling by TG101209 enhances radiotherapy in lung cancer models. *J Thorac Oncol* 2011;6:699-706.
29. Lu B, Mu Y, Cao C, et al. Survivin as a therapeutic target for radiation sensitization in lung cancer. *Cancer Res* 2004;64:2840-5.
30. Hanahan D, Weinberg RA. Hallmarks of cancer: the next generation. *Cell* 2011;144:646-74.
31. Shiao SL, Coussens LM. The tumor-immune microenvironment and response to radiation therapy. *J Mammary Gland Biol Neoplasia* 2010;15:411-21.
32. Cavallo F, De Giovanni C, Nanni P, et al. 2011: the immune hallmarks of cancer. *Cancer Immunol Immunother* 2011;60:319-26.
33. Suzuki K, Kyuichi K, Sima CS, et al. Clinical impact of immune microenvironment in stage I lung adenocarcinoma: tumor interleukin-12 receptor  $\beta 2$  (IL-12R $\beta 2$ ), IL-7R, and stromal foxP3/CD3 ratio are independent predictors of recurrence. *J Clin Oncol* 2013;31:490-8.
34. Hall RD, Gray JE, Chiappori AA. Beyond the standard of care: a review of novel immunotherapy trials for the treatment of lung cancer. *Cancer Control* 2013;20:22-31.
35. Rüttinger D, Winter H, van den Engel NK, et al. Immunotherapy of cancer: key findings and commentary on the third Tegernsee conference. *Oncologist* 2010;15:112-8.
36. Topalian SL, Hodi SF, Brahmer JR, et al. Safety, activity and immune correlates of anti-PD-1 antibody in cancer. *N Engl J Med* 2012;366:2443-54.
37. Tahara H, Sato M, Thurin M, et al. Emerging concepts in biomarker discovery; the US-Japan workshop on immunological molecular markers in oncology. *J Transl Med* 2009;7:45.
38. Romero P. Current state of vaccine therapies in non-small-cell lung cancer. *Clin Lung Cancer* 2008;9 Suppl 1:S28-36.
39. Schae D, Ratikan JA, Iwamoto KS, et al. Maximizing tumor immunity with fractionated radiation. *Int J Radiat Oncol Biol Phys* 2012;83:1306-10.
40. Formenti SC, Demaria S. Combining radiotherapy and cancer

- immunotherapy: a paradigm shift. *J Natl Cancer Inst* 2013;105:256-65.
41. Yuan X, Liao Z, Liu Z, et al. Single nucleotide polymorphism at rs11982073: T869C of the TGFβ1 gene is associated with the risk of radiation pneumonitis in patients with non-small-cell lung cancer treated with definitive radiotherapy. *J Clin Oncol* 2009;27:3370-8.
  42. Douillard JY, Shepherd FA, Hirsh V, et al. Molecular predictors of outcome with gefitinib and docetaxel in previously treated non-small-cell lung cancer: data from the randomized phase III INTEREST trial. *J Clin Oncol* 2010;28:744-52.
  43. Keedy VL, Argeaga CL, Johnson DH. Does gefitinib shorten lung cancer survival? Chaos redux. *J Clin Oncol* 2008;26:2428-30.
  44. Sandler AB, Schiller JH, Gray R, et al. Retrospective evaluation of the clinical and radiographic risk factors associated with severe pulmonary hemorrhage in first-line advanced, unresectable non-small-cell lung cancer treated with carboplatin and paclitaxel plus bevacizumab. *J Clin Oncol* 2009;27:1405-12.
  45. Cappuzzo F, Ciuleanu T, Stelmakh L, et al. Erlotinib as maintenance treatment in advanced non-small-cell lung cancer: a multicenter, randomized, placebo-controlled phase 3 study. *Lancet Oncol* 2010;11:521-9.
  46. Mok T, Yang JJ, Lam KC. Treating patients with EGFR-sensitizing mutations: first line or second line--is there a difference? *J Clin Oncol* 2013;31:1081-8.
  47. Kelly K, Chansky K, Gaspar LE, et al. Phase III trial of maintenance gefitinib or placebo after concurrent chemoradiotherapy and docetaxel consolidation in inoperable stage III non-small-cell lung cancer. *J Clin Oncol* 2008;26:2450-6.
  48. Fong T, Morgensztern D, Govindan R. EGFR inhibitors as first-line therapy in advanced non-small cell lung cancer. *J Thorac Oncol* 2008;3:303-10.
  49. Kwak EL, Bang YJ, Camidge DR, et al. Anaplastic lymphoma kinase inhibition in non-small-cell lung cancer. *N Engl J Med* 2010;363:1693-703.
  50. Chen HY, Yu SL, Chen CH, et al. A five-gene signature and clinical outcome in non-small-cell lung cancer. *N Engl J Med* 2007;356:11-20.
  51. Castañón E, Bosch-Barrera J, López I, et al. Id1 and Id3 co-expression correlates with clinical outcome in stage III-N2 non-small cell lung cancer patients treated with definitive chemoradiotherapy. *J Transl Med* 2013;11:13.
  52. Raben D, Bunn PA. Biologically targeted therapies plus chemotherapy plus radiotherapy in stage III non-small-cell lung cancer: a case of the Icarus syndrome? *J Clin Oncol* 2012;30:3909-12.
  53. Buettner R, Wolf J, Thomas, RK. Lessons learned from lung cancer genomics: the emerging concept of individualized diagnostics and treatment. *J Clin Oncol* 2013;31:1858-65.
  54. Marks LB, Bentzen SM, Deasy JO, et al. Radiation dose-volume effects in the lung. *Int J Radiat Oncol Biol Phys* 2010;76:S70-6.
  55. Marks LB, Yorke ED, Jackson A, et al. Use of normal tissue complication probability models in the clinic. *Int J Radiat Oncol Biol Phys* 2010;76:S10-9.
  56. Tsoutsou PG, Koukourakis MI. Radiation pneumonitis and fibrosis: mechanisms underlying its pathogenesis and implications for future research. *Int J Radiat Oncol Biol Phys* 2006;66:1281-93.
  57. Hartsell WF, Scott CB, Dundas GS, et al. Can serum markers be used to predict acute and late toxicity in patients with lung cancer? *Am J Clin Oncol* 2007;30:368-76.
  58. Zhao L, Wang L, Ji W, et al. Elevation of plasma TGF-β1 during radiation therapy predicts radiation-induced lung toxicity in patients with non-small-cell lung cancer: a combined analysis from Beijing and Michigan. *Int J Radiat Oncol Biol Phys* 2009;74:1385-90.
  59. Fu XL, Hong H, Bentel G, et al. Predicting the risk of symptomatic radiation-induced lung injury using both the physical and biologic parameters V30 and transforming growth factor beta. *Int J Radiat Oncol Biol Phys* 2001;50:899-908.
  60. Huang EX, Hope AJ, Lindsay PE, et al. Heart irradiation as a risk factor for radiation pneumonitis. *Acta Oncol* 2011;50:51-60.
  61. D'Errico MP, Grimaldi L, Petruzzelli MF, et al. N-terminal pro-B-type natriuretic peptide plasma levels as a potential biomarker for cardiac damage after radiotherapy in patients with left-sided breast cancer. *Int J Radiat Oncol Biol Phys* 2012;82:e239-46.
  62. Dienstmann R, Braña I, Rodon J, et al. Toxicity as a biomarker of efficacy of molecular targeted therapies: focus on EGFR and VEGF inhibiting anticancer drugs. *Oncologist* 2011;16:1729-40.
  63. Lind JS, Senan S, Smit EF. Pulmonary toxicity after bevacizumab and concurrent thoracic radiotherapy observed in a phase I study for inoperable stage III non-small-cell lung cancer. *J Clin Oncol* 2012;30:e104-8.
  64. Spigel DR, Hainsworth JD, Yardley DA, et al. Tracheoesophageal fistula formation in patients with lung cancer treated with chemoradiation and bevacizumab. *J Clin Oncol* 2010;28:43-48.
  65. Bradley JD, Paulus R, Komaki R, et al. A randomized phase III comparison of standard-dose (60 Gy) versus high-dose (74 Gy) conformal chemoradiotherapy ± cetuximab for stage III non-small cell lung cancer: results on radiation dose in RTOG 0617. *J Clin Oncol* 2013;31:abst 7501.
  66. Cannon DM, Mehta MP, Adkison JB, et al. Dose-limiting toxicity after hypofractionated dose-escalated radiotherapy in non-small-cell lung cancer. *J Clin Oncol* 2013;31:4343-8.
  67. Baker R, Han G, Saranqasin S, et al. Clinical and dosimetric predictors of radiation pneumonitis in a large series of patients treated with stereotactic body radiation therapy to the lung. *Int J Radiat Oncol Biol Phys* 2013;85:190-5.
  68. Bongers EM, Botticella A, Palma DA, et al. Predictive parameters of symptomatic radiation pneumonitis following stereotactic or hypofractionated radiotherapy delivered using volumetric modulated arcs. *Radiat Oncol* 2013;109:95-9.
  69. Palma DA, Senan S, Tsujino K, et al. Predicting radiation pneumonitis after chemoradiation therapy for lung cancer: an international individual patient data meta-analysis. *Int J Radiat Oncol Biol Phys* 2013;85:444-50.



**Cite this article as:** Palmer JD, Zaorsky NG, Witek M, Lu B. Molecular markers to predict clinical outcome and radiation induced toxicity in lung cancer. *J Thorac Dis* 2014;6(4):387-398. doi: 10.3978/j.issn.2072-1439.2013.12.04

# BETWEEN YOU AND ME

---

## Stories of Special K patients

*Special K* is street drug made from the anesthetic ketamine and it is abused by a select group of patients. They are usually young and come from wealthy families and have promising prospects for their lives. But due to various reasons they become drug abusers, and cannot extricate themselves from the drug habit. As a urologist, I thought I would never have contact with this group. However, by chance, I provided care for some of these patients and began to learn more about them. The underlying story with each of them poses an important question for physicians. When a disease has become a social problem, what role should medicine play in it?

The first time I met Mr. Huang, a *Special K* patient, was in 2007. He was tall and handsome, but slow and sluggish when talking and acting. In spite of having visited hospitals many times, no one could figure out the nature of his disease. When approaching diagnosis, I asked three questions. What brought you to the hospital? Tell me more? Do you have any questions for me? What happened later with Mr. Huang indicated how useful this approach can be. If I hadn't followed it, I probably would have missed the diagnosis.

He told me, *"I have to pee every couple of minutes. But each time I do not urinate very much. Plus, it is very painful"*. Actually, many patients with urinary tract infections have similar symptoms, and the patients usually recover with 2-3 days of treatment. So, I thought this case was not unusual. But the fact that Mr. Huang had received treatment in many different hospitals for more than six months without helping him was curious and it worried me a lot.

I handed Mr. Huang a questionnaire, since his simple subjective description of the disease didn't help me to understand his condition very well. It is helpful to quantify things and get more details. Astonishingly, what he wrote on the questionnaire indicated a very serious problem. *"I have to squat to pee, and I can't fall asleep at night. I even wish I could live on the toilet"*, Mr. Huang told me when he noticed that his questionnaire result was not what I expected. Reviewing the information I tried to decide which disease could account for his symptoms. Only tuberculosis seemed like it could explain his condition. Therefore, in the following days I started a work-up for tuberculosis. However, Mr. Huang had an imaging examination first, and it showed that his bladder was only the size of a ping-pong ball. Such severe organ damage was rare in my experience, and the existing medical knowledge I was aware of couldn't explain it!

A few days later, I realized that I needed to dig out the answer from the patient himself. So I asked my second question: tell me more? Mr. Huang then told me, *"I've been taking Special K. These urinary problems all appear after my using drugs, but I do not know whether they are related"*. I asked him, *"Is there anyone else around like you? I mean the ones who also take Special K, and have urinary problems?"* He said, *"Quite a few! They have problems in urinating as well, but do not have as much pain as I do"*.

Well, now I had a clue about what was going on. *Special K* is a new type of drug that is abused. It is especially popular in recent years. Traffickers grind the commonly used medical anesthetic ketamine into fine powder to sell as *Special K*. Due to its inexpensive price and the fact that people think they cannot get addicted to it as easily as to heroin, which has serious side effects, *Special K* has become particularly popular among young people. So this is how the responsibility of the government and the police came to be related to my medical practice.

At that time, my friend Peggy discovered in Hong Kong a patient with bladder contracture due to abuse of *Special K*. I did not expect the same disease to occur in the mainland so soon. Since then, if my patients have similar symptoms to those of Mr. Huang, I ask them: "Tell me more". Over time, I have learned to distinguish this group of patients from others. They are usually anxious and helpless young people, having long-term medical treatments but all ending up without a cure. But I have found that the people who are helpless may not only be the patients themselves, but also their families, and even we doctors.

All we can do is to give the patients symptomatic treatment to temporarily relieve pain. In the early stage of the disease, drug treatment is the most effective way to relieve the symptoms. When it progresses into the late stage and the bladder or kidneys are damaged, this cannot be reversed. "To cure sometimes, to relieve often and to comfort always" applies to such a disease. But in fact, the ones we comfort are more frequently the family members rather than the patients.

Young Jia came to the hospital accompanied by his mother. His father visited him once in a while but left in a hurry every time. All the clothing and personal belongings that Young Jia had were expensive. He was usually silent, and like many patients he looked forlorn. His father talked to me three times. I remember clearly what he said each time, *"I have money! Don't worry about the expense as long as you cure my son's disease"*. His mother looked older than her age. What she said the most was, *"Dr. Wu, please help me"*.

Young Jia gradually became comfortable with me, and he even burst into tears once when I had a long talk with him. Jia's father had deep pockets, and an affair that took up much of his time. Without his disease, Jia would rarely see his father. His mother could do nothing to help him but cry. Although Jia also had enough money, he felt doleful and vexed. That was probably the reason why he took

*Special K*. He was just killing time.

Jia's younger sister who was studying in France encouraged him to cheer up after she found out about his disease. She told Jia, "*Brother, you have to be all right and come to my commencement*". His sister was actually the impetus for Jia to come to the hospital. I told Jia, "Your mom and dad do love you, just the same as your sister does. They just express their love in different ways". He kept silent for a second, and then nodded.

Actually Jia's disease was not serious. He was discharged after a few days' treatment, and his whole family felt very happy with that, so did I. But unfortunately, he came back to the hospital a few months later. I've seen a lot of cases like Jia's family: a sick child, a seemingly successful father, and a helpless mother. In fact, they were all helpless, and they were so helpless that they frequently called me after their son was discharged from the hospital. They begged me to call their child to help to solve their continuing family problems. I could tell they did not trust each other anymore as they were unable to communicate effectively. Why did they attempt to get their doctor to shoulder the responsibility for maintaining their family relationships?

Ms. Meng was a civil servant who had a sinecure in a remote city. Her job was so easy that she had time to play cards regularly, and to kill time by taking *Special K*. She had been taking it for seven years, which was quite a long time. When she came to the hospital, her kidneys were seriously damaged.

She was a wife and mother. But now these two roles had disappeared. I had concerns about Ms. Meng, and I know I shouldn't let my emotions affect my relationship to patients. However, she had been deceiving everyone about her illness, including her colleagues for fear of losing her job. She also deluded her husband with the reason she needed to see a doctor, and attempted to talk me into concealing the fact. She also tried to hide the fact from me that she had been taking *Special K* when I first treated her. What's more, she cheated the patients in the same ward in the hospital. She said she had to borrow some money for an urgent problem but instead she used the money to buy drugs.

"Why can't you just extricate yourself from the drugs", I asked, though I felt it was useless to ask her such question right after I finished it. She said, "*When feeling painful, I feel much better after taking Special K*". I cannot enter their world, nor judge whether such words are real or not. I asked, "Have you ever thought about your children?". This was the only moment I saw the honesty from her eyes. She could not even believe what herself had said. The structures of her personality were completely in chaos.

Soon after Ms. Meng's discharge, she gave me a phone call saying she had relapsed. Still she poured out lies and concocted excuses. I know that no matter how painful she suffered physically and mentally, she could not find way out of this vicious circle of deception. Nobody knows what is going to happen to her.

As a urologist, I did not have much experience with drug addicts, and I still do not know how to communicate with them. But I do know that although they have physical disease, psychological problems are crux of their situation. More and more of my experience indicates how fragile the relationship established between these patients and me is. Equality, respect, and trust are the basic principles of communication between doctors and patients. As for this particular group, although they are overwhelmed with pain when they see doctors, they determine to stop taking *Special K*, their families advise them earnestly and kindly to stop, and the doctors try hard to persuade them and communicate with them, the outcome is more often than not disappointing.

The disaster brought about by taking drugs comes like a rain storm. All I can do is to hold up an umbrella for the patients, shielding them temporarily from the rain so that they won't get too wet, and lead them to where it does not rain. If they insist to stay in the rain and refuse to leave, how can I help them?

When the medical and social problems are intertwined, we all need to think how we can improve the outcome.

**Peng Wu**

Department of Urology, Nanfang Hospital, Southern Medical University, Guangzhou 510515, China

(Email: [doctorwupeng@gmail.com](mailto:doctorwupeng@gmail.com).)

doi: 10.3978/j.issn.2072-1439.2014.03.01

Disclosure: The author declares no conflict of interest.

